REPUBLIC OF IRAQ
MINISTRY OF HIGHER EDUCATION AND SCIENTIFIC RESEARCH
AL-FURAT AL-AWSAT TECHNICAL UNIVERSITY
ENGINEERING TECHNICAL COLLEGE- NAJAF
DEPARTMENT OF MECHANICAL ENGINEERING TECHNIQUES OF POWER

PARAMETRIC INVESTIGATION OF THERMAL PERFORMANCE FOR PARABOLIC TROUGH SOLAR COLLECTOR

HUSSEIN ALI JABBAR HAMMOUD

MSC.TECH.
IN MECHANICAL ENGINEERING TECHNIQUES OF POWER

2023

REPUBLIC OF IRAQ
MINISTRY OF HIGHER EDUCATION AND SCIENTIFIC RESEARCH
AL-FURAT AL-AWSAT TECHNICAL UNIVERSITY
ENGINEERING TECHNICAL COLLEGE- NAJAF
DEPARTMENT OF MECHANICAL ENGINEERING TECHNIQUES OF POWER

PARAMETRIC INVESTIGATION OF THERMAL PERFORMANCE FOR PARABOLIC TROUGH SOLAR COLLECTOR

A THESIS

SUBMITTED TO THE DEPARTMENT OF MECHANICAL ENGINEERING TECHNIQUES OF POWER

AS PARTIAL FULFILLMENT OF THE REQUIREMENTS FOR THE MASTER OF THERMAL TECHNOLOGIES DEGREE IN MECHANICAL ENGINEERING TECHNIQUES OF POWER (M.TECH.)

BY

HUSSEIN ALI JABBAR HAMMOUD

(B.Sc. Eng. Tech. Automobile. 2014)

Supervised by:

Prof. Dr. Dhafer Manea Hicham **Asst. Prof. Kareem Jafar Alwan**

2023

DECLARATION

I hereby declare that the work in this thesis is my own except for quotations and summaries, which have been duly acknowledged.

Signature:

Name: HUSSEIN ALI JABBAR

Date: / /2023

COMMITTEE REPORT

We certify that we have read this thesis titled **" PARAMETRIC INVESTIGATION OF THERMAL PERFORMANCE FOR PARABOLIC TROUGH SOLAR COLLECTOR "** submitted by **Hussein Ali Jabbar** as Examining Committee , examined the student in its contents. In our opinion, the thesis is adequate for an award of the Master's degree of Technical Thermal Engineering.

Signature :

Name :

(Supervisor)

Date : / / 2023

Signature :

Name :

(Co- Supervisor)

Date : / / 2023

Signature:

Name:

(Member)

Date : / / 2023

Signature:

Name :

(Member)

Date : / / 2023

Signature :

Name :

(Chairman)

Date : / / 2023

Approval of the Engineering Technical college – Najaf

Signature :

Name: **Asst. Prof. Dr. Hassanain G. Hameed**

Dean of Engineering Technical College – Najaf

Date : / / 2023

SUPERVISOR CERTIFICATION

We certify that this thesis, entitled **"PARAMETRIC INVESTIGATION OF THERMAL PERFORMANCE FOR PARABOLIC TROUGH SOLAR COLLECTOR "**, which is submitted by **Hussein Ali Jabbar**, has been prepared under my supervision at the Mechanical Techniques Engineering of Power Department, Engineering Technical College-Najaf, Al-Furat Al-Awsat Technical University, as partial fulfillment of the requirements for the Master's degree in Technical Thermal Engineering.

Signature:
Name: **Prof. Dr. Dhafer Manea Hachim**
(Supervisor)
Date: / / 2023

Signature :
Name**: Asst. Prof. Kareem Jafar Alwan**
(Supervisor)
Date: / / 2023

In view of the available recommendation, I forward this thesis for debate by the examining committee.

Signature:

Name: **Asst. Prof.Dr. Adeal A.Edan**

(Head Mechanical. Eng. Tech. of Power Dept.)

Date: / / 2023

LINGUISTIC CERTIFICATION

This is to certify that this thesis entitled "**PARAMETRIC INVESTIGATION OF THERMAL PERFORMANCE FOR PARABOLIC TROUGH SOLAR COLLECTOR** " was reviewed linguistically. Its language was amended to meet the style of the English language.

Signature:

Name:

Date: / / 2023

بِسْمِ اللَّهِ الرَّحْمَنِ الرَّحِيمِ

وَالشَّمْسُ تَجْرِي لِمُسْتَقَرٍّ لَهَا ذَلِكَ تَقْدِيرُ الْعَزِيزِ الْعَلِيمِ (38) وَالْقَمَرَ قَدَّرْنَاهُ مَنَازِلَ حَتَّى عَادَ كَالْعُرْجُونِ الْقَدِيمِ (39) لَا الشَّمْسُ يَنْبَغِي لَهَا أَنْ تُدْرِكَ الْقَمَرَ وَلَا اللَّيْلُ سَابِقُ النَّهَارِ وَكُلٌّ فِي فَلَكٍ يَسْبَحُونَ (40) .

صدق الله العلي العظيم

سورة يس

ACKNOWLEDGEMENT

Thanks to God the Compassionate, the Merciful and my God bestow peace on Prophet Mohammed, member of his family and his followers.

I would like to express my gratitude to my supervisors (**Prof. Dr. Dhafer Manea Hicham)** and **(Asst. Prof. Kareem Jafar Alwan)** for giving me the opportunity to work on this project and for their support of my master's thesis.

I extend my sincere thanks to the Dean (**Asst. Prof. Dr. Hassanain G. Hameed**) of the Technical College of Engineering, Najaf, and the esteemed head of the Mechanical Engineering and Technology of Power Department (**Asst. Prof. Dr. Adeal A.Edan)** for providing possible assistance to facilitate the study process. Special thanks go to the members of the department for their assistance.

Finally, my deepest gratitude goes to my family my dear parents, brothers, wife, and children for their patience, support, and encouragement throughout my life.

My God bestows health and happiness on all of them.

Hussein Ali Jabbar

2023

ABSTRACT

Parabolic trough collector is one of the solar concentrating technologies. The parabolic trough collector collects solar irradiation and uses a reflector on an absorber tube to heat a working fluid, which flows to a heat exchanger for the production of steam to generate electricity. Experimental and numerical steps are presented in this study to manufacture a parabolic trough collector with manual tracking system. The experiments test with water as the working fluid, the experiments included the effect of volume flow rate on the thermal performance of a parabolic trough collector and study the effect of direction on the thermal behavior of the parabolic trough collector. Experiments compare between the parabolic trough collector east-west line and south-north line directions ; the east-west line direction has four days (2^{nd} , 6^{th} , 7^{th} , and 10^{th}) of November with four ranges of volume flow rate (4, 1, 2, and 3) L/min respectively. South-north line direction has four days (13^{th} , 14^{th} , 20^{th} , and 21^{st}) of November with four ranges of volume flow rate (1, 2, 3, and 4) L/min, respectively.

The results found the maximum average value of output temperature of east-west line direction reached (336.65 K) on day 6 November with a volume flow rate of 1 L/min, and that more than (2^{nd} ,7^{th} , and 10^{th}) of November by (6.8%, 4%, and 5.6%) respectively. The maximum average value of output temperature of south-north line direction reached (328.35 K), on day 13^{th} of November, and more (14^{th} ,20^{th} , and 21^{st}) of November by (3%, 4%, and 5%) respectively.

The maximum value of thermal efficiency of east-west line direction was reached (68.7%) on day 6^{th} of November, and was higher than on other days (2^{nd} ,7^{th}, and 10^{th}) of November by (64%, 24%, and 33%) respectively. The maximum average value of thermal efficiency of south- north line direction on day 14^{th}

November reached (49.5 %), more than another day in south-north line direction (13^{th} ,20^{th} , and 21^{st}) of Novembor by (11 %, 8%, and 4%) respectively. According to the comparative analysis of thermal performance, the east-west line direction show the highest value for parabolic trough collector. This indicates that in comparison to the south-north line direction, the east-west line direction is the optimal choice maximuming the thermal efficiency of a parabolic trough collector.

A numerical study depending on COMSOL Multiphysics Version 6.0 simulation software is used to investigate the thermal behavior of a solar parabolic trough collector with the utilization of various working fluids (water, TherminolVP-1, and Syltherm800). The numerical study examined the effects of volume flow rate, the effect of the various ranges of absorptivity (0.5, 0.7, and 0.9), effect of the various ranges of reflectivity (0.225, 0.5, and 0.95), the effect of the weather condition of Al-Najaf city, the effect of mass flow rate, and the effect of inlet temperature.

The first step of a numerical study made validation with pervious study model with numerical present model. At last concluded Syltherm800 is the best working fluid that may be utilized in a parabolic trough collector when compared to other working fluids. Syltherm800 provides high output temperatures relative to water. Water best choice as working fluid with low range of input temperature and low mass flow rate. Syltherm800 best choice for high range of input temperature and high mass flow rate.

CONTENT

LIST OF FIGURES

LIST OF THE TABLES

NOMENCLATURE

Symbols	Definition	Unit
Aa	Aperture area of PTC	m^2
A_g	Glass Surface Area	m^2
A_p	Pipe Surface Area	m^2
A_{ri}	Inner Area of receiver tube	m^2
Cp	Specific heat capacity	J/Kg.K
D_{absi}	Receiver inner diameter	m
D_{abso}	Receiver outer diameter	m
D_{covi}	Cover inner diameter	m
D_{covo}	Cover outer diameter	m
D_{ri}	Receiver inner diameter	m
Ep_{cov}	Cover thickness	m
f	Focal length	m
G_b	Solar irradiation	W/m^2
h	Convection heat transfer coefficient	W/m^2. K
h_{out}	Convective heat transfer coefficient	W/m^2. K
K_{abs}	Absorber thermal conductivity	W/m . K
K_{cov}	Cover thermal conductivity	W/m . K

L	Length of collector	m
$\dot{m}$	Mass flow rate	Kg/s
Nu	Nusselt number	-
Pr	Prandtl number	-
Q	Volumetric flow rate	m^3/s
Q_{loss}	Heat losses	W
Q_s	Solar Energy	W
Q_u	Useful heat	W
Re	Reynolds number	-
R_g	Total Energy on Glass	W
R_p	Total Energy on Pipe	W
T_{am}	Ambient temperature	K
T_{ci}	Inner cover temperature	K
T_{co}	Outer cover temperature	K
T_{fm}	Mean fluid temperature	K
T_{in}	Input temperature	K
T_{out}	Output temperature	K
T_r	Receiver temperature	K

T_r	Receiver tube temperature	K
u	Flow velocity in X-direction	m/s
v	Flow velocity in Y-direction	m/s
w	Flow velocity in Z-direction	m/s
W	Width of PTC	m

GREEK SYMBOLS

Symbol	Definition	Unit
α_{cov}	Cover absorbance	-
α_g	Glass absorbance	-
α_p	Pipe absorbance	-
ΔP	Pressure drop	pa
ϵ_{cov}	Cover emittance	-
μ	Viscosity	Pa.s
ρ	Density	Kg/m^3
τ_{cov}	Cover transmittance	-
η_{th}	Thermal efficiency	-

ABBREVIATION

Symbol	Description
CC	Concentration ratio
CFD	Computional Fluid Dynamic
CPC	Compound Parabolic Collector
CSP	Concentrating Solar Plant
CTC	Cylinderical Trough Collector
EG	Ethylen Glycol
ETC	Evacuated Tube Collector
FPC	Flat Plate Collector
GHG	Green House Gas
HFC	Heliostat Field Collector
HTF	Heat Transfer Fluid
IPH	Industrial Process Heat
MWCNT	Multiwall Carbon Nano Tube
PDR	Parabolic Dish Reflector
PTC	Parabolic Trough Collector
SEGS	Solar Electric Generation System

Chapter One
Introduction

Chapter One

Introduction

1.1. General

Renewable energy is obtained from renewable resources that replace themselves organically over time. The sun, wind, biomass, hydro-electric, and geothermal heat are all examples of natural phenomena that produce renewable energy [1]. Renewable and non-renewable energy resources are the two types of energy resources now in use. Non-renewable energy sources include coal, oil, natural gas, and nuclear. Renewable energy comes from natural processes that are renewed on a regular basis. It comes directly from the sun in all of its forms. In contrast to fossil fuels, which are depleted significantly faster than they are regenerated, renewable energy is rapidly replenished [2]. Electricity generation, air and water heating and cooling, and transportation energy services are all common uses of renewable energy. Renewable energy accounts for around 20% of worldwide energy consumption, including about 30% of electricity [3].

Fossil fuels have provided nearly all of our energy needs for the past century because they are both much less costly and more practical than renewable energy sources. Another significant problem is the significant amount of hazardous gases discharged into the environment as a result of the burning of non-renewable energy sources like fossil fuels, which has also resulted in global warming [4]. Massive volumes of waste heat from the power station have been released, resulting in thermal pollution in streams and a variety of plant and animal species suffering. In addition, there are ongoing,

long-term issues with the disposal of radioactive waste from nuclear power plants and worries that radiation might be emitted into the atmosphere [5].

The amount of energy consumed in 2018 was more than double what it was in 2010, and as a result, carbon dioxide (CO_2) emissions soared to the highest level ever in 2018, reaching 33.1 gigatonnes [6]. As a result, increased generation of renewable energy is necessary to satisfy the energy needs of the world's rapidly developing economies. Renewable energy is never depleted and produces little or no waste, such as carbon dioxide or other chemical reactions. It has a minor influence on the environment. Renewable energy projects may be profitable for a variety of sites, and facility generators require less maintenance than traditional generators, resulting in cheaper maintenance and operation costs. Figure 1.1 below shows the contribution of renewable energy to world electricity production.

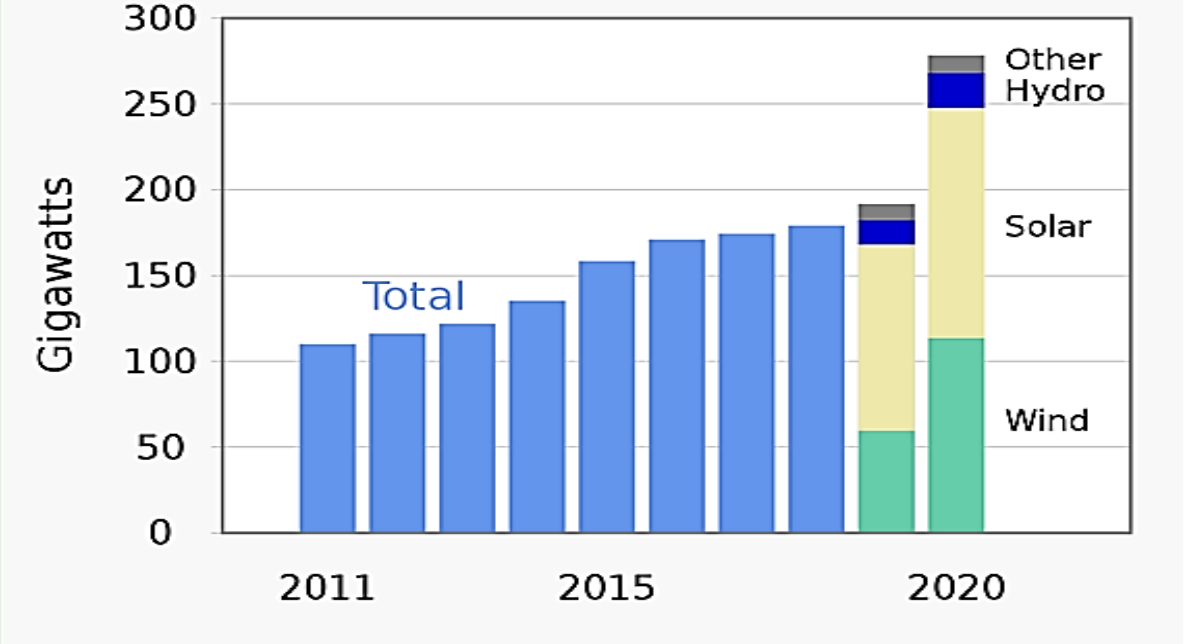

Fig 1.1.Contribution of Renewable Energy in World Electricity Production[7].

1.2. Solar Energy

The heat and radiant light from the sun may be used in several ways, such as solar power to produce electricity, solar thermal energy, which includes solar water heating, and solar photovoltaics. It is a significant source of renewable energy, and depending on how it collects and disseminates solar energy or transforms it into solar power, its technologies are categorized as passive or active solar. Solar power is pure, limitless, and secure. Even when it is converted into electricity through photovoltaic or thermodynamic plants, it does not produce harmful emissions. Solar energy is a particularly attractive source of electricity due to its vast scale.

The Carbon Tracker Initiative predicted in 2021 that the land area required to generate all of our energy from the sun alone would be 450,000 Km^2 roughly the same size as Sweden, Morocco, or California (0.3 percent of the total land area on Earth) [8]. The sun radiates a massive quantity of energy into its surroundings, which total 174 PW (1 PW = 10^{15} W) in the earth's upper atmosphere. Both the atmosphere (6 percent through reflection and 16 percent by absorption) and the clouds have attenuated the energy twice before it reaches the Earth's surface (20 percent by reflection and 3 percent by absorption, as shown in Fig.1.2). The land and seas get another 51% (89 PW) of the total incoming solar energy.

The visible and near-infrared wavelengths of solar radiation reach the Earth's surface in huge amounts, with a minor portion in the near-ultraviolet [9]. The majority of the world's population lives in locations with insolation values of 150–300 watts per square meter per day, or (3.5-7) KWh per square meter per day [10]. Because the total amount of solar energy available on

Earth remains large, but because of its low density and erratic nature, it must be efficiently gathered and stored. Figure 1.2. shows the earth's energy budget.

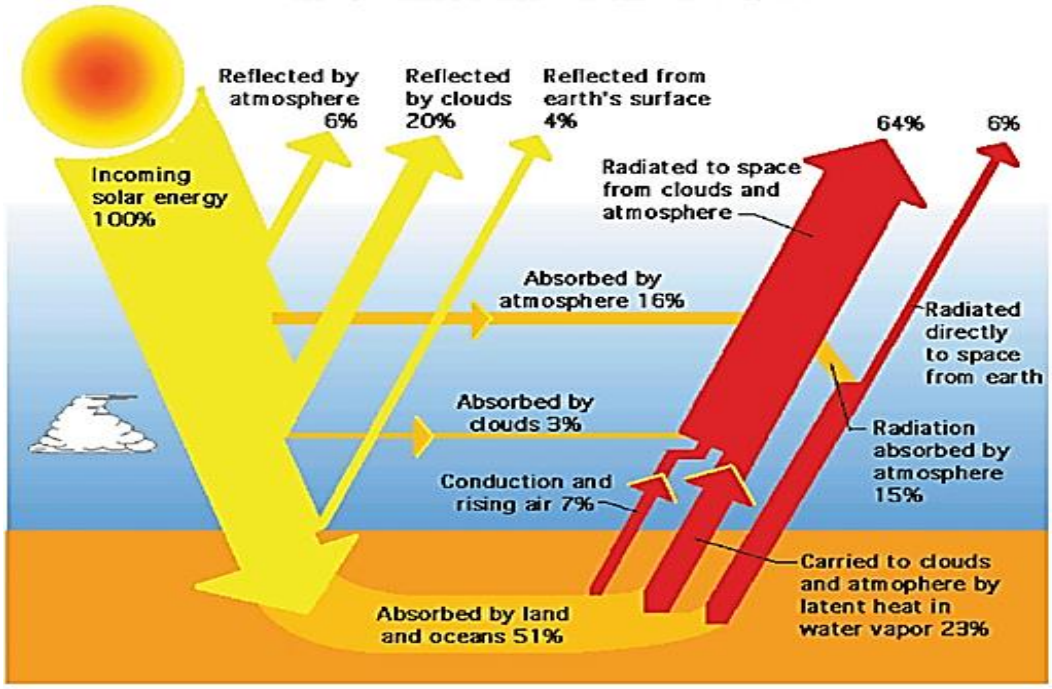

Fig.1.2. Earth's Energy Budget [11].

The sun emits (410 * 10^{15} J) of energy each hour on earth, which is more than the entire amount of energy consumed worldwide in 2001 [12]. As a result, solar energy is a possible option for meeting current energy demands. Solar energy can be used in three ways: solar photovoltaic, solar thermal, and solar hybrid technologies [13]. The sun's energy is focused on an absorber using mirrors or lenses in the solar thermal system.

Solar Concentrator Systems (SCSs) gather solar energy, which is then used for a variety of critical tasks in our everyday lives, including generating electricity, heating water, and air conditioning. Figure 1.3 shows the solar energy map of the world by KWh/m^2 .

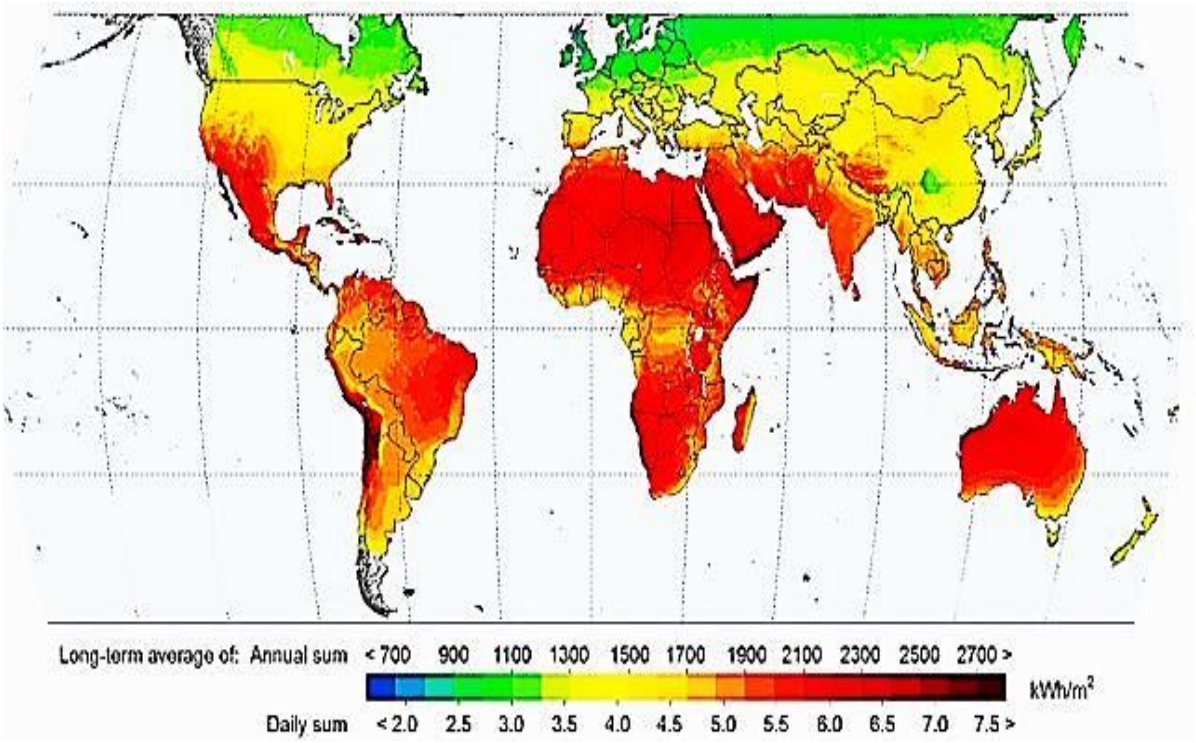

Fig.1.3. Solar Energy Map of the World by KWh/m^2 [14].

1.3. Concentrated Solar Thermal Systems

Sunlight is collected and used to generate heat by solar thermal collectors. Using a collector, thermal energy from sunlight or solar radiation is transformed into a form that may be used and stored. This energy is carried by electromagnetic radiation with wavelengths ranging from ultraviolet to infrared (short) [15]. Solar thermal collectors are divided into two categories : non-concentrating and concentrated. Solar ponds, flat plate collectors (FPC), and evacuated tube collectors (ETC) are examples of non-concentrating devices.

Non-tracking, single-axis tracking, and two-axis tracking are the three types of focusing systems. Concentrated solar thermal systems that do not require tracking, such as the compound parabolic collector (CPC). A compound parabolic collector (CPC), a linear fresnel reflector (LFR), a

cylindrical trough collector (CTC), and a parabolic trough collector (PTC) are included in the single axis tracking concentrating solar thermal [16].

The two-axis tracking solar thermal concentrate includes the parabolic dish reflector (PDR), and heliostat field collector (HFC). As a type of solar concentrator, the parabolic trough collector (PTC) is one of the most often used. The several solar thermal collector types, together with their motion, absorber type, concentrating ratio, and indicated temperature range [17], are shown in Table 1.1.

Table.1.1. Concentrated Solar Thermal Systems [17].

Motion	Collector type	Absorber type	Concentrating ratio	Indicative temperature range ^{o}C
Stationary	Flat Plate Collectors (FPC)	Flat	1	30-80
	Evacuated Tube Collectors (ETC)	Flat	1	50-200
	Compound Parabolic Collector (CPC)	Tubular	1-5	60-240
Single axis tracking	Compound Parabolic Collector (CPC)	Tubular	5-15	60-300
	Linear Fresnel Reflector (LFR)	Tubular	10-40	60-250
	Cylindrical Trough Collector (CTC)	Tubular	15-50	60-300

	Parabolic Trough Collector (PTC)	Tubular	10-85	60-400
Two axis tracking	Parabolic Dish Reflector (PDR)	Point	600-2000	100-1500
	Heliostat Field Collector (HFC)	Point	300-1500	150-2000

As a type of solar concentrator, the parabolic trough collector (PTC) is one of the most often used. The several solar thermal collector types, together with their motion, absorber type, concentrating ratio, and indicated temperature range It's also necessary to have a precise focusing equipment. As a result, a solar concentrator is made from :

I. a focusing device.

II. a receiver system .

III. a tracking arrangement.

A solar concentrator may produce temperatures of up to 2000 °C [18]. They therefore have the potential to be utilized in high delivery temperature thermal and electrical power production. The advantages of a concentrator by concentrating solar energy from a larger surface area onto a smaller one (the absorber), it increases solar intensity. The concentration on a smaller surface area reduces heat loss. The high delivery temperature results in a thermodynamic fit between the temperature level and the task, which helps to save money by replacing an expensive large receiver with a less expensive reflecting or refracting surface area.

1.4. Parabolic Trough Collector (PTC)

A polished metal mirror that is straight in one dimension and curved like a parabola a kind of solar thermal collector known as a parabolic trough collector. An absorber, a tracking system, a support structure, and a reflector surface main part of the parabolic trough collector (PTC). The focal line, which is where hot objects are positioned, is where the sunlight that enters the mirror and its plane of symmetry is focused. For further uses, a fluid-filled tube runs the whole length of the trough at its focal point.

The tube receives concentrated sunlight, which warms the fluid to a high degree, which uses the heat energy to produce electricity or mechanical power [19]. The most common and well-known form of parabolic trough is this solar energy collector. There are two types of applications for parabolic trough collectors (PTC), concentrated solar power (CSP) facilities, which will be built first and foremost. Several commercial collectors for such purposes have been successfully tested under real-world operational circumstances.

A typical aperture width is around 6 meters in total. The technique of geometrical concentration is applied. The lengths vary between 100 and 150 meters. The ratios range from 20 to 30. Temperatures range from 300 to 400 degrees Celsius. Solar power (CSP) facilities with PTCs are both directly and indirectly related to steam power cycles. Although the solar electric generation system (SEGS) facilities in the United States are the most well-known examples of concentrating solar plants (CSP) , a number of other projects are now being developed or built across the world [20].

The other set of applications necessitates temperatures ranging from 100 to 250 °C. Industrial process heat (IPH), low-temperature heat demand with large consumption rates (domestic hot water, DHW, space heating, and

swimming pool heating), and heat-driven refrigeration and cooling are the most common of these uses. Aperture widths range from 1 to 3 meters, total lengths from 2 to 10 meters, and geometrical concentrating ratios from 15 to 20. Although the majority of the facilities are in the United States, several have lately been erected in other nations[21]. Figure 1.4 shows the parabolic trough collector [22].

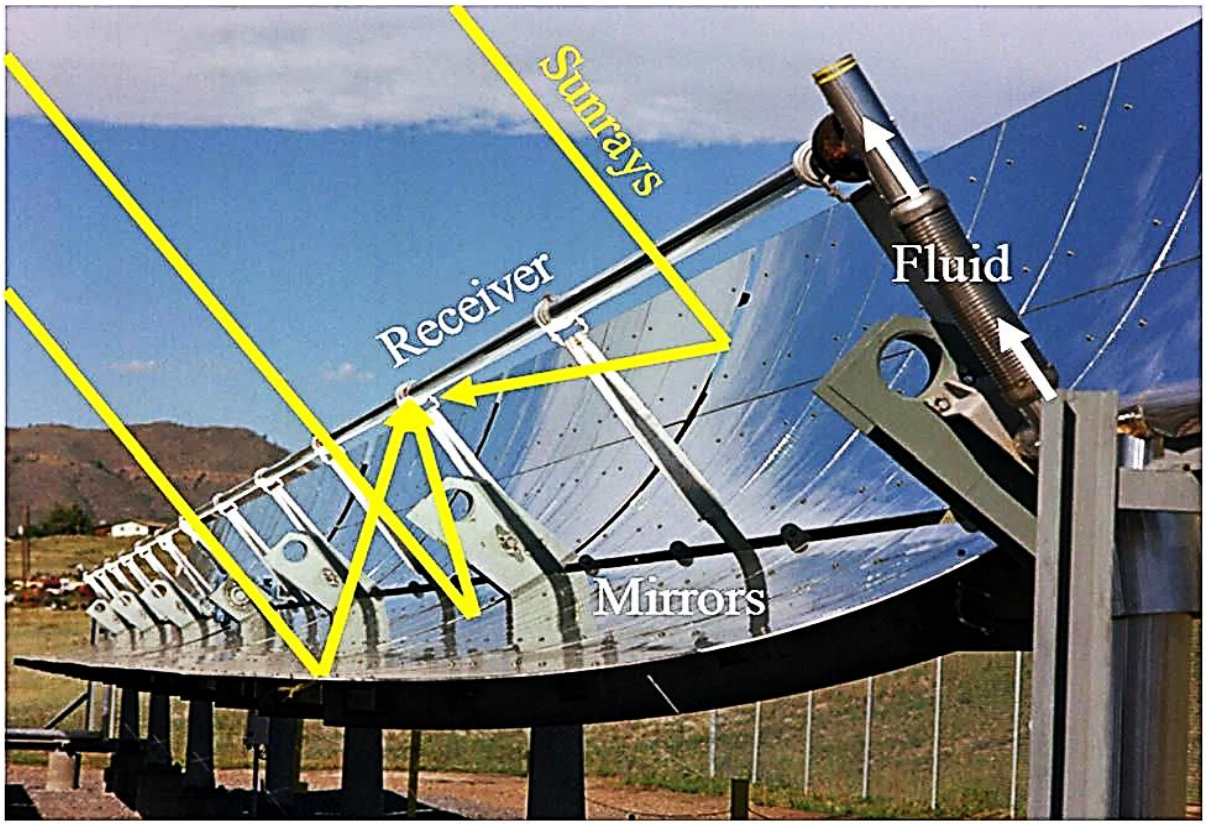

Fig.1.4. Parabolic Trough Collector [22].

1.5. Working Fluids in Parabolic Trough Collector (PTC)

A number of working fluids are utilized in concentrating solar systems, including pressurized water, molten salt, thermal oil, liquid sodium, Nano fluid, and gases. The working fluid function is characterized as a heat transmission medium [23]. Any sort of working fluid can be employed in a

temperature range operation. A pump or compressor pumps the working fluid through absorber tube the to the heat exchanger. The heat transfer process will take place between the absorber tube and the working fluid, and the absorber tube will serve as the receiver of the solar concentrating system's focused solar radiation.

Thermal energy is transferred from the working fluid to the heat exchanger, which is subsequently transformed into energy and utilized to generate electricity. Every working fluid has varied thermo-physical characteristics and reacts differently depending on the situation. Any working fluid's density, thermal conductivity, specific heat, and viscosity are all important aspects [24]. The thermal efficiency of a working fluid is calculated by the mass flow rate and specific heat when there is a temperature differential between the intake and output flow.

Parabolic trough collectors (PTCs), which employ thermal oil as the heat transfer fluid, are the most prevalent solar field technology. Alternative fluids such as water, molten salts, or pressured gas have been studied and tried due to environmental concerns and the thermal oil's temperature constraints. Using pressurized water has a number of advantages. a simpler plant layout, lower-temperature pressurized water, greater steam temperature without impurities, and lower-temperature pressurized water [25].

Molten salt is used as a heat transfer fluid in the American Solar-Two power tower project [26]. Because of its simple storage idea, it is also recommended for use in parabolic trough plants [27] . With a maximum working temperature of 600 ºC, a nitrate salt mixture (40 % $NaNO_3$, 60 % KNO_3) is employed [28]. In concentrating solar collectors, using gas-working fluids is a simple technique to function at high temperatures. The energy and

energetic properties of several gas working fluids in a commercial parabolic trough collector (PTC) are investigated in this study.

As working fluids, air, nitrogen, carbon dioxide, helium, neon, and argon were studied, researchers proposed using carbon dioxide (CO_2) as a heat transfer fluid (HTF) in the collector field [29]. Heat exchangers transfer heat from the collector field to a molten salt loop in the middle. Heat exchangers transfer heat from the collector field to a molten salt loop in the middle. Heat is transported and stored from the dispersed collector field to the power block through the molten salt loop.

In concentrating solar power systems, the working fluid is critical, and all recent attempts have been made to find a suitable fluid that can serve as the optimum heat transfer medium in these systems. Finally, the best thermophysical qualities, high thermal efficiency, and operation at high temperatures were used to choose the appropriate working fluid for the parabolic trough collector (PTC).

1.6. Temperature Operation Range of Working Fluids

The temperature operation range of working fluid in solar concentrating systems different from types to another depending on thermos-physical properties which control in the nature of working fluid and the temperature operation range. Water has temperature operation range between (300 - 600) K [23] , water has high thermal conductivity and low viscosity. Thermal oil has temperature range between (243- 673) K [23]. Molten salt has temperature operation range between (600 -800) K [28]. Liquid sodium has temperature operation range between (400– 1200) K [24] , has high thermal conductivity and low specific heat. Air, carbon dioxide, helium have temperature operation ranges between (300-1200)K, (300-1100)K ,(400-1200)K respectively[29].

1.7. Solar Concentrating Systems Power Plants

Renewable energy technologies are used to generate electricity. It is being promoted on a worldwide basis in order to meet rising demand in an environmentally friendly manner. Solar thermal power generation is one of the most significant renewable energy methods for generating electricity with a low environmental impact. Furthermore, a megawatt-scale grid linked to solar thermal power plants that can produce energy with high dispatch ability may be built.

To concentrate the sun's light energy onto a receiver and convert it to heat, all concentrating solar power (CSP) devices employ a mirror structure. The heat may then be utilized to generate steam, that can be used to power a turbine or directly as process heat in heavy industrial operations. Thermal energy storage devices are commonly used in concentrating solar power (CSP) plants to generate electricity on overcast days or hours after sunset or before sunrise. Concentrated solar power is a versatile and dispatchable renewable energy source because of its capacity to store solar energy.

Concentrating solar power (CSP) facilities had a total capacity of 4429 MW in operation across the world by the end of 2014, with plants with a total capacity of 5684 MW under construction or development [30]. Around the world, there are concentrating solar power (CSP) projects with plants that are either operating, under construction, or in the planning stages. Parabolic trough collector (PTC), solar power tower (SPT), linear fresnel reflector (LFR), and parabolic dish systems are the four extant concentrating solar power (CSP) technologies, as depicted in Figure 1.5.

Regardless of the technology utilized, all concentrating solar power (CSP) facilities have the same three basic components: the solar field, the power

block, and the storage system[31]. The solar field is made up of solar concentrators with different shapes depending on the technology. Their purpose is to reflect and focus direct sunlight (DNI) onto a tiny region known as the receiver, which heats the heat transfer fluid (HTF). The energy collected by the heat transfer fluid (HTF) is sent to the power block, where turbines convert it to electricity [32].

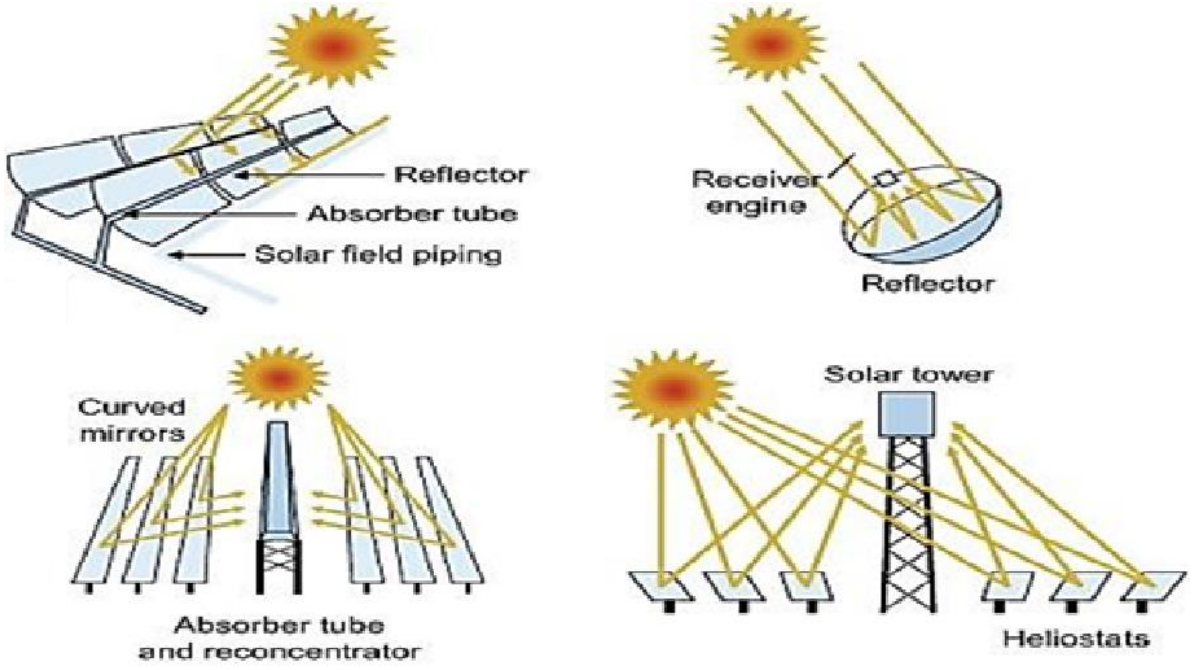

Fig.1.5. Types of Concentrating Solar Power Technology [33].

Solar concentrators of varying capacities have been used in electricity stations in twenty-three countries around the world. There are one or more stations in each country, in other countries, such as Spain, more than fifty stations may be found, each of which uses a different system of the aforementioned solar concentrators [34]. The parabolic trough collector is the most technically and commercially mature concentrating solar power plant

technology at the current time, as shown in Figure 1.6. The global concentrating solar power (CSP) plant capacity could reach 37 GW by 2025 and 600 GW by 2040 [35]. Such numbers confirm the promising future in this area.

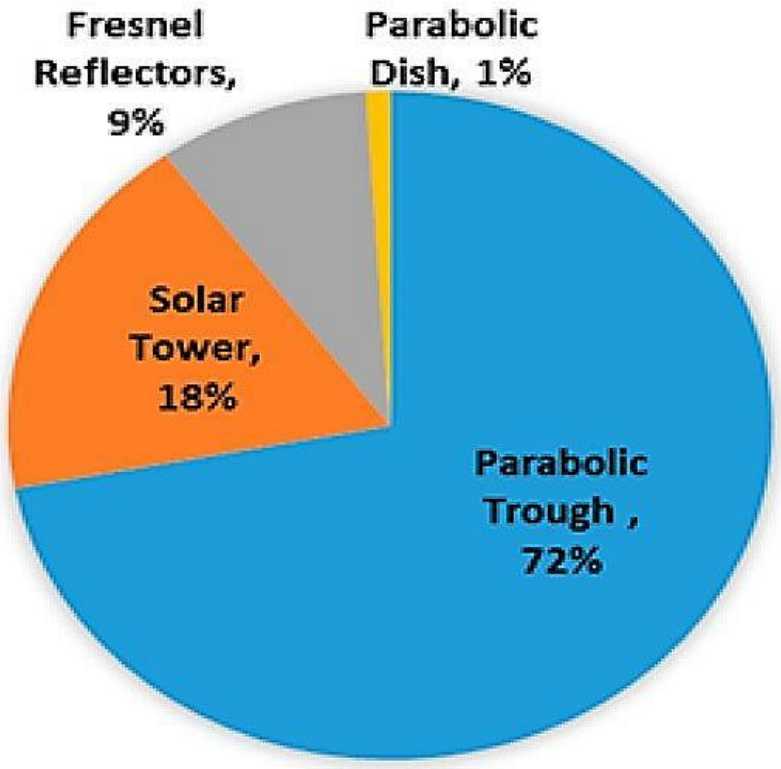

Fig.1.6. Percentage of CSP Technology Types [36].

1.8. Study Aims

The main objectives of the current study can be listed as :

- **Experimental work :** Manufacture parabolic trough collector apparatus for :
  1- The effect of direction on thermal performance of parabolic trough collector.
  2- The effect of volumetric flow rate on thermal performance of parabolic trough collector .
- **Numerical study :** Build and develop a numerical simulation model to examin the thermal performance of the parabolic trough collectors with various working fluids.

1. The Effect of Volumetric Flow Rate on Thermal Performance of PTC.
2. The Effect of Inlet Temperature on Thermal Performance of PTC.
3. The effect of weather condition on thermal performance of PTC.
4. The effect of reflectivity on thermal performance of PTC.
5. The effect of absorptivity on thermal performance of PTC.
6. The effect of mass flow rate on thermal performance of PTC.

1.9. Outlines of Thesis

This thesis consists of six chapters. They are briefly introduced as flows:

Chapter One presents a broad background and introduction about the renewable energy , solar collectors , parabolic trough technology and working fluids in parabolic trough collectors and Temperature ranges.

Chapter Two discusses the previous experimental , and numerical studies that have been carried out regarding the working fluids in parabolic trough technology , include the numerical and experimental studies .

Chapter Three presents a related theoritcal analysis and numerical simulation setup of the working fluids in parabolic trough collector (PTC).

Chapter Four presents a related experimental setup of the working fluids in parabolic trough collector (PTC), and all equipment used in the test are presented in detail.

Chapter Five presents the results and discussion of experimental and the numerical setups of working fluids in parabolic trough collector (PTC).

Chapter Six gives a conclusion of the study along with some recommendations that may be followed for future study and references.

Chapter Two
Literature Review

Chapter Two

Literature Review

2.1. Introduction

This chapter presents previous studies of the thermal performance of the parabolic trough collector (PTC) by using different working fluids; these studies include both experimental and numerical studies.

2.2. Experimental Studies of Thermal Performance of Parabolic Trough Collectors (PTC) by Using Different Working Fluids

Many studies have been presented to investigate the thermal performance of the parabolic trough collector by using various working fluids such as pressurized water, thermal oil, molten salts, pressurized gases, air, nitrogen, carbon dioxide, helium, nitrate salts, and nanofluids [36]. Each type of working fluid is employed in specified conditions and temperature ranges [37]. In this paragraph, I will review the experimental studies that investigated the thermal performance of parabolic trough collectors.

T.A. Yassen et al. 2010 [38] investigated experimental of the thermal performance of a parabolic trough collector using water as the working fluid. The studies were carried out in Tikrit, Iraq, over the winter and summer. Tikrit University's solar radiation was computed theoretically, and a theoretical analysis was conducted using the FORTRAN 90 software. To calculate the theoretical thermal efficiency, the dimensions and parameters of the collector were entered into the computer. The experimental thermal efficiency of the collector was found to be between (7-15)% lower than the theoretical.

The final results showed that an increase in mass flow rate led to an increase in thermal efficiency. When the water mass flow rate exceeds forty kilos per hour, there is no substantial change in efficiency, as shown in Figure 2.1 below:

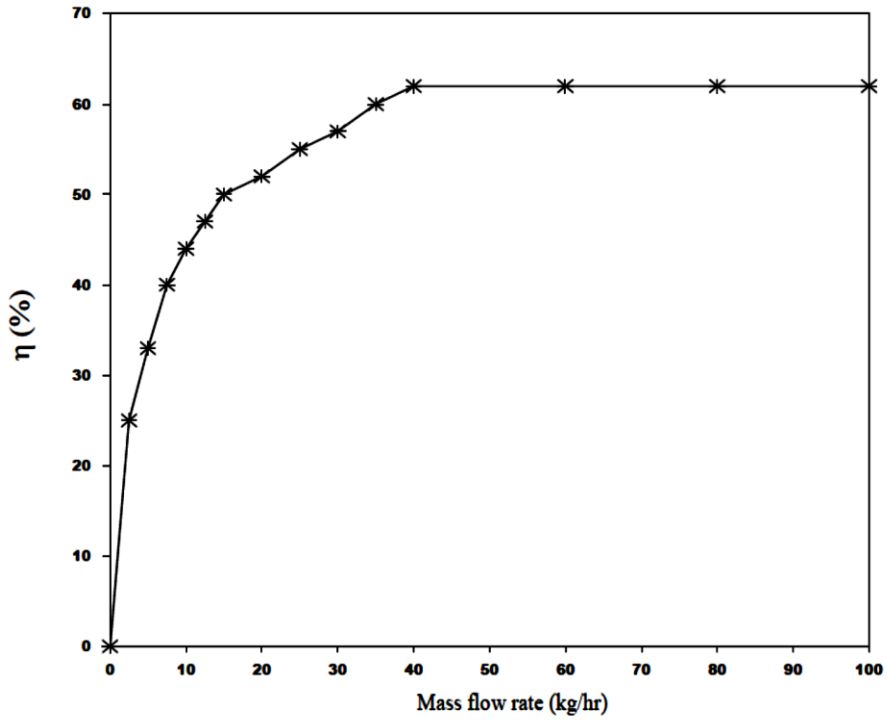

Fig.2.1. Thermal Efficiency of PTC with Different Mass Flow Rate [38].

M . Ouagued et al. 2013 [39] estimated thermal performance of PTC under Algerian climate conditions experimentally by using different thermal oils as heat transfer fluids (Syltherm 800, Marlotherm SH, Marlotherm X, Santotherm 59, Santotherm LT, Syltherm XLT, and Therminol D12), the final result found Syltherm 800 given the high output thermal performance of the parabolic trough collector as shown in Figures 2.2 and 2.3 below:

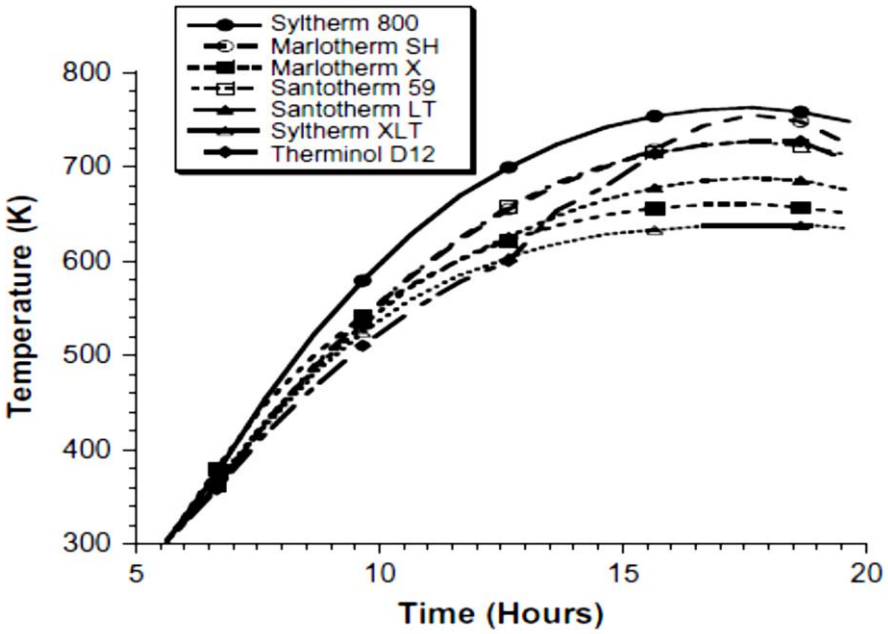

Fig. 2.2. Temperature Range of Different Thermal Oil [39].

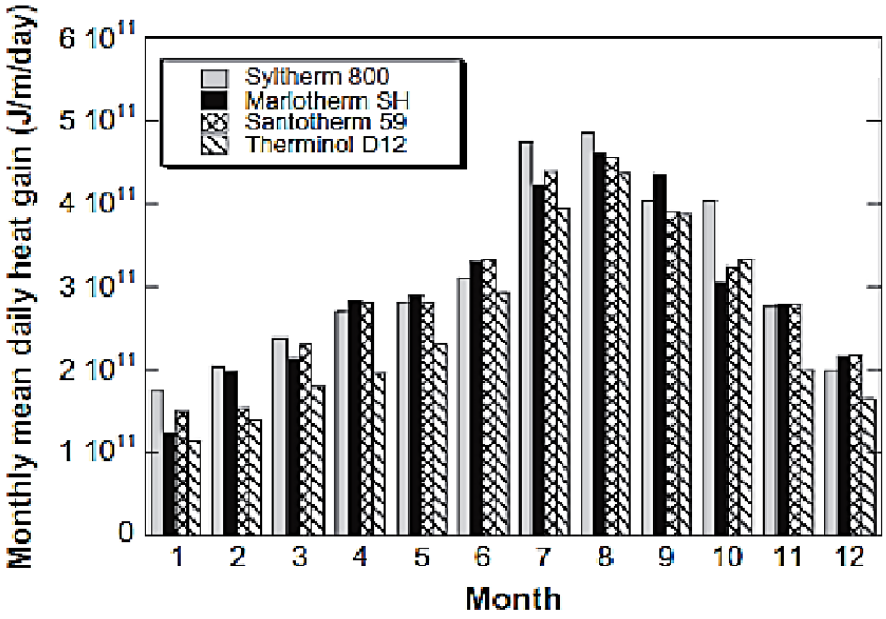

Fig. 2.3 . Monthly Mean Daily Heat Gain of Different Thermal Oil [39].

J. Muñoz-Anton et al. 2014 [40] investigated the thermal performance of a parabolic trough collector by using gases as working fluids experimentally. By comparing the performance of PTC with thermal oil (Syltherm800) and gas carbon dioxide (CO_2) as heat transfer fluids, they discovered that thermal oil (Syltherm800) has a limited operation temperature range below 673 K, whereas carbon dioxide (CO_2) operates well above 1100 K.

Y.T. Wu et al. 2015 [41] estimated the thermal performance of a parabolic trough collector experimentally by using molten salt as the heat transfer medium with a melting point of 359 K and operation temperature upper limits of 823 K, found the water-to-salt heat exchanger's overall heat transfer coefficient ranged from 600 to 1200 W/(m^2.K) in the ranges of 10,000 < Re < 21,000 , and 9.5 < Pr < 12.2. The experimental results were in good agreement with the Sieder-Tate and Gnielinski equations, which offer well-known correlations.

D. Rajput et al. 2016[42] investigated the effect of nanofluid on the thermal performance of a parabolic trough collector experimentally, using nanofluid Alumina (Al_2O_3) with synthetic oil as heat transfer fluid. The final result showed that by employing Al_2O_3/synthetic oil nanofluid, temperature gradients and maximum temperatures in the absorber are considerably minimized, and the parabolic trough collector was more efficient when using nanofluid (Al_2O_3) when compared with the thermal performance of a parabolic trough collector using synthetic oil, as shown in Figures. 2.4 and 2.5 below :

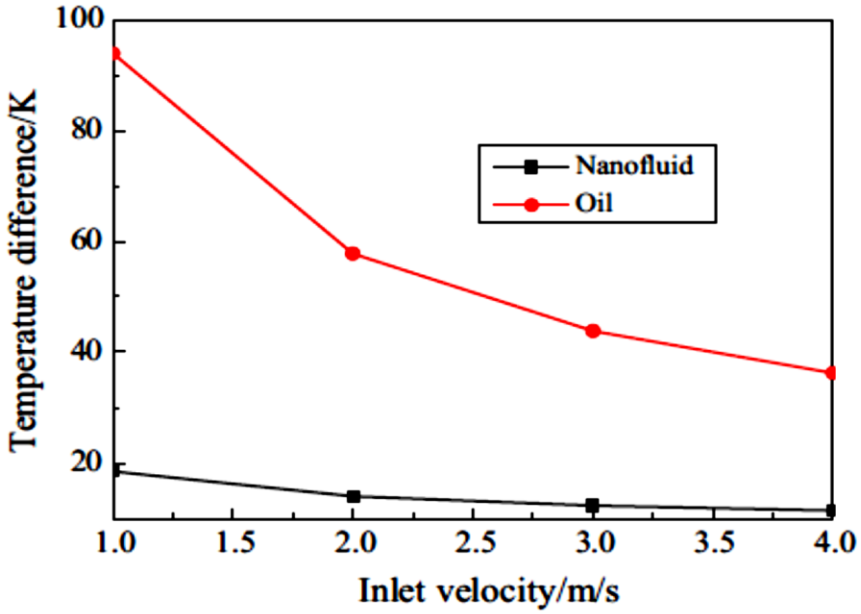

Fig.2.4.Temperature Difference Under Different Inlet Velocity [42].

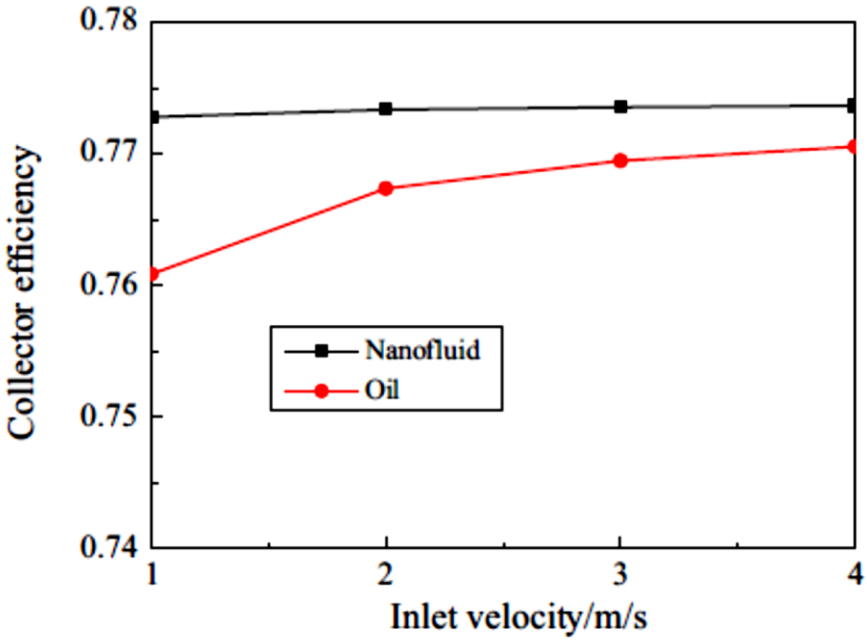

Fig.2.5. Collector Efficiency Under Different Inlet Velocity [42].

M . Chafie et al. 2017 [43] conducted experiments to evaluate the thermal behavior of a parabolic trough collector. They built and installed a PTC at labortary of thermal process in the Research and Technology Center of Energy (CRTEn), Borj Cedria-Tunisia. They investigated thermal performance by using Transcal N oil as a heat transfer medium. The final results showed that climate variables significantly impact on thermal performance, with the average energy and energy efficiency are higher on days with a clear sky days than on a cloudy sky days. Energy efficiency ranged from 19.7% to 52.6% on a daily basis, while daily exergy efficiency ranged from 8.51% to 32.34%.

Singh H et al. 2017 [44] evaluated thermal performance of parabolic trough collector experimentally by using an ethylene glycol and distilled water based mixture as working fluid. Experimental investigations have indicated that the total thermal efficiency of PTC while using a ethylene glycol and distilled water at 100 L/h is 6.4 %, which is much higher than the efficiency result at 160 L/h, which is roughly 5.89 %.

M. M. Tafarroj et al. 2018 [45] estimated the thermal performance of parabolic trough collector experimentally using two types of nanofluids as working fluid: nanosilica and multi-wall carbon nanotube (MWCNT) with used in ethylene glycol (EG). For nanosilica and MWCNT, the volume fractions of nanoparticles in the base fluid were 0.1- 0.5%, and 0.1 - 0.6 %, respectively. The final results showed that the nanofluid containing 0.6% MWCNT/EG had the greatest outlet temperature of 346.1 K.

S. T. Hamidi et al. 2018 [46] investigated thermal performance of parabolic trough collector experimentally using three types of working fluid (water, nanoparticles of CuO mixed with distilled water, and nanoparticles of Al_2O_3 mixed with distilled water) without a tracking system and a concentration ratio of 0.01% and a mass flow rate of 20L/h. The experiments were conducted at the Electro-mechanical Engineering Department at Baghdad University of technology in October 2017 during the daytime (9 a.m. – 15 p.m.). The final results show that using CuO with distilled water as a working fluid raised the average output temperature by 10.4%, the average usable heat gain by 11%, and the average collector efficiency by 15%. Using Al_2O_3 with distilled water as a working fluid raised average output temperatures by 4%, usable heat gains by 6.5 % , and collector efficiencies by 8.2 % as shown in Figures 2.6,2.7, and 2.8 below :

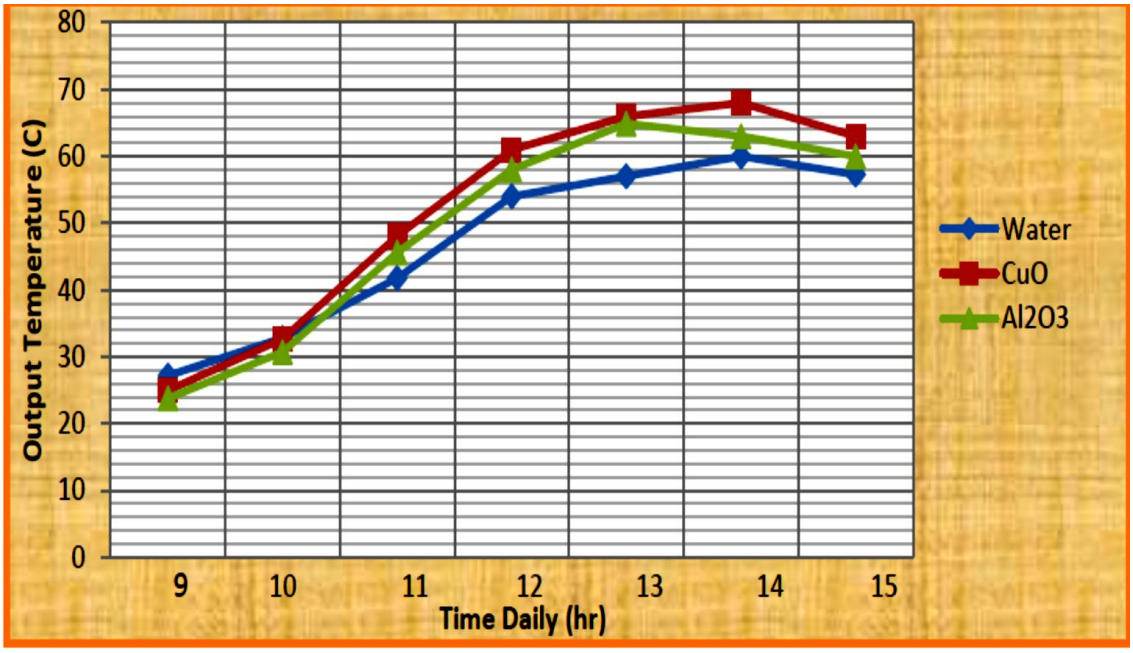

Fig.2.6. Output Temperature with Various Time [46].

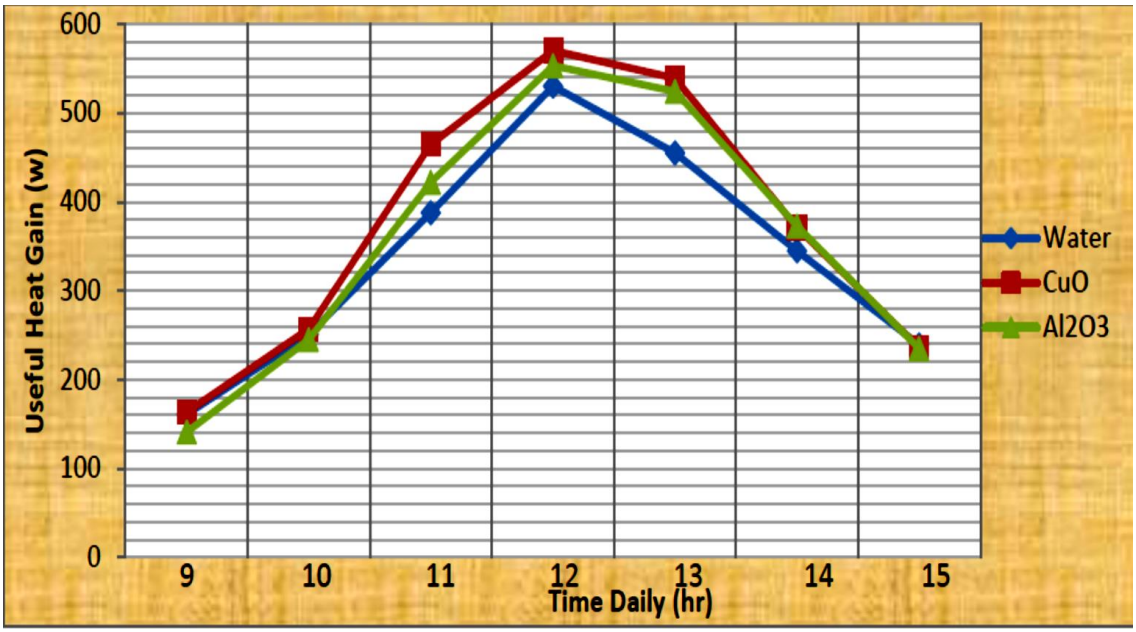

Fig.2.7. Useful Heat Gain with Various Time [46].

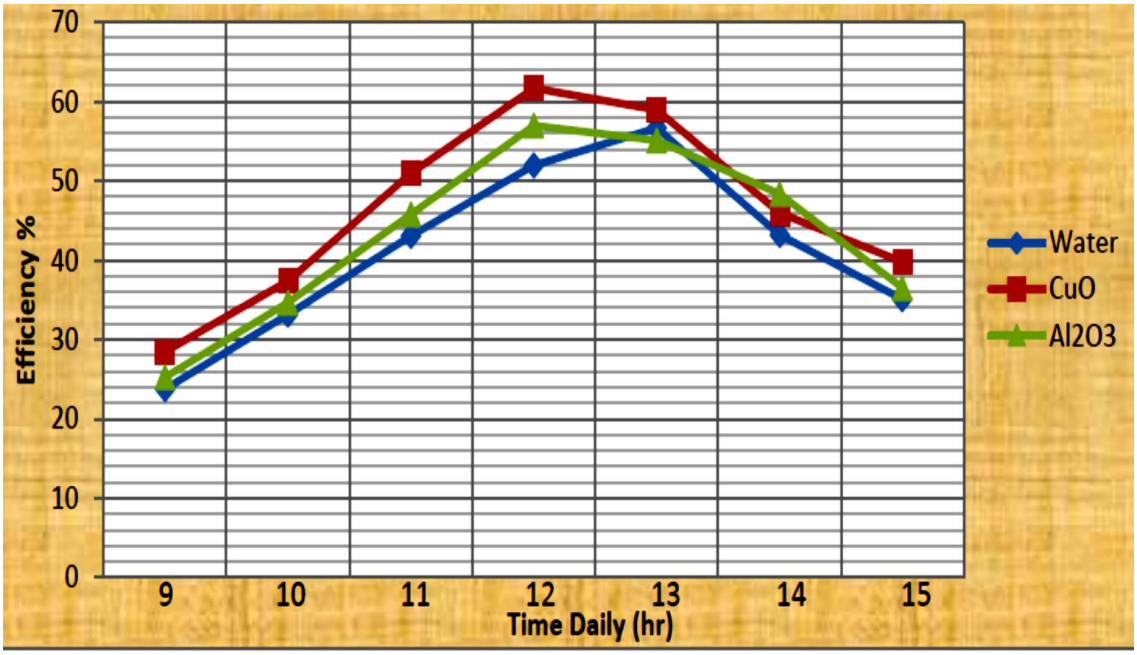

Fig.2.8. Thermal Efficiency with Various Time [46].

M. Malekan et al. 2019 [47] investigated the thermal performance of parabolic trough collector experimentally by using different working fluid, namely Fe_3O_4 and CuO / Therminol66 nanofluids. Improving the performance of a PTC can enhance a PTC power plant's efficiency and electricity generation, which has been identitied as one of the most signitication issues facing researchers in this discipline. In this research article the thermal performance behavior was evaluated with using nanofluid as heat transfer medium under external magnetic field with different volumetric fraction of nanfluid (Fe_3O_4/Therminol66 and CuO/ Therminol66) to enhance the working fluid characteristics. The final results showed an increase in the heat convection coefficient, and the maximum efficiency was obtained for using Fe_3O_4/ Therminol66 as heat transfer fluid.

R. Malviya et al. 2020 [48] estimated the thermal performance of parabolic trough collector experimentally using different working fluids as heat transfer medium. They examined three types of working fluid (water, TherminolVP-1, air). The final results indicated that the maximum collector efficient achieved using water as heat transfer fluid, give its high heat transfer coefficient. On the other hand, air had high pressure drop as shown in Figures 2.9, 2.10 below:

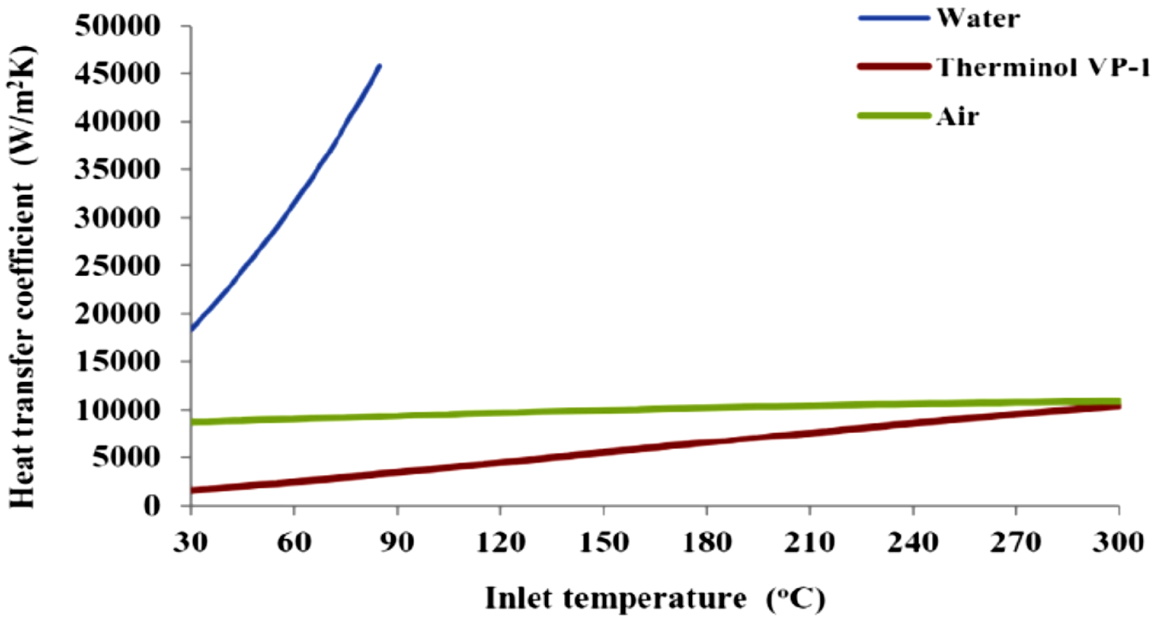

Fig.2.9. Heat Transfer Coefficient with Different Inlet Temperatures [48].

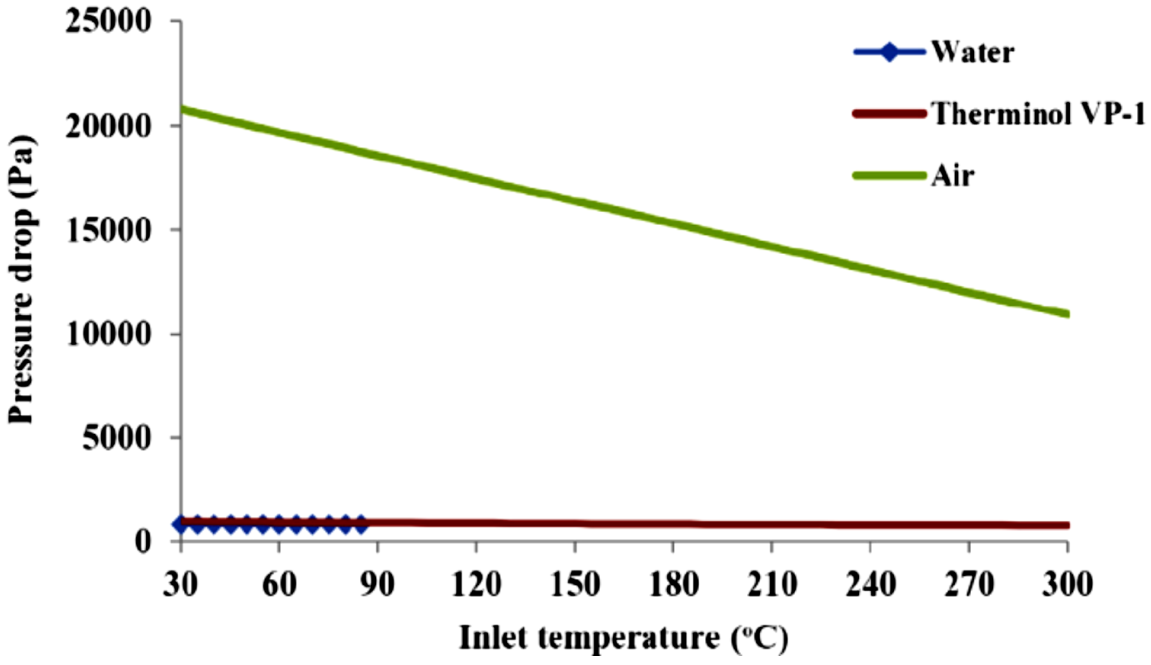

Fig.2.10. Pressure Drop with Different Inlet Temperatures [48].

2.3. Numerical Studies of Thermal Performance of Parabolic Trough Collectors (PTC) by Using Different Working Fluids

Many studies have been presented to numerically improve the thermal performance of the parabolic trough collector by using various working fluids such as pressurized water, thermal oil, molten salts, pressurized gases, air, nitrogen, carbon dioxide, helium, nitrate salts, and nano fluids, with each type of working fluid being used in specific conditions and temperature ranges [49]. The numerical literature studies that investigate the thermal performance of parabolic trough collectors with various working fluids will be reviewed in this paragraph.

N. Boerema et al. 2012 [50] use various working conditions, numerically investigated the thermal performance of parabolic trough collector behavior. They used molten salt and liquid sodium as heat transfer fluids in PTC. Molten salt has a high melting point (415–513 K) and an operation temperature range above 873 K. Liquid sodium high melting point (377.7 K) and high boiling point (1146 K) allow for a significantly wider temperature range of operation. Hitec (a ternary molten salt composed of 53% KNO_3 + 40% $NaNO_2$ + 7% $NaNO_3$) and liquid sodium (Na) were compared. When compared to Hitec, liquid sodium has a higher heat transfer coefficient (greater than Hitec), a lower heat capacity (30-50%), and a wider operating temperature range. The findings show efficient collectors when using liquid sodium.

M. Biencinto et al. 2014 [51] the thermal performance of a parabolic trough collector using different working fluids, including a comparison step with pressurized nitrogen and synthetic oil as heat transfer fluids in PTC. Synthetic oil has challenges when used as heat transfer due to its flammability, toxicity to the environment, and a temperature limit of roughly 400 degrees Celsius. The model of PTC has been designed and developed by the TRNSYS simulation software. The final results show that when nitrogen and synthetic oil are pressurized equally, PTC has the same net efficiency.

O. Behar et al. 2015 [52] analysis thermal performance of PTC numerical by using Sytherm 800 as working fluid , the model developed and design by Engineering Equation Solver (EES), the result of numerical study validation with results of experimental study, Sandia LS-2 test data were used to create and validate the suggested model. According to the final results, the model developed in this study forecasts thermal efficiency more correctly than EES, with an average uncertainty of 0.64 % to 1.11 % for ESS,

E. Papanicolaou et al. 2016 [53] investigated thermal performance of parabolic trough collect numerically with using nanofluid as working fluid, thermal oil Syltherm800 / Al_2O_3 utilization as heat transfer fluid, numerical results validated with experimental finding of SEGS LS-2 module PTC. Using nanofluid (Al_2O_3) with base fluid enhancement the thermal properties of the base fluid , the results of validation showed that maximum relative error of output temperature and thermal efficiency are 0.3% and 7.3% respectively. The final results of numerical simulation found the thermal efficient of parabolic trough collector increase by 10 % with using concentrating 4% of nanofluid.

E. Bellos et al. 2016 [54] estimated thermal performance behavior of parabolic trough collector numerically by using numerical model developed under Engineering Equation Solver (EES) software with utilization gases as heat transfer fluids, the comparison thermal performance of PTC including six gases (air, nitrogen, carbon dioxide, helium, neon and argon) are examined as heat transfer fluid. When using helium, the exergetic efficiency is 0.4338, but when using carbon dioxide, it is 0.431. Air and nitrogen with 0.4174 and 0.4167 respectively, while neon and argon come with 0.4047 and 0.3857, respectively. The final results showed that helium is the greatest working fluid for input temperatures up to 700K, while carbon dioxide is the best choice for temperatures greater than that. Helium operating at 640 K inlet temperature and 0.035kg/s mass flow rate achieves the worldwide maximum exergetic efficiency. Furthermore, the optimal mass flow rate for each investigated working fluid is dependent on the operating temperature level as shown in Figures 2.11, 2.12, and 2.13 below :

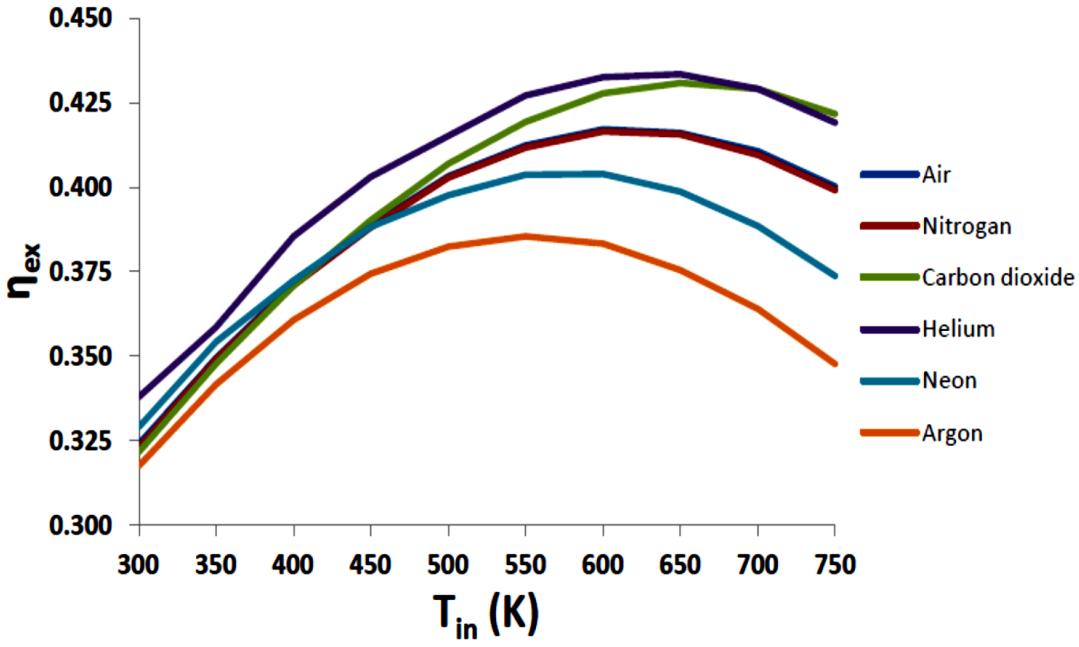

Fig. 2.11. Exergy Efficiency with Different Input Temperatures [54].

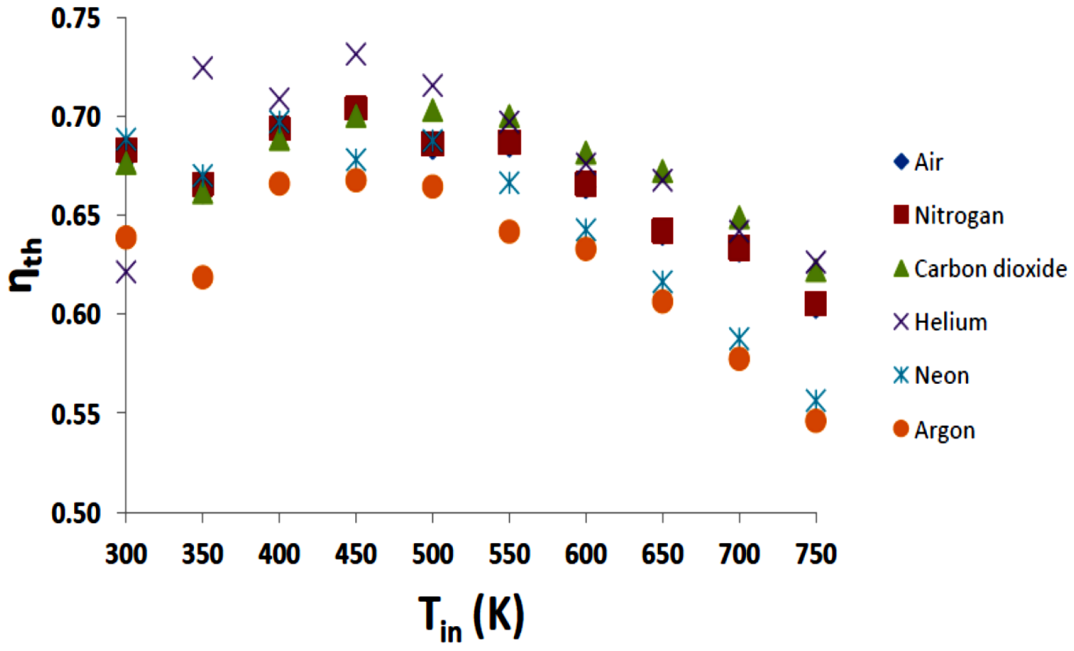

Fig.2.12. Thermal Efficiency with Different Input Temperature [54].

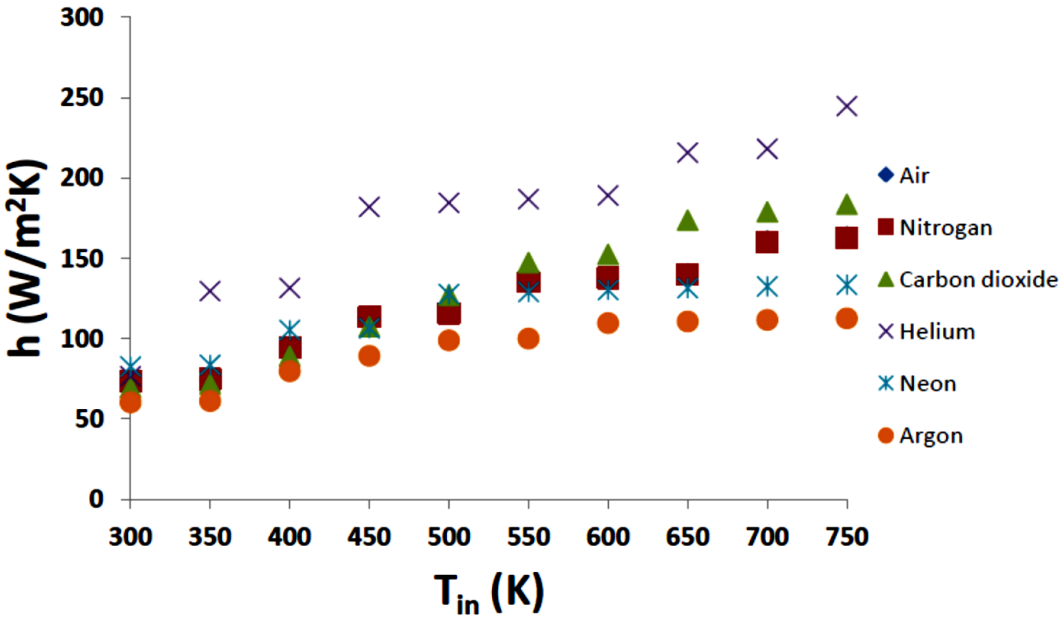

Fig.2.13. Heat Transfer Coefficient with Different Input Temperatures [54].

S. E. Ghasemi et al. 2016 [22] investigated the effective nanofluid on the thermal performance behavior of parabolic trough collector numerically with utilization water / Al_2O_3 and water /CuO nanofluid. Computational Fluid Dynamics (CFD) trade code for finding fluid dynamics and heat transfer coefficients using the finite volume method. The analysis is based on a turbulent k-ε-RNG model for different heat flow conditions. Volume fraction (φ) of nanofluid versus thermal and the hydrodynamic performance of the parabolic trough is discussed. the result shows compared with pure water, nanofluids improved the heat transfer performance of parabolic trough collectors. The final results show that increasing the volume fraction of nanoparticles increases the average Nusselt number and coefficient of friction for both nanofluids. In addition, Al_2O_3 and CuO nanoparticles were added (φ=3%), Water improved heat transfer by 28% and 35%, respectively.

C. Tzivanidis et al. 2016 [55] estimated thermal performance of parabolic trough collector numerically, The model was designed in the commercial software Solid works and simulated in its flow simulation studio. The estimating comparison between water and TherminolVP-1 as working fluid in PTC, the final results found water give high thermal performance of PTC than TherminolVP-1 as shown in Figure 2.14, and 2.15 below :

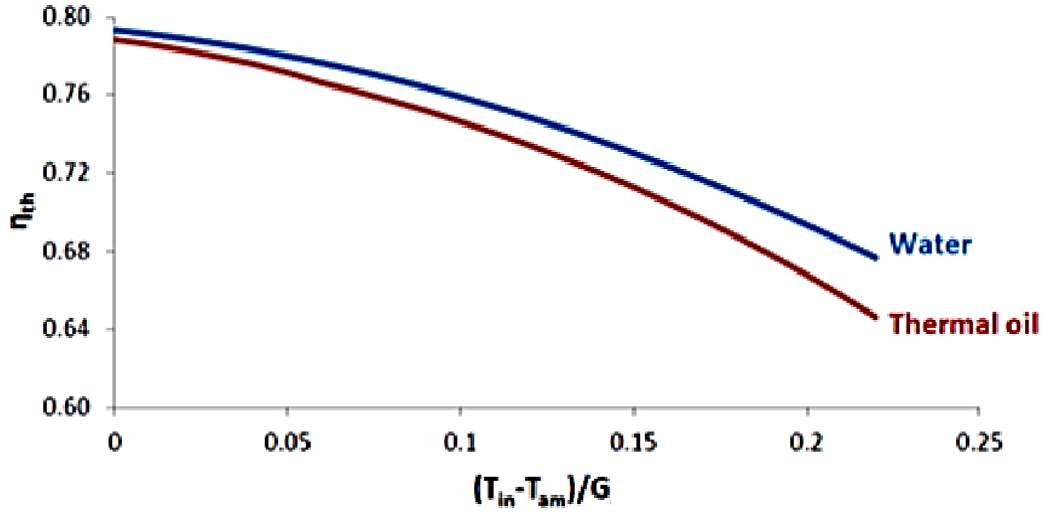

Fig. 2.14. Thermal Efficiency with Different Operation Conditions[55].

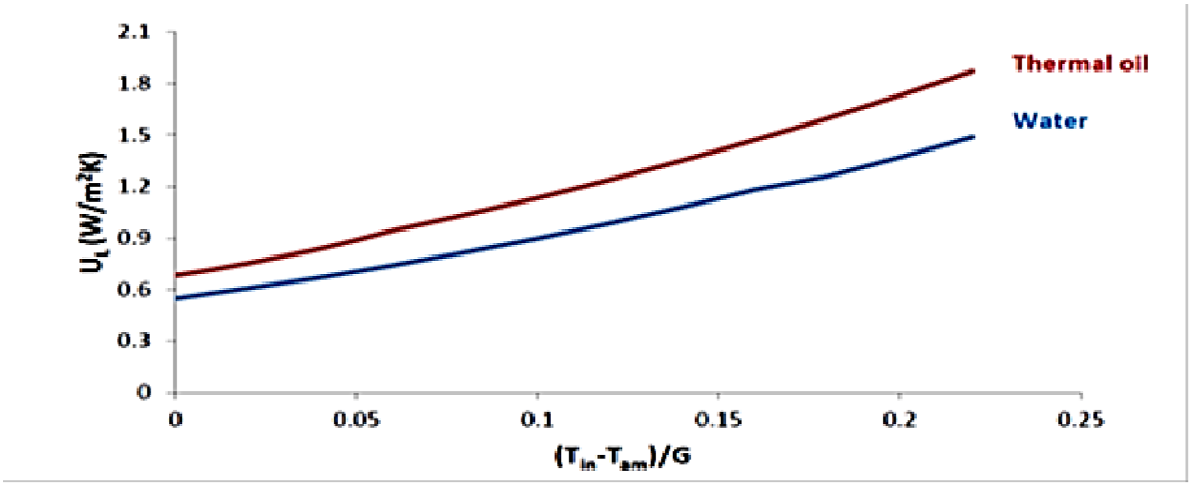

Fig. 2.15. Heat Losses with Different Operation Conditions [55].

Y. Qiu et al. 2017 [56] investigated the thermal behavior of parabolic trough collector numerically with using supercritical CO_2 (s-CO_2) as working fluid, the final results found that the thermal efficiency of PTC increase with decrease the input temperature and increase the inlet velocity of working fluid.

E. Bellos et al. 2017 [57] evaluated exergetic analysis of PTC numerically with using thermal oil (TherminolVP-1), and air as working fluid, the model of PTC LS-2 developed by EES (Engineering Equation Solver), according to the final data with an input temperature of 500 K and a flow rate of 10,000 l/min, the worldwide maximum exergetic efficiency for operation with air is 25.62 %, while for TherminolVP1 it is 31.67 % for 500 K and 100 l/min, at last found Thermal oil give high thermal performance of PTC than air as heat transfer fluid.

K. A. Antonopoulos et al. 2017 [58] analysis thermal performance of parabolic trough collector numerically with using different heat transfer fluid, numerical model of PTC (Euro trough ET-150) is design and develop by Engineering Equation Solver (EES), the numerical simulation comparison between different working fluids (pressurized water, TherminolVP-1, nitrate molten salt, sodium liquid, air, carbon dioxide and helium), with operation input temperature range (300-1300 K). The final results show that liquid sodium has the highest worldwide exergetic efficiency 47.48 % at 800 K inlet temperature, whereas helium, carbon dioxide, and air have maximum exergetic performance of 42.21 %, 42.06 %, and 40.12 %, respectively. Furthermore, at temperatures up to 550 K, pressurized water is the optimum working medium, whereas for temperatures beyond 1100 K, carbon dioxide and helium are the only options, as shown in Figure 2.14 below :

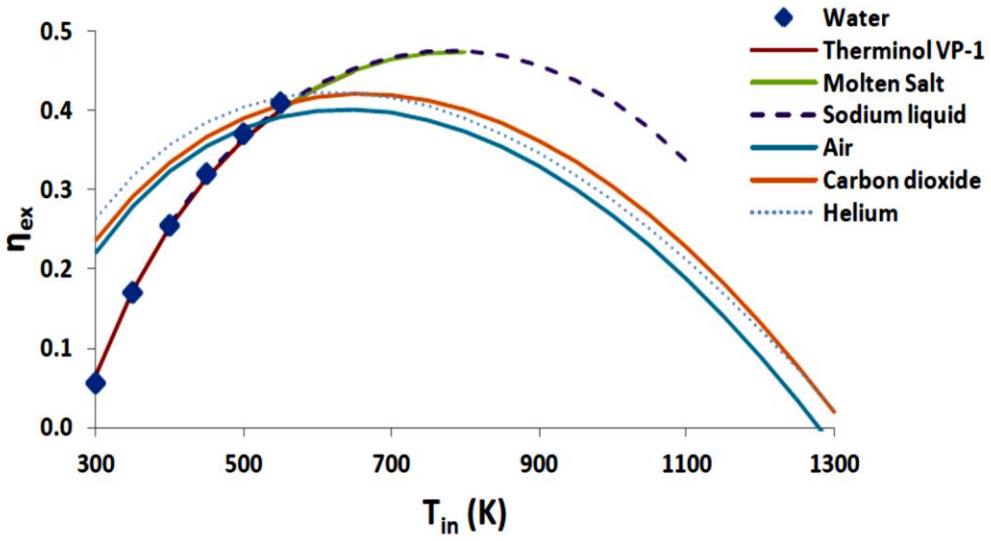

Fig. 2.16. Exergy Efficiency with Different Input Temperatures [58].

C. Tzivanidis et al. 2017 [59] examined the thermal behavior and performance of a parabolic trough collector numerically with the utilization of nanofluid as a heat transfer fluid, they used two types of nanoparticles, Al_2O_3 and CuO, with thermal oil (Syltherm800). EES (Engineering Equator Solver) is used to build a complete thermal model, which is then validated using experimental evidence from the literature. In the first part of the analysis, the Eurotrough ET-150 module was tested at different inlet temperatures (289–598 K) for three working fluids (Syltherm800, Syltherm800/CuO, and Syltherm800/Al_2O_3). The final results prove that both nanofluids are more efficient than Syltherm 800. The best option appears to be Syltherm 800/CuO. The employed of nanofluids has been shown to improve heat transmission by around 50%, with the increase being greater at higher temperatures. When the concentration ratio is optimized and the flow rate is relatively low, CuO can enhance thermal efficiency up to 1.26 % and Al_2O_3 can increase thermal

efficiency up to 1.13 %. At last, Syltherm800/CuO is the best choice as a working fluid, as shown in figures 2.15, 2.16, 2.17, and 2.18 below:

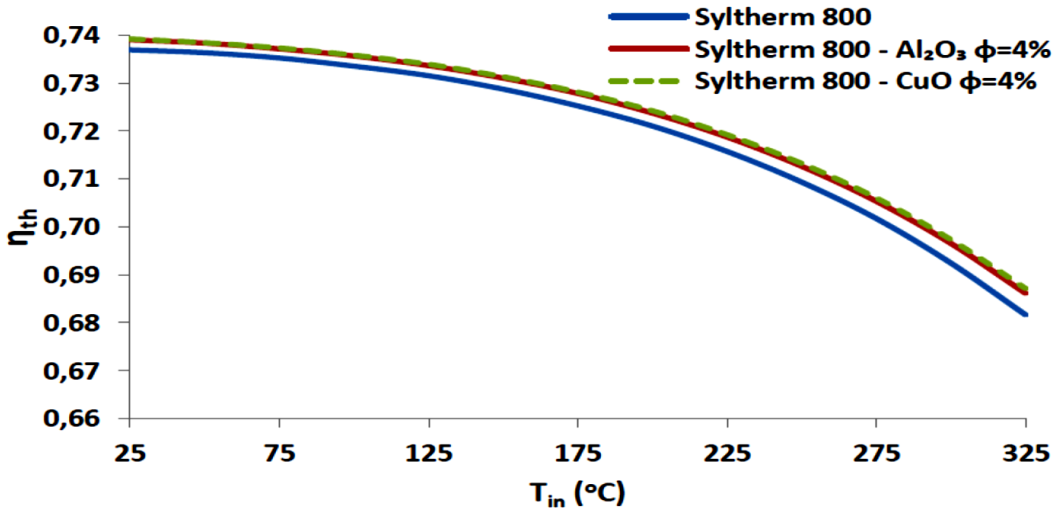

Fig.2.17. Thermal Efficiency with Different Input Temperatures [59].

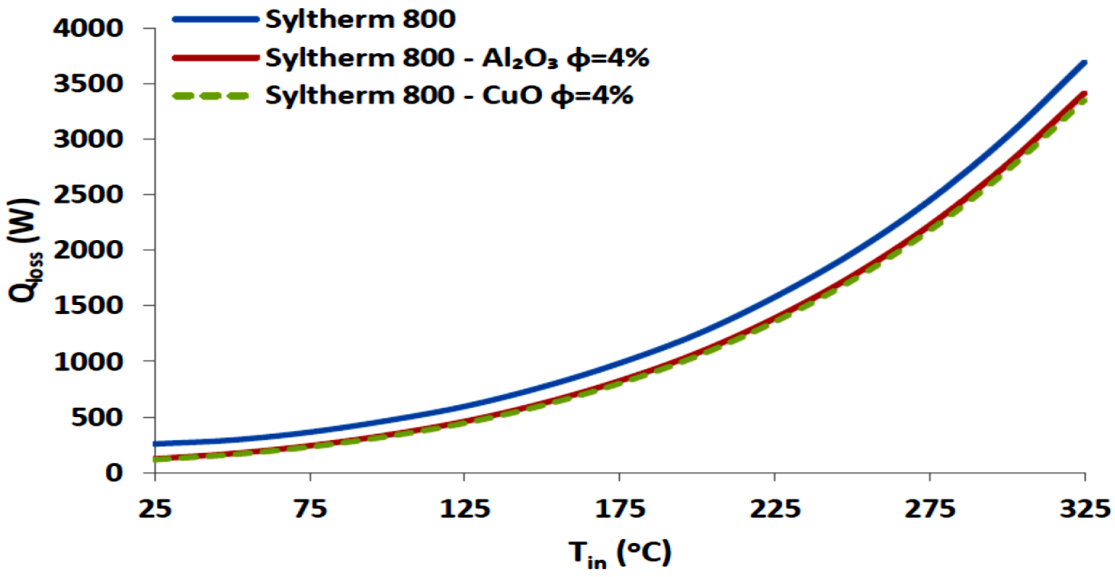

Fig.2.18. Heat Losses with Different Input Temperatures [59].

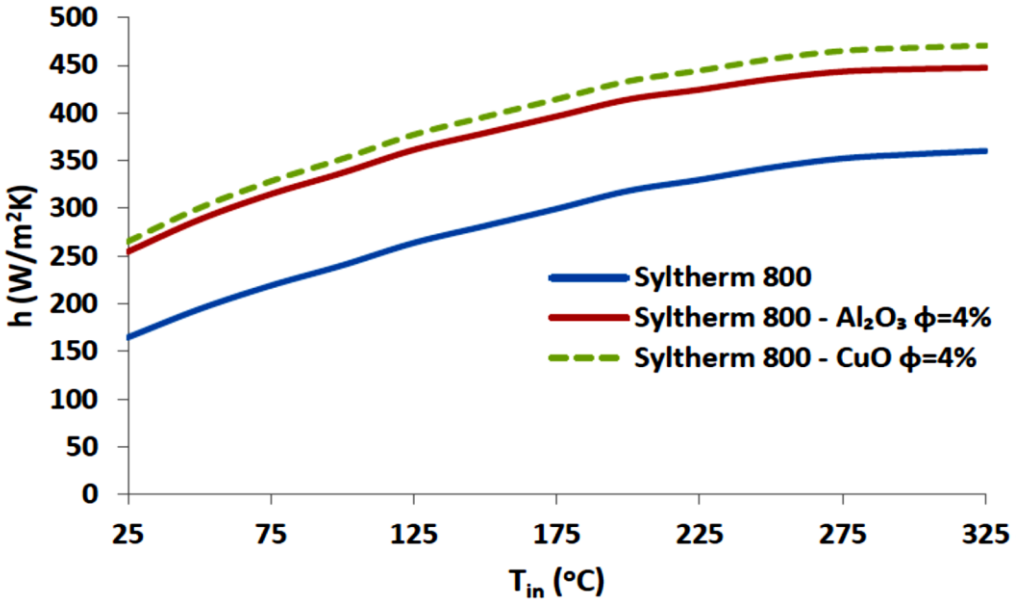

Fig.2.19. Heat Convection Coefficient with Different Input Temperatures [59].

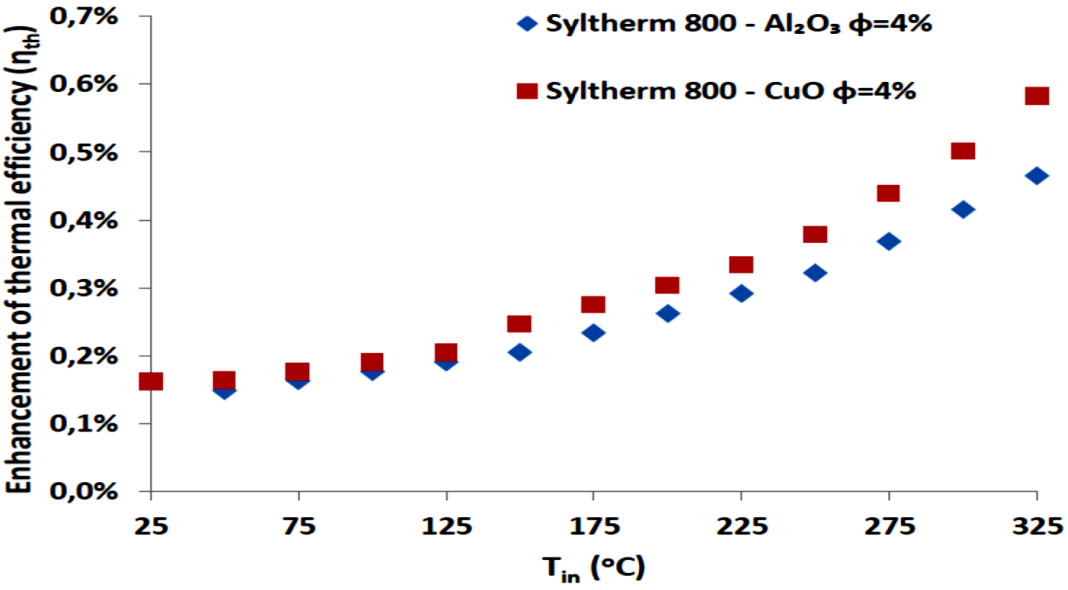

Fig.2.20. Enhancement of Thermal Efficiency with Different Input Temperatures[59].

I. Daniil et al. 2017 [60] investigated thermal performance of PTC numerically with using gases (air, helium, carbon dioxide) as working fluid, the final results show that helium has high thermal exergy at operation temperature range up to 563 K , while carbon dioxide is best chose at high temperature operation ranges.

P. D. Tagle-Salazar et al. 2018 [61] investigated the thermal performance of a parabolic trough collector numerically with nanofluid as a heat transfer fluid; the simulation model was designed and developed by EES (Engineering Equation Solver), numerical results show the best agreement with the experimental results; the nanofluid utilization is alumina, and the base fluid is water. The final results show that combining nanoporous (Al_2O_3) with water improves PTC thermal performance over using water as a heat transfer fluid.

E. Bellos et al. 2018 [62] Using mono- and hybrid-nanofluids, the thermal performance of a parabolic trough collector was numerically evaluated. The LS-2 PTC module is being investigated for use with Syltherm800 as a base fluid, the mononanofluids studied are 3% Al_2O_3 / Syltherm800, 3% TiO_2 in Syltherm 800, and hybrid nanofluids 1.5 percent and Al_2O_3, 1.5 percent TiO_2 / Syltherm800, respectively. The final results found that the thermal efficiency improvement for hybrid nanofluids is up to 1.8 %, whereas as for nanofluids is up to 0.7 %. The greater Nusselt number enhancement for the hybrid nanofluid situation, which is around 2.2 higher than the equivalent for operation with pure thermal oil, accounts for the

increased thermal efficiency as shown in Figures 2.19,2.20, and 2.21 below.

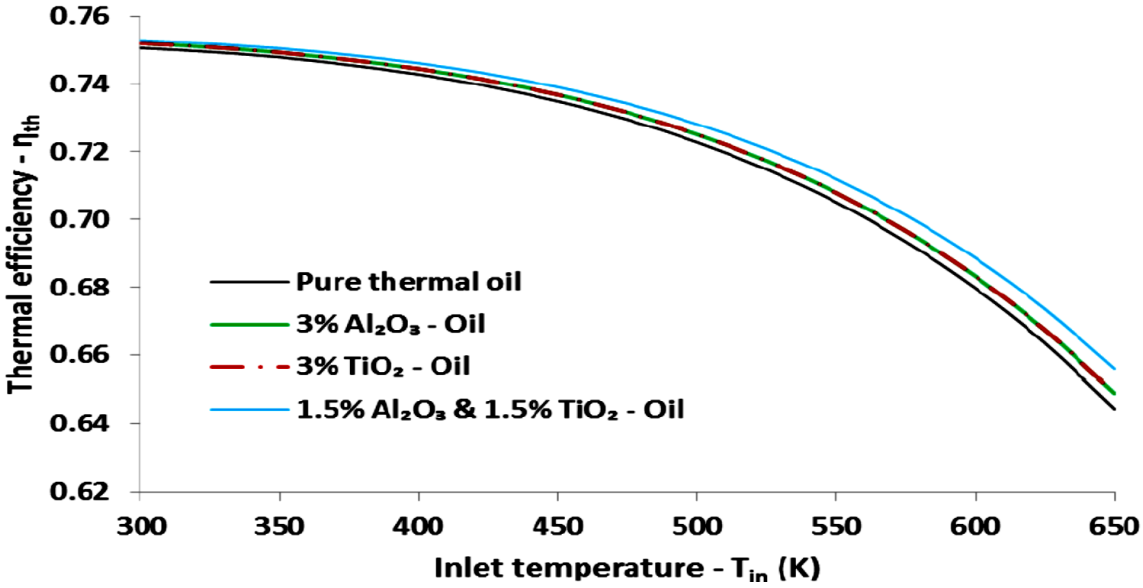

Fig.2.21. Thermal Efficiency with Different Inlet Temperatures [62].

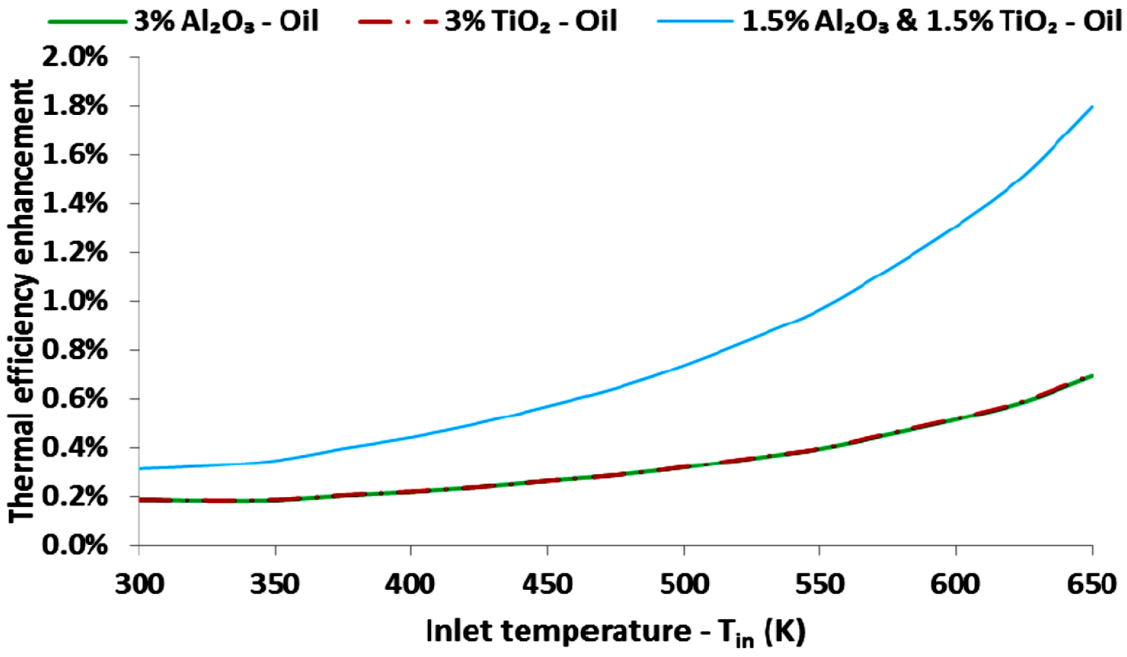

Fig.2.22. Thermal Efficiency Enhancement with Different Inlet Temperatures [62].

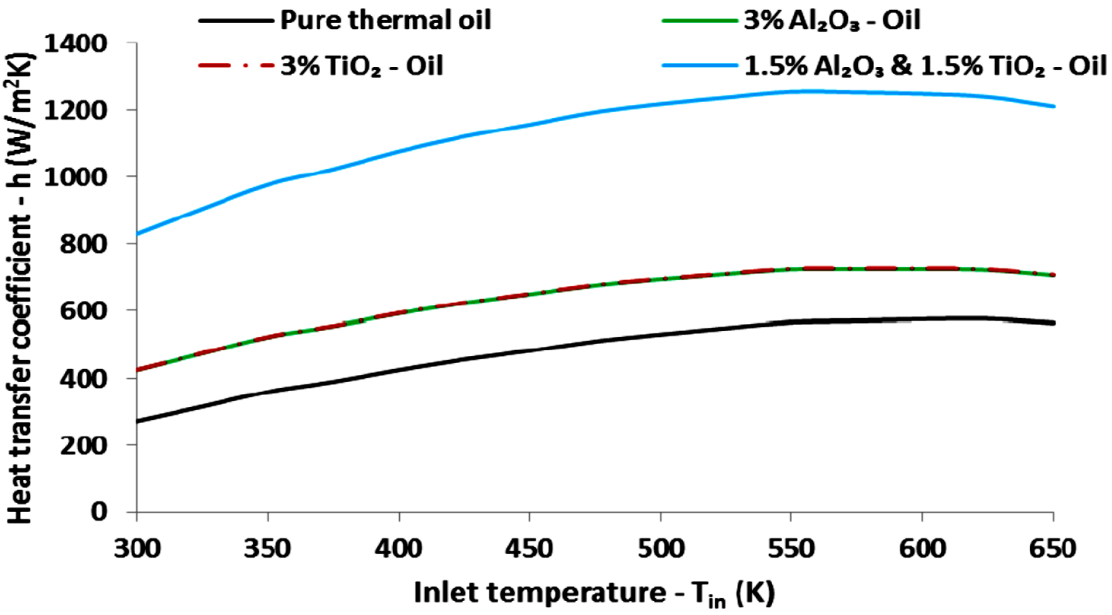

Fig.2.23. Heat Transfer Coefficient with Different Inlet Temperatures [62].

B. LAMRANI et al. 2018 [63] investigated thermal performance of parabolic trough collector numerically under transient climate condition with using two types of working fluid are water and oil thermal (Syltherm800) as working fluid, the final results show that thermal oil (Syltherm800) give maximum output temperature than water.

A. A. Hachicha et al. 2018 [64] conducted analysis an on the thermal performance of PTC. They used Engineering Equation Solver (EES) to analyze and simulate the LS-2 parabolic trough collector with using six different working fluids : pressurized water, supercritical CO_2, TherminolVP-1, and the addition of CuO, Fe_3O_4, and Al_2O_3 nanoparticles to TherminolVP-1. The Al_2O_3/TherminolVP-1 based nanofluid improved thermal efficiency the most, by 0.22 %, compared to 0.18 % and 0.15 % for CuO/TherminolVP-1 and Fe_3O_4/ TherminolVP-1 respectively, while pressurized water proved to be the

ideal working fluid at lower temperatures, its high-pressure needs have imposed a technical restraint on its use due to the receiver tube's material limitations.

D. Korres et al. 2019 [65] estimated the thermal performance of parabolic trough collector numerically with thermal oil (Syltherm800) and nanofluid CuO/Syltherm800 in 5% volumetric nanoparticle concentration ,with different operation temperature range (298K to 573K), using a created computational fluid dynamics model, the study is carried out in SolidWorks flow simulation studio under laminar flow. Thermal efficiency is determined to have a mean value of 1.24 % and a maximum value of 2.76 % at input temperatures of 573 K. Furthermore, the mean and maximum heat transfer coefficient improvements were determined to be 16.16% and 17.41%, respectively, with a 16.09% growth in pumping work. With the usage of nanofluid, exergy efficiency may be increased by up to 2.60 %, while total efficiency can be increased by up to 2.76 %, as shown in Figures 2.22, 2.23, and 2.24 below :

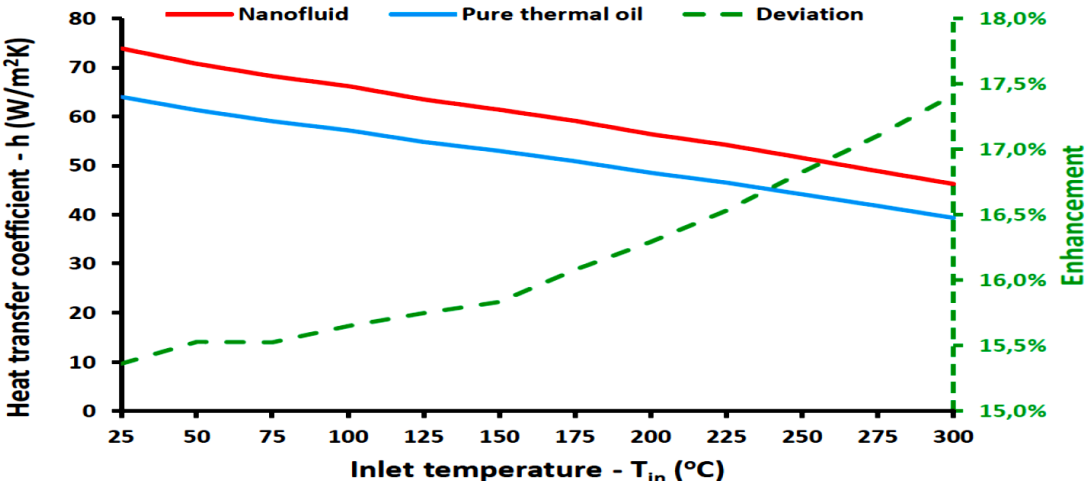

Fig.2.24. Heat Transfer Coefficient with Different Inlet Temperatures [65].

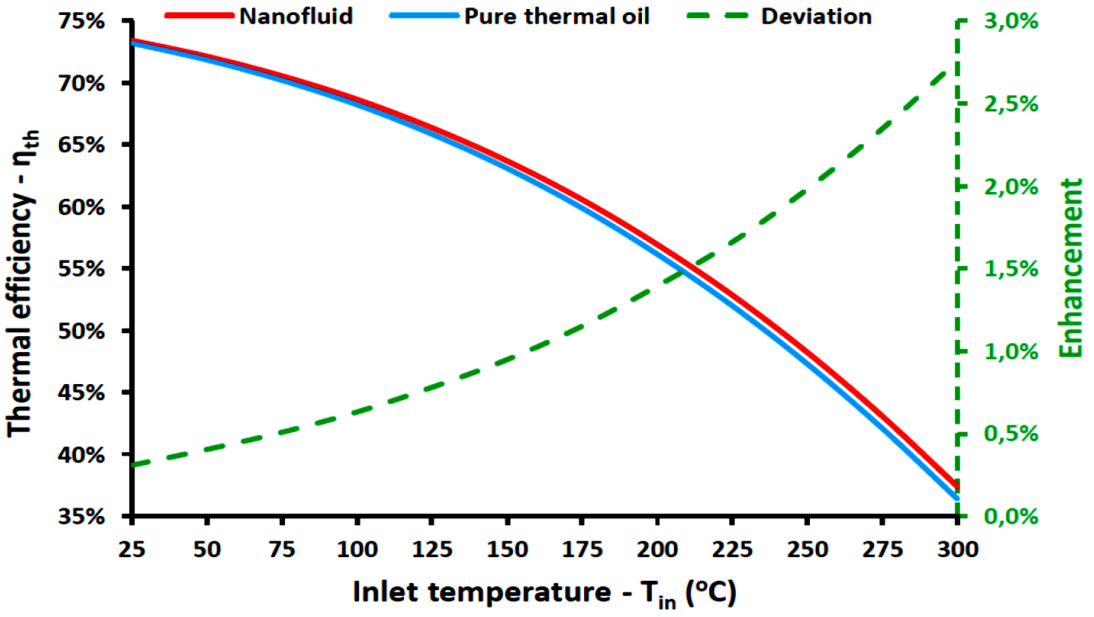

Fig.2.25. Thermal Efficiency with Different Inlet Temperatures [65].

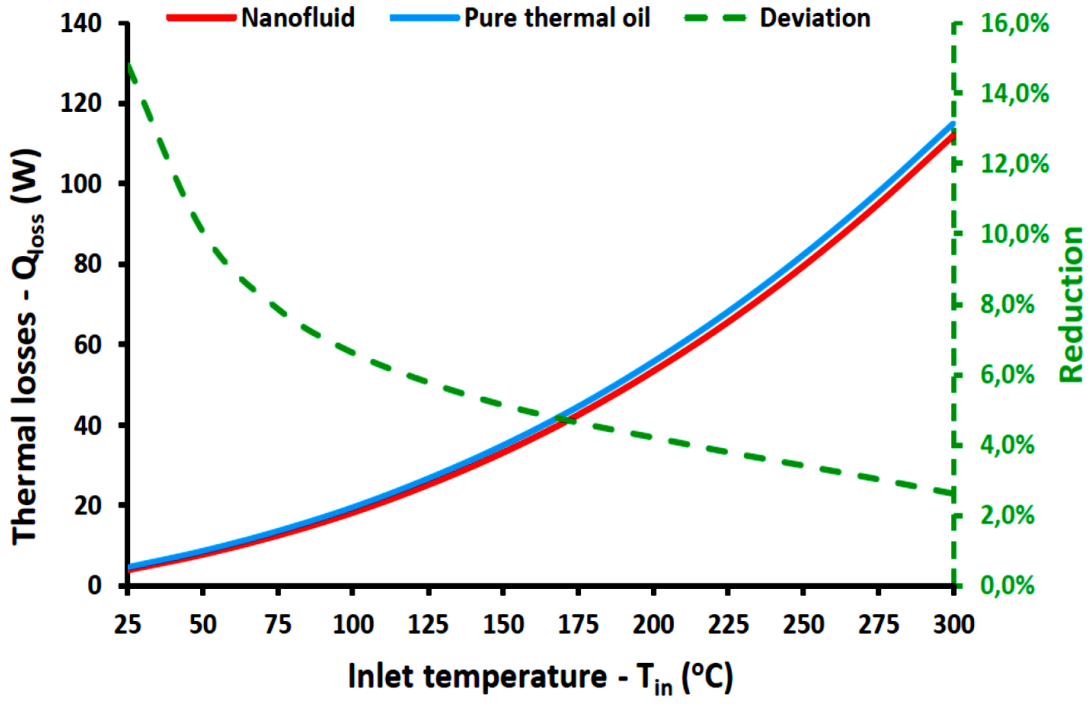

Fig.2.26. Thermal Losses with Different Inlet Temperatures [65].

C. Tzivanidis et al. 2018 [66] investigated the thermal performance of parabolic trough collector numerically with high temperature operation range up to 800 K, using thermal oil (Syltherm800) as heat transfer fluid, numerical model design and developed Engineering Equation Solver (EES) software, numerical model of PTC construction and simulation under energy balance concept. Numerical model results with experimental literature results, The influence of input fluid temperature, flow rate, ambient temperature, sun beam irradiation, and the heat transfer coefficient between cover and ambient are explored factors for model accuracy testing. The final results show that numerical model give high thermal efficiency accuracy with deviation 0.2%.

D. Kavaz et al. 2018 [67] estimated thermal behavior of PTC experimentally and numerical, numerical model developed by using Engineering Equation Solver (EES) software and validated with experimental results of the Sandia National Laboratory (SNL), AZTRAK platform LS-2 test , with utilization pressurized water, nanoparticles synthesized from green bio-matter(Olive leaf extract OLE) and agricultural waste (barley husk BH), When compared to ordinary nanoparticles, the synthesized nanoparticles proved to be effective corrosion inhibitors, non-toxic, and inexpensive to create. A green-synthesized nanofluids: water/BH-SiO_2 and water/OLE-TiO_2. The usage of water/BH-SiO_2 nanofluids resulted in a 0.073% mean increase in thermal efficiency, whereas water/OLE-TiO_2 nanofluids results in a 0.077% mean increase. The heat transfer performance of the nanofluids exhibits a 128% and 138% increase in heat transfer coefficient for water/OLE-TiO_2 and water/BH-SiO_2 nanofluids, respectively. At a 3% volumetric fraction of nanoparticles, the

mean variance in pressure losses between the nanofluids and the base fluid was likewise less than 14.85%.

J. Liu et al. 2019 [68] determined thermal performance of parabolic trough collector using different working fluid numerically, present study comparing between three types of working fluid (liquid sodium, Hitec, and solar salt), with operation temperature range (550 to 800 K). Solar salt is (60% $NaNO_3$ and 40% KNO_3), and Hitec is (53% KNO_3 + 40% $NaNO_2$ + 7% $NaNO_3$), the final results found liquid sodium given heat transfer coefficient 2.5 to 5 times than Hitec, and solar salt. At last liquid sodium more efficient than solar salt, and Hitec as shown in figures 2.24, and 2.25 below :

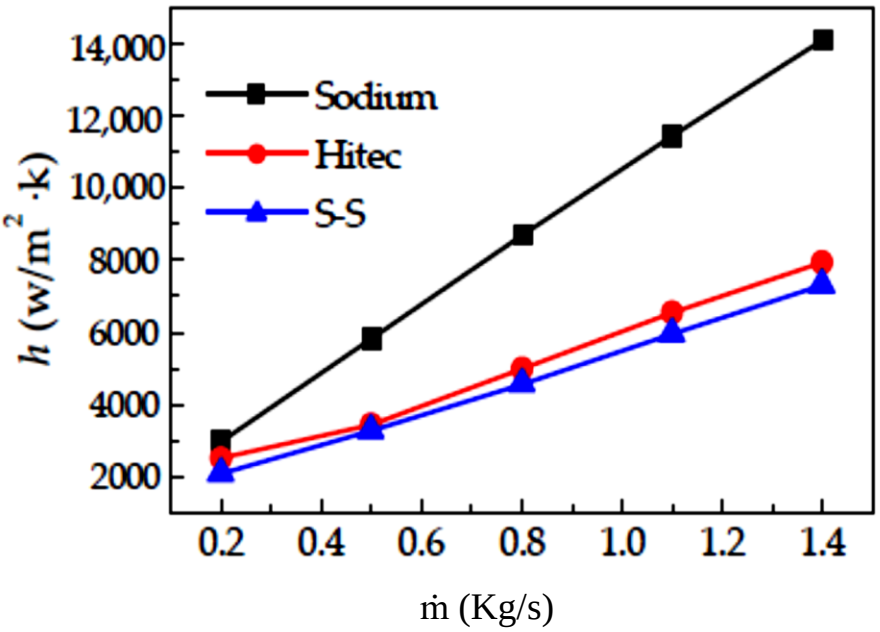

Fig.2.27. Heat Transfer Coefficient with Different Mass Flow rate[68].

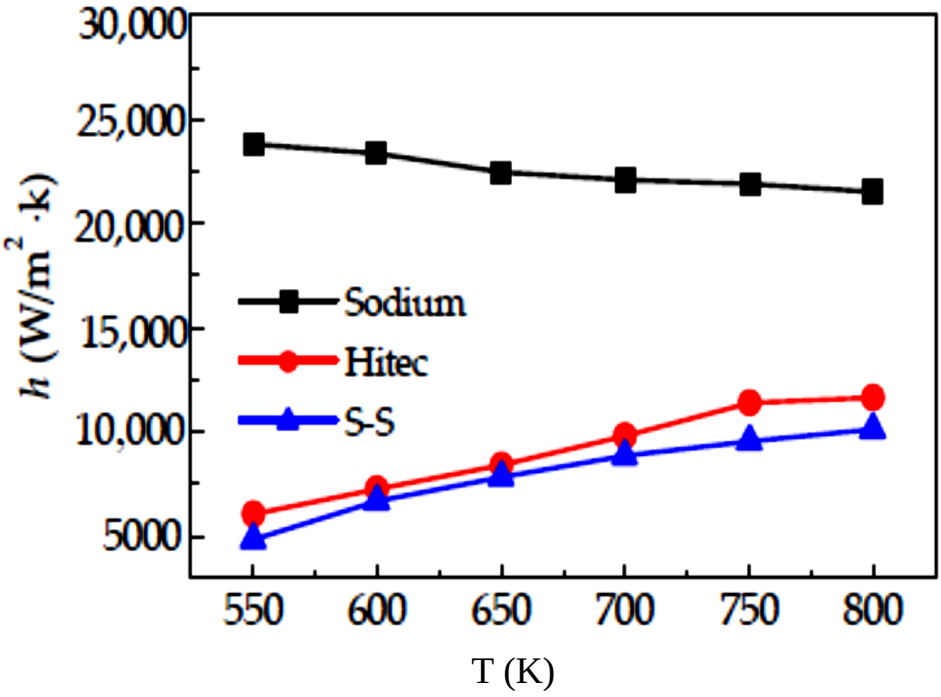

Fig.2.28. Heat Transfer Coefficient with Different Operation Temperature Range[68].

A. Ahmadi et al. 2019 [69] estimated the effect different of working fluids on the thermal behavior of parabolic trough collector by using numerical simulation by MATLAB simulation program to investigation energy and exergy efficiency of PTC with utilization two types of base fluid (water, and thermal oil TherminolVP-1) and nanopartical of (CuO, and Al_2O_3) with different volumetric concentrating (1%, 3%, and 5%). The numerical model is validation with experimental results and found best agreement between them. For low enthalpy, water as a basefluid exceeds oil, nanoparticles do not have a significant impact on system performance in generally. Adding nanoparticles improves energy efficiency while lowering exergy efficiency (very little change), when using oil as a basefluid, adding nanoparticles outperforms using

water. CuO has a greater impact on system energy and efficiency than Al_2O_3 as a nanoparticle. CuO is more dense and has a greater thermal conductivity than other materials. The final results show that water as a basefluid has better energy and exergy efficiency than oil, according to numerical calculations. PTC using water as a basefluid has greater annual average energy and exergy efficiencies (10.81 % and 9.44 %) than PTC using oil as a basefluid (10.64 % and 9.07 %).

K. A. Ahmed et al. 2020 [70] investigated the thermal performance of parabolic trough collector with using different working fluid numerically, present study determined influence of gases (air, helium, and carbon dioxide) as working fluid on thermal behavior of parabolic trough collector, For the design and simulation of the SPTC(Solar Parabolic Trough Collector), ANSYS FLUENT 15 computer programs were employed. The study of effect of varies heat transfer fluid on the thermal performance of PTC was with different input temperature, and different mass flow rate of working fluids. the final results show that helium has maximum collector efficient when compare with air, and carbon dioxide.

I. H. Yılmaz et al. 2020 [71] estimated the influence of using various working fluid on thermal performance of parabolic trough collector numerically with using ten types of working fluids, They are liquid metals : liquid sodium, Lead-Bismuth Eutectic (LBE), molten salts (solar salt, Hitec, Hitec XL), a ternary salt mixture (18 % $LiNO_3$ + 52% $NaNO_3$ + 30% KNO_3), a quaternary salt mixture (9%$NaNO_3$+ 54% KNO_3 + 18% $LiNO_3$+ 18% $Ca(NO_3)_2$), a new salt mixture(7.5% NaCl + 23.9% KCl+ 68.6% $ZnCl_2$), and

Thermal oils (Therminol VP-1 and Dowtherm A). the final results show that liquid sodium give high thermal efficiency, high heat transfer coefficient, LBE is second types efficient working fluid, as shown in Figures 2.26, and 2.27 below :

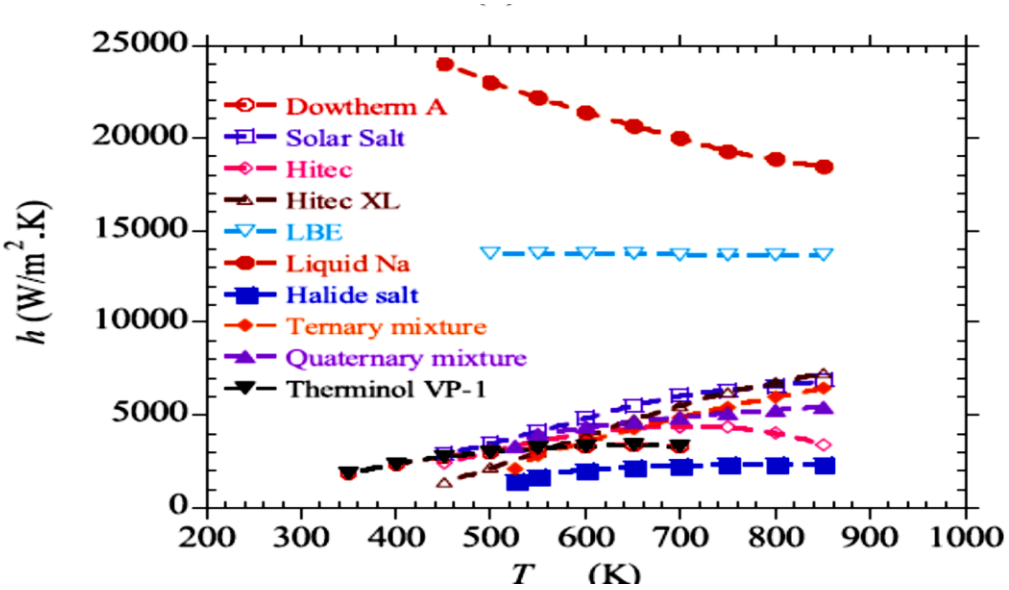

Fig.2.29. Heat Transfer Coefficient with Different Inlet Temperatures [71].

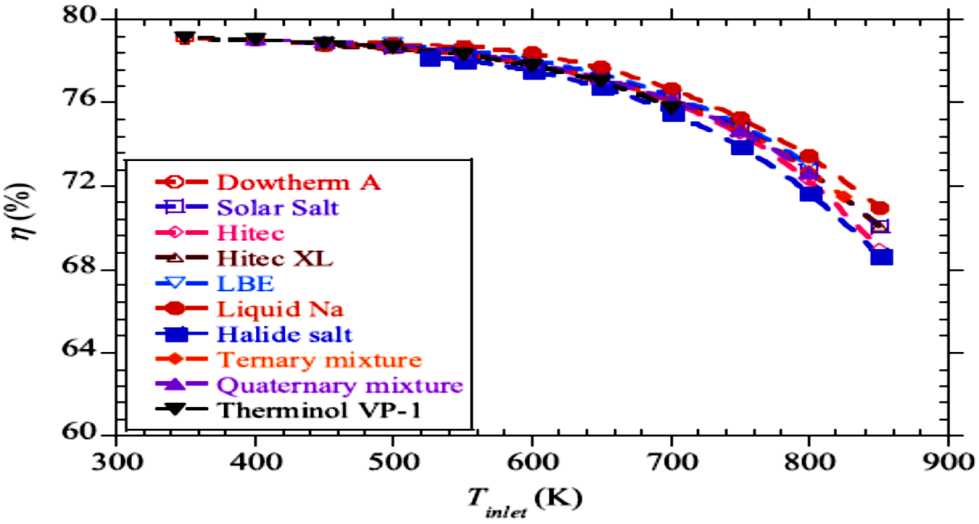

Fig.2.30. Thermal Efficiency with Different Inlet Temperatures [71].

N. Abed et al. 2020 [72] estimated thermal and hydraulic performance of parabolic trough collector numerically by using open-source CFD software Open Field Operation and Manipulation (OpenFOAM), with three types of working fluid (water, TherminolVP-1, and molten salt), with verity input temperature range (320 - 500 K). The final results show that at high range of Reynolds (Re) number, TherminolVP-1 outperformed water, with greater Nusselt number values, lower thermal stresses, and higher thermal efficiency. The optimum choice for high working temperatures (up to 873 K) is molten salt since it does not show any substantial drop in overall thermal efficiency at high temperatures, resulting in higher performance.

Y. M. Abdullatif et al. 2021[73] investigated thermal performance of parabolic trough collector numerically, the numerical simulation modeled depending on engineering equation solver (EES) software and validated with literature results of LS-2 parabolic trough collector. Performance comparison between different working fluid, gases (air, helium, and carbon dioxide) liquid (pressurized water, TherminolVP-1, and Syltherm800), and nanofluid (Cu/ pressurized water, Cu/ TherminolVP-1, and Cu/ Syltherm800). The final results show that Cu/Syltherm 800 nanofluid exhibited the highest thermal efficiency gain of 0.141%, followed by Cu/water and Cu/Therminol VP1 with 0.037% and 0.088 %, respectively. The gases had pressure drop more than liquids, Pressurized water had the best energy efficiency values in the temperature range of (300 - 400 K), whereas liquid sodium had the highest energy efficiency values in the temperature range of (400 - 1100 K). Helium has the maximum energy efficiency at temperatures over 1100 K.

2.4. Summary of Literature Review :

After reviewing the previous studies above about the impact different of working fluid on thermal performance of parabolic trough collector, author name, year of study, types of working fluids, investigation method, and results can be summarize in table 2.1 as shown below. In this thesis, the thermal performance of a PTC was investigated through both experimental an numerical approaches, taking into account a range of factors such as volume and mass flow rates, weather, conditions, direction, reflectivity of the reflector surface, absorption coefficient, and working fluid properties. The novelty of the research lies in using a numerical unsteady-state flow solution to exmine the thermal behavior of a PTC with different working fluids, which is in contrast to the previous studies that mainly utilizaed steady-state flow solutions. By combing experimental and numerical methods, a comprehensive under standing of the impact of different working fluid on the thermal performance of a PTC was provided, which can contribute to the design and optimization of efficient and sustainable solar energy systems.

Table 2.1 : Summarize of literature review about investigation thermal performance of PTC with different working fluids.

Researcher's name	Types of working fluid	Investigation method	Results
T. A. Yassen 2010 [38]	water	Experimentally	The experimental thermal efficiency of the collector was found to be between (7 – 15) % lower than the theoretical one, the final results showed that increase mass flow rate lead to increase thermal efficiency, and When the water mass flow rate exceeds forty kilos per hour, there is no substantial change in efficiency.
M. Ouagued et al. 2013 [39]	Syltherm800, Marlotherm SH, Marlotherm X, Santotherm 59, Santotherm LT, Syltherm XLT, and Therminol D12	Experimentally	the final result found Syltherm 800 given high output thermal performance of parabolic trough collector.
J. Muñoz-Anton et al. 2014 [40]	Syltherm800 carbon dioxide (CO_2)	Experimentally	found thermal oil (Syltherm800) has limitation operation temperature range below (673 K), while carbon dioxide (CO_2) operate great than (1100 K).

Y.T. Wu et al. 2015 [41]	molten salt	Experimentally	found The water-to-salt heat exchanger's overall heat transfer coefficient ranged from 600 to 1200 W/(m^2.K) in the ranges of 10,000 < Re < 21,000 , and 9.5 < Pr < 12.2.
Y.Wang et al. 2016[42]	nanofluid Alumina (Al_2O_3) with synthetic oil	Experimentally	The final result showed that by employing Al_2O_3/synthetic oil nanofluid, temperature gradients and maximum temperature in the absorber are considerably minimized, the parabolic trough collector is efficient with using nanofluid (Al_2O_3) when comparing with thermal performance of parabolic trough collector using synthetic oil.
M. Chafie et al. 2017 [43]	Transcal N oil	Experimentally	Energy efficiency ranged from 19.7% to 52.6 % on a daily basis, While daily exergy efficiency ranged between 8.51 % to 32.34 % .
Singh H et al. 2017 [44]	Ethylene glycol and distilled water based mixture	Experimentally	the total thermal efficiency of PTC while using a ethylene glycol and distilled water at 100 L/h is 6.4 %, which is much higher than the efficiency result at 160 L/h, which is roughly 5.89 %.
M. M. Tafarroj et al. 2018 [45]	(Nanosilica + MWCT) with ethylene glycol(EG)	Experimentally	The final results showed that the Nano fluid that contains 0.6% MWCNT/EG had the greatest outlet temperature of 346.1 K.

S. T. Hamidi et al. 2018 [46]	Water Water/Cuo Water/Al_2O_3	Experimentally + Numerically	The final results obtained Using CuO with distilled water as a working fluid raises the average output temperature by 10.4%, the average usable heat gain by 11%, and the average collector efficiency by 15% , Using Al_2O_3 with distilled water as a working fluid raised average output temperatures by 4%, usable heat gains by 6.5% , and collector efficiencies by 8.2 %.
M. Malekan et al. 2019 [47]	Fe_3O_4 and CuO / Therminol66 nanofluids	Experimentally	The final results found the increase the heat convection coefficient, and the maximum efficiency was obtained for using Fe_3O_4/ Therminol66 as heat transfer fluid.
R. Malviya et al. 2020 [48]	Water, TherminolVP-1, air	Experimentally	final results found the maximum collector efficient when using water as heat transfer fluid, water has high heat transfer coefficient, and air has high pressure drop.
N. Boerema et al. 2012 [50]	molten salt and liquid sodium	Numerically	The comparison between molten salt and liquid sodium (Na) by use steady state solution liquid sodium has high heat transfer coefficient greater than molten salt , less heat capacity (30-50 %) when comparing with molten salt, and liquid sodium show wide operation temperature range. The finding show efficient collector with using liquid sodium.

M. Biencinto et al. 2014 [51]	pressurized nitrogen and synthetic oil	Numerically	The final results show that equal net efficiency of PTC when equal pressurizes nitrogen and synthetic oil by using steady state flow splution method.
O.Behar et al. 2015 [52]	Sytherm800	Numerically	the final results, the model developed in this study forecasts thermal efficiency more correctly than EES, with an average uncertainty of 0.64 % to 1.11 % for ESS by steady state method.
E. Papanicolaou et al. 2016 [53]	thermal oil Syltherm800 / Al_2O_3	Numerically	maximum relative error of output temperature and thermal efficiency are 0.3% and 7.3% respectively. The final results of numerical simulation found the thermal efficient of parabolic trough collector increase by 10 % with using concentrating 4% of Nano fluid.
E. Bellos et al. 2016 [54]	air, nitrogen, carbon dioxide, helium, neon and argon	Numerically	The final results showed that helium is the greatest working fluid for input temperatures up to 700K, while carbon dioxide is the best choice for temperatures greater than that. Helium operating at 640K inlet temperature and 0.035kg/s mass flow rate achieves the worldwide maximum exergetic efficiency by using steady state solution.
S. E. Ghasemi et al. 2016 [22]	water / Al_2O_3 and water /CuO nanofluid	Numerically	increasing the volume fraction of nanoparticles increases the average Nusselt number and coefficient of friction for both nanofluids. In addition,

			Al_2O_3 and CuO nanoparticles were added (φ=3%), Water improved heat transfer by 28% and 35% respectively.
C. Tzivanidis et al. 2016 [55]	water TherminolVP-1	Numerically	The final results found water give high thermal performance of PTC than TherminolVP-1by using steady state solution.
K. A. Antonopoulos et al. 2017 [58]	pressurized water, TherminolVP-1, nitrate molten salt, sodium liquid, air, carbon dioxide, and helium	Numerically	The final results show that liquid sodium has the highest worldwide exergetic efficiency 47.48 % at 800 K inlet temperature, whereas helium, carbon dioxide, and air have maximum exergetic performance of 42.21 %, 42.06 %, and 40.12 %, respectively. Furthermore, at temperatures up to 550 K, pressurized water is the optimum working medium, whereas for temperatures beyond 1100 K, carbon dioxide and helium are the only options.
C.Tzivanidis et al. 2017 [59]	Syltherm800, Syltherm800/CuO, Syltherm800/Al_2O_3	Numerically	Nano fluid efficient than Syltherm800, The best option appears to be Syltherm 800/CuO. The use of nanofluids has been shown to improve heat transmission by around 50%, with the increase being greater at higher temperatures, When the concentration ratio is optimized and the flow rate is relatively low, CuO can enhance thermal efficiency up to 1.26 % and Al_2O_3 can increase thermal

			efficiency up to 1.13 %. At last Syltherm800/CuO is best choice as working fluid with steady state solution.
P. D. Tagle-Salazar et al. 2018 [61]	water, water/ Al_2O_3	Numerically	The final result show that using nanoparitcal (Al_2O_3) with water given high thermal performance of PTC than using water as heat transfer fluid . with steady state solution.
A. Ahmadi et al. 2019 [69]	nanopartical of (CuO, and Al_2O_3), with base fluid (water, and thermal oil TherminolVP-1)	Numerically	The final results show that water as a basefluid has better energy and exergy efficiency than thermal oil, according to numerical calculations. PTC using water as a basefluid has greater annual average energy and exergy efficiencies (10.81 % and 9.44 %) than PTC using oil as a basefluid (10.64 % and 9.07 %) with steady state method.
K. A. Ahmed et al. 2020 [70]	air, helium, and carbon dioxide	Numerically	the final results show that helium has maximum collector efficient when compare with air, and carbon dioxide with steady state solution.

Chapter Three

THEORETICAL ANALYSIS AND NUMERICAL SIMULATION

Chapter Three

THEORETICAL ANALYSIS AND NUMERICAL SIMULATION

3.1. Introduction

In this chapter, a three-dimensional numerical analysis of a parabolic trough collector absorber tube is presented for estimating the thermal performance of a parabolic trough collector with different working fluids. Three types of working fluid were investigated in this numerical study: water, TherminolVP-1, and Syltherm800. The effect of the weather condition of Al-Najaf city in Iraq, was studied using the weather station data. Weather conditions, volumetric flow rate, absorber tube absorptivity, reflectivity of the reflector surface, and mass flow rate were all considered to impact the thermal behavior of the parabolic trough collector. The COMSOL Multiphysics 6.0 software program was used to build and develop a numerical model resolves fluid flow and heat transfer cases. The developed numerical model was validated based on the literature's experimental results. The solution of a high-performance parabolic trough collector was presented using governor equations, initial and boundary conditions, and an unsteady state flow condition.

3.2. Mathematical Model

The fundamental mathematical model for the examined collector is presented in this paragraph. These equations describe the energetic and thermal. It operates as an image concentrator that only makes use of the direct solar radiation (G_b) that enters its aperture (Aa). Equation (3.1)[74] calculates the total available solar irradiation (Q_s) in the collection:

$$Q_s = A_a \cdot G_b \quad \ldots\ldots\ldots\ldots\ldots\ldots\ldots\ldots \quad (3.1)$$

Some of the sun energy is absorbed by the working fluid, which increases its temperature. The amount of energy that can be easily described using the energy balance in the fluid volume is called the useful energy (Q_u), ($\dot{m}$) mass flow rate of working fluid, (Cp) specific heat of working fluid, (T_{out}) output temperature of working fluid, (T_{in}) input tempertature of working fluid, as expressed in equation (3.2) [75] below :

$$Q_u = \dot{m} \cdot Cp \,.\, (T_{out} - T_{in}) \quad \ldots\ldots\ldots\ldots\ldots\ldots (3.2)$$

The most important performance measure is the thermal efficiency of the solar collector (η_{th}), which is the ratio of useful energy to solar radiation available, as described in equation (3.3) below :

$$\eta_{th} = \frac{Qu}{Qs} \quad \ldots\ldots\ldots\ldots\ldots\ldots\ldots\ldots\ldots\ldots (3.3)$$

By examining the heat transport processes inside the absorber tube, equation (3.4) may be used to calculate the useable energy in a second method. This equation describes the heat transmission from the hot absorber to the flowing working fluid,

$$Q_u = h \cdot A_{ri} \,.\, (T_r - T_{fm}) \quad \ldots\ldots\ldots\ldots\ldots\ldots\ldots (3.4)$$

Where (h) heat transfer coefficient,(A_{ri}) inner cross section area of receiver tube (T_r) temperature of receiver tube,(T_{fm}) mean temperature of working fluid.

Heat transfer theory and the Nusselt number (Nu) may be used to estimate the heat transfer coefficient (h) for the tube internal flow, (D_{ri}) hydraulic inner diameter of receiver tube, (K) thermal conductivity of working

fluid . More specifically, Equation (3.5) shows the connection between Nusselt number and heat transmission coefficient.

$$Nu = \frac{h \,.\, Dri}{K} \quad \text{.....(3.5)}$$

The Reynolds (Re) number and the Prandtl (Pr) number are defined belo .

$$Re = \frac{\rho \,.V.D}{\mu} \quad \text{.....(3.6)}$$

$$Pr = \frac{\mu \,.\, Cp}{K} \quad \text{.....(3.7)}$$

Where (ρ) density of working fluid, (V) velocity of working fluid, (D) absorber tube diameter, (μ) viscosity of working fluid.

The next important element of the thermal analysis is the thermal loss calculations. This value can be calculated in a number of methods, and the necessary equations for the analysis are given below. It merely states that all of the aforementioned equations are included in the created model. According to equation(3.8)[78], the energy balance in the absorber demonstrates that the absorbed solar energy is divided into useable energy output and thermal losses (Q_{loss}).

$$Q_s \cdot \eta_{opt} = Q_u + Q_{loss} \quad \text{.....(3.8)}$$

By carefully monitoring the heat transport activities inside the receiver, thermal losses may be calculated. In essence, it implies that thermal energy is exchanged between the absorber and the cover, and between the cover and the environment. Under unsteady-state conditions, these energy levels correspond to the thermal losses. Equation(3.9) [74]describes the heat exchange between

the cover and the absorber. In this case, just the radiation losses are taken into account since the heat convection losses may be disregarded.

$$Q_{loss} = A_{co} \cdot h_{ca}.(T_{co} - T_{fm}) + \epsilon_c . A_{co} \cdot \sigma . (T^4_{co} - T^4_{ci}) \quad \text{……..(3.9)}$$

3.3. Numerical Simulation

The COMSOL Multiphysics 6.0 software program is used to calculate important parameters such as output temperature, useful heat, total heat loss, thermal efficiency, Nusselt number, and Reynold number of working fluids based on the thermos-physical characteristics of the working fluids and the verifiable input temperature used in the simulation program with input parameters of numerical simulation such as :

- Solar irradiation equation

$$R_g = I * A_g * \alpha_g \quad \text{……..(3.10)}$$

$$R_p = I * A_p * \alpha_p \quad \text{……..(3.11)}$$

Where R_g total energy on glass cover (W), I amount of solar radiation (W/m^2), A_g area of glass cover (m^2), α_g Absorption coefficient of glass. (R_p) total energy on absorber tube (W), A_p area of absorber tube (m^2), α_p Absorption coefficient of absorber tube.

- Ambient temperature .

- Wind speed

- The convective heat transfer coefficient ($W/m^2.^oC$)

$$h_{out} = 5.7 + 3.8\ V_{out} \quad \text{……..(3.12) [75]}$$

where V_{out} is wind speed (m/s), and h_{out} is the convective heat transfer coefficient ($W/m^2.ºC$).

3.3.1. Assumption of Numerical Simulation

- Unsteady state flow.
- Three-dimension flow.
- Laminar flow.
- Weakly compressible flow (the density changes with temperature).
- There are no thermal losses due to contact.
- The receiver is an evacuated tube and the heat convection losses between absorber and cover are neglected.
- There is uniform heat flux over the absorber.
- Non constant properties fluid flow.
- Fully developed flow.

3.3.2. Geometry

Especially on the absorber tube, the effect of the heat transfer of parabolic trough collector studied numerically. The working fluid flow through absorber tube and gain heat energy by convection process with absorber wall. Table 3.1 shown the all detail of parabolic trough collector and absorber tube geometry of previous study B. LAMRANI et al. 2018 [63], which validated with it. The numerical study based on COMSOL Multiphysics 6.0 software. Figure 3.1 shown parabolic trough collector absorber tube of previous study B. Lamrani et al. 2018 [63].

Table 3.1. Characteristics of PTC of previous study B. LAMRANI et al. 2018 [63].

Symbol	Parameter	Value	Unit
L	Collector length	5	m
W	Collector aperture width	3.4	m
Aa	Aperture area of PTC	17	m^2
F	Focal length	1.84	m
D_{abso}	Receiver outer diameter	0.070	m
D_{absi}	Receiver inner diameter	0.066	m
D_{covo}	Cover outer diameter	0.115	m
D_{covi}	Cover inner diameter	0.109	m
Ep_{cov}	Cover thickness	0.006	m
K_{abs}	Absorber thermal conductivity	54	W/m . K
K_{cov}	Cover thermal conductivity	0.78	W/m . K
ϵ_{cov}	Cover emittance	0.86	–
τ_{cov}	Cover transmittance	0.95	–
α_{cov}	Cover absorbance	0.02	–
CC	Concentrating ratio	22.7	–

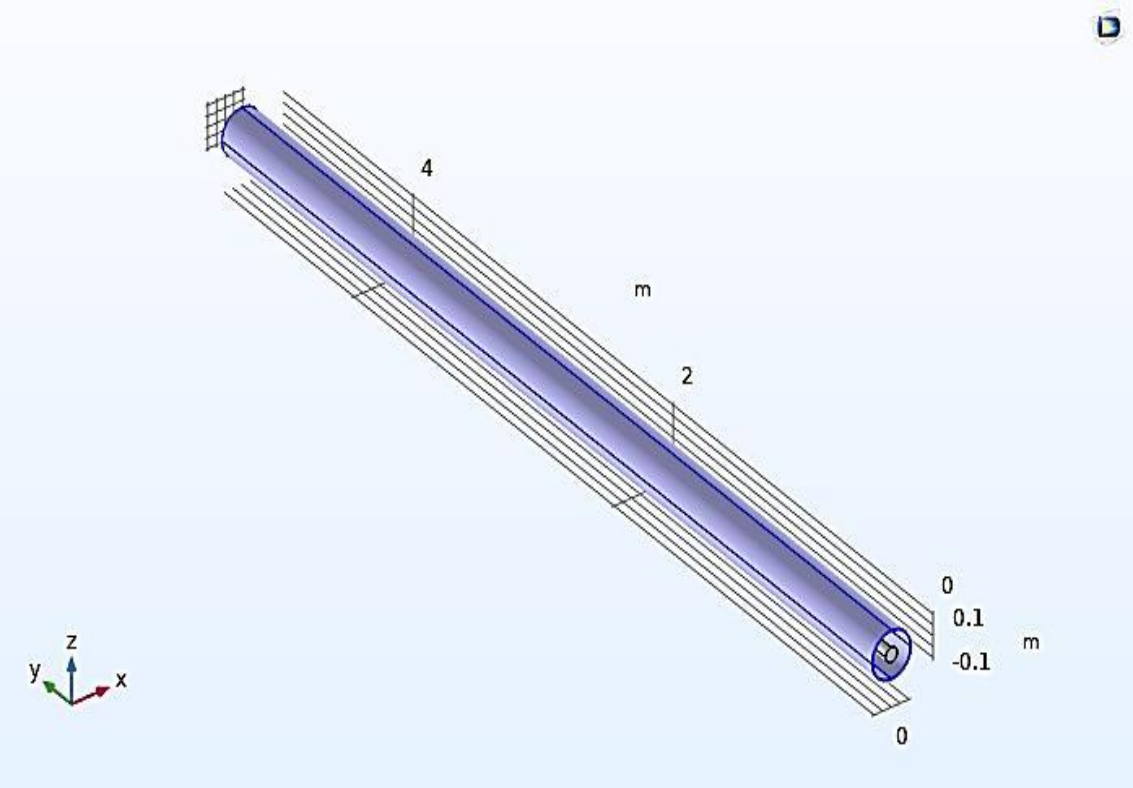

Fig.3.1.Geometry of Absorber Tube of PTC.

3.3.3. Governing Equations

The following are the governing equations for forced convection of incompressible, unsteady state , and laminar flow in the collector's absorber tube [79]:

3.3.3.1. Continuity Equation :

$$\frac{\partial \rho}{\partial t}+\frac{\partial}{\partial x}(\rho u)+\frac{\partial}{\partial y}(\rho v)+\frac{\partial}{\partial z}(\rho w)=0 \quad \text{.....(3.13)}$$

3.3.3.2. Momentum Equation :

$$\frac{\partial u}{\partial t}+\left(u\frac{\partial \rho u}{\partial x}+v\frac{\partial \rho u}{\partial y}+w\frac{\partial \rho u}{\partial z}\right)=-\frac{\partial p}{\partial x}+\mu\left(\frac{\partial^2 u}{\partial x^2}+\frac{\partial^2 u}{\partial y^2}+\frac{\partial^2 u}{\partial z^2}\right) \quad \text{.....(3.14)}$$

$$\frac{\partial v}{\partial t}+\left(u\frac{\partial \rho v}{\partial x}+v\frac{\partial \rho v}{\partial y}+w\frac{\partial \rho v}{\partial z}\right)=-\frac{\partial p}{\partial y}+\mu\left(\frac{\partial^2 v}{\partial x^2}+\frac{\partial^2 v}{\partial y^2}+\frac{\partial^2 v}{\partial z^2}\right) \quad \text{.....(3.15)}$$

$$\frac{\partial w}{\partial t}+\left(u\frac{\partial \rho w}{\partial x}+v\frac{\partial \rho w}{\partial y}+w\frac{\partial \rho w}{\partial z}\right)=-\frac{\partial p}{\partial z}+\mu\left(\frac{\partial^2 w}{\partial x^2}+\frac{\partial^2 w}{\partial y^2}+\frac{\partial^2 w}{\partial z^2}\right) \quad \text{.....(3.16)}$$

3.3.3.3. Energy Equation :

$$\frac{\partial T}{\partial t}+u\frac{\partial T}{\partial x}+v\frac{\partial T}{\partial y}+w\frac{\partial T}{\partial z}=\alpha(\frac{\partial^2 T}{\partial x^2}+\frac{\partial^2 T}{\partial y^2}+\frac{\partial^2 T}{\partial z^2}) \quad \text{…….(3.17)}$$

Where (u) is the velocity vector (m/s), (ρ) the fluid density (kg/m^3), (P) is the static pressure (Pa),(Cp) the fluid specific heat at constant pressure (J/kg. K) , (T) temperature of flow (K), and (k) is the fluid thermal conductivity (W/m. K).

3.3.4. Initial and Boundary Conditions:

- Initial boundary condition: the velocity, pressure and temperature at initial time as the flowing:

  $u = v = w = 0$ …….(3. 18)

  $p = 0$ …….(3. 19)

  $T = T_{inial}$ …….(3. 20)

- Inlet boundary condition: The flow has a constant mass flow rate at inlet and constant inlet temperature at the receiver inlet.

  $\dot{m} = \int \rho\ (\boldsymbol{u}\cdot\boldsymbol{n})\ A$, $T = T_{in}$, y = 0 , $0 \le r \le \frac{d}{2}$ …….(3. 21)

- Wall boundary condition: No-slip conditions exist at inside the pipe wall.

  $u = v = w = 0$ at $r = \frac{d}{2}$, $0 \le L \le 5$. …….(3. 22)

- Outlet boundary condition:

  P= 0 , y = L = 5m , $0 \le r \le \frac{d}{2}$ …….(3. 23)

3.3.5. Mesh Independent

In this model, a tetrahedral mesh was employed. as shown in Figure 3.2. For five different mesh sizes, many numerical efforts have been made to get and confirm the results. The chosen mesh and the solution approved contained 987015 elements with a minimum quality of 0.04998 and an average quality of 0.6498. Figures 3.3 and 3.4 show mesh independence with outlet temperature and useful energy.

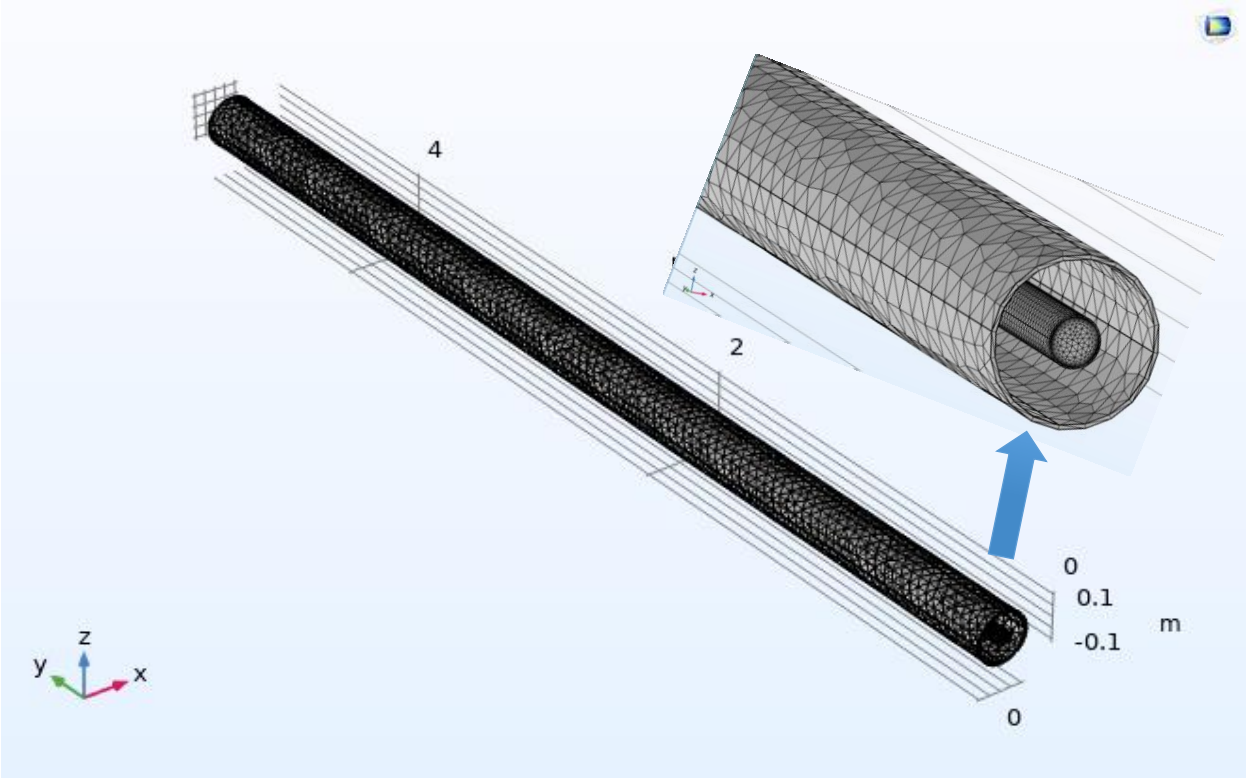

Fig.3.2. Absorber Tube Mesh.

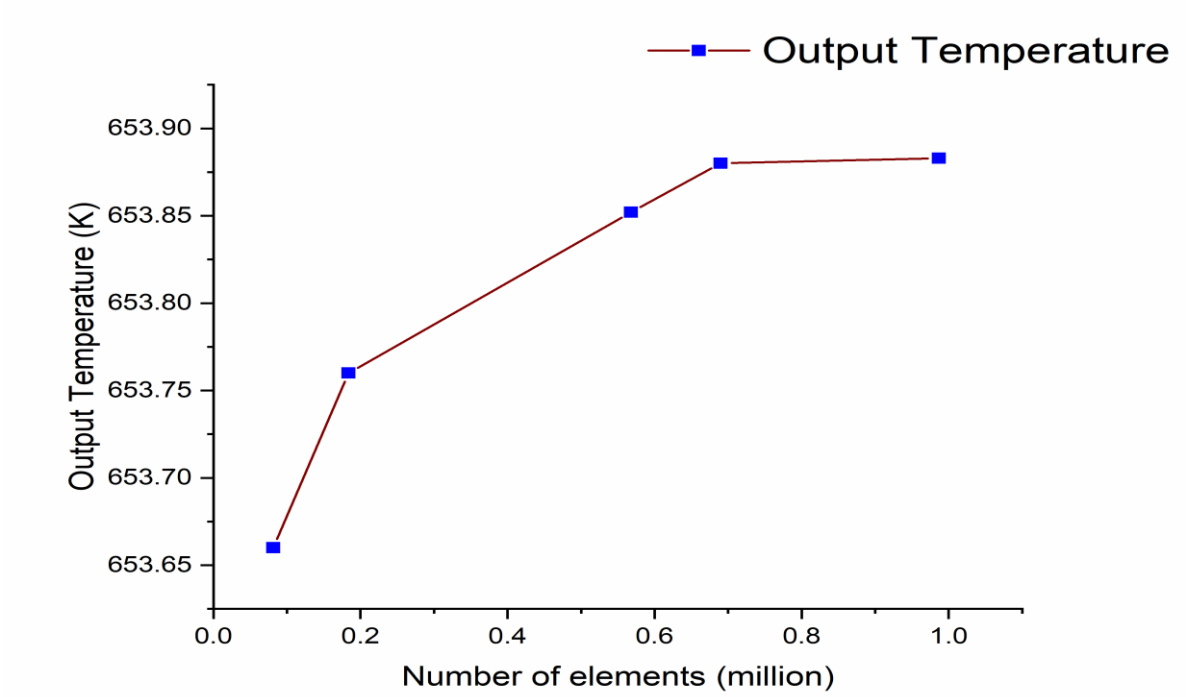

Fig.3.3. Mesh Independency Curve with Outlet Temperature.

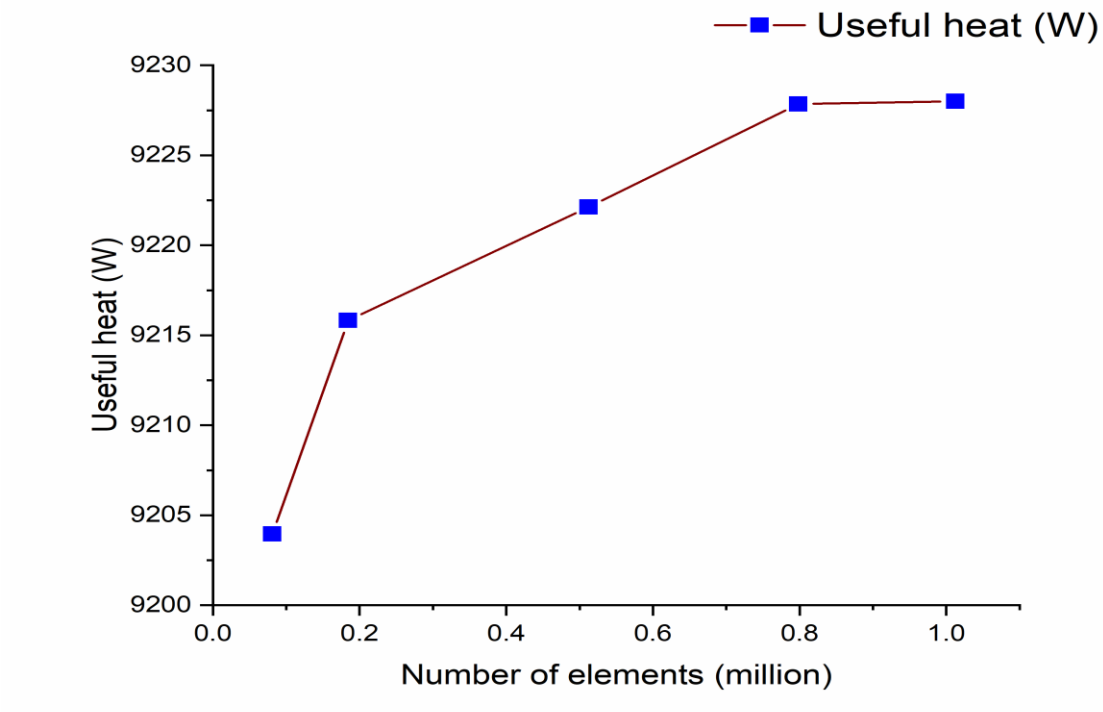

Fig.3.4. Mesh Independency Curve with Useful Heat.

3.3.6. Thermophysical Properties of Working Fluids

Each type of working fluid in concentrating solar systems has different thermal behavior due to its thermophysical properties. Many thermal properties have an effect on the nature of the thermal behavior of a working fluid, The important properties that have a great effect on thermal behavior include density, specific heat, thermal conductivity, and viscosity. Table 3.1 shows how the thermo-physical properties of the working fluid change with the amount of input temperature. The nature of the working fluid has a significant impact on the thermal performance of the parabolic trough collector. The thermo-physical properties of the working fluid are responsible for its temperature operation range, and the temperature operation range varies from one type to another according to the thermo-physical properties of the working fluid.

Table3.2. Thermo-physical Properties of Working Fluids [80-83].

Working fluid	Thermal properties
Water	**ρ (Kg/m^3)** = 1031.84412 + 18.53*10^{-3} T - 4.68515*10^{-4} T^2. **K (W/m.K)** = -0.34149+4.97*10^{-3} T - 6.00979*10^{-6} T^2. **Cp (J/kg.K)** = 5543.35375 – 8425.29*10^{-3} T+0.01305 T^2. **μ (pa.s)** = 0.03537-2.55881*10^{-4}T+6.21204*10^{-7}T^2-5.03136*10^{-12} T^3.
Oil Syltherm800	**ρ (Kg/m^3)** = 1115.80363 – 0.45272 T – 5.74009*10^{-4} T^2. **K (W/m.K)** = 0.19006-1.87724*10^{-4} T - 3.64219*10^{-10} T^2. **Cp (J/kg.K)** = 1107.93118 +1.70727 T – 4.02061*10^{-18} T^2. **μ (pa.s)** = 0.28141- 0.000217 T+6.26795*10^{-6} T^2 - 8.02194*10^{-9} T^3+ 3.82122*10^{-12} T^4.

Oil TherminolVP-1	**ρ (kg/m^3)** = - 0.90797 * T+ 0.00078116 * T^2- 2.367 * 10^{-6} * T^3+ 1083.25. **K (W/m.K)** = - 8.19477 * 10^{-5} * T- 1.92257 * 10^{-7} * T^2 + 2.5034 * 10^{-11} * T^3- 7.2974 * 10^{-15} * T^4+ 0.137743. **Cp(J/kg.K)**=0.002414*T+5.9591*10^{-6}*T^2-2.9879*10^{-8} * T^3+4.4172*10^{-11} * T^4 +1.498. **μ(pa.s)** = (1e-6*exp((544.19/(T-159.07))-2.59578))*(-0.90797 * T+ 0.00078116 * T^2 - 2.367 * 10^{-6} * T^3 + 1083.25).

CHAPTER FOUR
EXPERIMENTAL WORK

Chapter Four

Experimental Work

4.1. Introduction

In general, the objective of the experimental work to investigate the effect of working fluid (water) on thermal behavior of parabolic trough collector. The experimental parameters considered are ; output temperature, thermal efficiency, useful heat, total heat losses, Nusselt number, and Reynold number with variables flow rate. The heat transfer fluid used in the experiment is water.

4.2. Experimental Setup

The final form of the experimental parabolic trough collector is depicted in Figure 4.2. The Figure 4.2 shows the parts and equipment used to study the effect of water on the thermal performance of a parabolic trough collector. The experimental setup consist of a reflector parabola surface with an aperture area of 4.6 m^2, an absorber tube with a length of 2 m, a parabolic trough structure, a working fluid tank with a capacity of 0.072 m^3 , pipes and connections, a circular section with diameter 19.05 mm, a 373W centrifugal pump, and a flowmeter were used. Twelve thermocouples were employed to measure the temperatures of working fluid and ambient. Fluid pressure gauges were fixed at the working fluid tank to measure the static pressure. Figure 4.1 shows the schematic diagram of an experimental setup of parabolic trough collector.

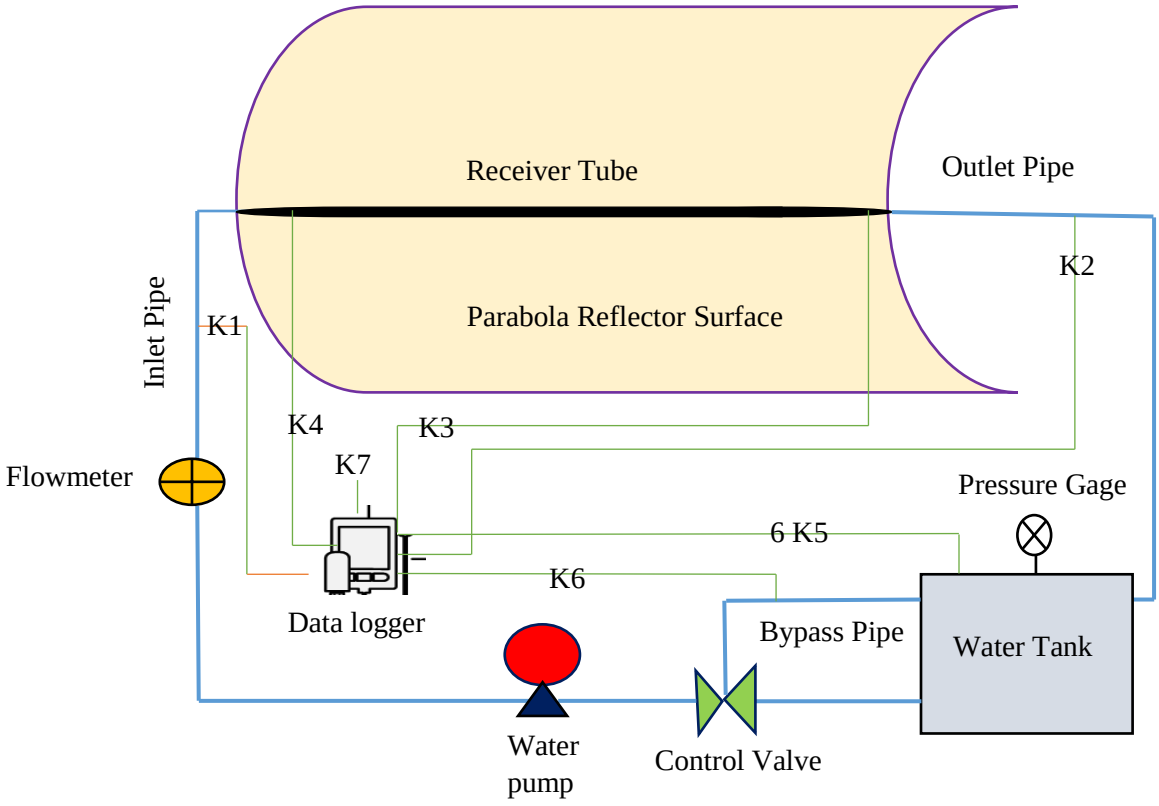

Fig.4.1. The Schematic Diagram of an Experimental Setup.

K1 = Inlet temperature of woking fluid thermocouple.

K2 = Outlet temperature of working fluid thermocouple.

K3 & K4 = absorber tube surface temperature thermocouple.

K5 = Water tank surface temperature thermocouple (six thermocouples).

K6 = Bypass pipe working fluid temperature thermocouple.

K7 = Ambient temperature thermocouple

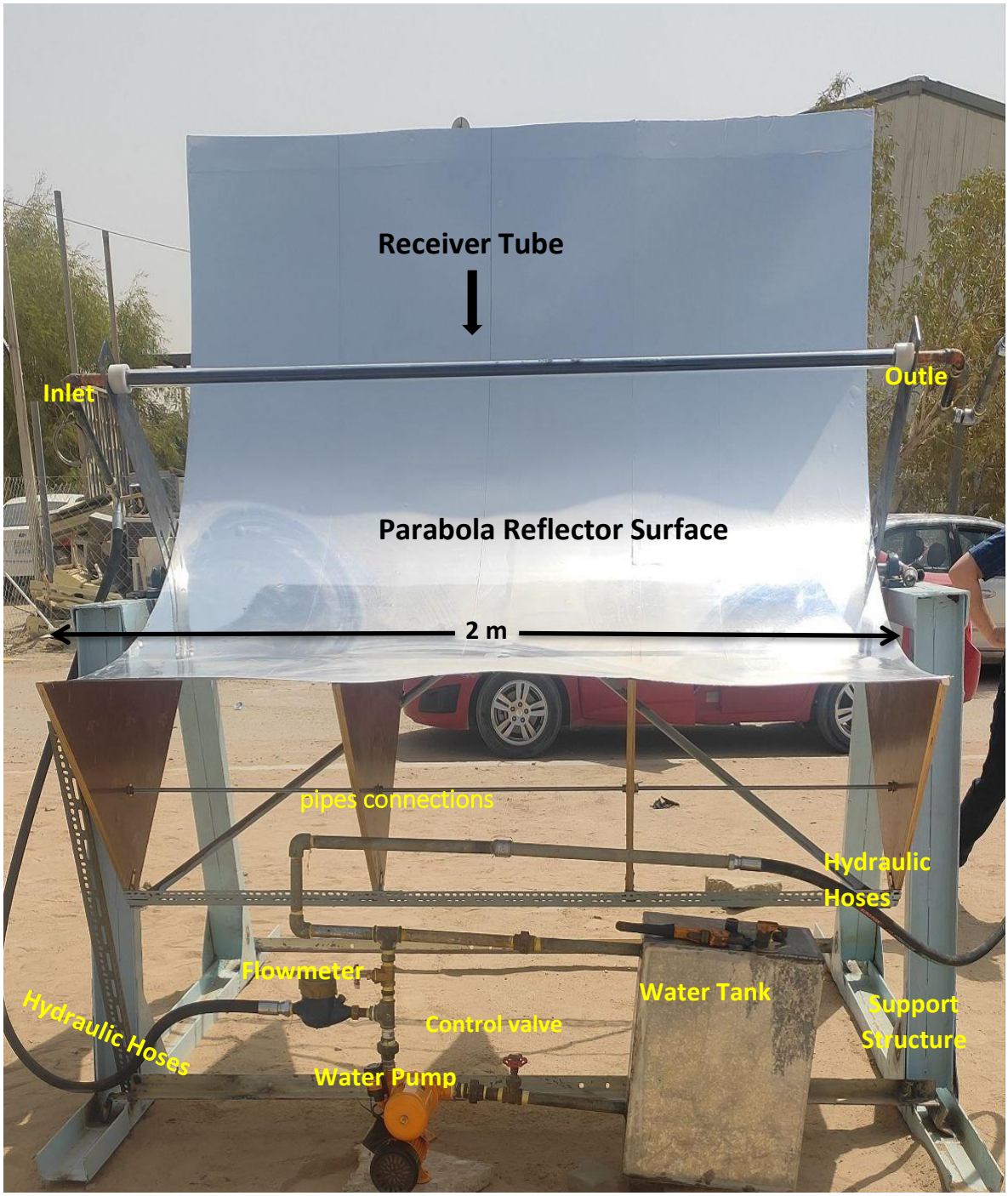

Fig.4.2. Experimental Apparatus Parabolic Trough Collector Testing.

Table 4.1: Characteristics of The Experimental Apparatus of PTC.

Symbol	Parameter	Value	Unit
L	Collector length	2	m
W	Collector aperture width	2.3	m
Aa	Aperture area of PTC	4.6	m^2
CC	Concertation ratio of PTC	18.3	-
F	Focal length	0.5	m
D_{abso}	Absorber tube outer diameter	0.025	m
D_{absi}	Absorber tube inner diameter	0.0235	m
Ep_{cov}	Cover thickness	0.003	m
K_{abs}	Absorber thermal conductivity	401	W/m . K

4.2.1. Reflector Surface

The main part of a parabolic trough collector is the reflector surface. It is used to reflect solar radiation onto the receiver, and it has a low absorptivity of solar radiation. The parabola arches shape, reflector tape, thin iron plate, carrier rod, and stud screw are all important components of reflector surfaces. The first step in creating a parabola reflector surface is to design the primary model in a computer using a software design program, then manufacture the primary model in a CNC machine using an iron plate, as shown in Figure 4.3 below.

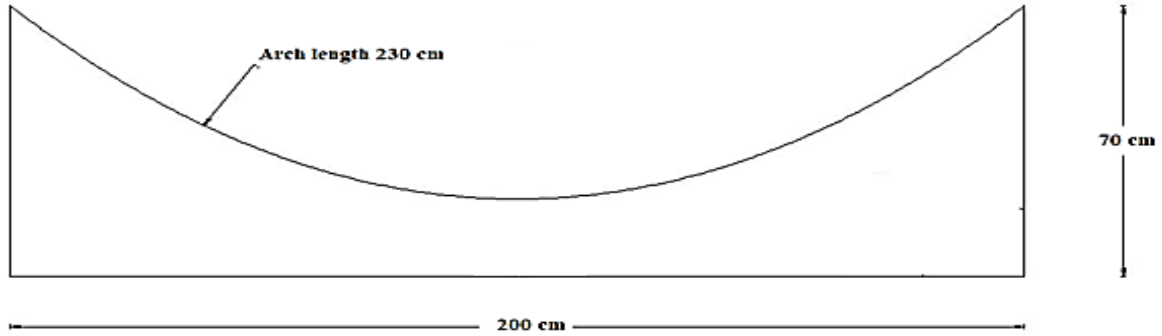

Fig.4.3. Sechmatic Parabolic Reflector Surface Design.

After creating the primary model, the dimensions of the parbolic trough arch were cheched with respect to the X and Y axis , according to the parabolic trough eqation. Next the final model was creatd using four pieces of 2 cm thick plywood, as shown in Fig.4.4. The carrier rod, with diameter of 32mm, was installed in the center of the parabolic pieces using two meter screws with a diameter of 16 mm on both sides.

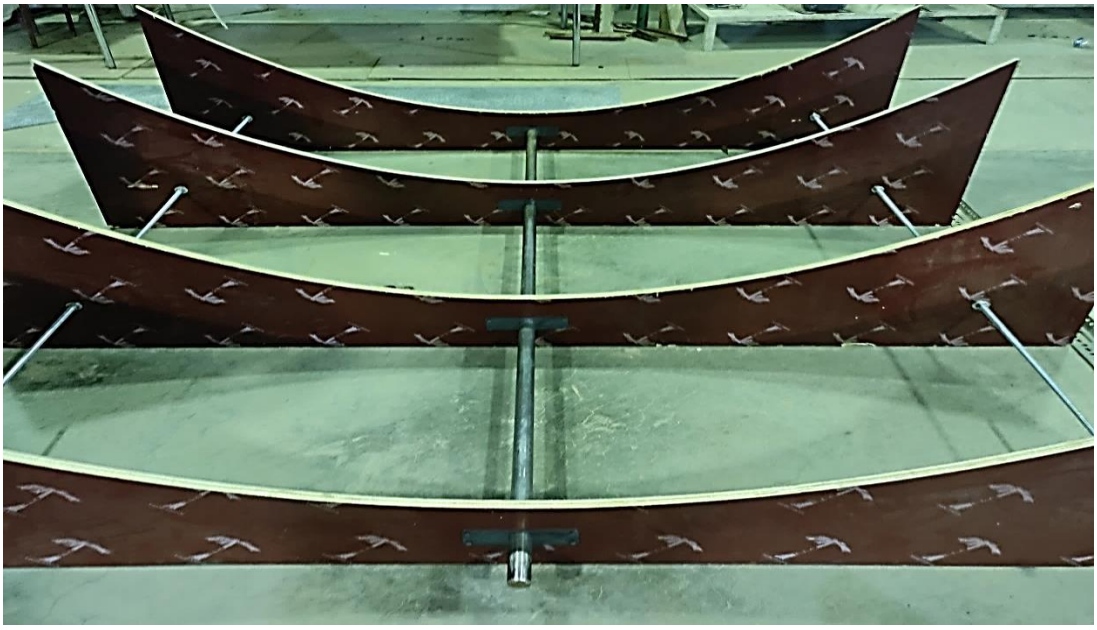

Fig.4.4. Plywood Parabola Mold.

Then, as shown in figure 4.5, the thin iron plate with a thickness of 1 mm was placed along the plywood parabolic shape. The iron plate was secure with small nails.

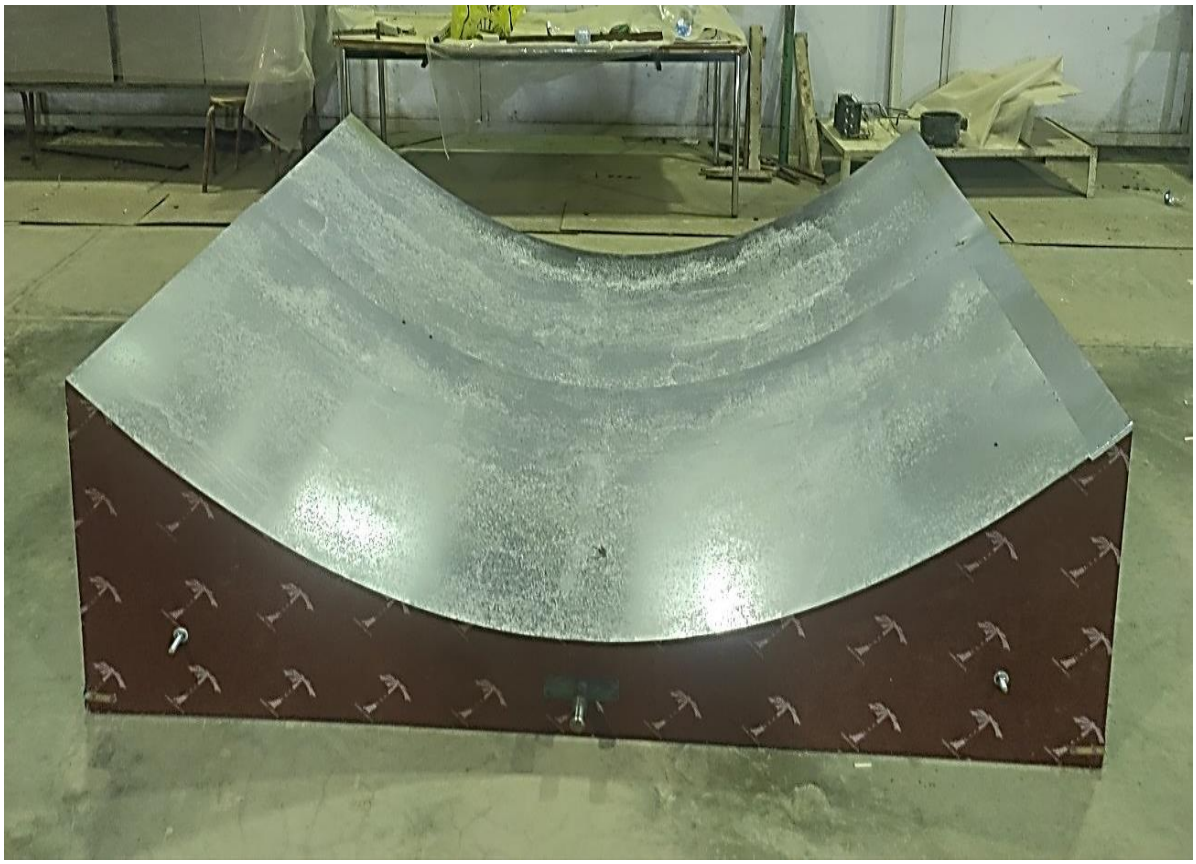

Fig.4.5. Parabola Mold with Thin Iron Plate Cover.

The final step in creating the reflective surface is to paste the sliver reflector straps onto thin iron plate above the parabolic shape as shown in figure 4.6 below :

Fig.4.6. Reflective Surface with Reflector Tape.

4.2.2. Receiver

Figure 4.7 shows a parabolic trough collector and receiver. The receiver tube is made up of a copper absorber tube. The receiver's function is to absorb solar radiation from the reflector's surface. The heat-transfer fluid flows through the absorber tube and gains heat energy by convection. The receiver is connected by hydraulic hoses on two sides. The amount of heat energy depends on the aperture area. Aperture area is the multiply by the width and the arch length of parabolic trough collector ; the diameter and length of the receiver have an effect on the thermal performance of a parabolic trough collector. The receiver used in this experiment has a 2 m long absorber copper tube with black thermal coating, and the main details are shown in table 4.1.

Fig.4.7. Experimental Receiver Tube.

4.2.3. Structure

The parabolic trough reflector surface and absorber carrier are supported by the iron structure. The design and manufacture methods of parabolic structures vary from type to type depending on the dimensions of the trough and the nature of the materials used during the manufacture of the reflector surface. The support structure is formed by four legs that are welded together by straight pieces of the same material, as shown in figure

4.8. The function of the structure is carry and fix the main part of the parabolic trough collector, especially the reflector surface carrier rod, which is fixed to the structure by a ball bearing.

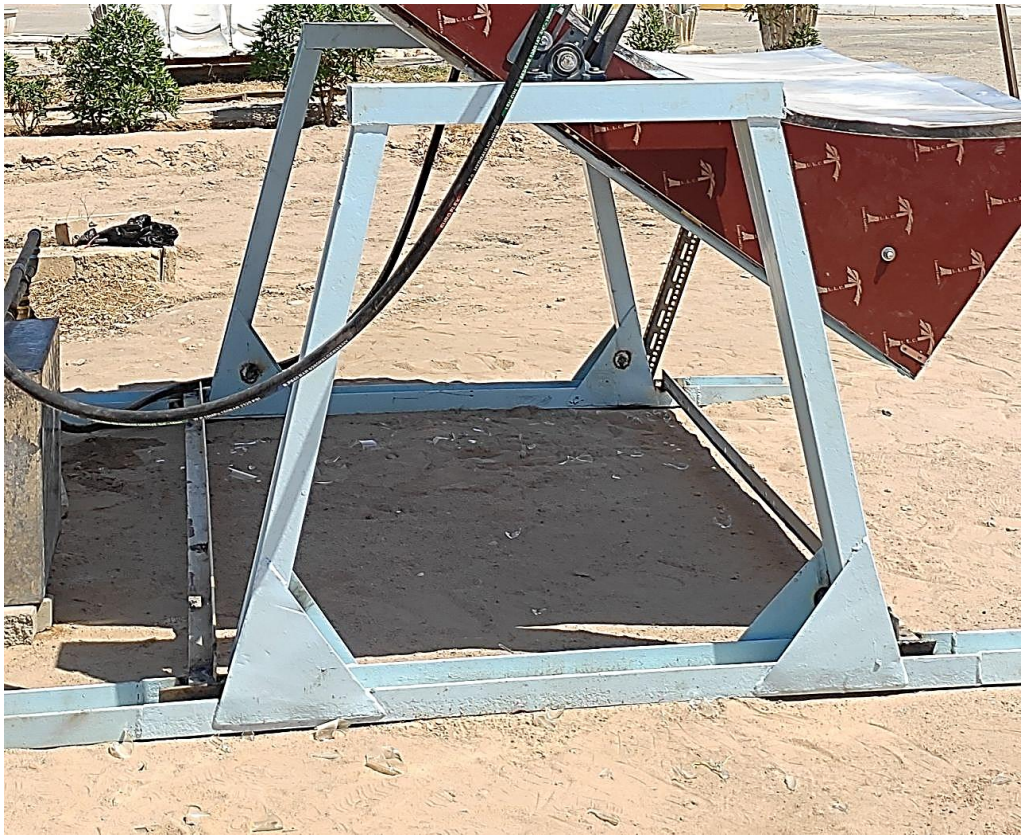

Fig.4.8. Support Structure.

4.2.4. Water Tank

Figure 4.9 shows a cubic water tank with a capacity of 0.072 m^3, dimensions of 60 cm in height and a width of 30 cm and a length of 40 cm. The tank contains three holes with a diameter of 3/4 inch for the inlet and outlet of the fluid and another hole to fill water tank with fluid and to install a pressure gage.

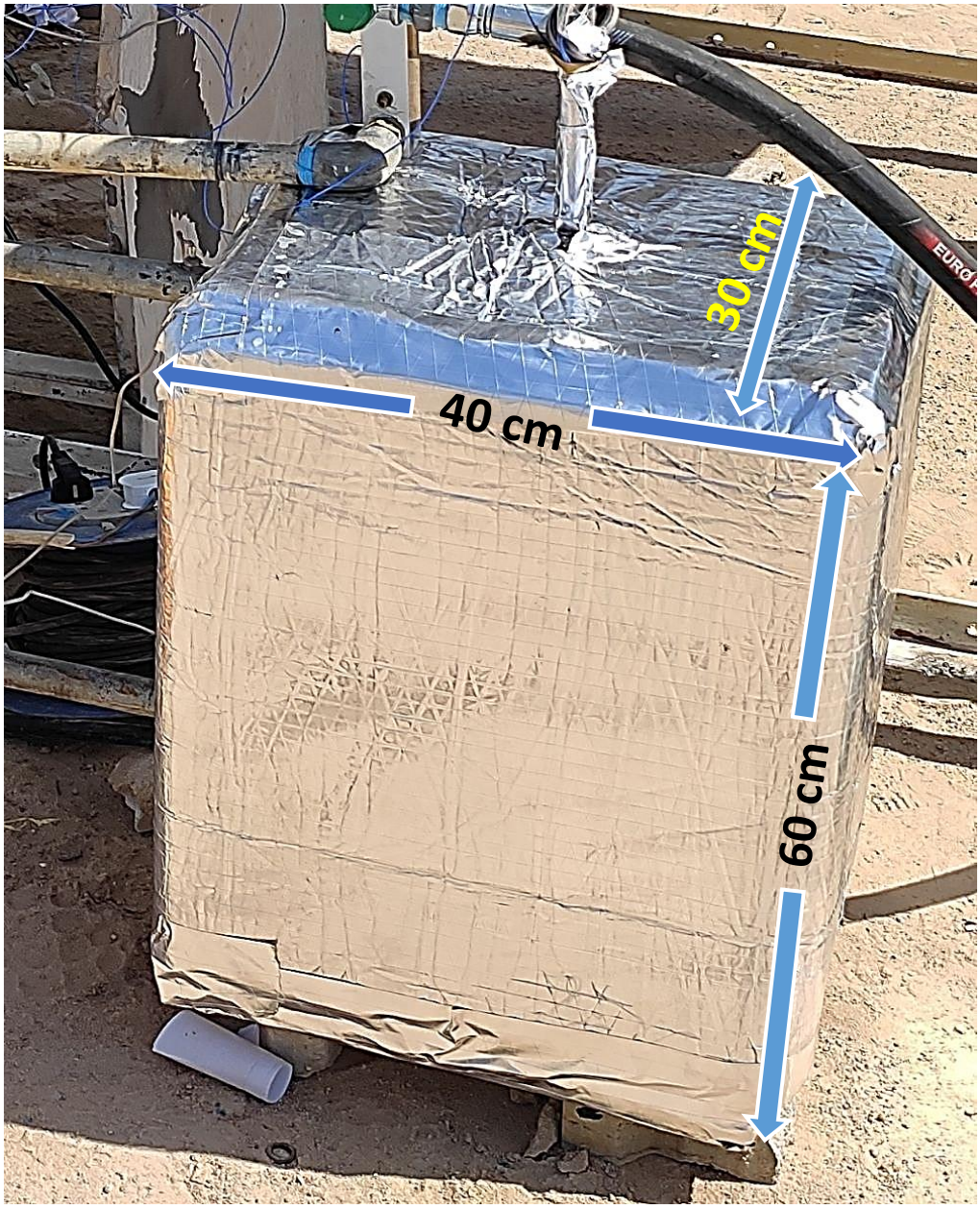

Fig.4.9. Water Tank.

4.2.5. Water Pump

A Centrifugal pump with a capacity of 373W and a speed of 2850 rpm, as shown in Figure 4.10, continuously circulates the fluid from the water tank to the receiver tube and back to the water tank .

Fig.4.10. Water Pump.

4.2.6. Thermocouples

Twelve K- types of thermocouples were used in the experimental study at the inlet and outlet of the fluid to measure water temperature, as shown in Figure 4.11 with twelve channels data logger were used to record temperatures during the test. K-types thermocouple provide wide range of operation temperature measurement.

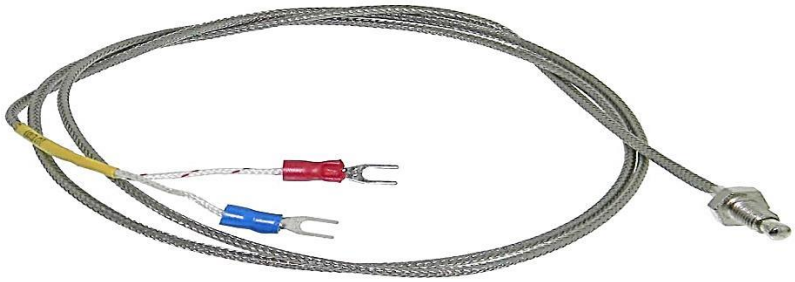

Fig.4.11. K-Type Thermocouple.

4.2.7. Flowmeter

Liquid flowmeter with 0.75 inch used in the experimental test to measure the amount of water flow in the test. Figure 4.12 show the mechanical flowmeter and it suitable for water and used at the cooling tower, boiling , and another industrial application. Liguid flowmeter used for wide range of water flow with low head losses. In the experimental test flowmeter connected between outlet pipe of water tank and inlet of absorber tube.

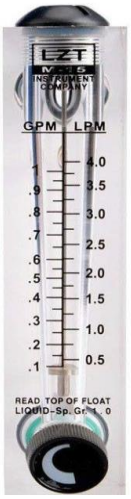

Fig.4.12. Liquid Flowmeter.

4.2.8. Pressure Gauge

Pressure gauge used to measurement the static and dynamic pressure of fluid. Installation in the top port of the water tank, Figure 4.13 show the pressure gage which used in the experimental study. There are many types of pressure gauge. The pressure gauge assist to diagnosis the pressure drop or fluid leak of system.

Fig.4.13. Pressure Gauge.

4.2.9. Solar power meter

Digital apparatus model (SM206-SOLAR) used to measure intensity of solar radation in (W/m^2) which reach to the parabolic trough reflector surface as shown in Figure 4.14.

Fig.4.14. Solar Power Meter.

4.2.10. Air Flow Anemometer

A device that use to measure air speed contain from two main part , a stick small fan and digitat meter as shown in Figure 4.15.

Fig.4.15. Air Flow Anemometer.

4.2.11. Multi-Channel Temperature Data Logger

A digital advice that use to recorder temperature contain from muti-chanal input to connect the thermocouple with it as shown in figure 4.16.

Fig.4.16. Multi-Channel Temperature Data Logger.

4.3. Experimental Procedures

1- After assembling all of the device's component parts, the measuring devices need to be set up and fixed. The following explanation applies to the measuring tools used:

a- Solar radiation measuring : The solar radiation meter is positioned at the same tilt angle of PTC. Direct incident radiation is measured every 15 minutes. The work starts from 7 am to 5 or 6 pm.

b- The K-type thermocouples are used to measure temperatures in 12 locations in the device. One thermocouple at the fluid inlet to the receiving tube and another at the fluid outlet. Other six thermocouples are located in all external faces of water tank. One of

thermocouple measure the ambient temperature. One thermocouple measure the outlet and backward of water tank. Two thermocouples measure the surface temperature of receiver tube .These thermocouples were connected to a 32-channel data logger to record all temperature data. A calibration of all these thermocouples was done in comparison with a mercury thermometer to obtain the best measurement accuracy.

c- Wind speed and ambient temperature measuring : An anemometer probe is placed near the receiver tube of the parabolic trough collector to measure wind speed every 15 minutes. The ambient temperature is also measured by placing an anemometer probe in the shade every 15 minutes.

2- The measuring devices work from the time the experiment began from 7:00 am in the morning until 5:00 pm in the evening.

3- Some readings are recorded manually (such as recording data of solar radiation, ambient temperature, and wind speed) every 15 minutes.

4- Experiments were conducted in Technical Engineering college of Najaf/Iraq.

CHAPTER FIVE

RESULTS AND DISCUSSIONS

Chapter Five

Results and Discussions

5.1. Introduction

In this chapter, the experimental and numerical results are presented and discussed. The results include experimentally and numerically derived effects of working fluids on the thermal performance of a parabolic trough collector with different working fluids and different fluid flow rates.

5.2. Experimental Results

After manufactured the parabolic trough collector in the workshops of Al-Najaf Engineering Technical College and conducting numerous experiments, an experimental study based on real results was conducted. In experimental steps, study the effect of collector direction on the thermal behavior of a parabolic trough collector and the effect of working fluid flow rate for four ranges 1, 2, 3, and 4 L/min. The experiments were conducted in two directions, one on the east-west line and the other on the south-north line. The experiment's results include measurements of parameters related to thermal performance, such as output temperature, temperature difference between inlet and outlet temperatures of the working fluids, useful heat, total heat losses, thermal efficiency, Nusselt number, and Reynold number when the working fluid is water.

5.2.1. The Effect of The Direction on Performance of PTC

There are two experimental direction conducted on four days each, namely November 2nd,6th, 7th, and 10th for the east – west line direction, and November 13th, 14th, 20th, and 21st for the south – north direction. The important parameters to measure the thermal performance were identified for each direction, including output temperature of working fluid, useful heat, heat losses, thermal efficiency, Nussult number, and Reynold number.

5.2.1.1. The Direction from East to West

The parabolic trough collector was positioned on the east – west line direction, the weather conditions of this direction, such as solar radiation, wind speed, ambient temperature were manually measured, four days November 2nd,6th, 7th, and 10th for the east – west line direction. Figure 5.1 depicts the solar radiation intensity of four days of East – West line direction. The maximum value of solar radiation intensity occurred with, November 2nd, which reached (811 W/m^2) more than November 6th, 7th, and 10th by 15%, 22%, and 28.3% respectively.

Figure 5.2 depicts the ambient temperature of the east – west line direction, the maximum value of ambient temperature occurred with November 2nd, with reached (304.65 K), and it is more than the ambient temperature of November 6th, 7th, and 10th by 1.2%, 6.6%, and 6.3% respectively. Figure 5.3 depicts the wind speed of East – West line direction, the maximum value of wind speed occurred with November 2nd reach (4.1 m/s), and it is more than wind speed of November 6th, 7th, and 10th by 19.5%, 8%, and 7.3% respectively.

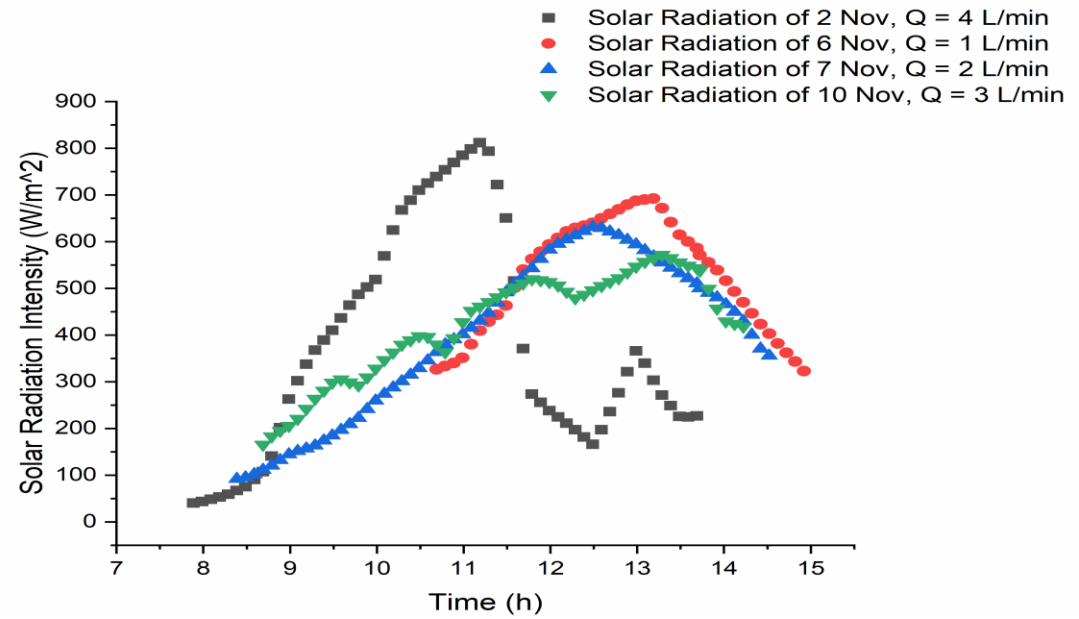

Fig.5.1. Solar Radiation Intensity of East – West Line Direction of Four Days November 2nd,6th, 7th, and 10th .

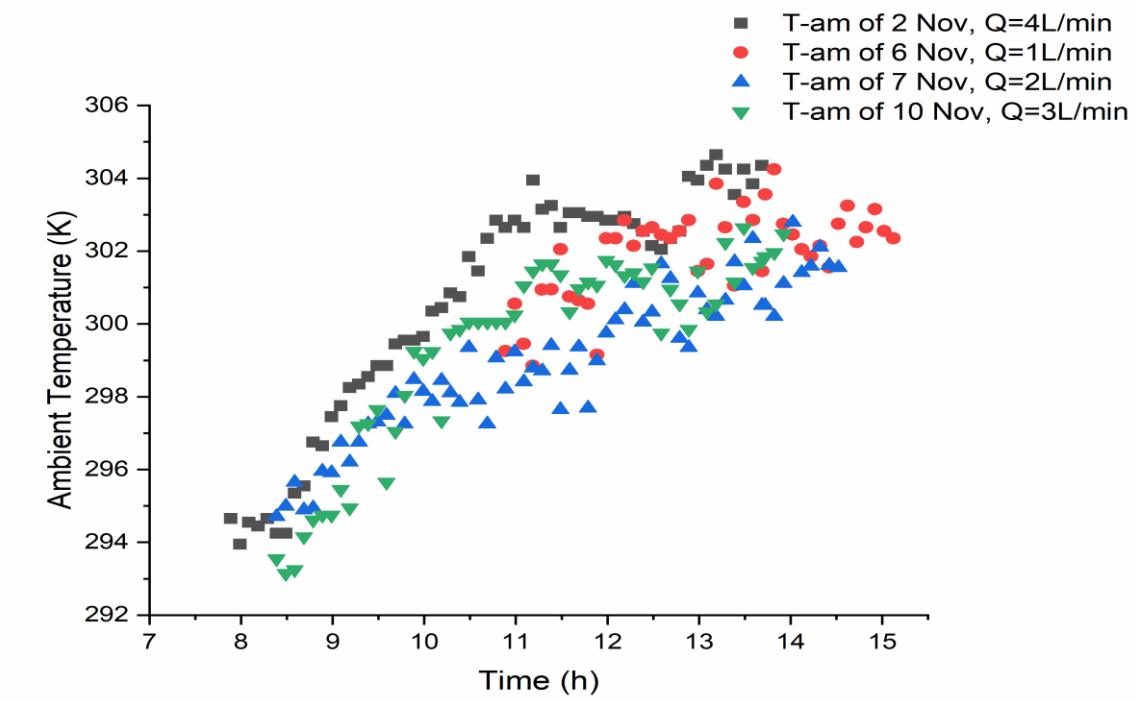

Fig.5.2. Ambient Temperature of East – West Line Direction of Four Days November 2nd,6th, 7th, and 10th .

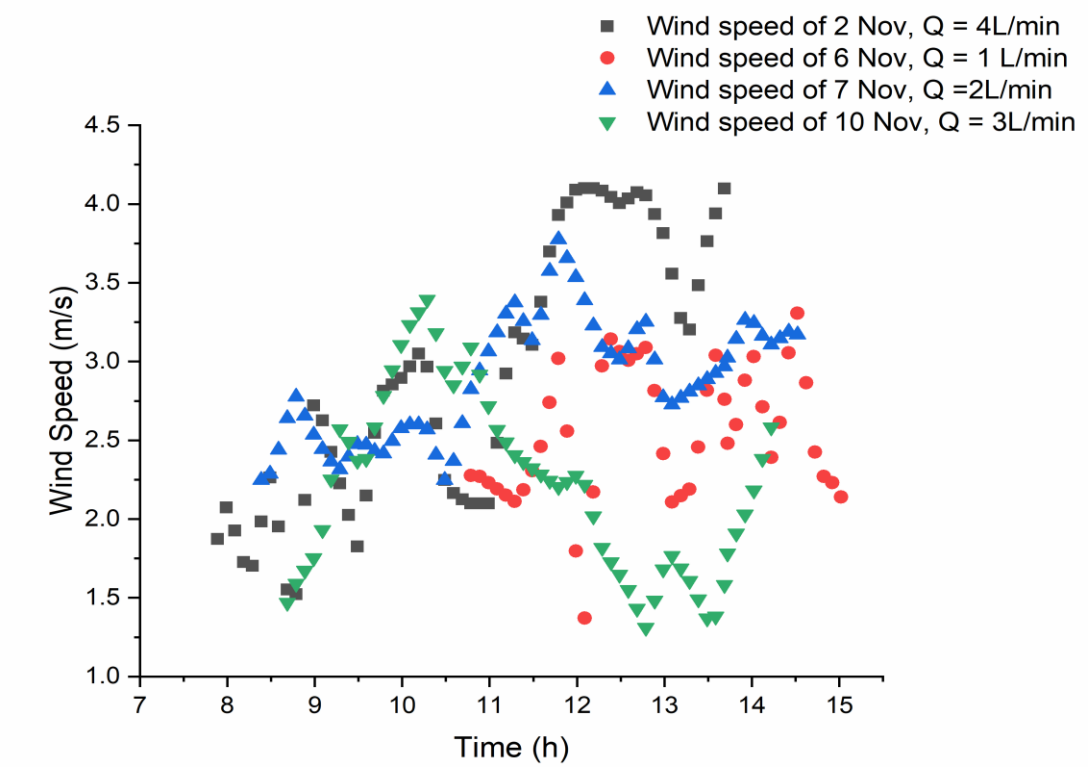

Fig.5.3. Wind Speed of East – West Line Direction of Four Days November 2nd,6th, 7th, and 10th .

The results of the experiments show the important parameters that indicate the thermal performance of a parabolic trough collector. The flow rate of heat transfer fluid used in experiments remained constant at single flow rate each day. Specifically, the flow rates for November 2nd,6th, 7th, and 10th were 4,1,2, and 3 L/min respectively. The working fluid used in experiments is water.

Figure 5.4 shows that the output temperature of four days of east-west direction the maximum value reached on November 6th is 336.65 K, which that is more than November 2nd,7th, and 10th by 6.8%, 4.4%, and 5.6% respectively. The maximum value of output temperature on November 6th is due to the fact that the water flow rate on this day is less

than the range of 1 L/min between other ranges on other days. November 7^{th} = 2 L/min, November 10^{th} = 3 L/min, andNovember 2^{nd} = 4 L/min.

The flow rate has an effect on the output temperature range because decrese flow rate leads to high number of water molecular flowing through a given point, resulting in a long time needed to heat them up.

Figure 5.5 depicts the temperature difference between the output temperature and the input temperature; the maximum value is reached on November 6^{th} with 22 K, which is greater than the values on November 2^{nd} , 7^{th} , and 10^{th} with 84%, 56%, and 77.7%, respectively, because a large volume of water will need more energy to heat up than a small volume, resulting in less significant temperature rise.

Figure 5.6 depicts the useful heat of working fluid and the maximum value obtained on November 6^{th} at 1485 W, which is greater than the values obtained on November 2^{nd} , 7^{th} , and 10^{th} by (50.6%,12%, and 42%) respectively, because the useful heat is directly proportional to temperature difference, and the value of temperature difference on November 6^{th} is greater than another day.

Figure 5.7 depicts the total heat losses of the parabolic trough collector, and heat losses occur as a result of convection process by ambient condition and absorber tube, and heat losses occur as a result of radiation process by absorber tube. The less range of heat losses refers to the best experiment, the less value of heat losses with November 2^{nd} with an average value of 192 W, which is less than November 6^{th} , 7^{th} , and 10^{th} by 56%, 66%, and 34% respectively.

Figure 5.8 shows the thermal efficiency of four days of east–west direction. The maximum value of thermal efficiency is reached on November 6th reached 68.7%, which is higher than the values on November 2nd , 7th , and 10th by 64%, 24%, and 33%, respectively. The maximum value of thermal efficiency is directly proportional to useful heat.

Figure 5.9 shows the value of the Nusselt number of four days of east–west line direction. The maximum value of the Nusselt number is (34) with day November 2nd , which is greater than the values of November 6th , 7th , and 10th by 58%, 29%, and 6% respectively. The maximum value of the Nusselt number is equivalent to a high range of flow rate because the Nusselt number is directly proportional to the heat convection coefficient which increase with flow rate of the working fluid increase.

Figure 5.10 shows the Reynolds number for four days in the east-west line direction November 2nd , 6th , 7th , and 10th with flow rates 4, 1, 2, and 3 L/min respectively. The maximum value of the Reynold number occurred on day of November 2nd , when Q = 4 L/min, which reached 4428.5, was higher than other days of November 6th , 7th , and 10th by 61.6%, 30.5%, and 12.2%, respectively. This result because there is a direct relationship between Reynolds number and working fluid (water) velocity; as water velocity increases lead to increase the Reynold number.

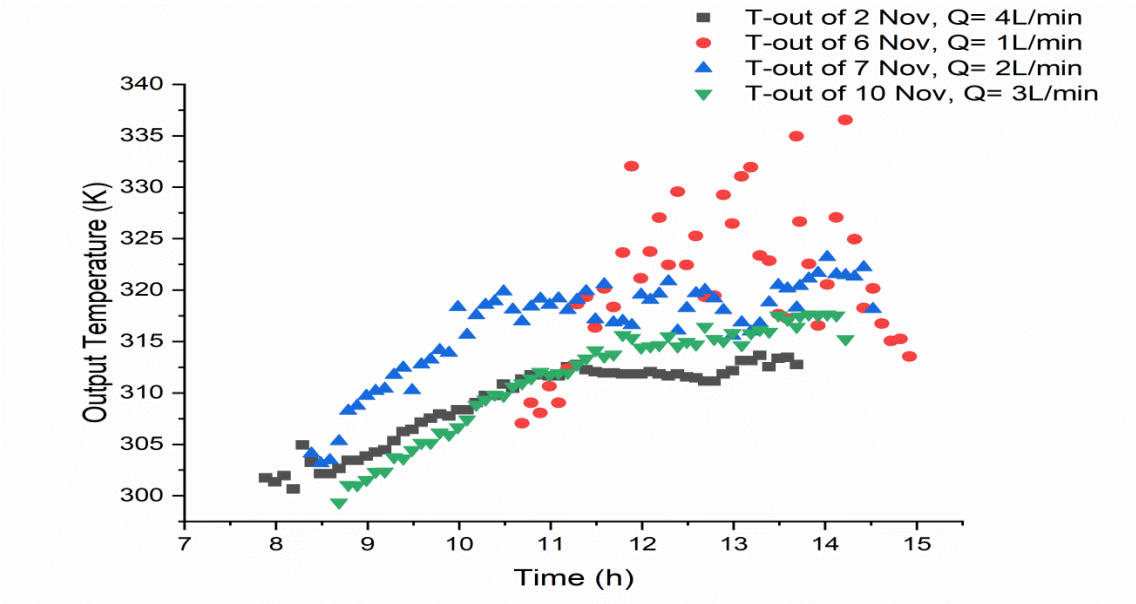

Fig.5.4.Output Temperature of East – West Line Direction of Four Days November 2nd,6th, 7th, and 10th with Flow rate (4,1,2, and 3) L/min Respectively.

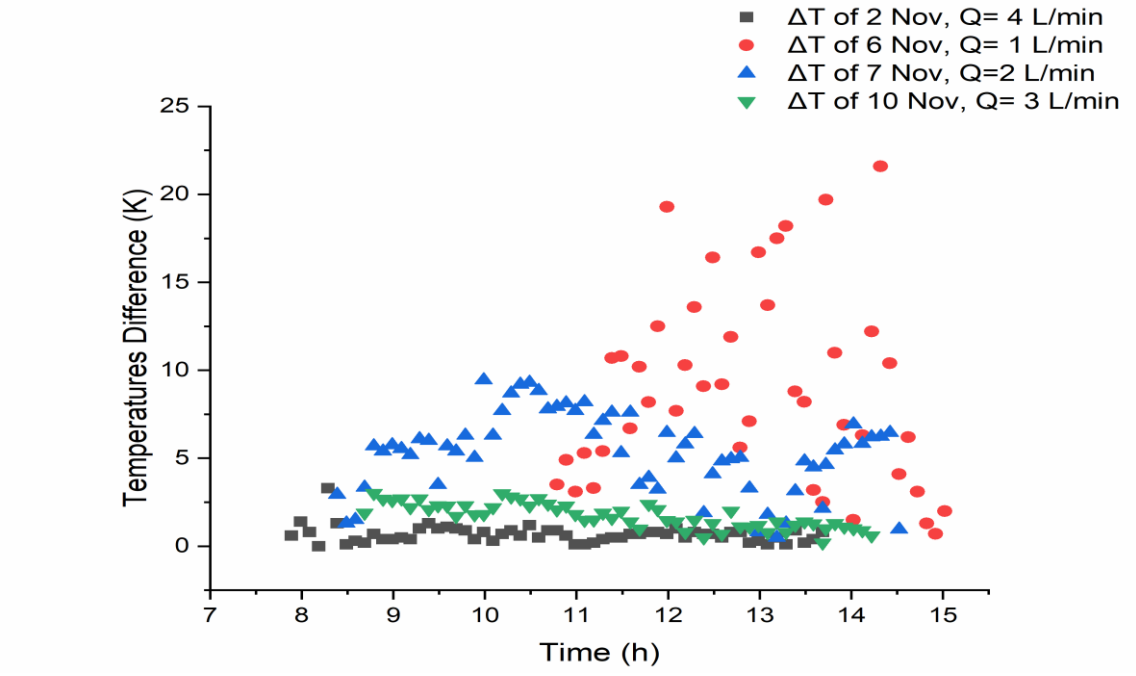

Fig.5.5. Temperature Difference of East – West Line Direction of Four Days November 2nd,6th, 7th, and 10th with Flow rate (4,1,2, and 3) L/min respectively.

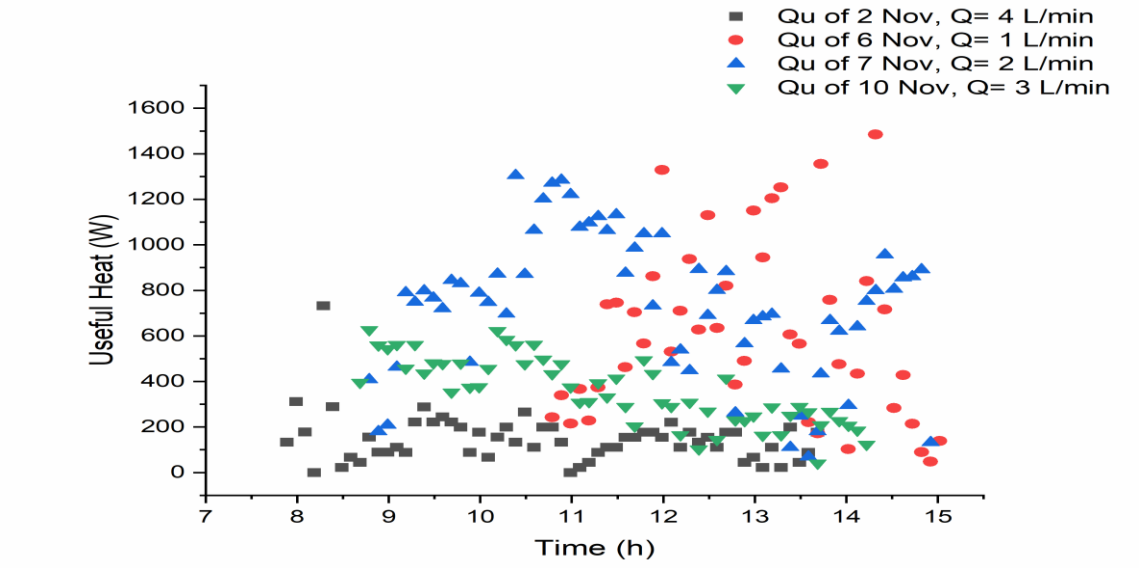

Fig.5.6.Useful Heat of East – West Line Direction of Four Days November 2^{nd},6^{th}, 7^{th}, and 10^{th} with Flow Rate (4,1,2, and 3) L/min Respectively.

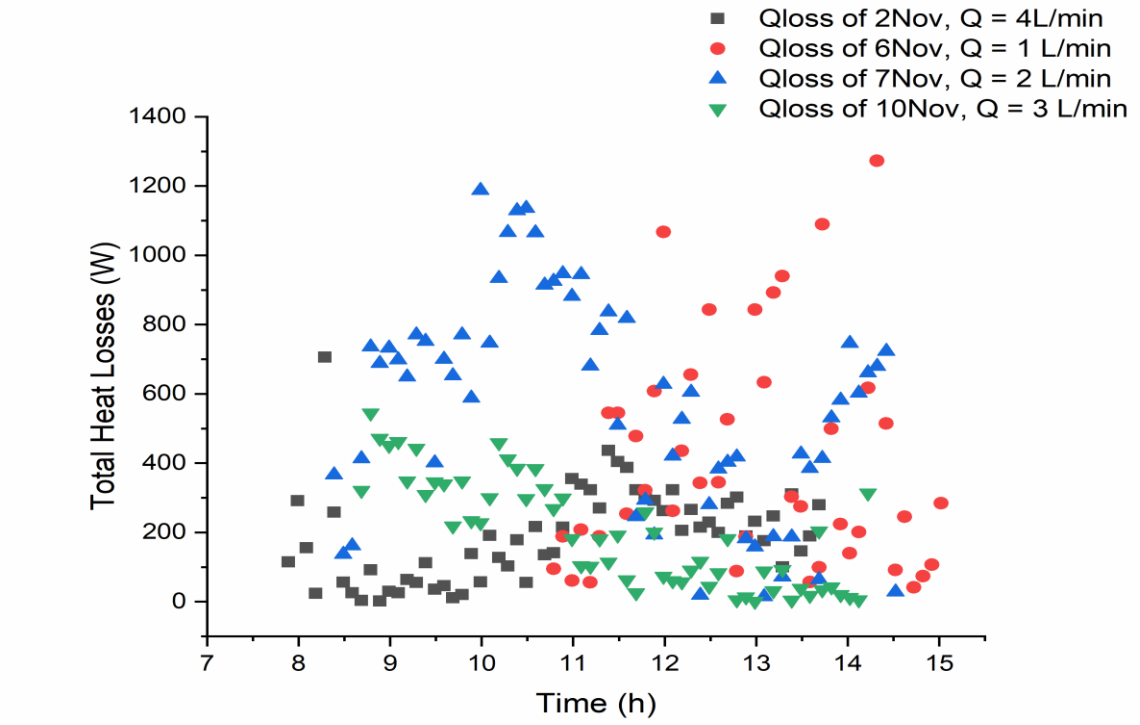

Fig.5.7.Total Heat Losses of East – West Line Direction of Four Days November 2^{nd},6^{th}, 7^{th}, and 10^{th} with Flow Rate (4,1,2, and 3) L/min Respectively.

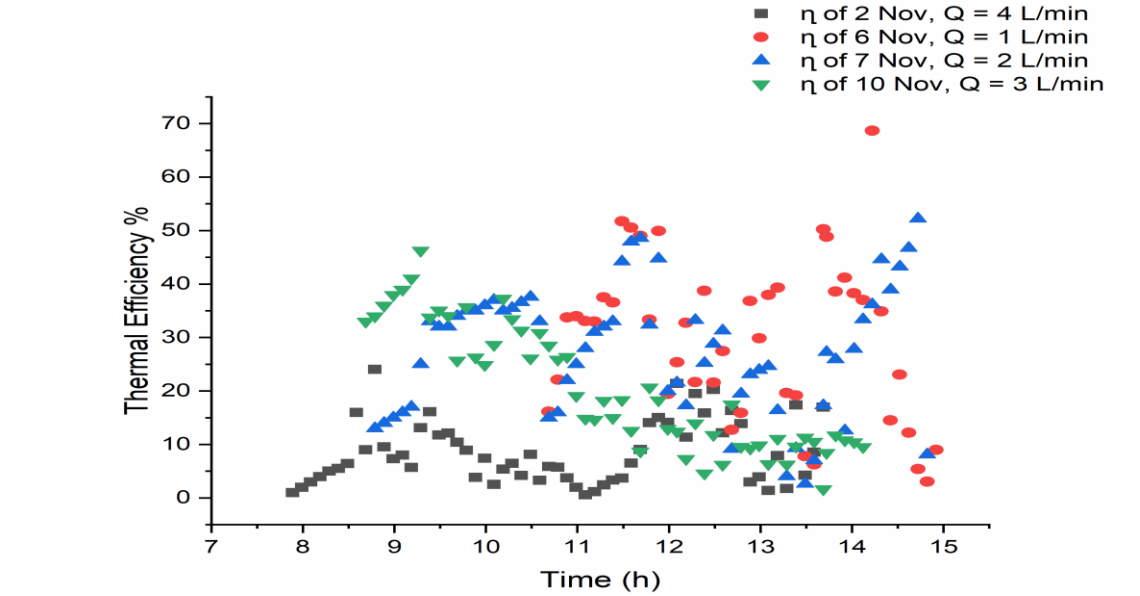

Fig.5.8. Thermal Efficiency of East – West Line Direction of Four Days November 2nd,6th, 7th, and 10th with Flow Rate (4,1,2, and 3) L/min Respectively.

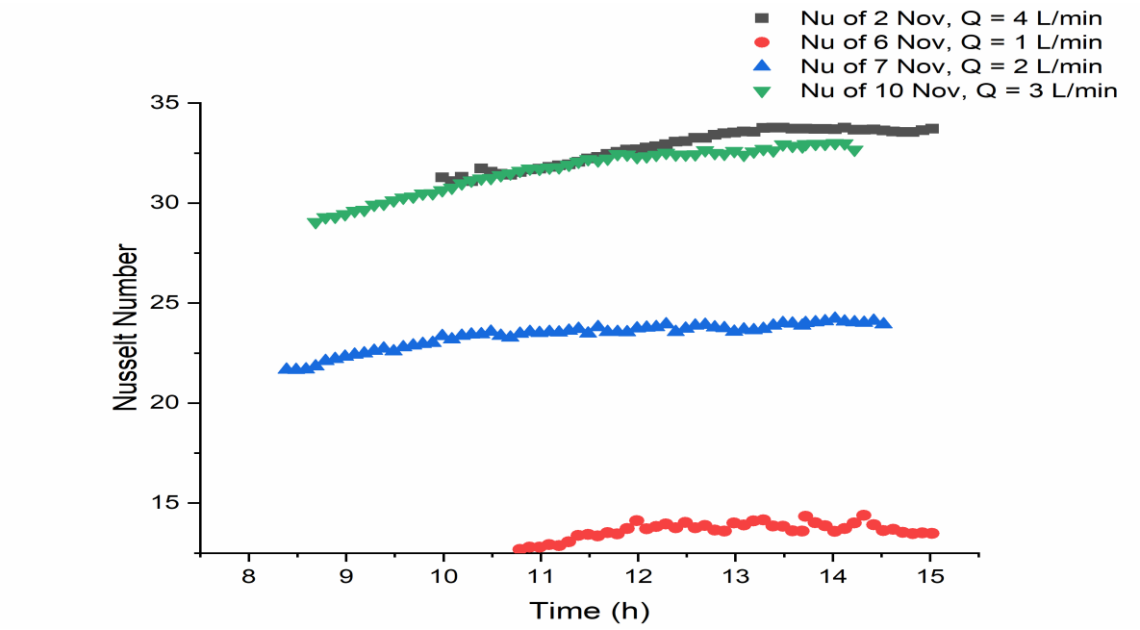

Fig.5.9. Nusselt Number of East – West Line Direction of Four Days November 2nd,6th, 7th, and 10th with Flow Rate (4,1,2, and 3) L/min Respectively.

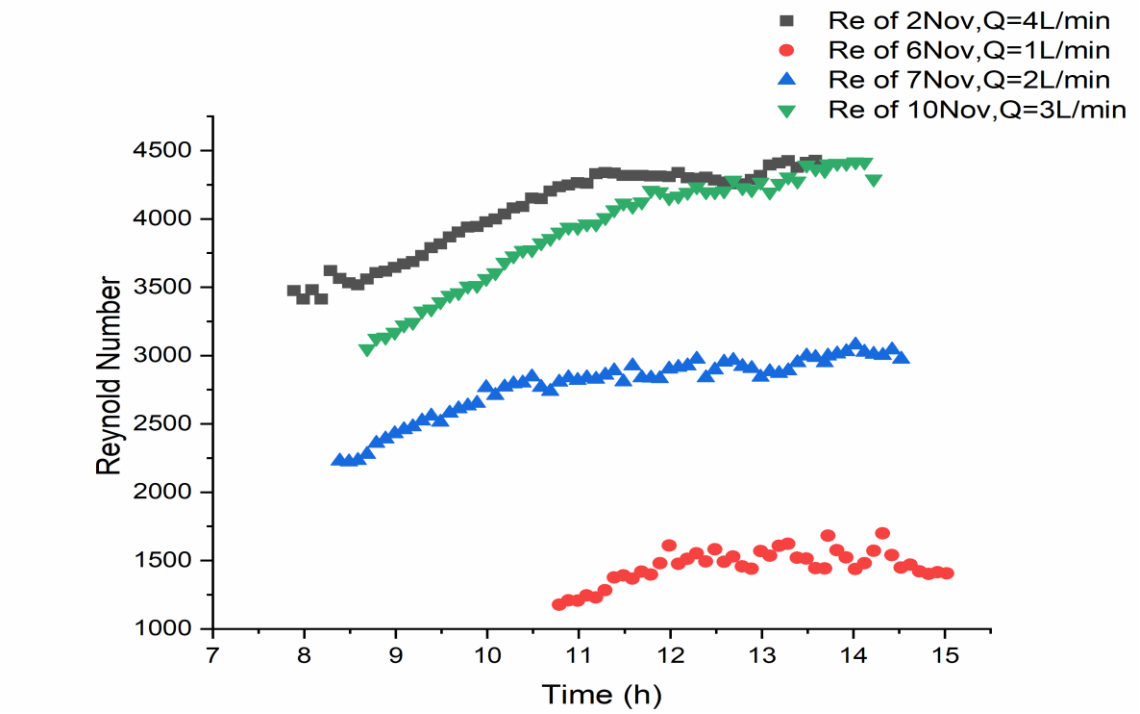

Fig.5.10. Reynold Number of East – West Line Direction of Four Days November 2nd,6th, 7th, and 10th with Flow Rate (4,1,2, and 3) L/min Respectively.

5.2.1.2. The Direction from South to North

The experiments were also conducted the south-north line direction, with working fluid (water) flow rates of 1, 2, 3, and 4 L/min on November 13th, 14th, 20th, and 21st respectively. The important thermal behavior parameters are established, including output temperature, temperature difference, useful heat or heat gain, total heat losses, thermal efficiency, Nusselt number, and Reynold number. The results explain the thermal performance of a parabolic trough collector. The weather conditions of the days of the south-north line direction, such as solar radiation intensity, ambient temperature, and wind speed, were manually recrded.

Figure 5.11 depicts the solar radiation intensity over four days in the south–north line direction. The maximum value of solar radiation intensity was reached on November 13th (656.8 W/m^2), which is higher than the other south-north line direction days of November 14th,20th, and 21st by 11.5%,14.8%, and14.7% respectively.

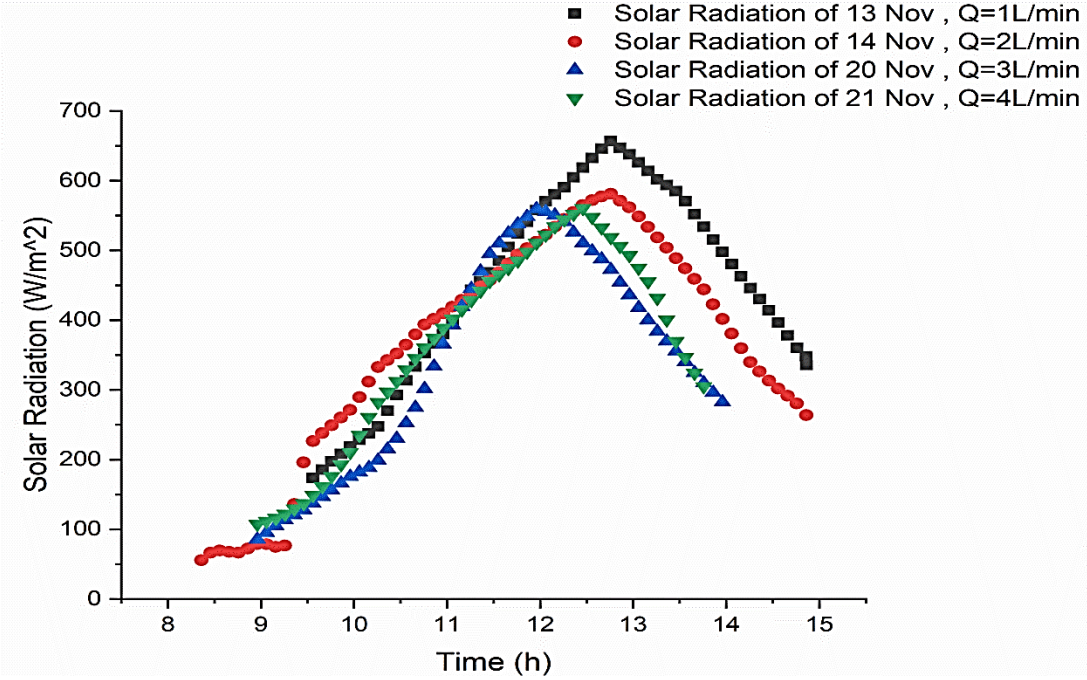

Fig.5.11. Solar Radiation Intensity of South – North Line Direction of Four Days November 13th, 14th, 20th, and 21st Respectively.

Figure 5.12 depicts the ambient temperature in the south-to-north direction; the maximum value occurred on November 13th and reached 300.35 K, which is 0.03%, 0.89%, and 0.26% higher than the ambient temperatures of November 14th, 20th, and 21st respectively. The wind speed of the south- -north line direction is depicted in Figure 5.13; the maximum value of wind speed occurred with a November 13th reached (5.18 m/s),

and it is greater than the wind speed of 14th, 20th, and 21st respectively by 11.1%, 9.4%, and 7.3%, respectively.

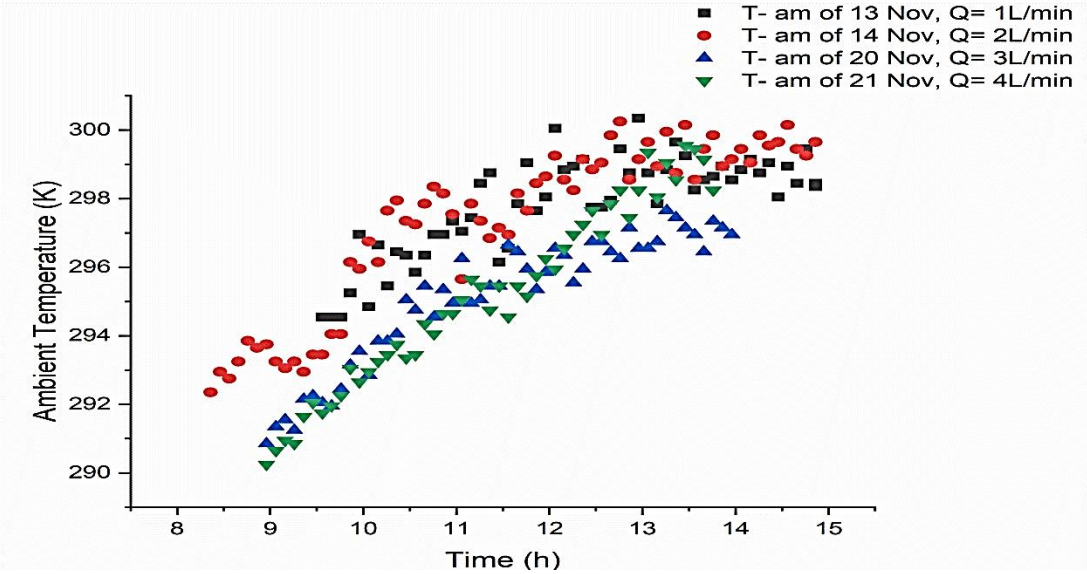

Fig.5.12. Ambient Temperature of South – North Line Direction of Four Days November 13th, 14th, 20th, and 21st Respectively.

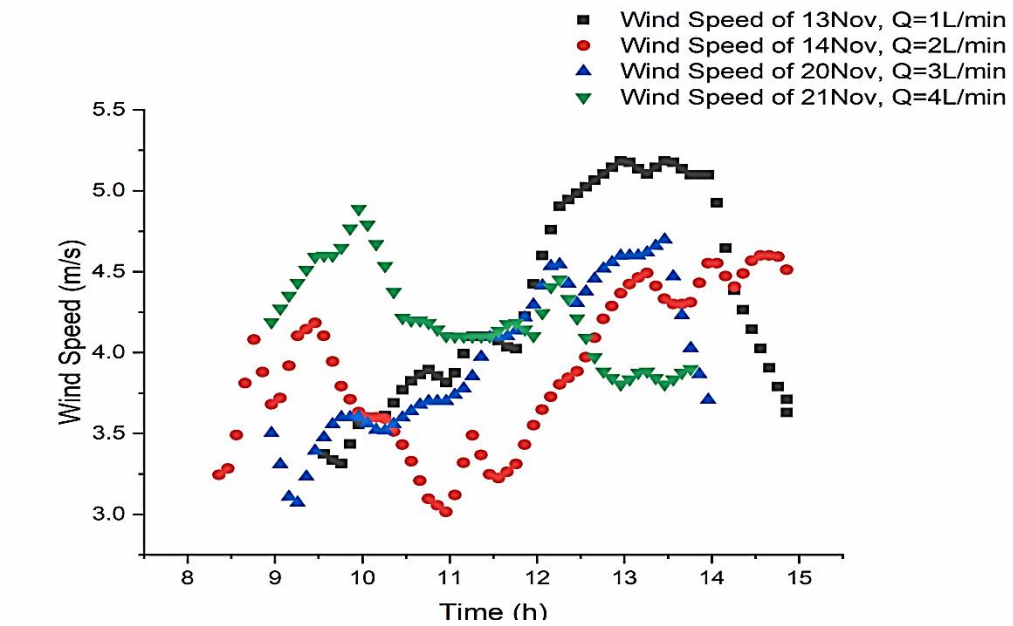

Fig.5.13. Wind Speed of South – North Line Direction of Four Days November 13th, 14th, 20th, and 21st Respectively.

Figure 5.14 depicts the output temperature of the south-north line direction, with the maximum value of the output temperature founded with day November 13th reached 328.35 K, which is 3%, 4%, and 5% higher than the other days November 14th, 20th, and 21st respectively. Because of the decrese flow rate leads to high number of water molecular flowing through a given point, resulting in a long time needed to heat them up, resulting in a higher output temperature.

Figure 5.15 shows the temperature difference of four days in the south–north line direction with different working fluid flow rates November 13th, 14th, 20th, and 21st with flow rates (1, 2, 3, and 4) L/min respectively. The maximum four-day temperature difference in the south-north line direction with November 13th reached (14 K), which was greater than November 14th, 20th, and 21st by (35.7 %, 59.2%, and 75%) respectively.

Figure 5.16 shows the useful heat of working fluid (water) over four days in the south–north line direction. The maximum value occurred on November 14th , reached 1241.2 W, which is more than days November 13th, 20th, and 21st by (22%, 5%, and 24%), respectively. The reason for this result is that the maximum value of useful heat occurred on November 14th because the flow rate on this day was 2 L/min and the temperature difference was high. The useful heat depends on the first step fluid flow rate and temperature difference, so the maximum value of useful heat occurred on November 14th.

Figure 5.17 depicts the total heat losses and the average less value of heat losses on November 21st reached 252.2 W, which is less than the other days November 13th, 14th, 20th, and 21st by (25%, 11.5%, and 23%),

respectively. The reason is increasing the mass flow rate leads to a higher number of water molecular flowing through a given point.

Figure 5.18 depicts the thermal efficiency of a parabolic trough collector with working fluid (water) over four days November 13th, 14th, 20th, and 21st. Because thermal efficiency has a direct proportional relationship with useful heat, the maximum value of thermal efficiency occurred on November 14th reached 49.5%, which was higher than other days in the south-north line direction November 13th, 20th, and 21st by (11%, 8%, and 4%) respectively.

Figure 5.19 depicts the Nusselt number of four days in a south-to-north direction, with the maximum value appearing on day of November 21st , Q = 4 L/min reaching 42.78, which is greater than any other day November 13th, 14th, and 20th by 67%, 43%, and 22%, respectively. The reason for this is that as the fluid flow rate increases, Nusselt number has a direct proportional relationship with the heat transfer coefficient and the heat transfer coefficient increasing with velocity of working fluid.

Figure 5.20 depicts the value of the Reynold number for four days in the south-north line direction, with the maximum value occurring on November 21st, when Q = 4 L/min, and Re = 6428.963, which was greater than the other days November 13th, 14th, and 20th by 75.3%, 52.5%, and 31% respectively. The reason for this is that the Reynolds number is proportional to the velocity of the working fluid, as the velocity of the working fluid increases, so does the Reynolds number.

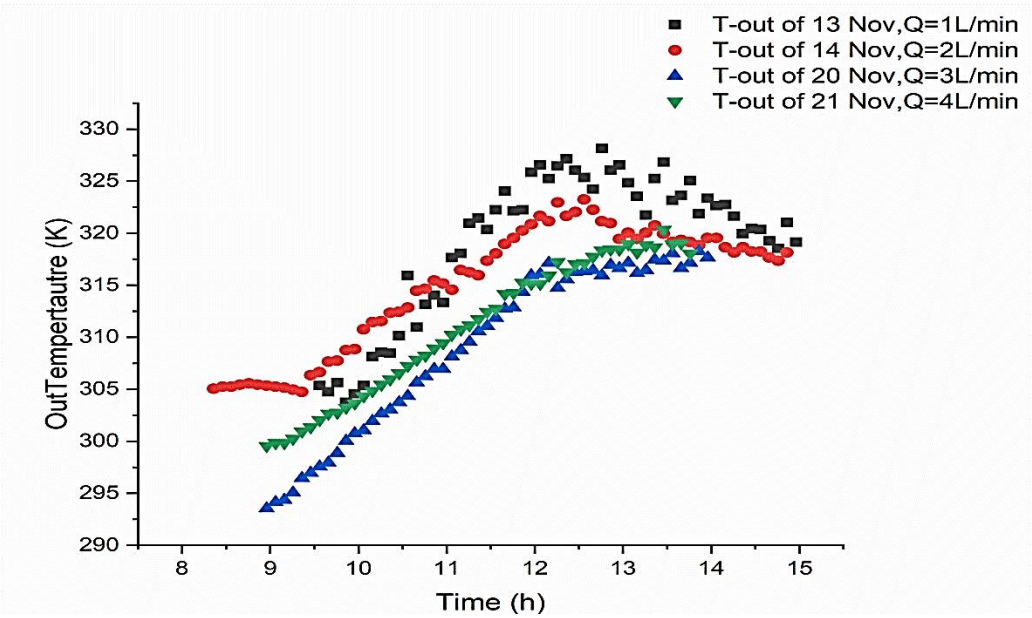

Fig.5.14. Output Temperature of South – North Line Direction Days November 13th, 14th, 20th, and 21st with Flow Rate 1,2,3, and 4 L/min Respectively.

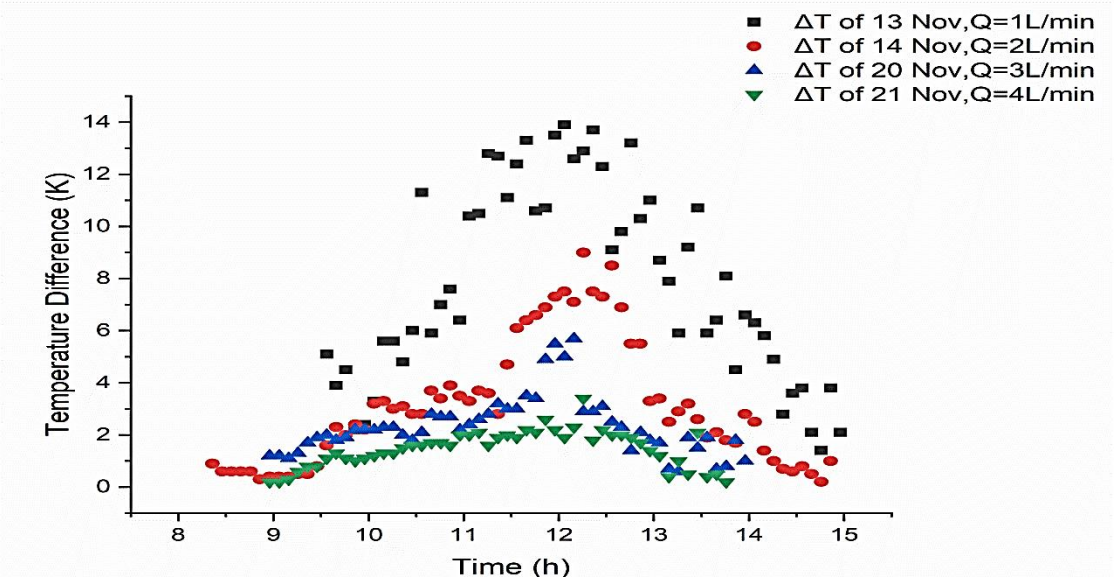

Fig.5.15. Temperature Difference of South – North Line Direction Days November 13th, 14th, 20th, and 21st with Flow Rate 1,2,3, and 4 L/min Respectively.

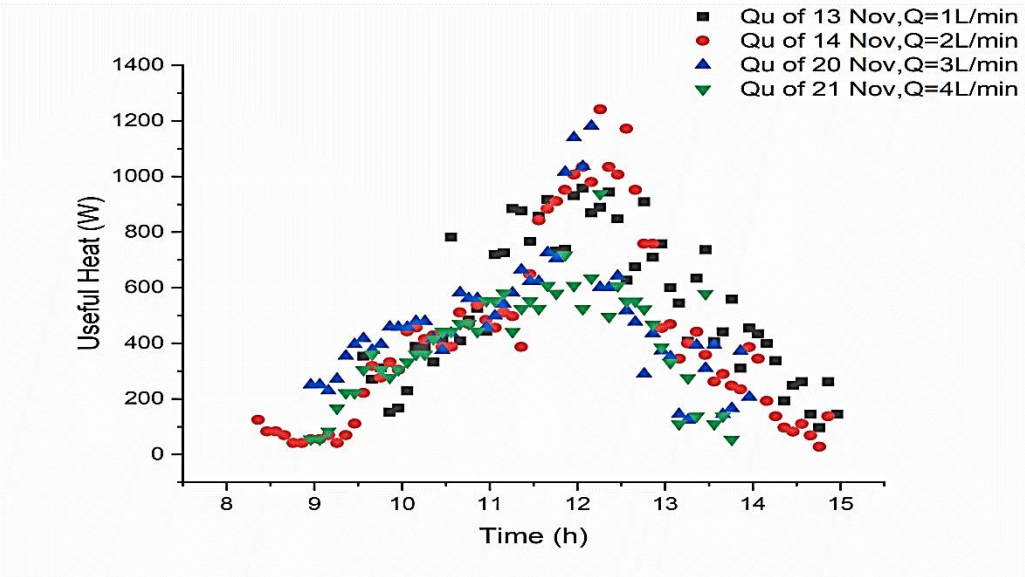

Fig.5.16. Useful Heat of South – North Line Direction Days November 13th, 14th, 20th, and 21st with Flow Rate 1,2,3, and 4 L/min Respectively.

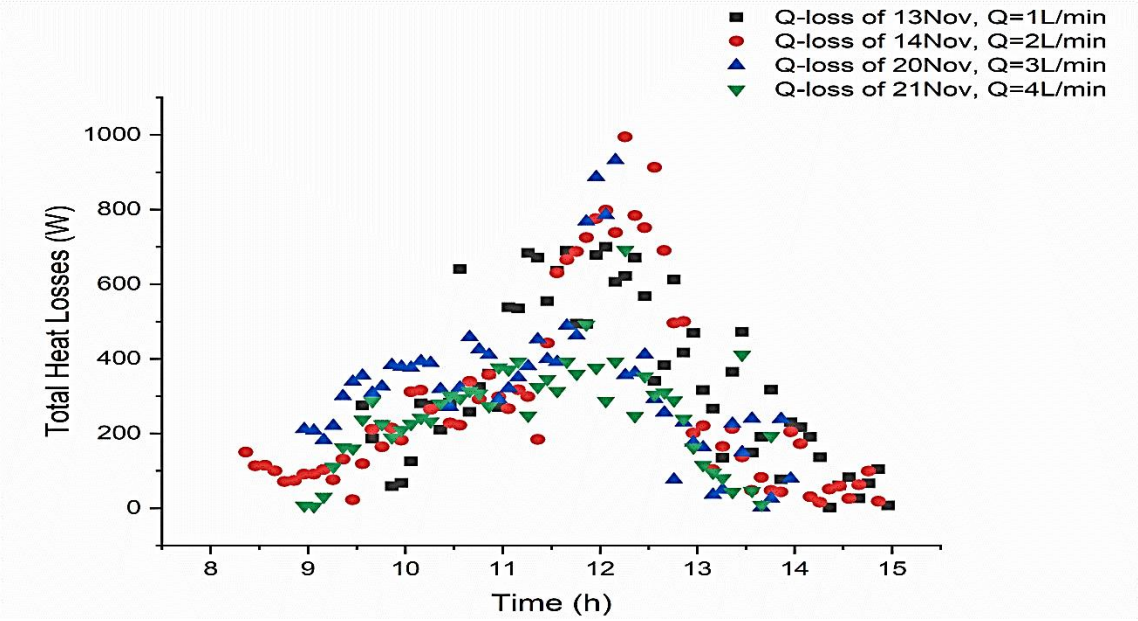

Fig.5.17. Total Heat Losses of South – North Line Direction Days November 13th, 14th, 20th, and 21st with Flow Rate 1,2,3, and 4 L/min Respectively.

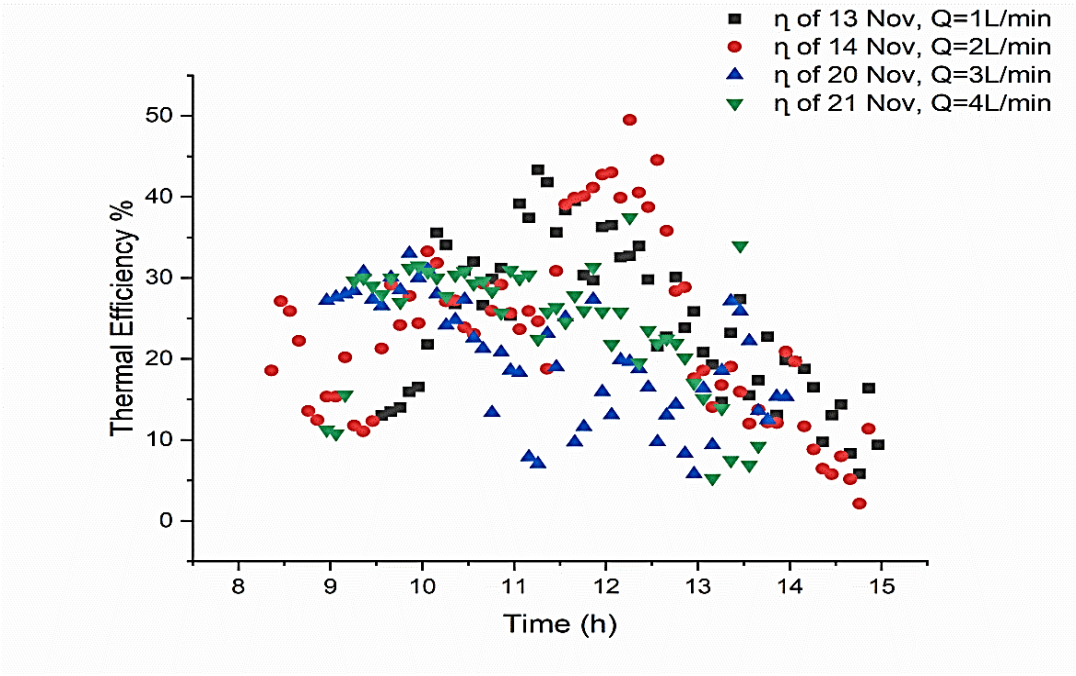

Fig.5.18. Thermal Efficiency of South – North Line Direction Days November 13th, 14th, 20th, and 21st with Flow Rate 1,2,3, and 4 L/min Respectively.

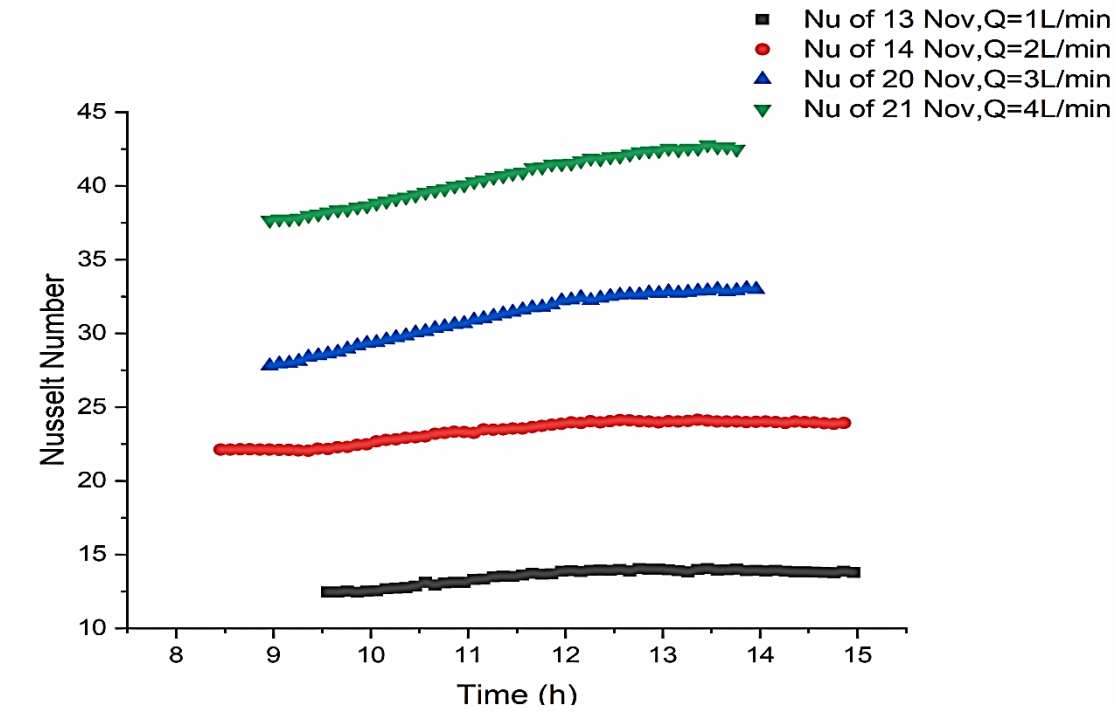

Fig.5.19. Nusselt Number of South – North Line Direction Days November 13th, 14th, 20th, and 21st with Flow Rate 1,2,3, and 4 L/min Respectively.

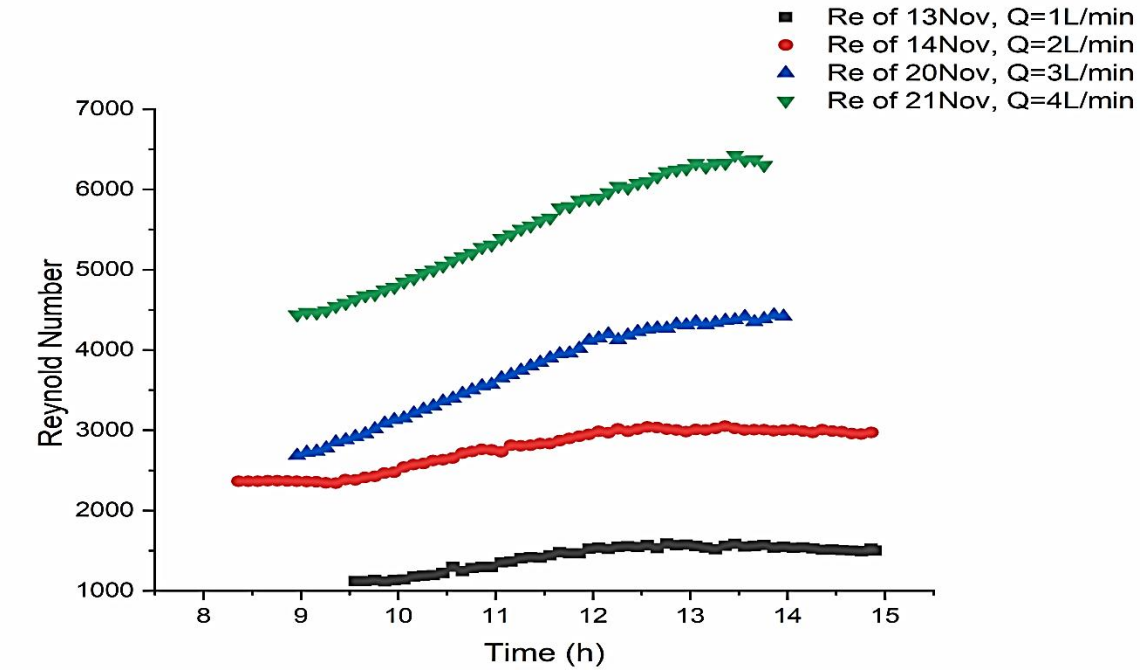

Fig.5.20. Reynold Number of South – North Line Direction Days November 13th, 14th, 20th, and 21st with Flow Rate 1,2,3, and 4 L/min Respectively.

5.2.1.3. Comparing between Two Lines Direction (East – West)&(South – North) of PTC.

When comparing two lines of parabolic trough collector direction in terms of the effect on thermal performance of parabolic trough collector. In the experiments, there are two lines direction : one from east to west and another from south to north. The day of the east-west line direction with a flow rate equal to 1 L/min is November 6th , and the day of the south-north line direction with a flow rate equal to 1 L/min is November 13th.

Figure 5.21 depicts the solar radiation over two days in the parabolic trough collector's two line directions (east-west and south-north). The maximum value of solar radiation occurred on the east–west line direction

day of Novembern 6th, which reached (692.313 W/m^2), which was more than the other south–north line direction day of November 13th by (5.1%).

Figure 5.22 depicts the ambient temperature of two days for both line directions of the parabolic trough collector (east-west and south-north); the maximum value of the ambient temperature occurred on day November 6th for the east-west line direction, which reached 304.25K, 1.3% higher than the other south-north line direction day November 13th.

Figure 5.23 depicts the wind speed over two days for two parabolic trough collector line directions (east-west and south-north). The maximum value of wind speed occurred on the south-north line direction day November 13th, reached 5.18 m/s, which was 36.3% higher than the other east-west line direction day November 6th.

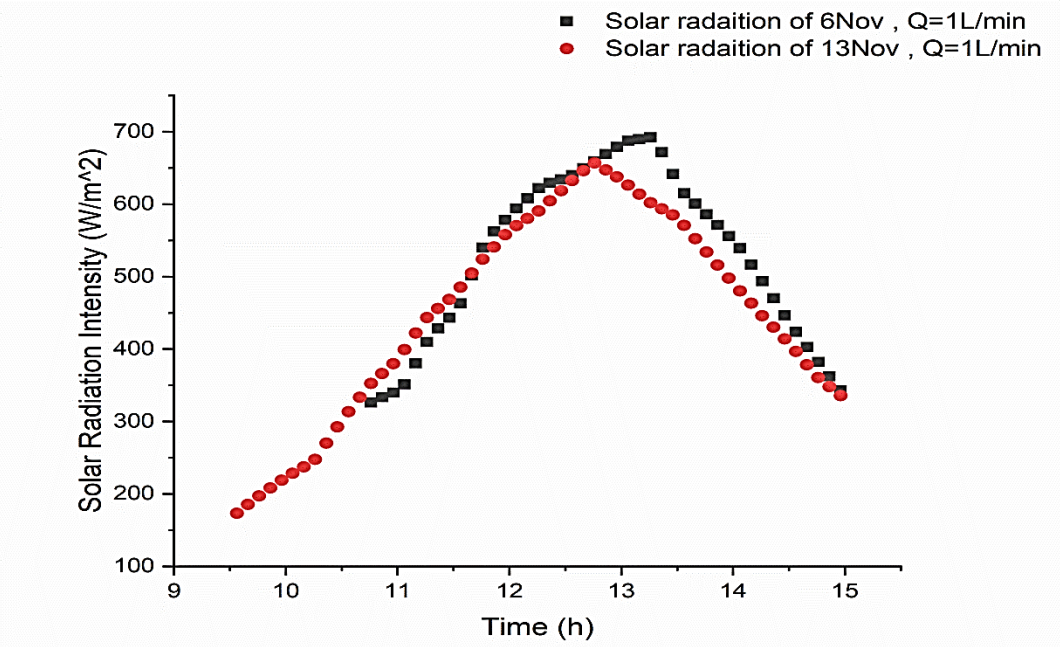

Fig.5.21. Solar Radiation of Two Days of East-West & South-North Line Direction with Constant Flow Rate Q=1 L/min.

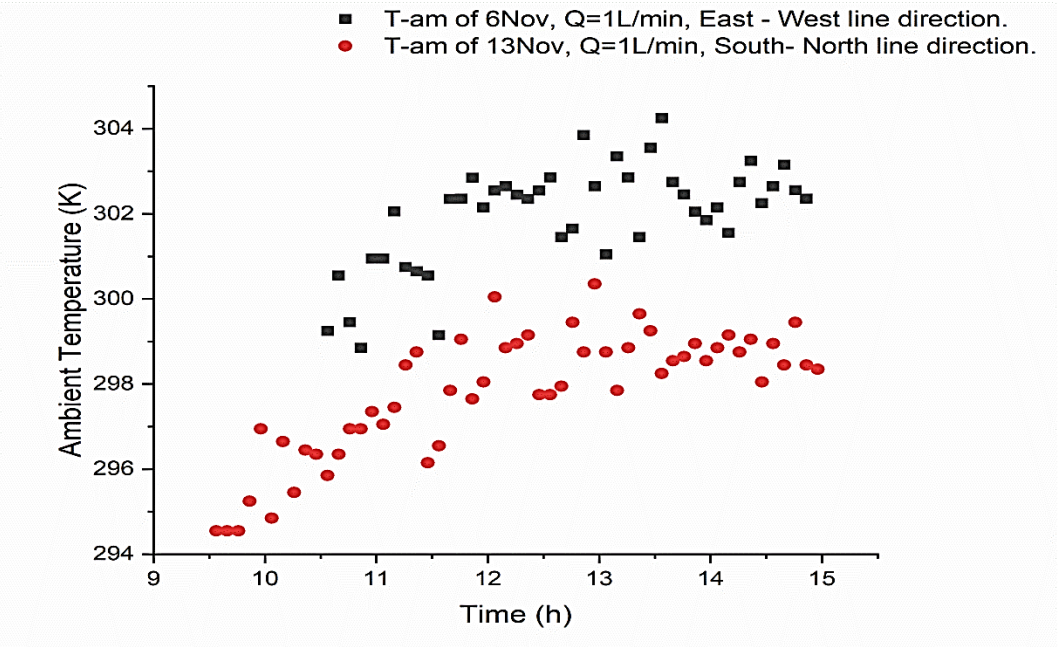

Fig.5.22. Ambient Temperature of Two Days of East-West & South-North Line Direction with Constant Flow Rate Q=1 L/min.

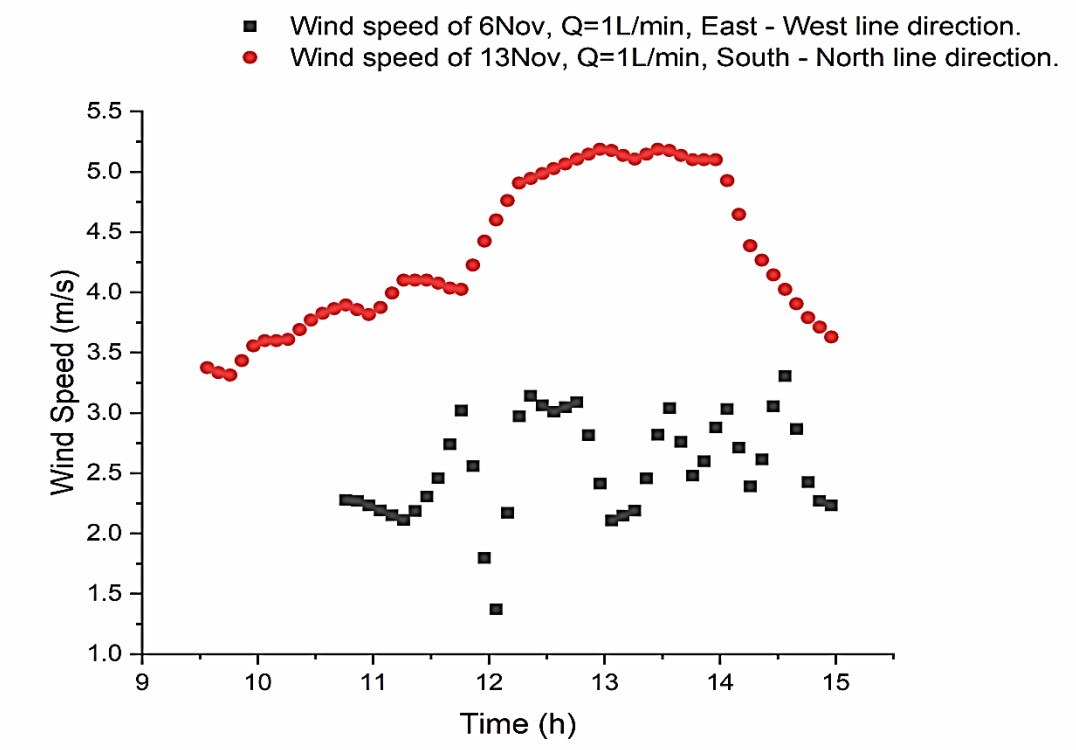

Fig.5.23. Wind Speed of Two Days of East-West & South-North Line Direction with Constant Flow Rate Q=1 L/min.

Figure 5.24 compares the outlet temperature on two line direction days: November 6th (east-west line direction) and November 13th (south-north line direction). The output temperature of both days with a constant flow rate of Q = 1 L/min reached 336.54 K on east-west day of November 6th, which was 2.53% higher than the other day of south-north day. Given the high value of the output temperature compared to east-west day November 13th, the reason for these results is the high amount of solar radiation intensity, high ambient temperature, and low wind speed of east-west day November 6th.

Figure 5.25 shows the temperature difference of two line direction days, east–west line direction day November 6th and south–north line direction day November 13th. The temperature difference of both days with a constant flow rate of Q=1 L/min reached a maximum value on the east-west day of November 6th, which reached (22 K), which was 35.6 % greater than the other day of the south-north day.

Figure 5.26 shows the useful heat of two line direction days, east–west line direction day November 6th and south–north line direction day November 13th . The useful heat of both days with a constant flow rate of Q = 1 L/min reached its maximum value on the east-west day of November 6th , which reached 1485.117 W, and this was more than the other day of the south-north day by 33.6%. This is because useful heat has a direct proportional relationship with temperature difference, and the day of November 6th had a higher temperature difference than the other day, November 13th, in the south-north line direction.

Figure 5.27 depicts the thermal efficiency of two line direction days, east–west line direction day November 6th and south–north line direction day November 13th. The thermal efficiency of both days with a constant flow rate of 1 L/min reached a maximum on November 6th, in the east-west direction, at 68.6% , which was 21% higher than the other day, November 13th , in the south-north direction.

Figure 5.28 depicts the Nusselt number of two line direction days, east–west line direction day November 6th and south–north line direction day November 13th . The Nusselt number reached 14.39 on both days with a constant flow rate of Q = 1 L/min, which was 2.3% higher than the other day November 13th in the south-north direction. Nusselt number has a inverse proportional relationship with the thermal conductivity, which decrese with increase of temperature difference of working fluid.

Figure 5.29 depicts Reynolds number of two line direction days, east–west line direction day November 6th and south–north line direction day November 13th. Reynolds number (1698.49) was reached on November 6th in the east-west direction, which was 6.5% higher than the other day, November 13th, in the south-north direction. Reynold number has a reverse proportional relationship with the dynamic viscosity of working fluid, which decreases with increasing output temperature, which leads to an increase in Reynold number.

As result, when comparing the thermal performance of a parabolic trough collector with an east–west line direction and a south–north line direction depending on the weather conditions and the important paramertes , the suitable direction for a parabolic trough collector was found to be the

east–west line direction, which has a high value for the thermal performance of a parabolic trough collector, as shown in the figures below.

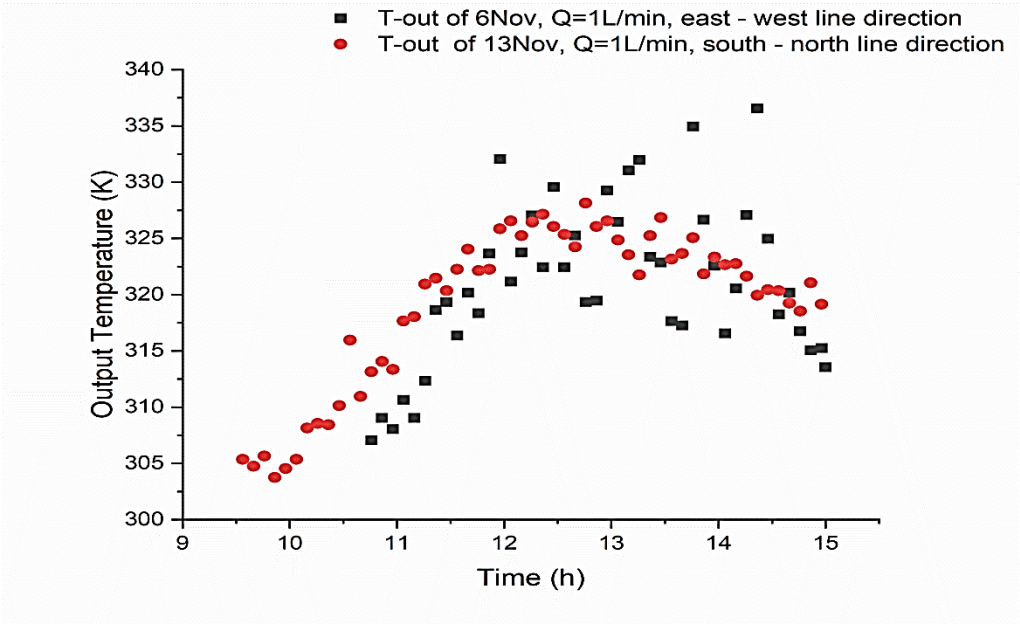

Fig.5.24. Output Temperature of Two Days of East - West & South - North Line Direction with Constant Flow Rate Q=1 L/min.

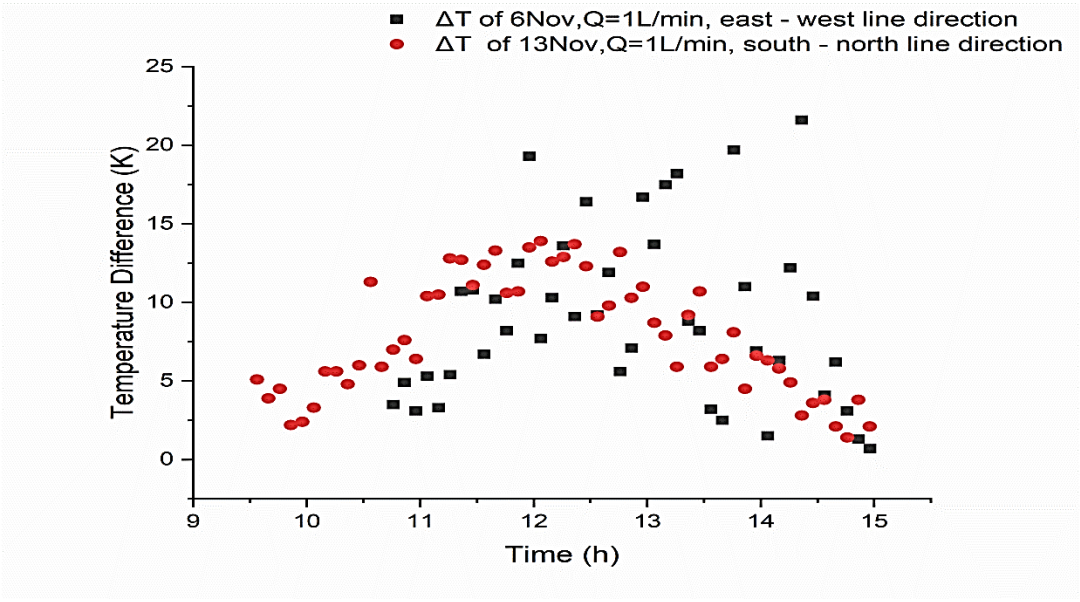

Fig.5.25.Temperature Difference of Two Days of East - West & South - North Line Direction with Constant Flow Rate Q=1 L/min.

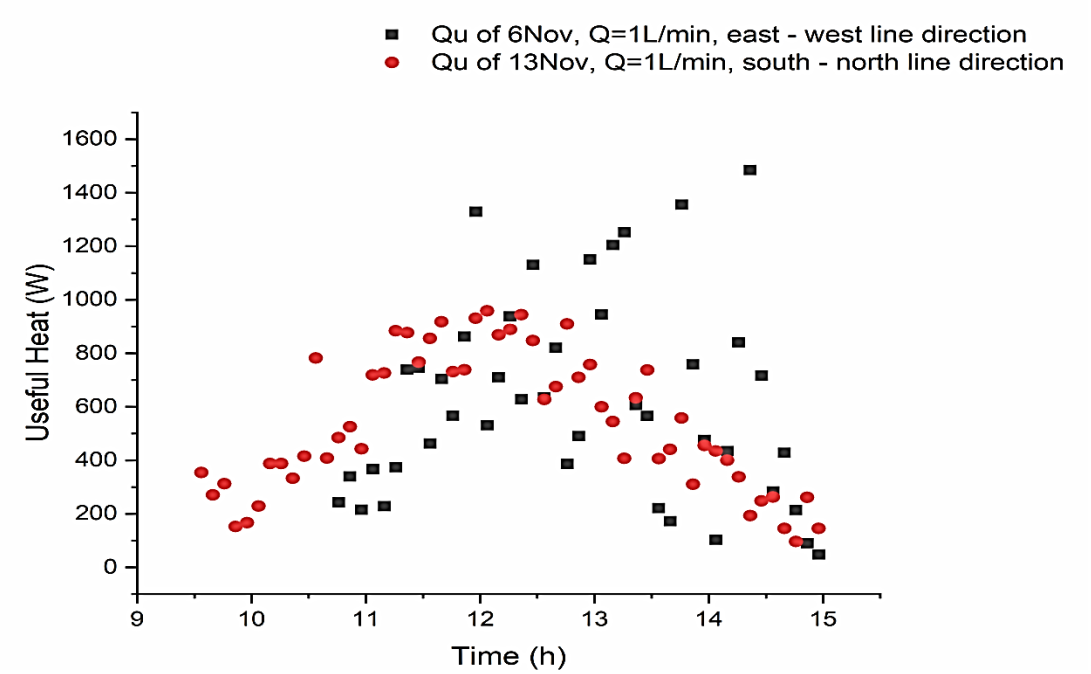

Fig.5.26.Useful Heat of Two Days of East - West & South - North Line Direction with Constant Flow Rate Q=1 L/min.

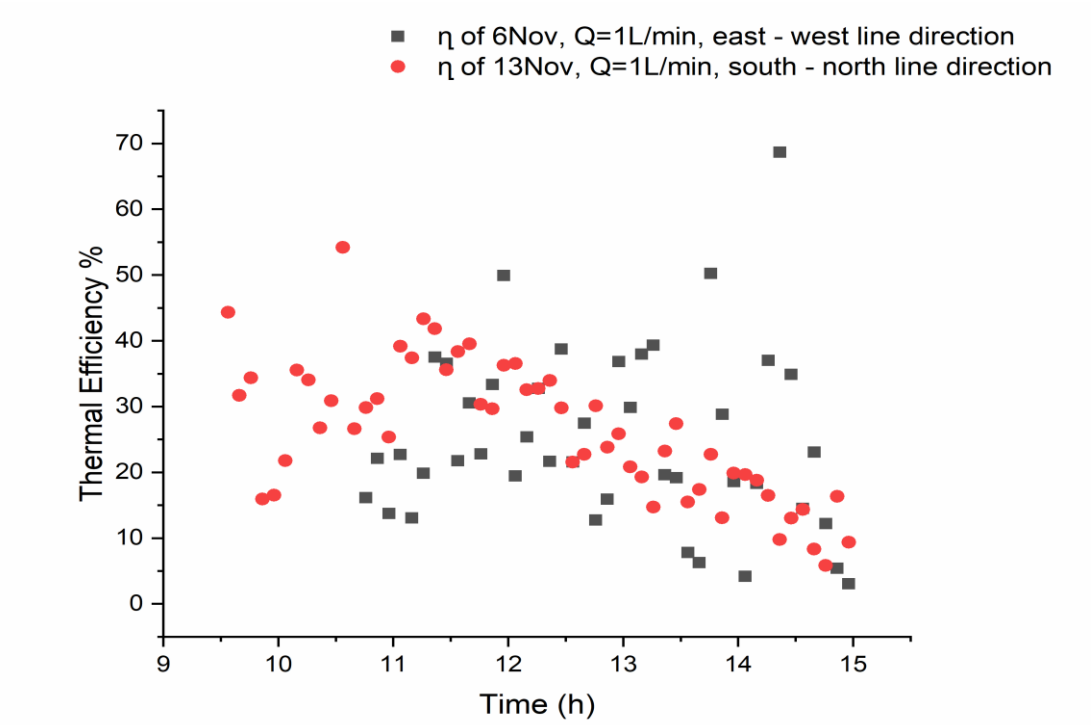

Fig.5.27.Thermal Efficiency of Two Days of East - West & South - North Line Direction with Constant Flow Rate Q=1 L/min.

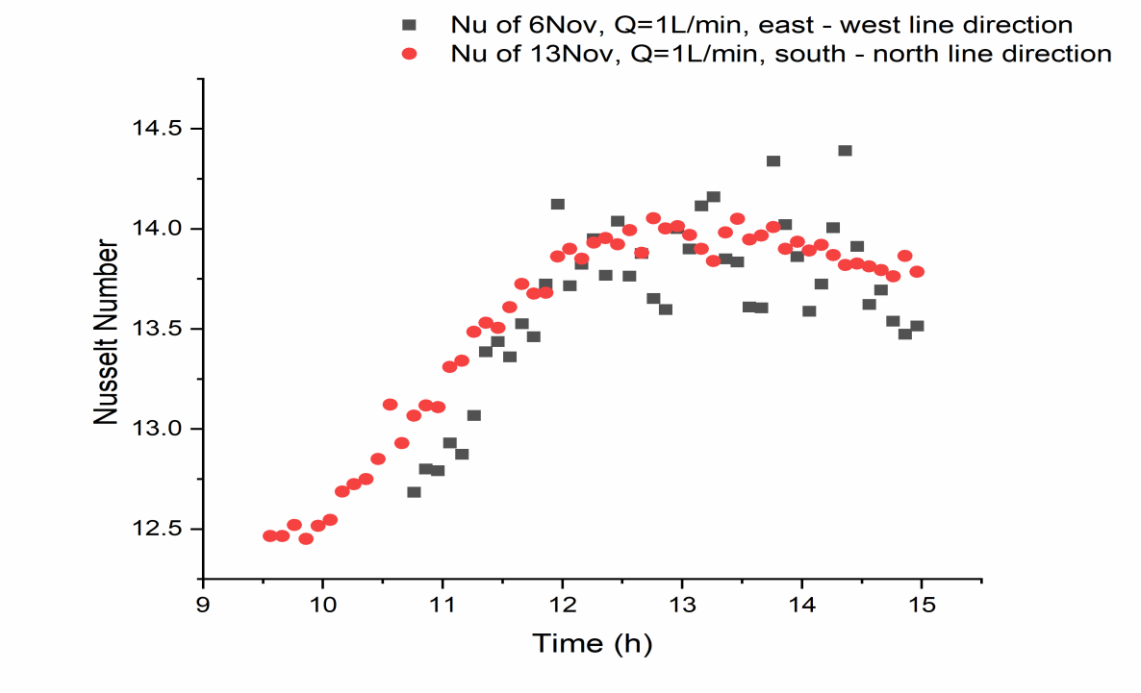

Fig.5.28.Nussult Number of Two Days of East - West & South - North Line Direction with Constant Flow Rate Q=1 L/min.

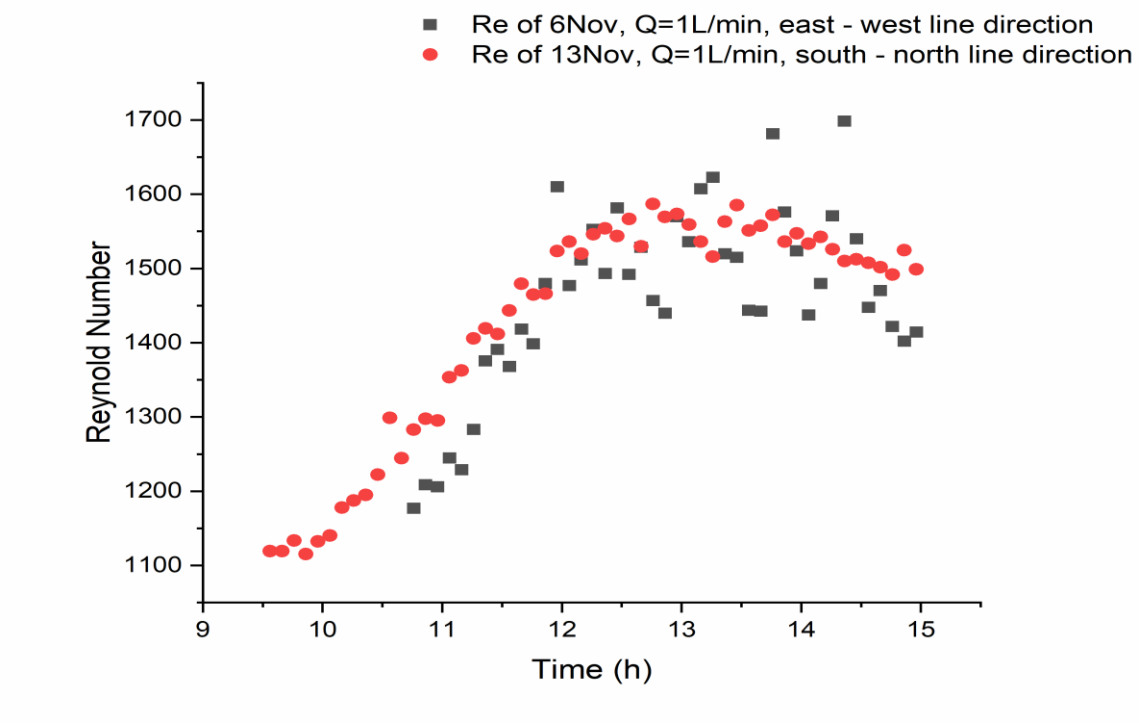

Fig.5.29.Reynold Number of Two Days of East - West & South - North Line Direction with Constant Flow Rate Q=1 L/min.

5.3. Numerical Results

A numerical simulation study based on the computational fluid dynamics (CFD) principle was conducted to compare the numerical results with experimental results. In this study, the first step of numerical simulation is chosen from a previous study based on model parameters and its results are compared to complete the validation process. A numerical model was built and developed by using COMSOL Multiphysics Version 6.0 simulation software according to Table 3.1 the characteristics of Balil Lamrani et al. 2018 [63], to investigate the thermal behavior of a solar parabolic trough collector with the utilization of various working fluids (water, Therminol VP-1, and Syltherm 800), study the effect of weather conditions, the effect of mass flow rate of working fluids, and the effect of inlet temperature of working fluids on thermal performance of PTC. The second step is buit and developed model according to Table 4.1 characteristics experimental apparatuse to comparing between numerical and experimental results, study the effect of volumetric flow rate, study the effect of reflectivity of reflective surface, and study the effect of absorptivity of absorber tube on thermal performance of parabolic trough collector.

5.3.1. Model's Validation

A comparison with previous work was carried out to verify the model used to study thermal performance of parabolic trough collector with using different working fluid. **Bilal LAMRANI et al. 2018 [63]** investigated thermal performance of parabolic trough collector numerically under transient climate condition with using two types of working fluid are water and thermal oil (Syltherm800) as working fluid. The thermal performance of the Parabolic Trough Collector (PTC) was investigated using numerical simulations for various operating fluids. The model will be used for validation build and development by using COMSOL Multiphysics 6.0 simulation software according to Table 3.1 the characteristics. The present model absorber tube material is a Steel AISI 4340 and can get its physical properties from material library of COMSOL Multiphysics 6.0 program ,with the PTC parameter and the thermos-physical properties of various working fluids as well as the under operation conditions parameter. The absorber tube consist of four domains (Glass, air, Steel AISI 4340, working fluid). The validation results are compared with the literature study. The average error percentage of validation for output temperature , thermal efficiency, useful heat, and total heat losses are (0.337 % , 5.34 % , 5.02 % , 5.2%) respectively, and they are acceptable percentages as shown in figures below :

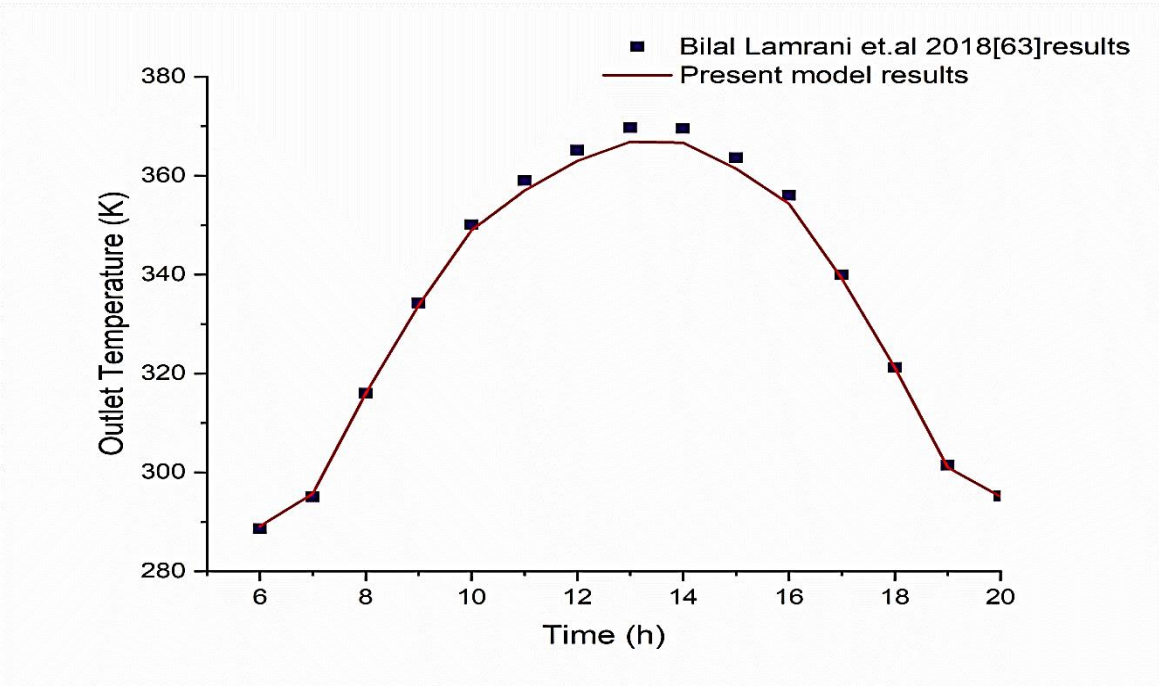

Fig.5.30. Output Temperature results validation.

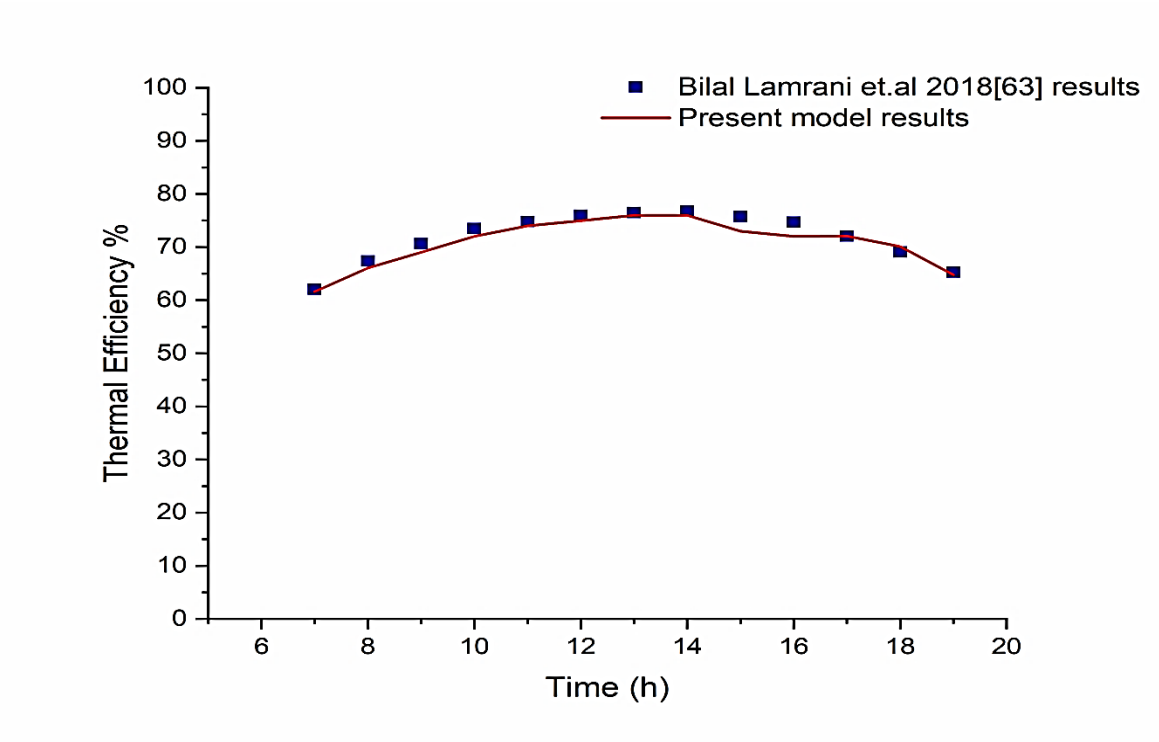

Fig.5.31. Thermal Efficiency results validation.

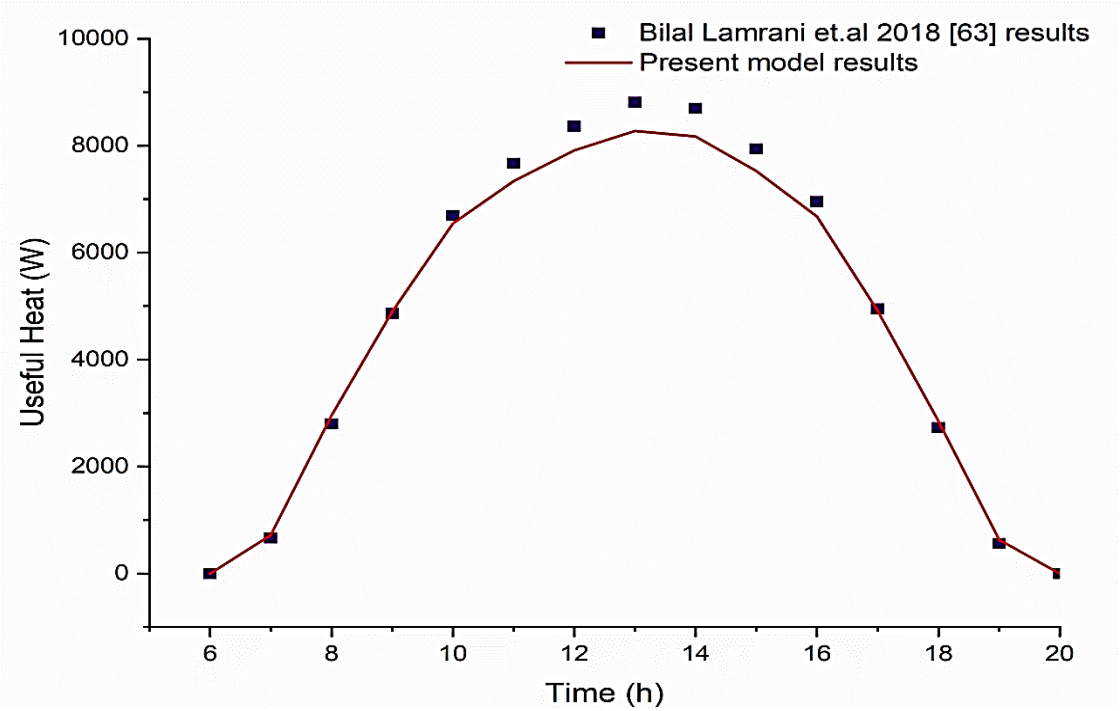

Fig.5.32 Useful heat results validation.

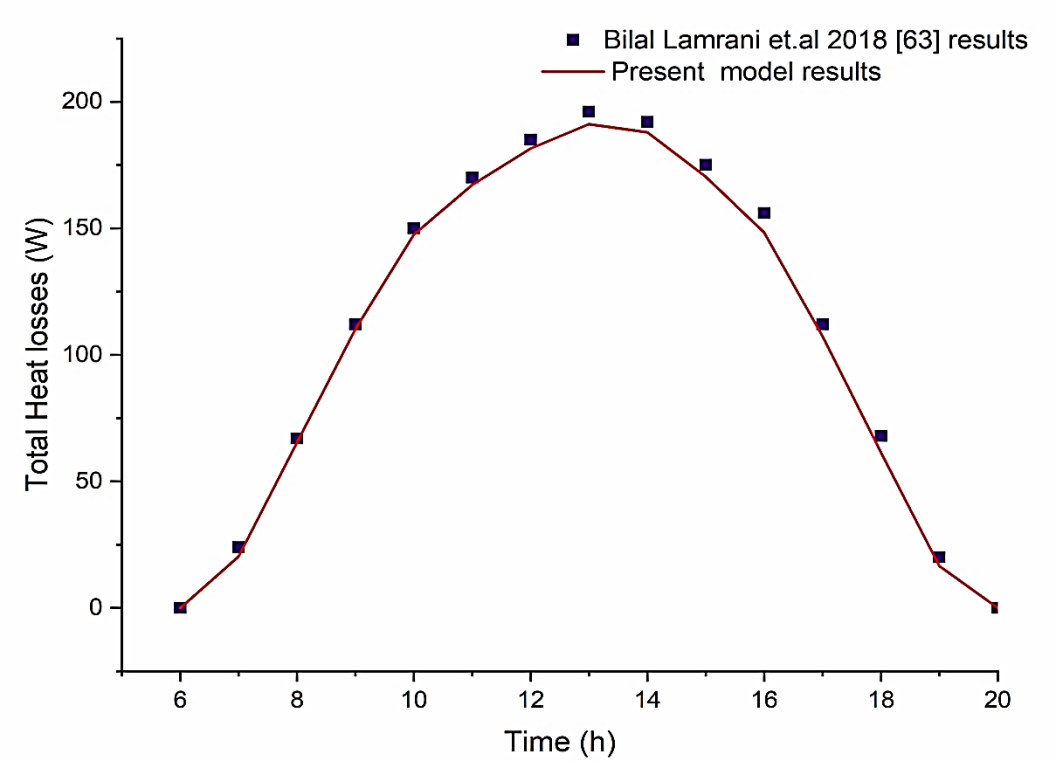

Fig.5.33.Total Heat losses results validation.

5.3.2.Comparing Numerical & Experimental Results

The comparing process between numerical result and experimental results lead more comfortable for the study of thermal behavior of parabolic trough collector and to know the range approach of numerical results with experimental results, buit model according to Table 4.1 characteristics experimental apparatuse to comparing between numerical and experimental results. Figure 5.34, and 5.35 show the comparing between numerical and experimental results by output temperature, Nussult number for two days one in east-west line direction is November 10th. Figure 5.34 show the comparing output temperature results of day November 10th between numerical and experimental results, the error percentage of average value of output temperature results between experimental and numerical is (0.4%). Figure 5.35 depicts comparing results of November 10th between numerical and experimental Nussult number results. The error percentage of comparing average value of Nusselt number of numerical and experimental is (0.22%).

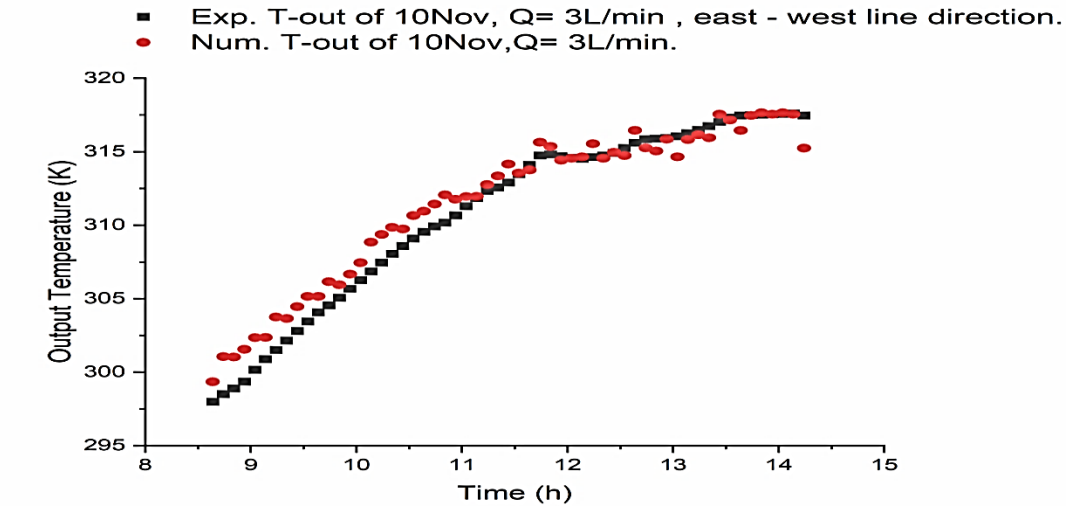

Fig.5.34. Output Temperature of Experimental & Numerical Results of 10Nov, East-West Line Direction with Flow Rate Q= 3 L/min.

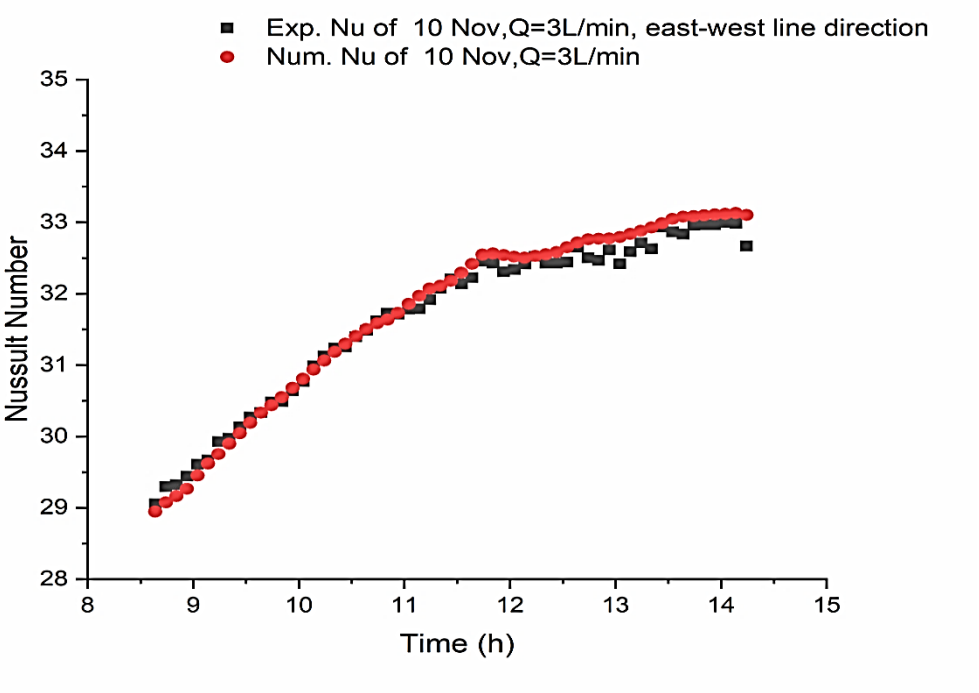

Fig.5.35. Nusselt number of Experimental & Numerical Results of 10Nov, East-West Line Direction with Flow Rate Q= 3 L/min.

The other comparing with south – north line direction day November 20th. Figure 5.36 show output temperature of November 20th comparing between numerical and experimental results. The error percentage of comparing output temperature results is (0.7%). Figure 5.37 show Nusselt number of comparing between numerical and experimental results of south –north line direction November 20th. the error percentage of Nusselt number results comparing is (0.18%).

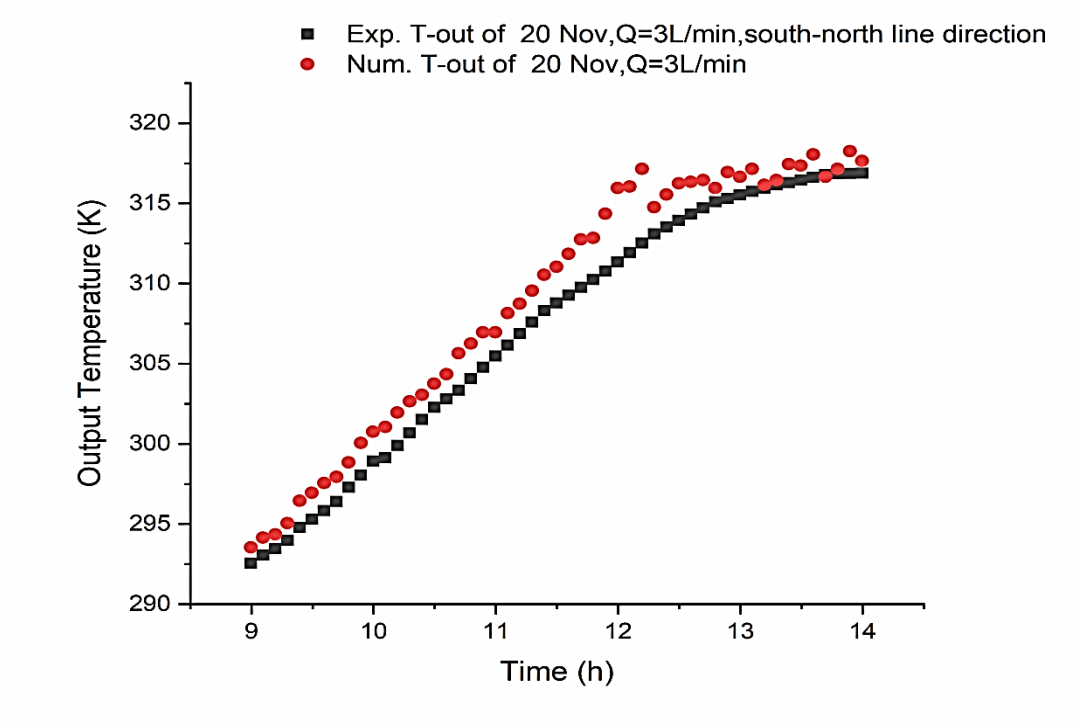

Fig.5.36. Output Temperature of Experimental & Numerical Results of 10Nov, East-West Line Direction with Flow Rate Q= 3 L/min.

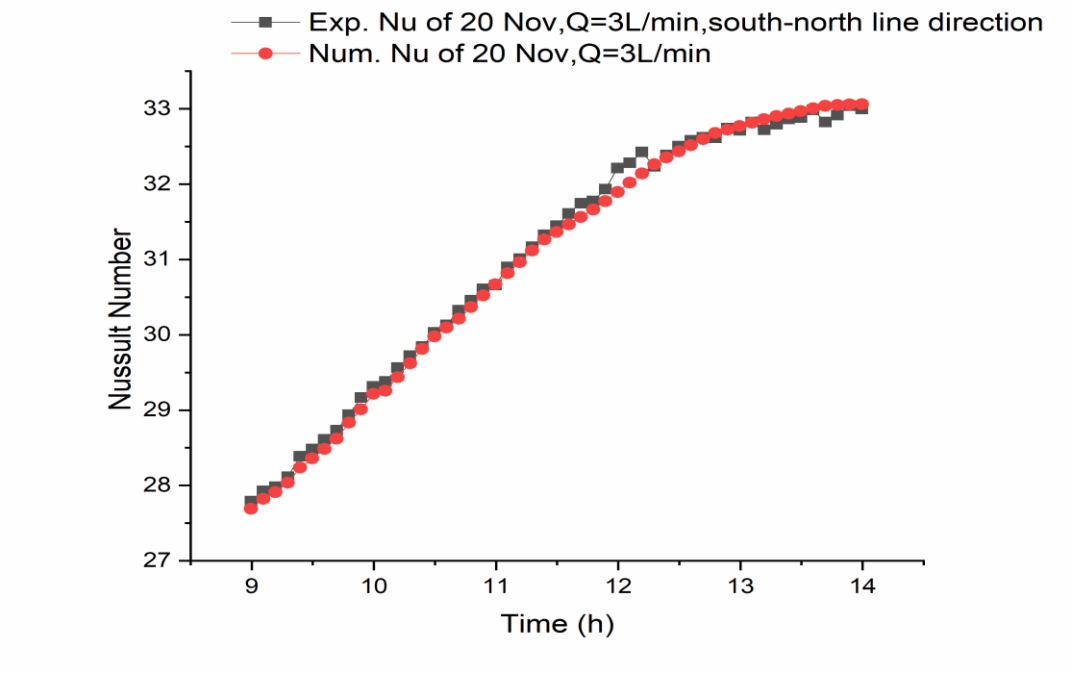

Fig.5.37. Nusselt Number of Experimental & Numerical Results of 10Nov, East-West Line Direction with Flow Rate Q= 3 L/min.

5.3.3. The Effect of Working Fluid Flow Rate on Performance of PTC

Present study the effect the flow rate of working fluid on thermal performance of parabolic trough collector numerically by using water as heat transfer fluid with the capacity of reflectivity equal 0.95 and absorptivity equal 0.9. The range of flow rate tested (1,2,3, and 4) L/min, the important parameters which measure thermal performance of parabolic trough collector such as output temperature, temperature difference, useful heat, total heat losses, thermal efficiency, cumulative heat, Nusselt number, pumping power, and Reynold number are found.

Figure 5.38 show the output temperature of working fluid with four flow rate ranges. The results founded the maximum output temperature with flow rate equal 1 L/min reached (338.02 K), that more than the other flow rate ranges (2,3, and 4) L/min by (3.4%, 4.6%, and 5.8%) respectively. Increase the mass flow rate leads to ahigher number of wter molecules flowing through a given point, resulting in a longer time needed to heat them up.

Figure 5.39 shows the temperature difference of flow rate ranges of working fluid. The maximum value of temperature difference occurred with flow rate with 1 L/min reached (26.69 degree), that more than other flow rates (2,3, and 4) L/min by (46%,62%, and 71%) respectively. The high value of the temperature difference with 1 L/min back to high convection heat transfer process with less flow rate between working fluid (water) and absorber tube.

Figure 5.40 show useful heat of working fluid with four ranges of flow rate. The maximum value of useful heat occurred with 4 L/min

reached (1913.65W), and that more than other flow rate ranges (1,2, and 3) by (1.6%, 0.77%, and 0.13 %) respectively. The high value of useful heat appeared with flow rate 4 L/min because the useful heat with directly proportional relationship with flow rate.

Figure 5.41 show the total heat losses of four ranges of working fluid (water) flow rate with reflectivity equal to (0.95), and absorptivity equal to (0.9), to comparing between all ranges of flow rate (1,2,3, and 4) L/min, the less value of heat losses lead to the best rage of flow rate, the less value of heat losses occurred with flow rate equal 4 L/min reached (13.38 W) that less than other flow rates (1,2, and 3) L/min by (33%, 25%, and 7%) respectively.

Figure 5.42 show the cumulative heat of working fluid (water) of four ranges of flow rates. The maximum cumulative heat appear with flow rate equal 4 L/min reached (17.55 W), that more the other flow rate ranges (1,2, and 3) L/min by (4.9%, 25%, and 29.6%) respectively. The reason of maximum cumulative with high range of flow rate because of the high flow rate of working fluid means more times of heat transfer between working fluid and absorber tube and more heat gain storage.

Figure 5.43 show thermal efficiency of working fluid of four ranges of flow rate (1,2,3, and 4) L/min with water as heat transfer fluid and with reflectivity equal (0.95) and absorptivity (0.9), the maximum value of thermal efficiency occurred with flow rate 4 L/min reached (76.18%), that more than (1,2, and 3) L/min by (1.34%,1.39%, and 1.46%) respectively. The reason of the high range of flow rate has maximum value of thermal

efficiency is the high rage of flow rate lead to more useful heat, and the thermal efficiency with directly proportional relationship useful heat.

Figure 5.44 show Nusselt number of four ranges of working fluid flow rate, the maximum value of Nusselt number occurred with high range of flow rate 4 L/min reached (42.08), that more than other flow rates (1,2, and 3) L/min by (65%,35%, and 20%) respectively. Nusselt number directly proportional relationship with heat transfer coefficient, which directly proportional relationship with velocity of fluid flow.

Figure 5.45 show the pumping power of four ranges of working fluid flow rate, the maximum pumping power occurred with flow rate range equal 4 L/min reached (0.00219 W), that more than other flow rates rages (1,2, and 3) L/min by (95.5%, 78.6%, and 47.1%) respectively, because the pumping power increase with the flow rate increase.

Figure 5.46 depicts Reynold number of four ranges of working fluid flow rate (1,2,3, and 4) L/min, the maximum value of Reynold number occurred with high range of flow rate 4 L/min reached (6064.75), that more than other flow rates (1,2, and 3) L/min by (71.8%,48.2%, and 24.17%) respectively. The maximum flow rate mean leads to high Reynold number, which Reynold number directly proportional relationship with velocity of fluid flow.

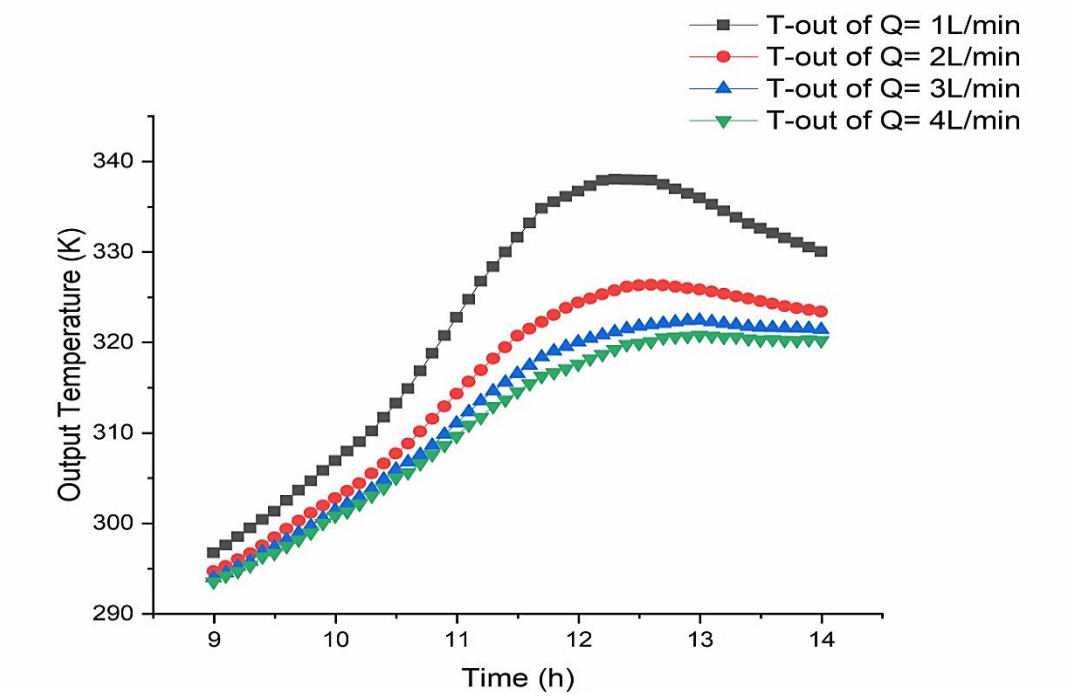

Fig.5.38.Output Temperature of Four Ranges Flow Rate of Water (1,2,3, and 4) L/min with Reflectivity = 0.95, and Absorptivity = 0.9.

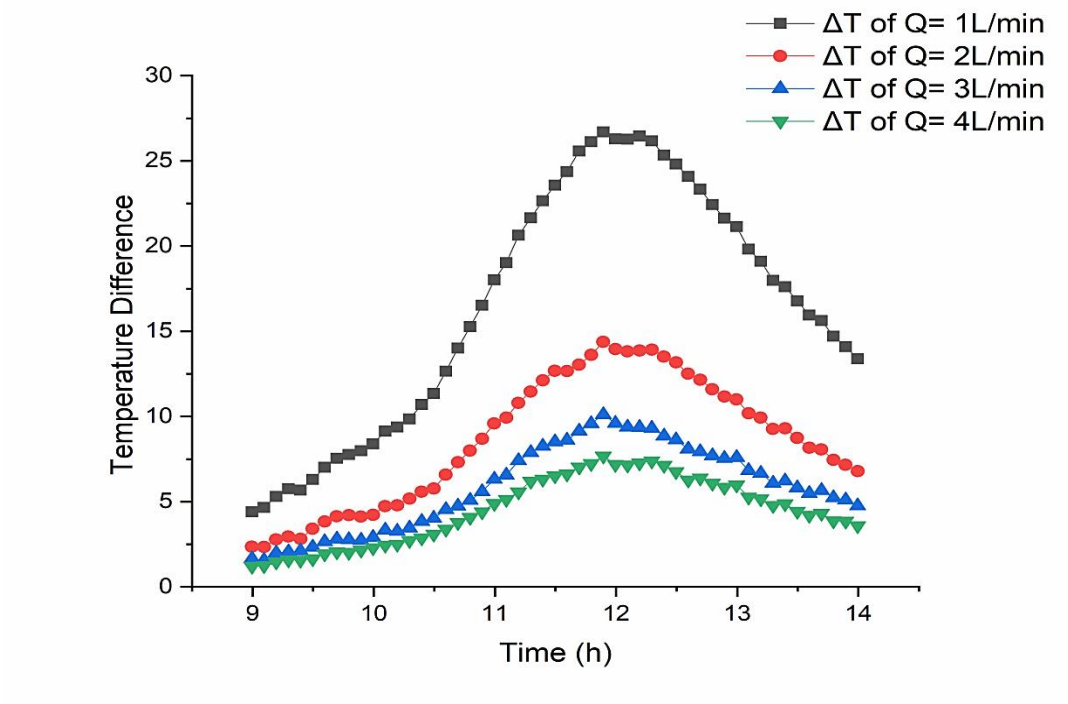

Fig.5.39. Temperature Difference of of Four Ranges Flow Rate of Water (1,2,3, and 4) L/min with Reflectivity = 0.95, and Absorptivity = 0.9.

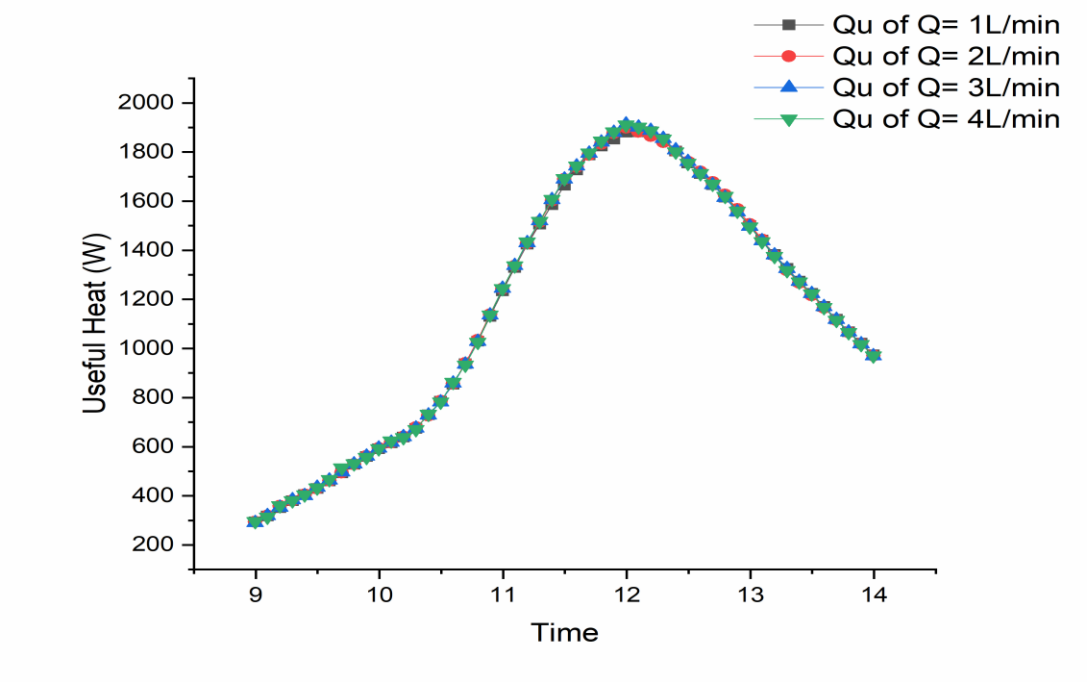

Fig.5.40. Useful Heat of of Four Ranges Flow Rate of Water (1,2,3, and 4) L/min with Reflectivity = 0.95, and Absorptivity = 0.9.

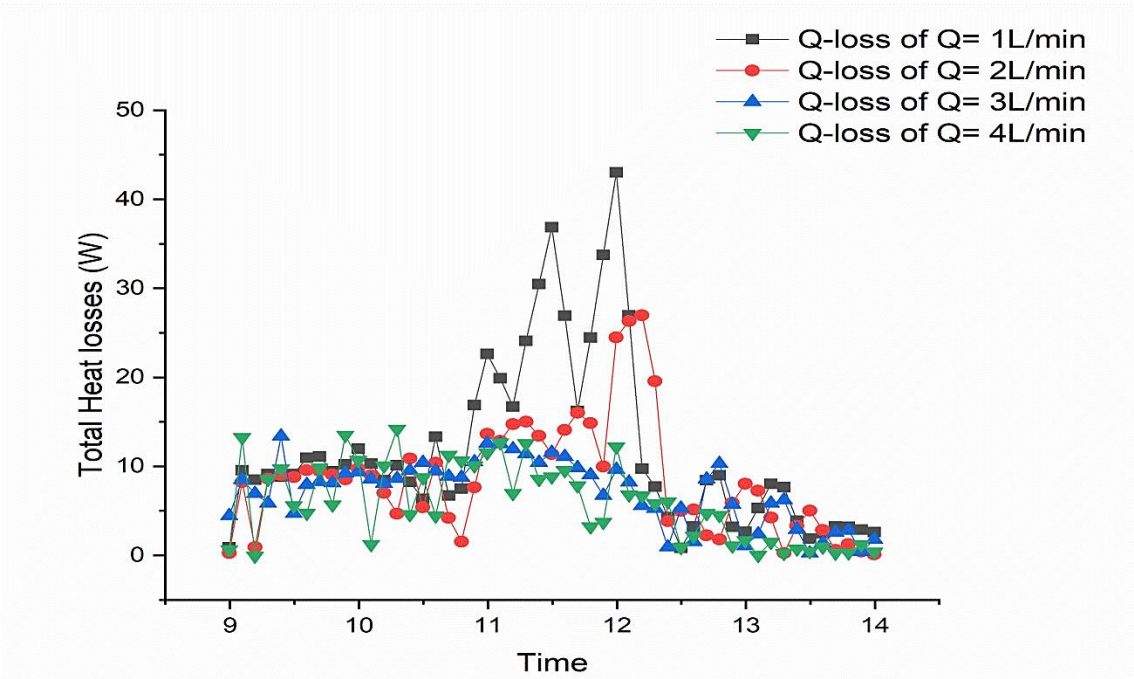

Fig.5.41. Total Heat losses of of Four Ranges Flow Rate of Water (1,2,3, and 4) L/min with Reflectivity = 0.95, and Absorptivity = 0.9.

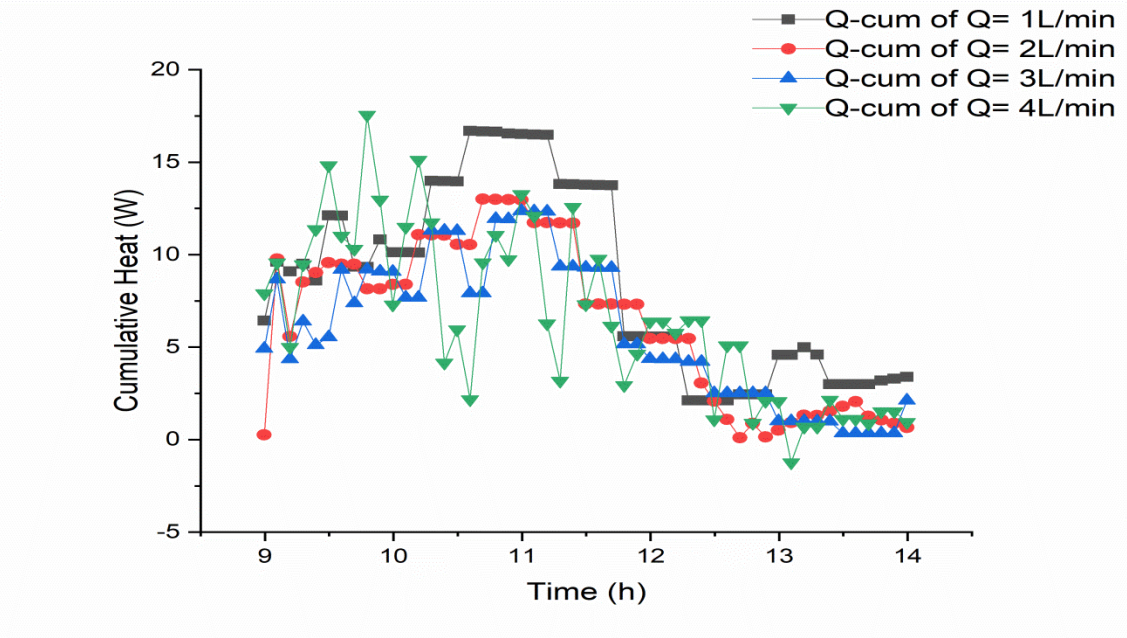

Fig.5.42. Cumulative Heat of of Four Ranges Flow Rate of Water (1,2,3, and 4) L/min with Reflectivity = 0.95, and Absorptivity = 0.9.

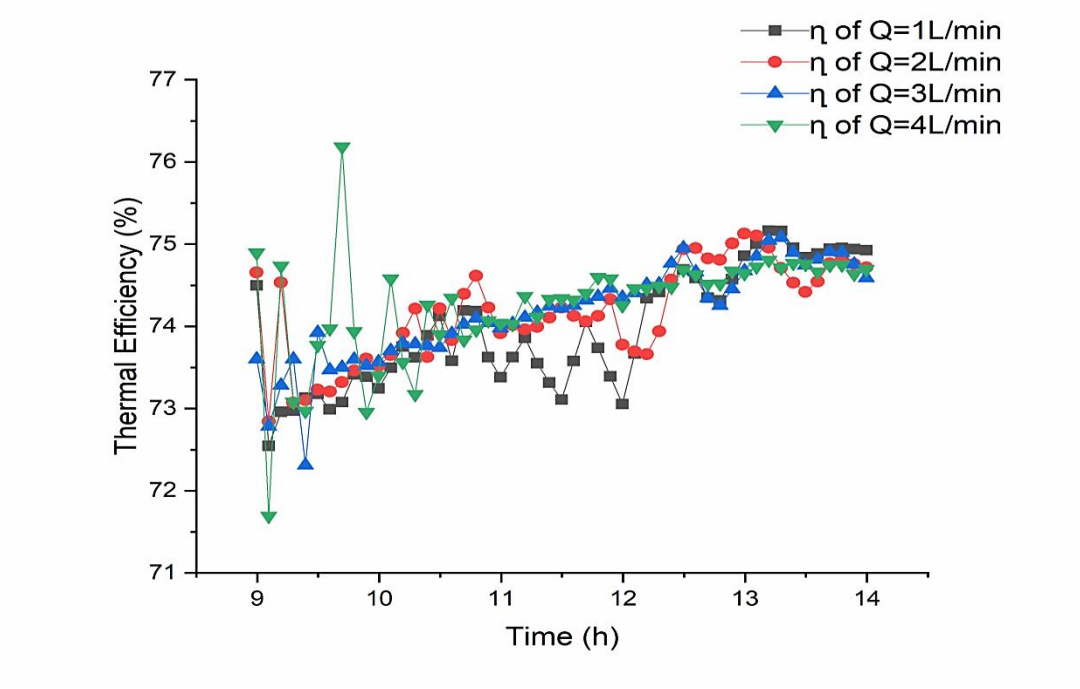

Fig.5.43. Thermal Efficiency of of Four Ranges Flow Rate of Water (1,2,3, and 4) L/min with Reflectivity = 0.95, and Absorptivity = 0.9.

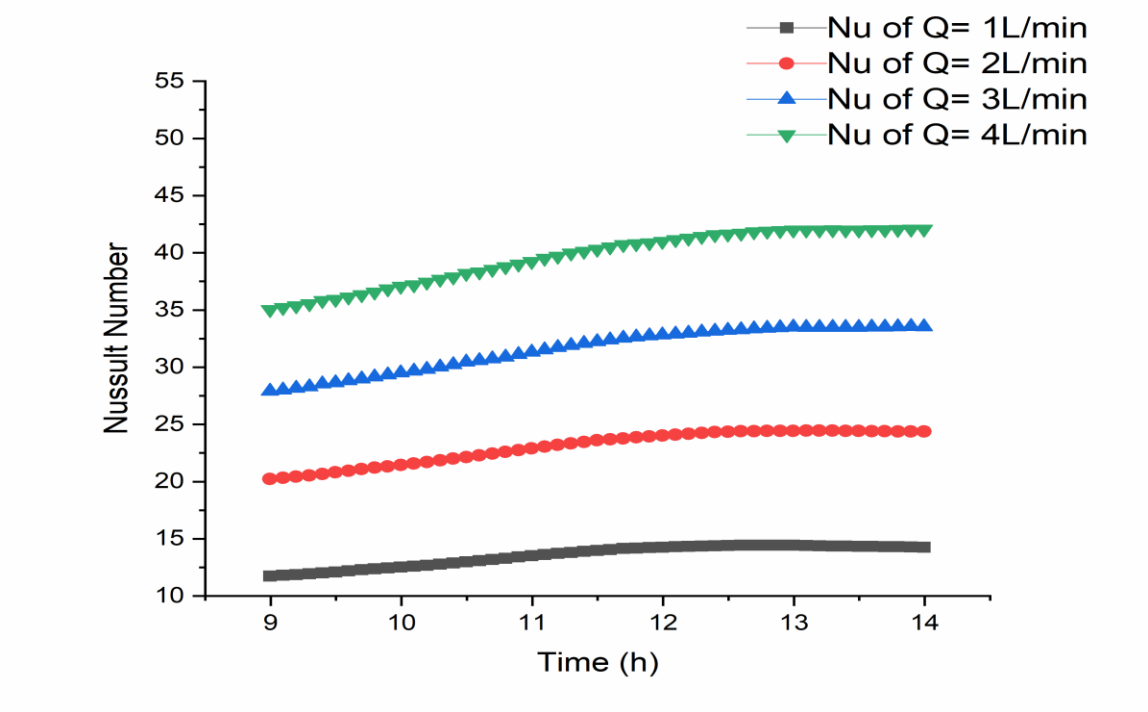

Fig.5.44. Nusselt Number of of Four Ranges Flow Rate of Water (1,2,3, and 4) L/min with Reflectivity = 0.95, and Absorptivity = 0.9.

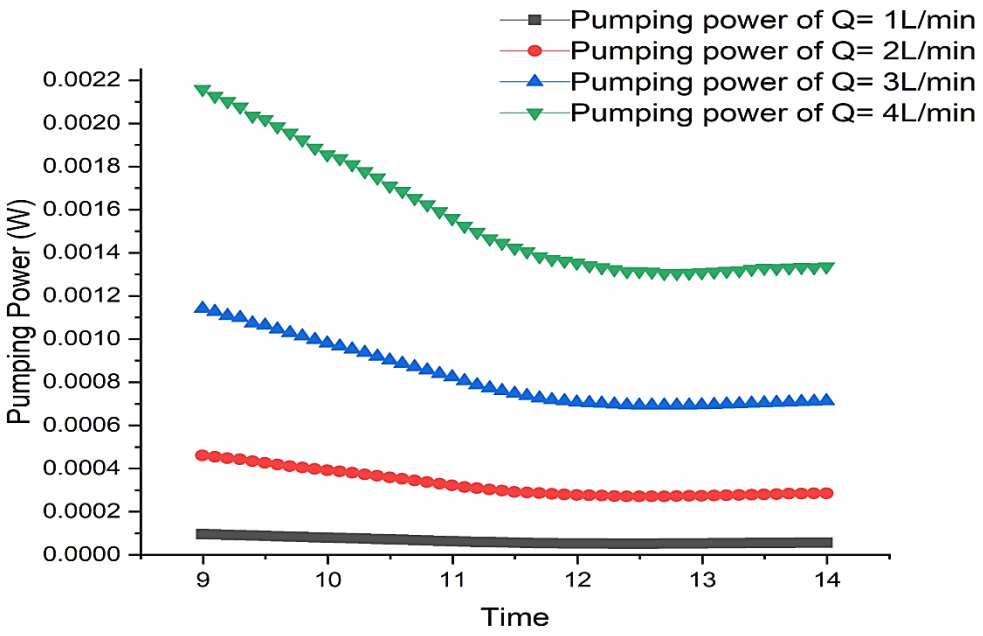

Fig.5.45. Pumping Power of of Four Ranges Flow Rate of Water (1,2,3, and 4) L/min with Reflectivity = 0.95, and Absorptivity = 0.9.

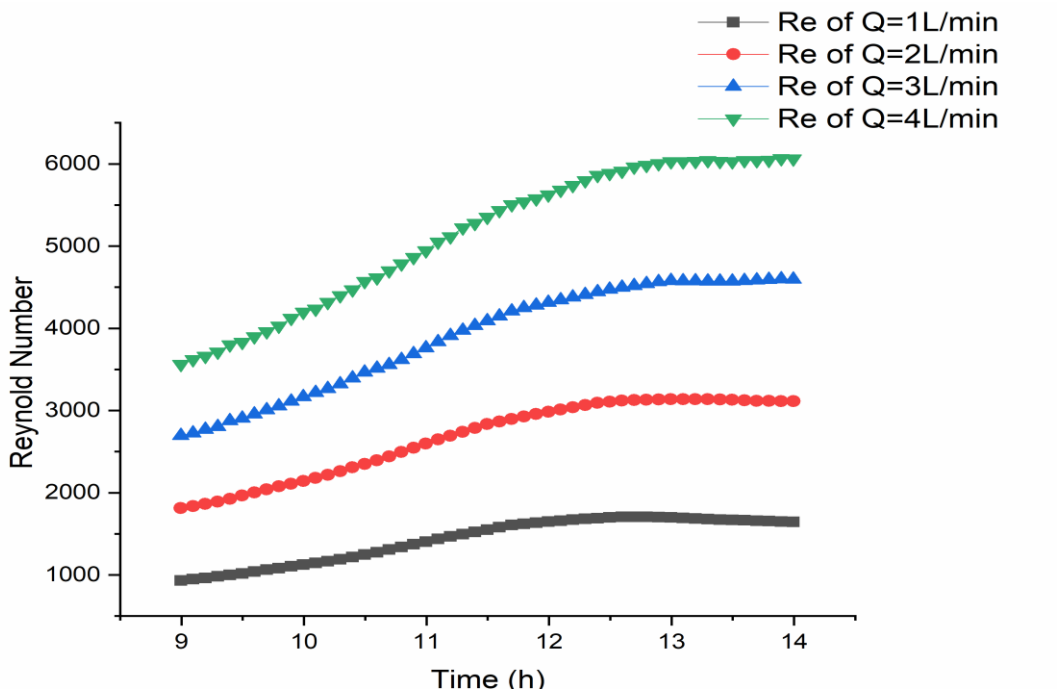

Fig.5.46. Reynold Number of of Four Ranges Flow Rate of Water (1,2,3, and 4) L/min with Reflectivity = 0.95, and Absorptivity = 0.9.

5.3.4. The Effect of Reflectivity on Performance of PTC

This study investigates the effect of reflectivity on the thermal performance of a parabolic trough collector using water as the heat transfer fluid with a flow rate of 4 L/min and absorptivity (α = 0.9) for three reflectivity ranges (0.225, 0.5, and 0.95) respectively. The important parameters such as output temperature, temperature difference, useful heat, total heat losses, cumulative heat, thermal efficiency, Nusselt number, pumping power, and Reynold number are founded numerically.

Figure 5.47 depicts the output temperature of the working fluid (water) with a flow rate of 4 L/min and absorptivity (α= 0.9) for three ranges of reflectivity (0.225, 0.5, and 0.95), with reflectivity (0.95) reached (320.8 K) higher value than the other ranges of reflectivity (0.225, and 0.5)

by 1.12% and 0.83%, respectively. That result occurred because the high range of reflectivity mean high solar energy reflected on the absorber tube, which lead to more heat from the working fluid and a high output temperature.

Figure 5.48 depicts the temperature difference of the working fluid (water) for three reflectivity ranges (0.225,0.5, and 0.95) respectively, with a flow rate of 4 L/min and absorptivity (α= 0.9). The maximum value of temperature difference occurred with reflectivity (0.95), which reached 7.67 degrees; this was more than other ranges of reflectivity (0.225, and 0.5) by 77% and 48.2%, respectively. This result is due to the high reflectivity range, which means high temperatures in the absorber, resulting in a large temperature difference.

Figure 5.49 depicts useful heat of water as heat transfer fluid with flow rate 4 L/min, and absorptivity equal 0.9, with three range of reflectivity (0.225,0.5, and 0.95) respectively. The maximum value of useful heat occurred with reflectivity (0.95), which reached (1911.1 W), this was more than other ranges of reflectivity (0.225, and 0.5) by 76.4% and 47.3%, respectively. That result occurred because the high range of reflectivity mean high solar energy reflected on the absorber tube, which led to more useful heat of working fluid.

Figure 5.50 depicts total heat losses of energy of parabolic trough collector by using water as heat transfer fluid with flow rate 4 L/min and absorptivity 0.9. The less average value of heat losses appeared with reflectivity (0.95), which reached (5.6 W), this was more than other ranges of reflectivity (0.225, and 0.5) by 10.7% and 5.3%, respectively. That result

occurred because the high range of reflectivity mean high solar energy reflected on the absorber tube that led to more heat gain and less heat losses.

Figure 5.51 depicts the cumulative heat of working fluid (water) with flow rate 4 L/min, and absorptivity 0.9, with three ranges of reflectivity (0.225,0.5, and 0.95) respectively. The maximum value of cumulative heat appeared with (0.95), which reached (17.55 W), this was more than other ranges of reflectivity (0.225, and 0.5) by 10.7% and 5.3%, respectively. That result occurred because the high range of reflectivity mean high solar energy reflected on the absorber tube that led to more cumulative heat.

Figure 5.52 show the thermal efficiency of working fluid with flow rate 4 L/min, and absorptivity 0.9 for three ranges of reflectivity (0.225,0.5, and 0.95) respectively. The maximum value of thermal efficiency occurred with reflectivity (0.95), which reached (76.18%),this was more than other ranges of reflectivity (0.225, and 0.5) by 73.4% and 45.1%, respectively. That result occurred because the high range of reflectivity mean high solar energy reflected on the absorber tube that led to more useful heat, and thermal efficiency with directly proportional relationship with useful heat, so that thermal efficiency increase with reflectivity increase.

Figure 5.53 depicts Nusselt number of water as heat transfer fluid with flow rate 4 L/min, and with absorptivity equal 0.9 for three ranges of reflectivity (0.225,0.5, and 0.95) respectively. The maximum value of Nusselt number occurred with (0.95), which reached (42.08), this was more than other ranges of reflectivity (0.225, and 0.5) by 17% and 0.7%, respectively. That result occurred because the high range of reflectivity

mean high solar energy reflected on the absorber tube that led to more useful heat so that mean high value of heat convection coefficient, and Nusselt number with directly proportional relationship with heat convection coefficient. Another reason of increase Nusselt number with increase value of reflectivity, when increase reflectivity lead to increase temperature which decrease thermal conductivity of working fluid and that lead to Nussult number increase, Nusselt number with reverse proportional relationship with thermal conductivity.

Figure 5.54 depicts pumping power of water as heat transfer fluid with flow rate 4 L/min, and with absorptivity equal 0.9 for three ranges of reflectivity (0.225,0.5, and 0.95) respectively. The maximum value of pumping power occurred with reflectivity equal (0.225), which reached (0.002155W), this was more than other ranges of reflectivity (0.225, and 0.5) by 24% and 27.4%, respectively. The increase of reflectivity mean increase thermal energy that lead to decrease of viscosity of working fluid and decrease pumping power.

Figure 5.54 depicts Reynold number of water as heat transfer fluid with flow rate 4 L/min, and with absorptivity equal 0.9 for three ranges of reflectivity (0.225,0.5, and 0.95) respectively. The maximum value of Reynold number occurred with (0.95), which reached (6064.75), this was more than other ranges of reflectivity (0.225, and 0.5) by 3% and 2%, respectively. That result occurred because high range of reflectivity mean high temperature range of water that lead to decrease dynamic viscosity, Reynold number reverse proportional relationship with dynamic viscosity.

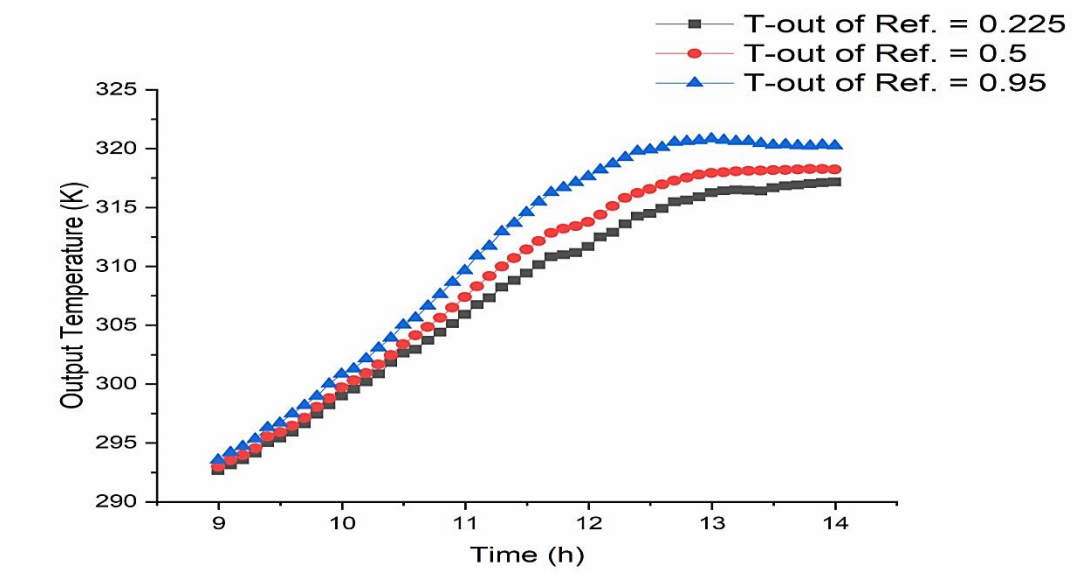

Fig.5.47. Output Temperature of Three Ranges of Reflectivity (0.225, 0.5, 0.95) with Flow rate Q = 4 L/min, and Absorptivity = 0.9.

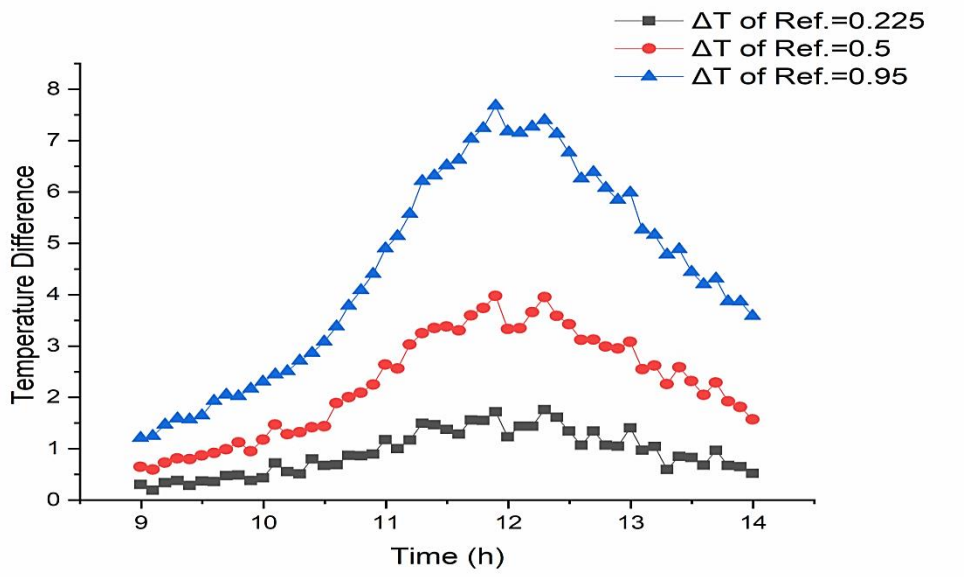

Fig.5.48.Temperature difference of Three Ranges of Reflectivity (0.225, 0.5, 0.95) with Flow rate Q = 4 L/min, and Absorptivity = 0.9.

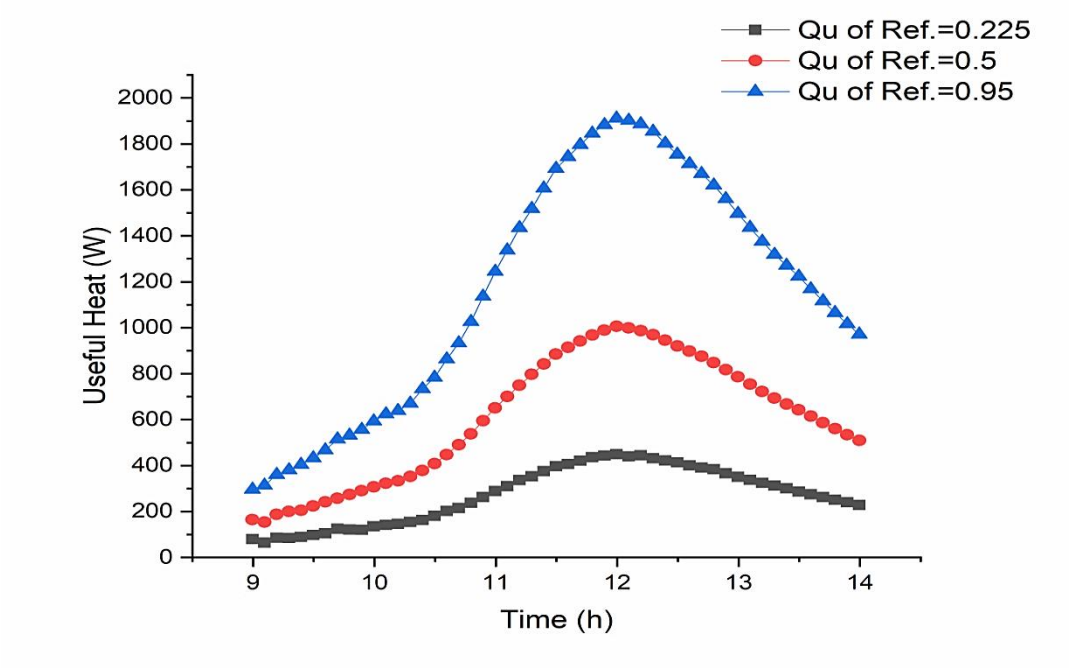

Fig.5.49.Useful Heat of Three Ranges of Reflectivity (0.225, 0.5, 0.95) with Flow rate Q = 4 L/min, and Absorptivity = 0.9.

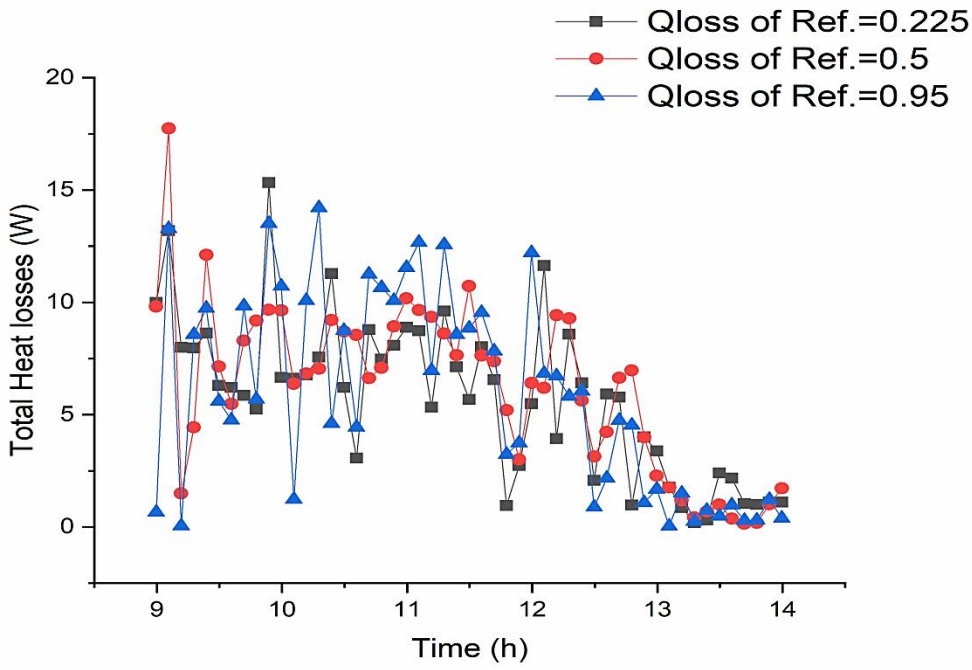

Fig.5.50.Total Heat Losses of Three Ranges of Reflectivity (0.225, 0.5, 0.95) with Flow rate Q = 4 L/min, and Absorptivity = 0.9.

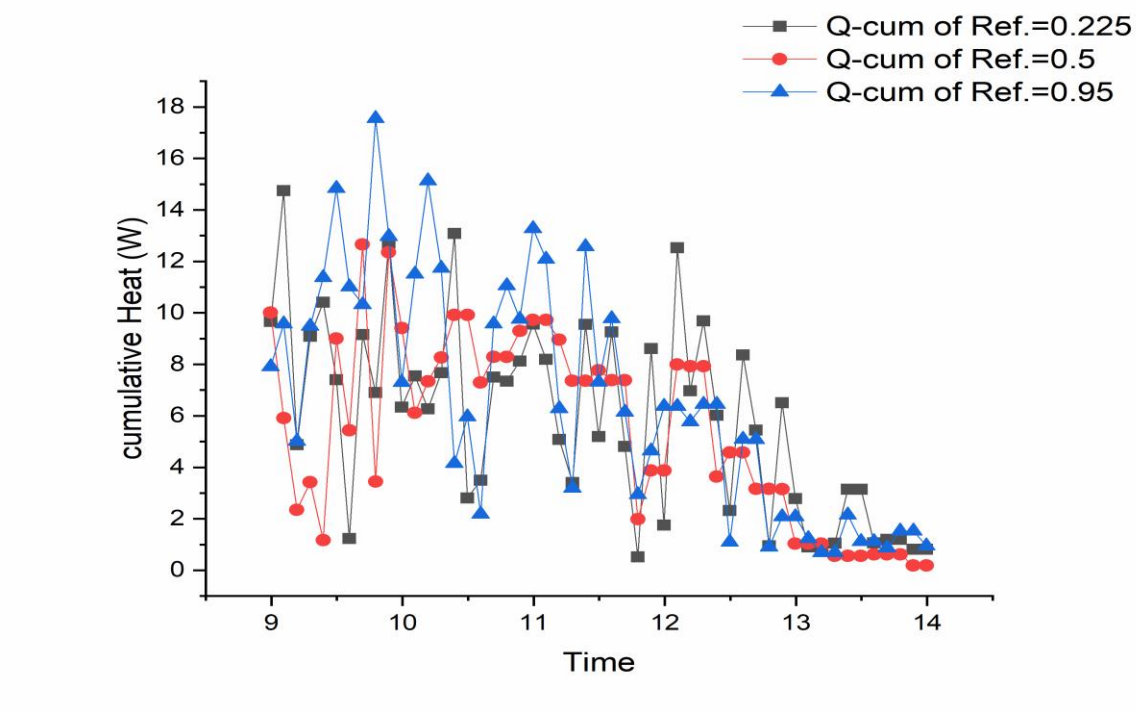

Fig.5.51. Cumulative Heat of Three Ranges of Reflectivity (0.225, 0.5, 0.95) with Flow rate Q = 4 L/min, and Absorptivity = 0.9.

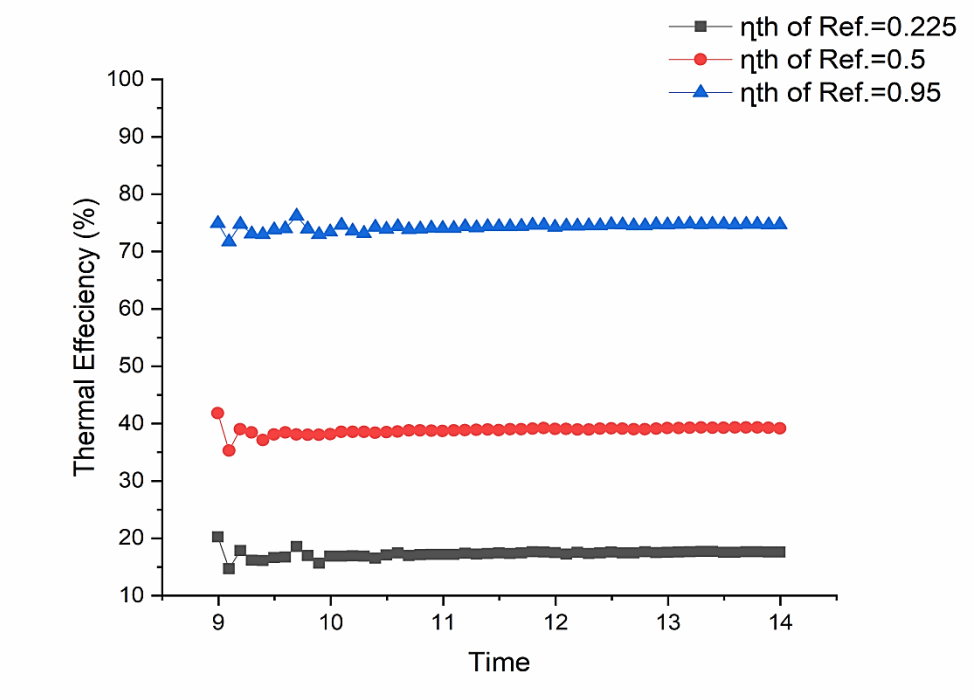

Fig.5.52. Thermal Efficiency of Three Ranges of Reflectivity (0.225, 0.5, 0.95) with Flow rate Q = 4 L/min, and Absorptivity = 0.9.

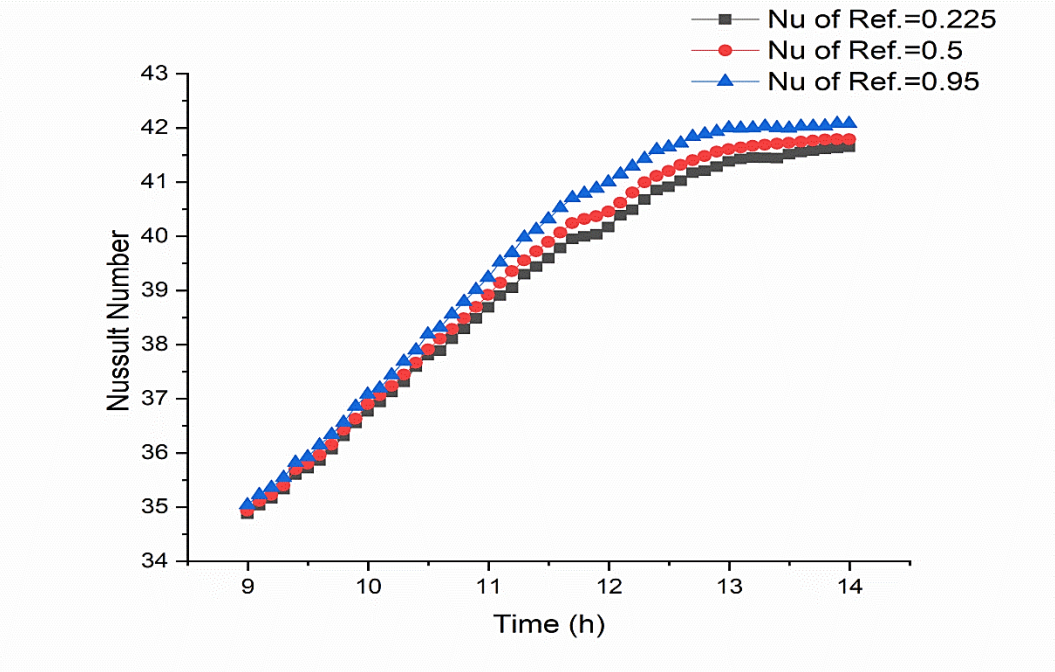

Fig.5.53. Nusselt Number of Three Ranges of Reflectivity (0.225, 0.5, 0.95) with Flow rate Q = 4 L/min, and Absorptivity = 0.9.

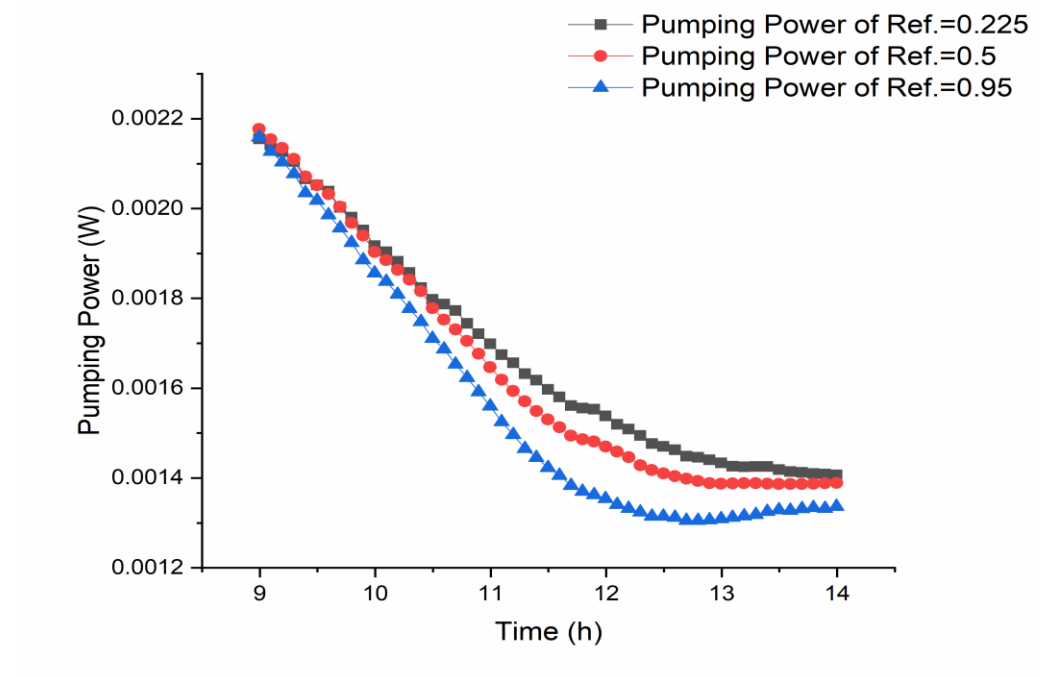

Fig.5.54. Pumping Power of Three Ranges of Reflectivity (0.225, 0.5, 0.95) with Flow rate Q = 4 L/min, and Absorptivity = 0.9.

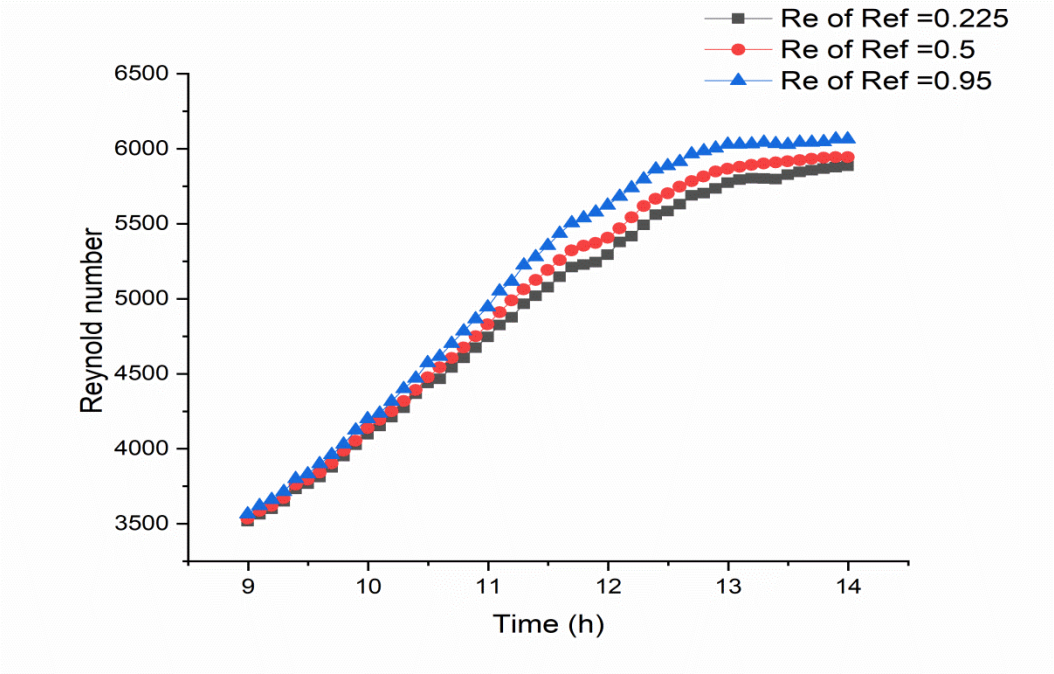

Fig.5.55. Reynold number of Three Ranges of Reflectivity (0.225, 0.5, 0.95) with Flow rate Q = 4 L/min, and Absorptivity = 0.9.

5.3.5. The Effect of Absorptivity on Performance of PTC

this study present the effect of the absorptivity of absorber tube on thermal performance of parabolic trough collector with using water as working fluid with flow rate 4 L/min, and reflectivity 0.95, and three ranges of absorptivity (0.5,0.7, and 0.9). Figure 5.56 depicts the output temperature of working fluid (water) with three ranges of absorptivity (0.5,0.7, and 0.9) with flow rate 4 L/min, and reflectivity 0.95. The maximum value of output temperature occurred with absorptivity 0.9, which reach (320.85K), this was more than other ranges of absorptivity (0.5, and 0.7) by (0.66%, and 0.42%) respectively. The increase of absorptivity of absorber tube lead to increase the surface temperature of absorber tube and increase output temperature of working due convection heat transfer process between absorber tube and working fluid (water).

Figure 5.57 depicts temperature difference of working fluid (water) with three ranges of absorptivity (0.5,0.7, and 0.9) with flow rate 4 L/min, and reflectivity 0.95. The maximum value of temperature difference occurred with absorptivity 0.9, which reach (7.67 degree), this was more than other ranges of absorptivity (0.5, and 0.7) by (42%, and 21%) respectively. The increase of absorptivity of absorber tube lead to increase the surface temperature of absorber tube and increase temperature difference of working due convection heat transfer process between absorber tube and working fluid (water).

Figure 5.58 depicts the useful heat of working fluid (water) with three ranges of absorptivity (0.5,0.7, and 0.9) with flow rate 4 L/min, and reflectivity 0.95. The maximum value of useful heat occurred with absorptivity 0.9, which reach (1911.1W), this was more than other ranges of absorptivity (0.5, and 0.7) by (44.6%, and 22.2%) respectively. The increase of absorptivity of absorber tube lead to increase the temperature of absorber tube and increase output temperature of working due convection heat transfer process between absorber tube and working fluid (water) and that lead to increase useful heat because of the useful directly proportional relationship with temperature difference.

Figure 5.59 depicts total heat losses of parabolic trough collector by using water as working fluid with three ranges of absorptivity (0.5,0.7, and 0.9) with flow rate 4 L/min, and reflectivity 0.95. The less average value of heat losses occurred with absorptivity 0.9, which reach (5.05 W), this was more than other ranges of absorptivity (0.5, and 0.7) by (12%, and 18%) respectively. The increase of absorptivity of absorber tube lead to increase the heat gain and decrease heat losses.

Figure 5.60 depicts cumulative of working fluid (water) with three ranges of absorptivity (0.5,0.7, and 0.9) with flow rate 4 L/min, and reflectivity 0.95. The maximum value of cumulative heat occurred with absorptivity 0.9, which reach (17.55 W), this was more than other ranges of absorptivity (0.5, and 0.7) by (7.2%, and 2%) respectively. The absorptivity of the absorber tube increased, which increased the surface temperature of the absorber tube and increased the heat transfer process between the working fluid and absorber tube, increasing the total heat of the working fluid (water).

Figure 5.61 shows the parabolic trough's thermal efficiency while utilizing water as the heat transfer fluid. The flow rate is 4 L/min, the reflectivity is 0.95, and there are three absorptivity bands (0.5,0.7, and 0.9). The thermal efficiency reached its highest point at absorptivity 0.9, reaching (76.1%), outpacing absorptivity ranges (0.5 and 0.7) by (42%, and 22%) respectively. Due to the convection heat transfer process between the absorber tube and working fluid (water), an increase in the absorber tube's absorptivity causes an increase in the surface temperature of the absorber tube and an increase in the output temperature of the working. Thermal efficiency and useful heat have a direct proportional relationship.

Figure 5.62 show Nusselt number of working fluid (water) with flow rate 4 L/min, reflectivity of reflector surface 0.95, and with three ranges of absorptivity of absorber tube (0.5,0.7, and 0.9). The maximum value of Nussult number occurred with absorptivity 0.9, which reached (42.08), this was more than other ranges of absorptivity (0.5, and 0.7) by (0.45%, and 0.27%) respectively. When increase absorptivity of absorber tube increase working fluid (water) temperature and that lead to decrease thermal

conductivity of working fluid which Nusselt number reverse proportional relationship with thermal conductivity.

Figure 5.63 depicts pumping power of water as heat transfer fluid with flow rate 4 L/min, reflectivity 0.95, and three ranges of absorptivity (0.5,0.7, and 0.9). The maximum value of pumping power occurred with absorptivity 0.5, which reach (0.002176W), this was more than other ranges of absorptivity (0.7, and 0.9) respectively. The increase of absorptivity of absorber tube lead to increase the surface temperature of absorber tube mean increase thermal energy that lead to decrease of viscosity of working fluid and decrease pumping power.

Figure 5.64 show Reynold number of water as heat transfer fluid with flow rate 4 L/min, reflectivity 0.95, and three ranges of absorptivity (0.5,0.7, and 0.9). With an absorptivity of 0.9, Reynold number achieved its highest value, which was (6064.75), outperforming absorptivity ranges of (0.5) and (0.7) by 1.2% and 0.8%, respectively. A high absorptivity value raises water temperature, which reduces dynamic viscosity and has an inversely proportional connection with the Reynolds number.

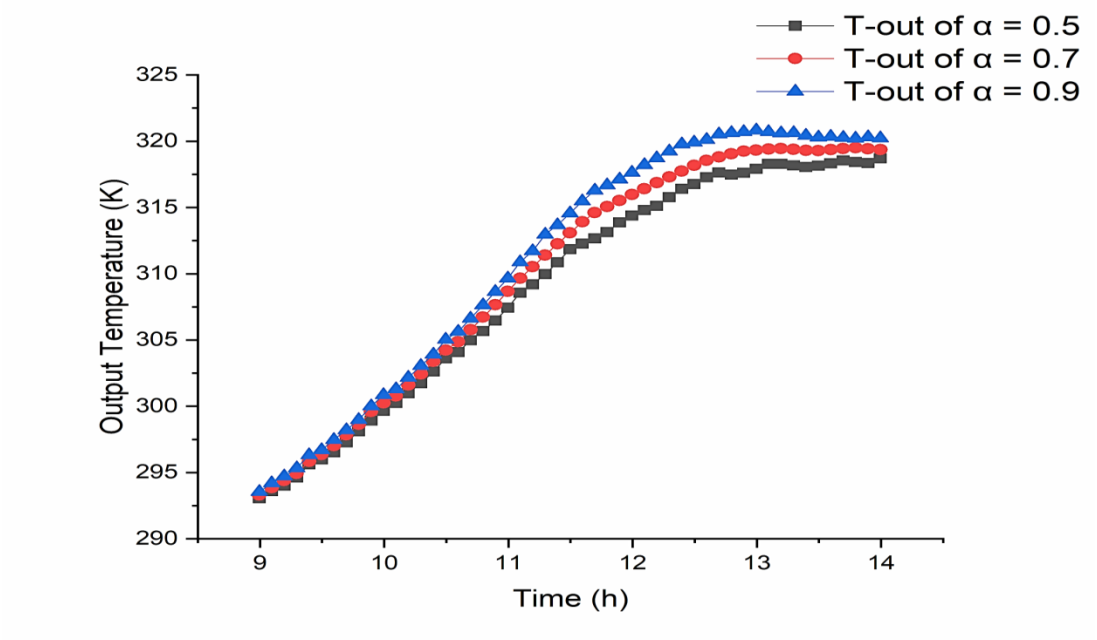

Fig.5.56. Output Temperature of Three Ranges of Absorptivity (0.5, 0.7, 0.9) with Flow rate Q = 4 L/min, and Reflectivity = 0.95.

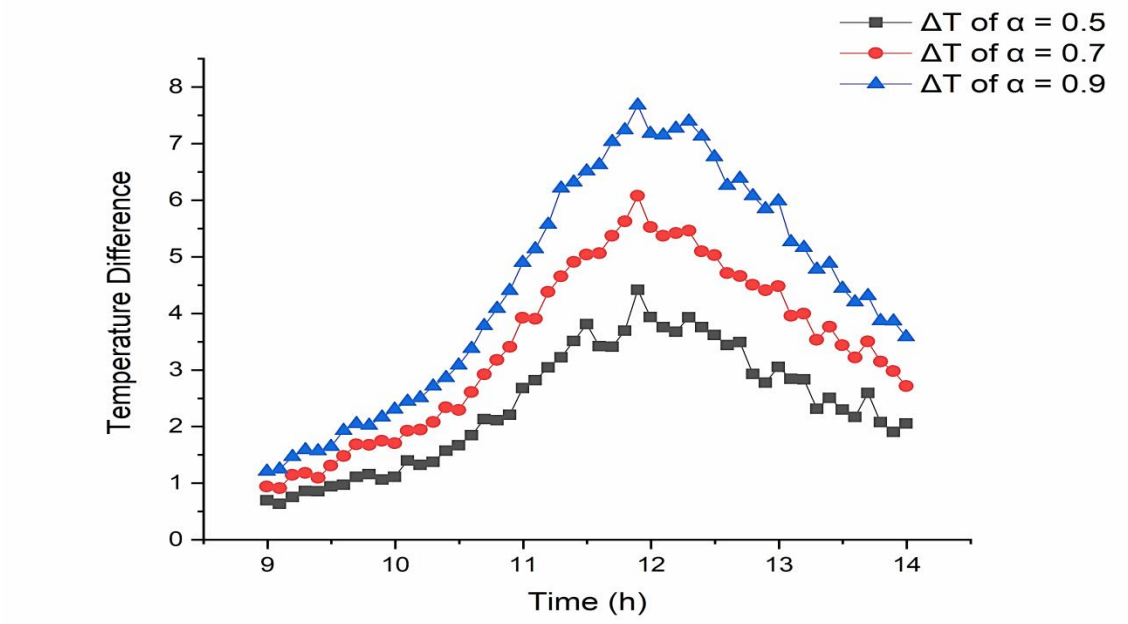

Fig.5.57. Temperature Difference of Three Ranges of Absorptivity (0.5, 0.7, 0.9) with Flow rate Q = 4 L/min, and Reflectivity = 0.95.

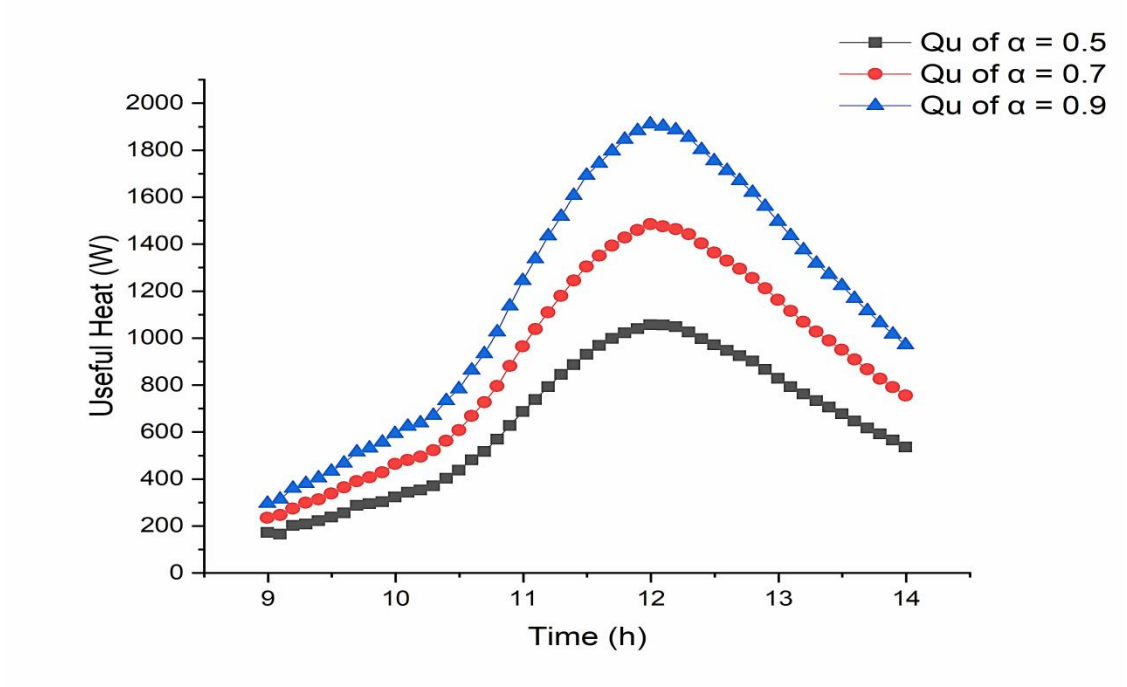

Fig.5.58. Useful Heat of Three ranges of Three Ranges of Absorptivity (0.5, 0.7, 0.9) with Flow rate Q = 4 L/min, and Reflectivity = 0.95.

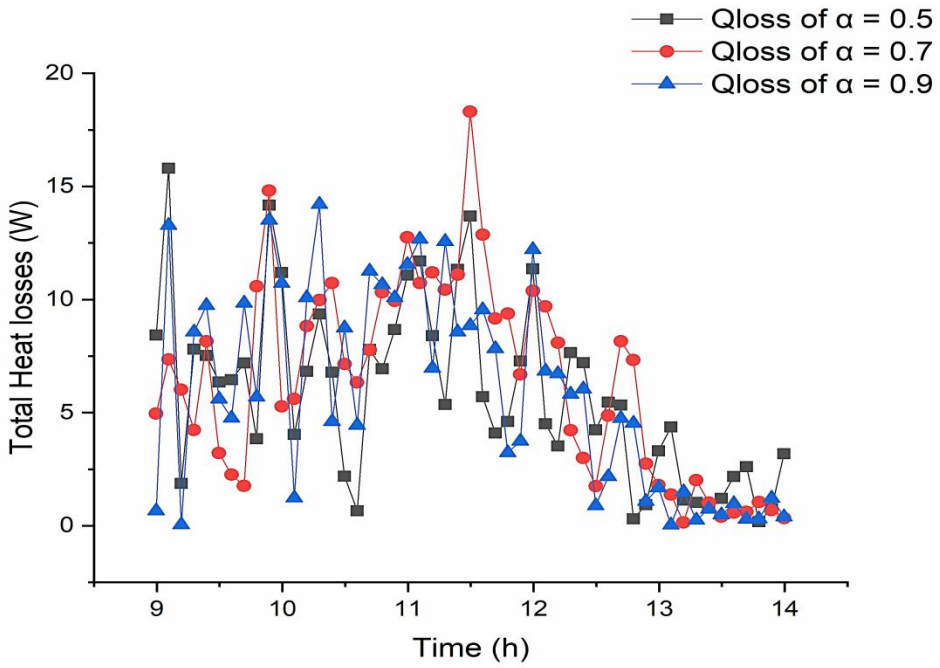

Fig.5.59. Total Heat Losses of Three Ranges of Absorptivity (0.5, 0.7, 0.9) with Flow rate Q = 4 L/min, and Reflectivity = 0.95.

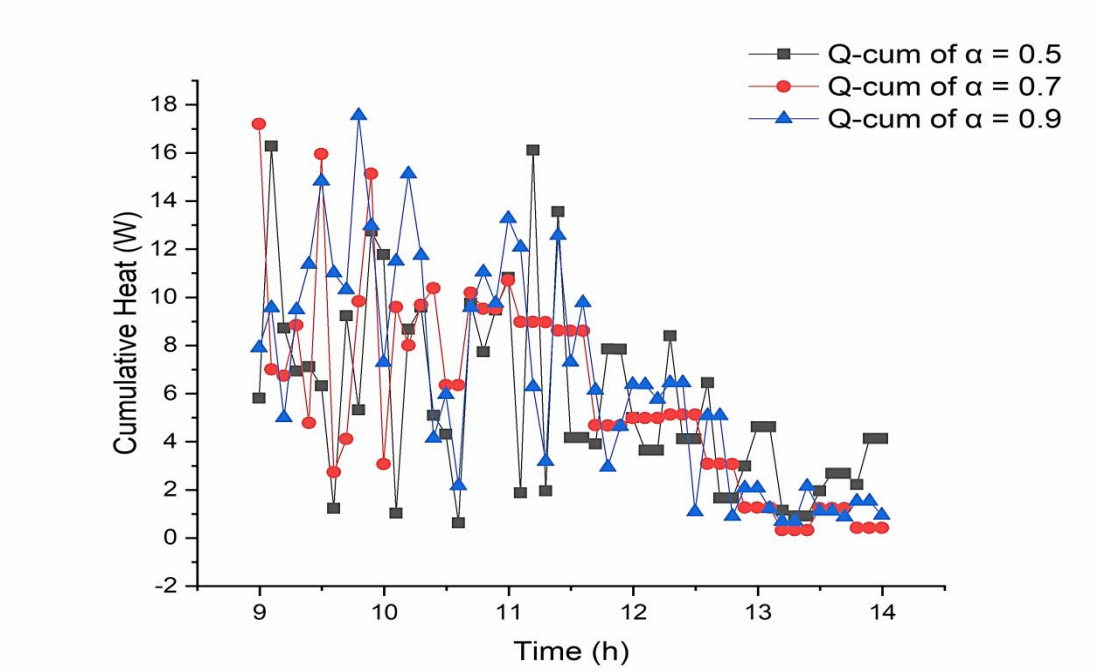

Fig.5.60. Cumulative Heat of Three Ranges of Absorptivity (0.5, 0.7, 0.9) with Flow rate Q = 4 L/min, and Reflectivity = 0.95.

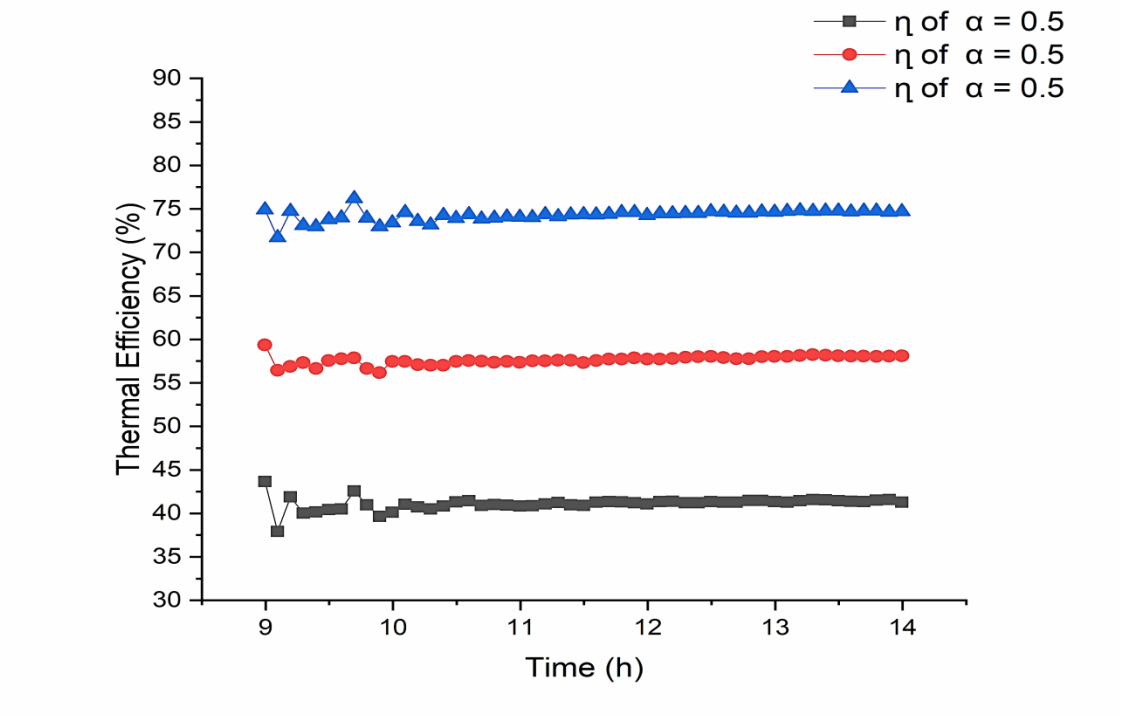

Fig.5.61. Thermal Efficiency of Three Ranges of Absorptivity (0.5, 0.7, 0.9) with Flow rate Q = 4 L/min, and Reflectivity = 0.95.

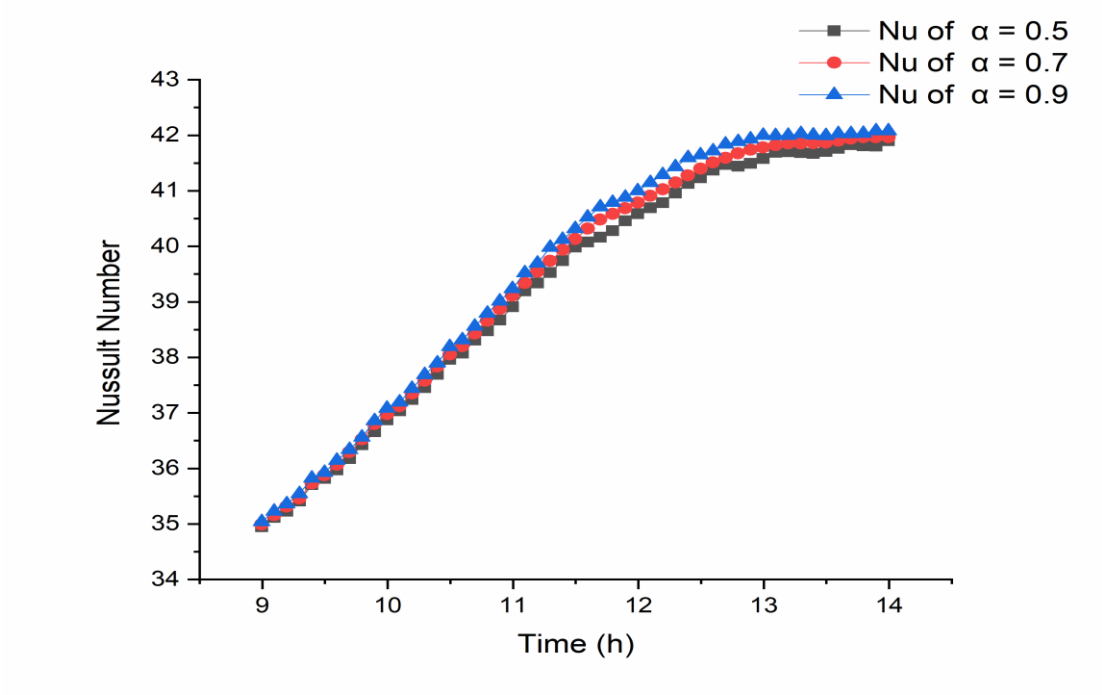

Fig.5.62. Nusselt Number of Three Ranges of Absorptivity (0.5, 0.7, 0.9) with Flow rate Q = 4 L/min, and Reflectivity = 0.95.

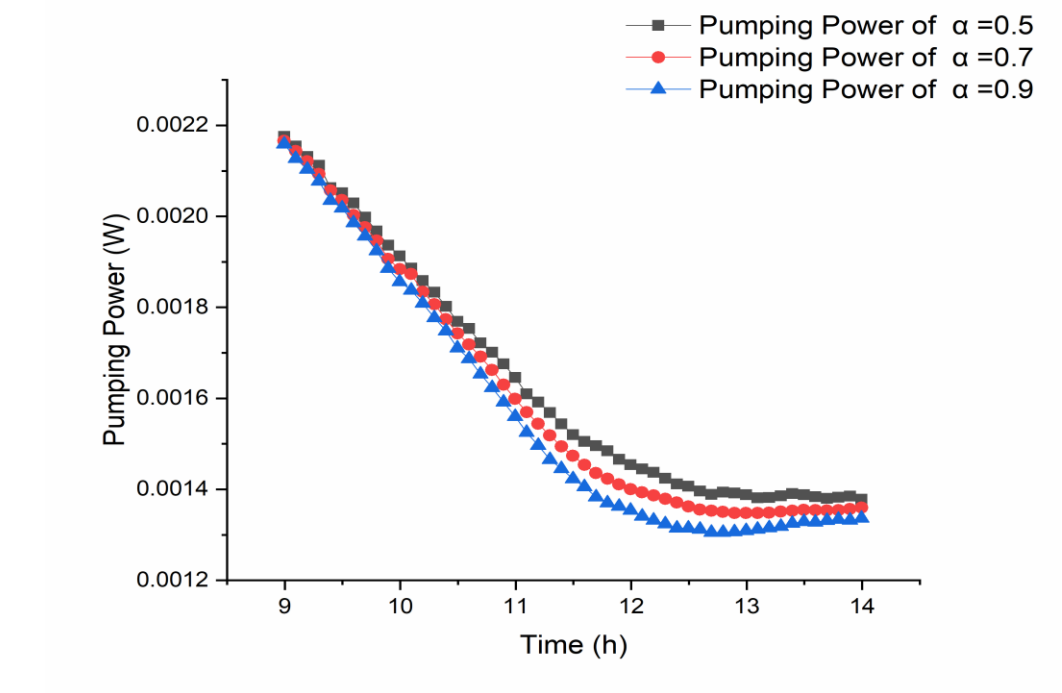

Fig.5.63. Pumping Power of Three Ranges of Absorptivity (0.5, 0.7, 0.9) with Flow rate Q = 4 L/min, and Reflectivity = 0.95.

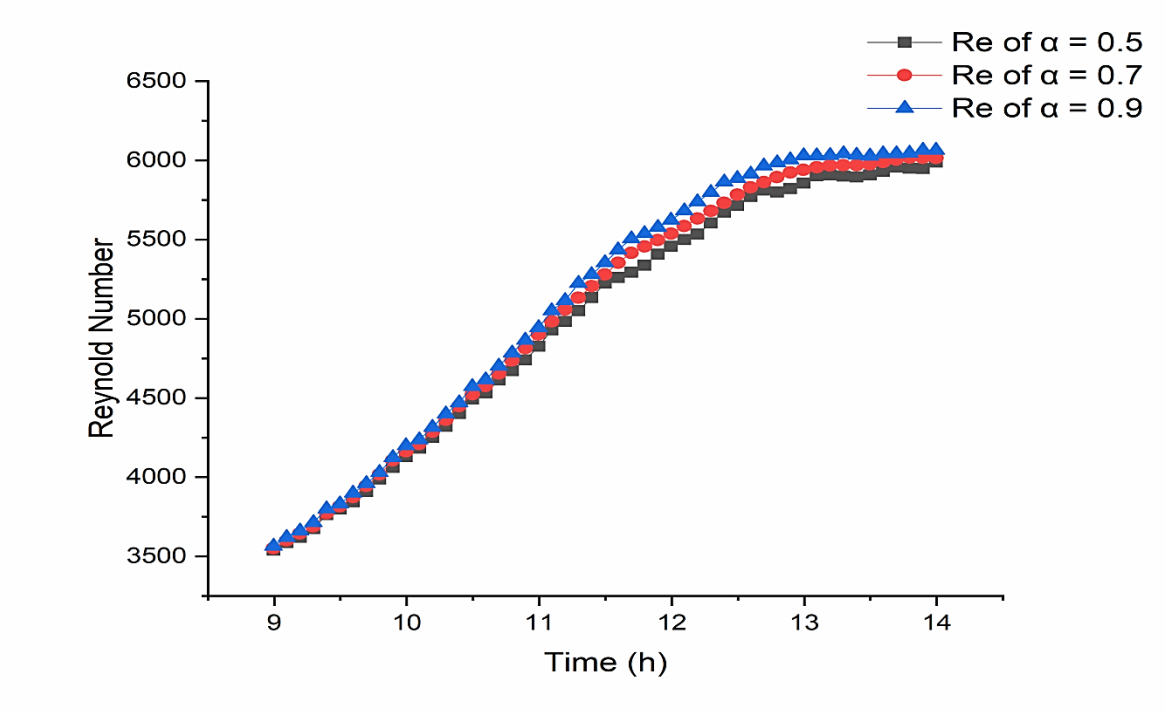

Fig.5.64. Reynold Number of Three Ranges of Absorptivity (0.5, 0.7, 0.9) with Flow rate Q = 4 L/min, and Reflectivity = 0.95.

5.3.6. The Effect of Weather Conditions of Performance of PTC

The effect of the climate on the performance of PTC depending on the weather conditions data of Al-Najaf city at four seasons in year, the data which including the solar radiation intensity, ambient temperature, and wind speed at (15 Jan, 15Mar, 15July, and 15 Oct) of year 2018 as shown in Figure (5.65, 5.66 and 5.67) respectively, numerical model was built and developed by using COMSOL Multiphysics Version 6.0 simulation software according to Table 3.1 the characteristics of Balil Lamrani et al. 2018 [63], to investigate the thermal behavior of a solar parabolic trough collector with the utilization of various working fluids (water, Therminol VP-1, and Syltherm 800).

Figure 5.65 depicts the solar radiation intensity at 15 July is reach the maximum value, and average of solar radiation intensity of 15 July reach (869 W/m^2) more than the 15 Jan by (56.7%), 15 Mar by (15.86%), 15 Oct by (58.84%). While Figure 5.66 show the maximum ambient temperature value found at 15July with average value reach (305.831 K), and it is more than the ambient temperature of 15 Jan by (5.9%), 15 Mar by (1.8%), and 15 Oct by (0.18%). And also figure 5.67 show the maximum wind speed at 15 Oct, average value of wind speed at 15 Oct reach (3.153 m/s), and it is more than the average value of 15 Jan by (50%), 15 Mar by (77%), and 15 July by (48%).

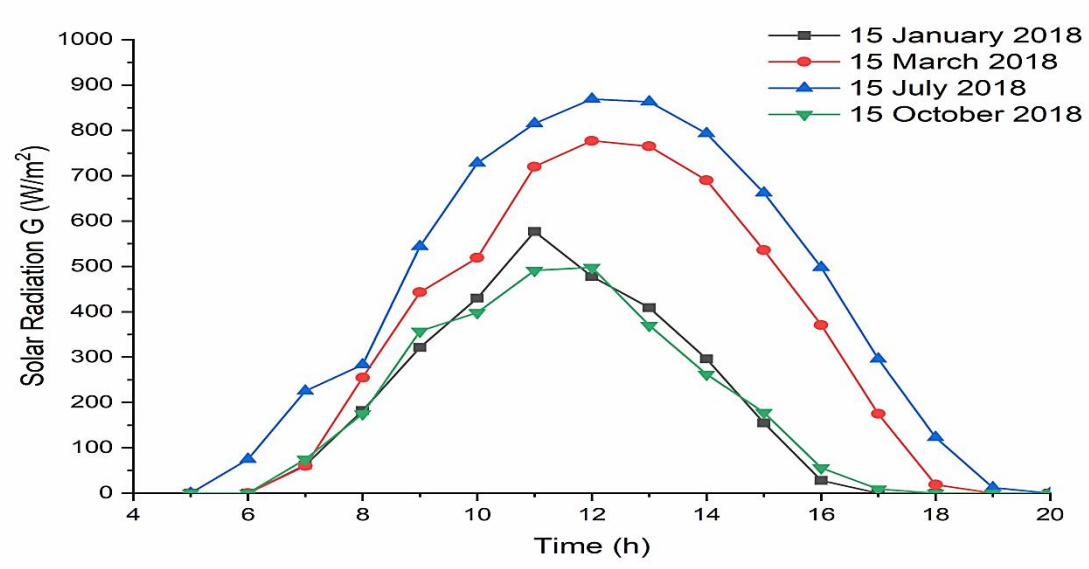

Fig.5.65. Solar Radiation Intensity for 4- Days in Year 2018.

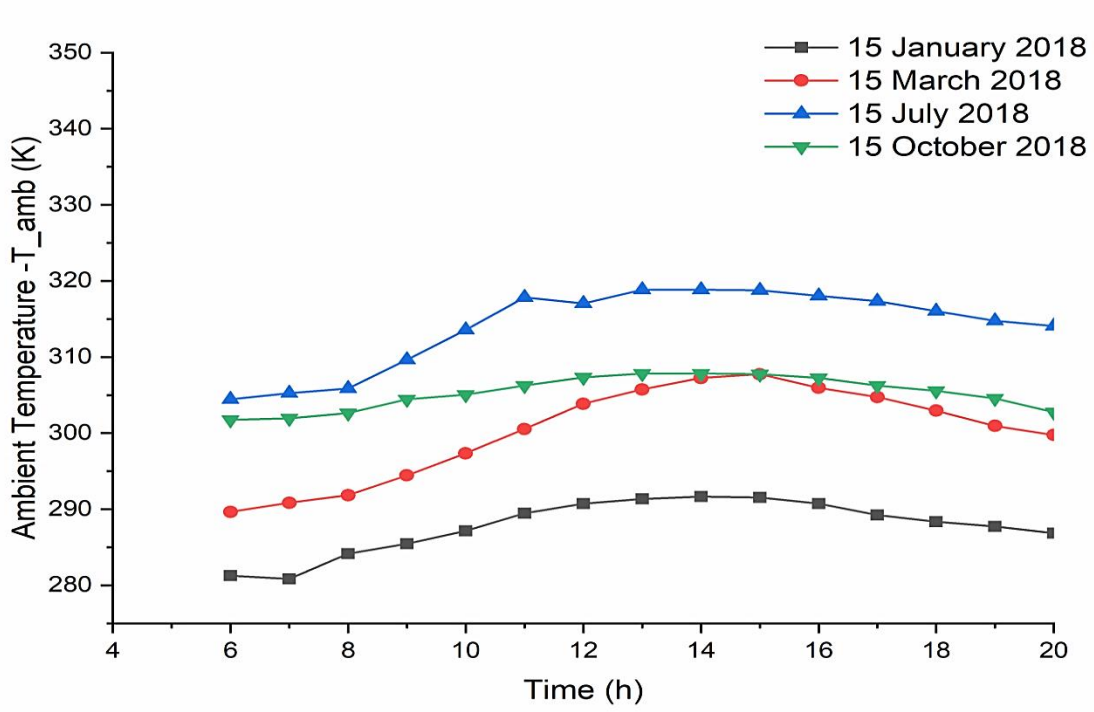

Fig.5.66. Ambient Temperature for 4- Days in Year 2018.

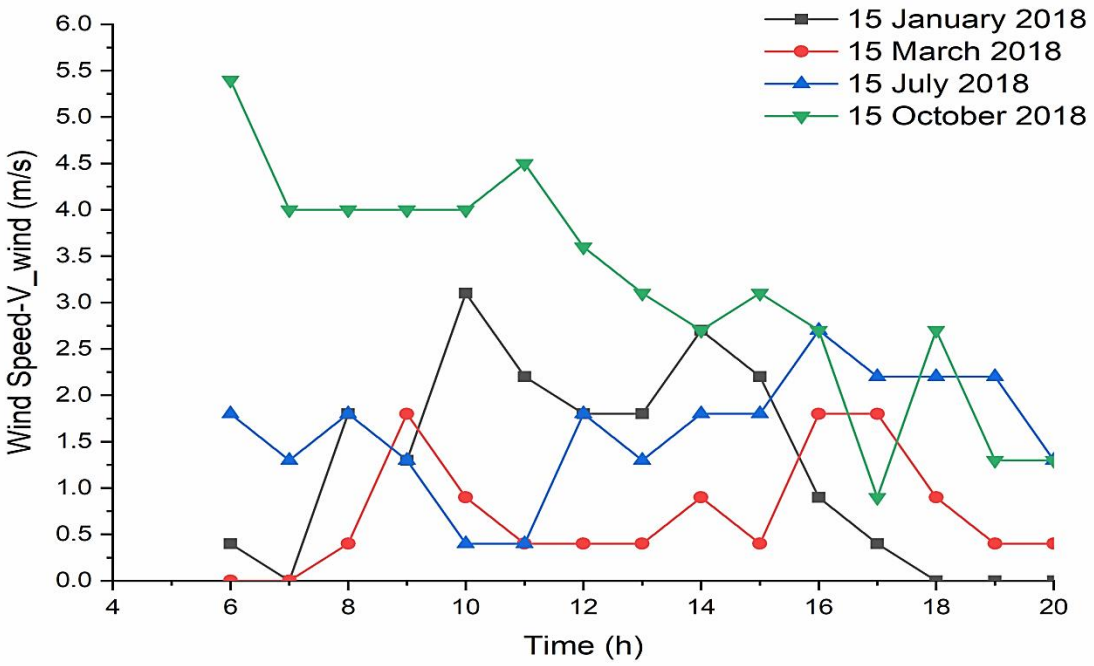

Fig.5.67.Wind Speed for 4- Days in Year 2018.

Figure 5.68 shows the outlet temperature of PTC variation with time, for difference working fluid, at four month of year. Where these months represent season winter, spring, summer, and autumn in Iraq. The results show the maximum outlet temperature obtained in a month of July. Because of high solar radiation and high ambient temperature, comparison with other months. So this lead to increase the outlet temperature of PTC. Also when comparison between the outlet temperature, for three working fluid used in this study, note that the Syltherm800 and TherminolVP-1, have higher outlet temperature comparison with water.

Figure 5.69 show the useful heat variation with time from PTC, with difference working fluid, at four month of year. The results show the maximum average value of useful heat obtained. when using working fluid water, Syltherm800 and TherminolVP-1, are 3175.5 W, 2694.9W, and 2860.01W respectively, at 15 October 2018. While the maximum average useful heat obtained. when using working fluid water, Syltherm800 and TherminolVP-1, are 5800.2 W, 4377.5 W, and 4732.1 W respectively, at 15 July 2018. Where the water has the high useful heat comparison with other working fluid, because of the water have high specific heat capacity, and also its flow with low mass flow rate.

The heat loss from PTC dependent on the following factors, weather conditions (solar radiation, ambient temperature, and wind speed), mass flow rate of working fluid, input temperature of working fluid, and type of working fluid (depend on its thermal properties). Figure 5.70 show the heat loss variation with time from PTC, with difference working fluid, at four months. The results shown the minimum average heat loss obtained. when

using working fluid water, Syltherm800 and TherminolVP-1, are 161.79 W, 642.42 W, and 477.15 W respectively, at 15 October. While the maximum average heat loss obtained, when using working fluid water, Syltherm800 and TherminolVP-1, are 401.9 W, 1824.6 W, and 1470.1 W respectively, at 15 July. This results refer to when increasing the solar energy, lead to increase the loss, when the mass flow rate is low, because of the heat loss to atmosphere increase by convection and radiation. Also the heat loss of Syltherm800 and TherminolVP-1 are more than of water, because these working fluid have less specific heat capacity comparison with water, and this leads to rapid heat gain and rapid loss.

Figure 5.71 shows the thermal efficiency variation with time for PTC, with difference working fluid, at four month of year. The results showed that the average thermal efficiency, using water, during four months was about 70%, despite the change in solar radiation, air temperature and wind speed. While the other fluids (Syltherm800 and TherminolVP-1) showed variation in thermal efficiency during these months. The Maximum average thermal efficiency of TherminolVP-1 and Syltherm800 are 62% and 65% respectively, in 15 Jan and 15 Oct. While the minimum average thermal efficiency of TherminolVP-1 and Syltherm800 are 57% and 61% respectively, in 15 Mar and 15 July. This large difference in the thermal efficiency of the working fluids used is due to their thermal properties and the effect of mass flow rate, as well as the heat loss that results when the flow rate is low. As a result, the useful heat decreases and the thermal efficiency decreases with it.

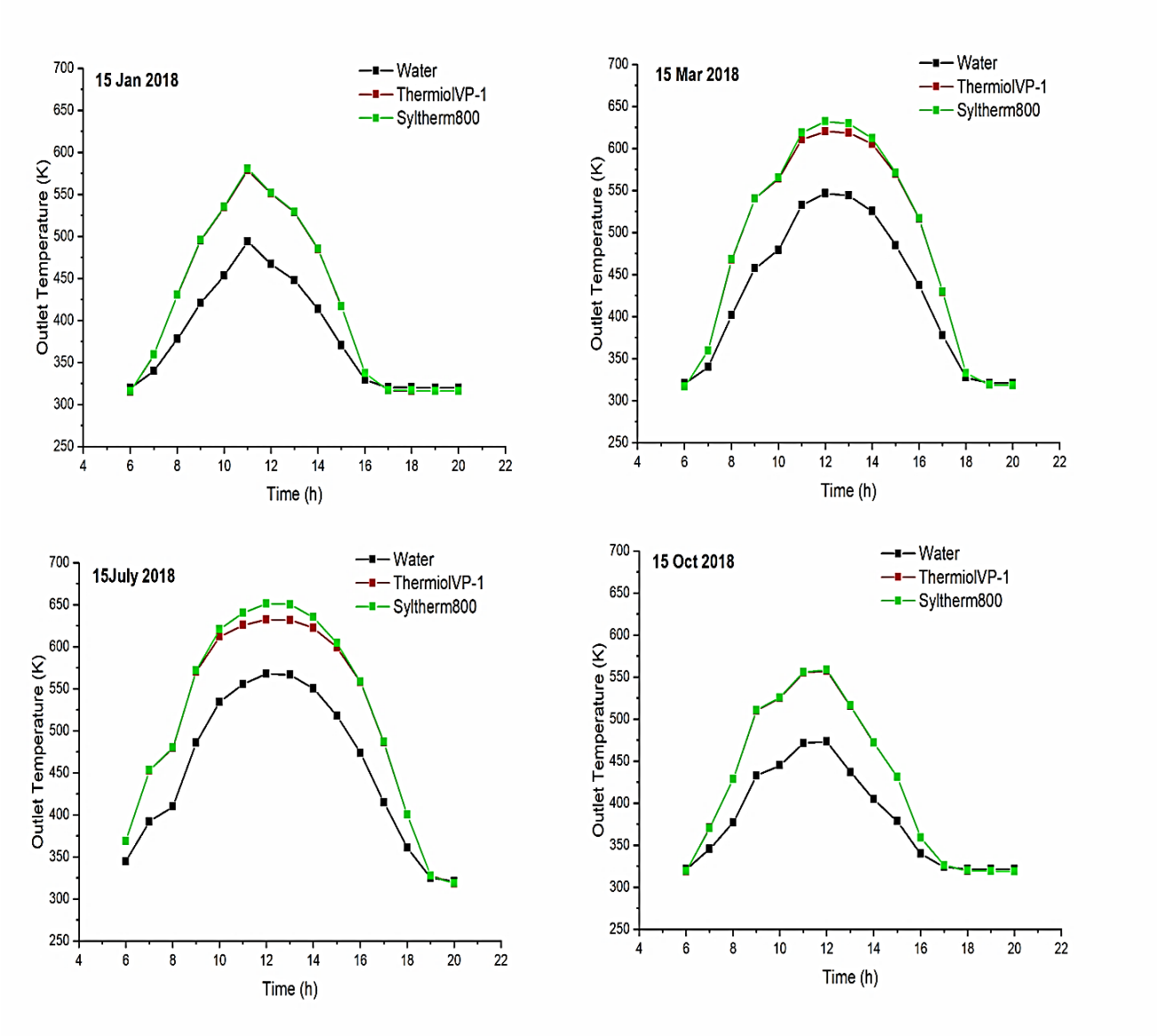

Fig.5.68.Variation of Outlet Temperature of Three Working Fluid with Time at Four Days in Year at Constant Mass Flow Rate ($\dot{m} = 0 \cdot 009267\ kg/s$)and Constant Inlet Temperature ($T_{in} = 323 \cdot 15K$).

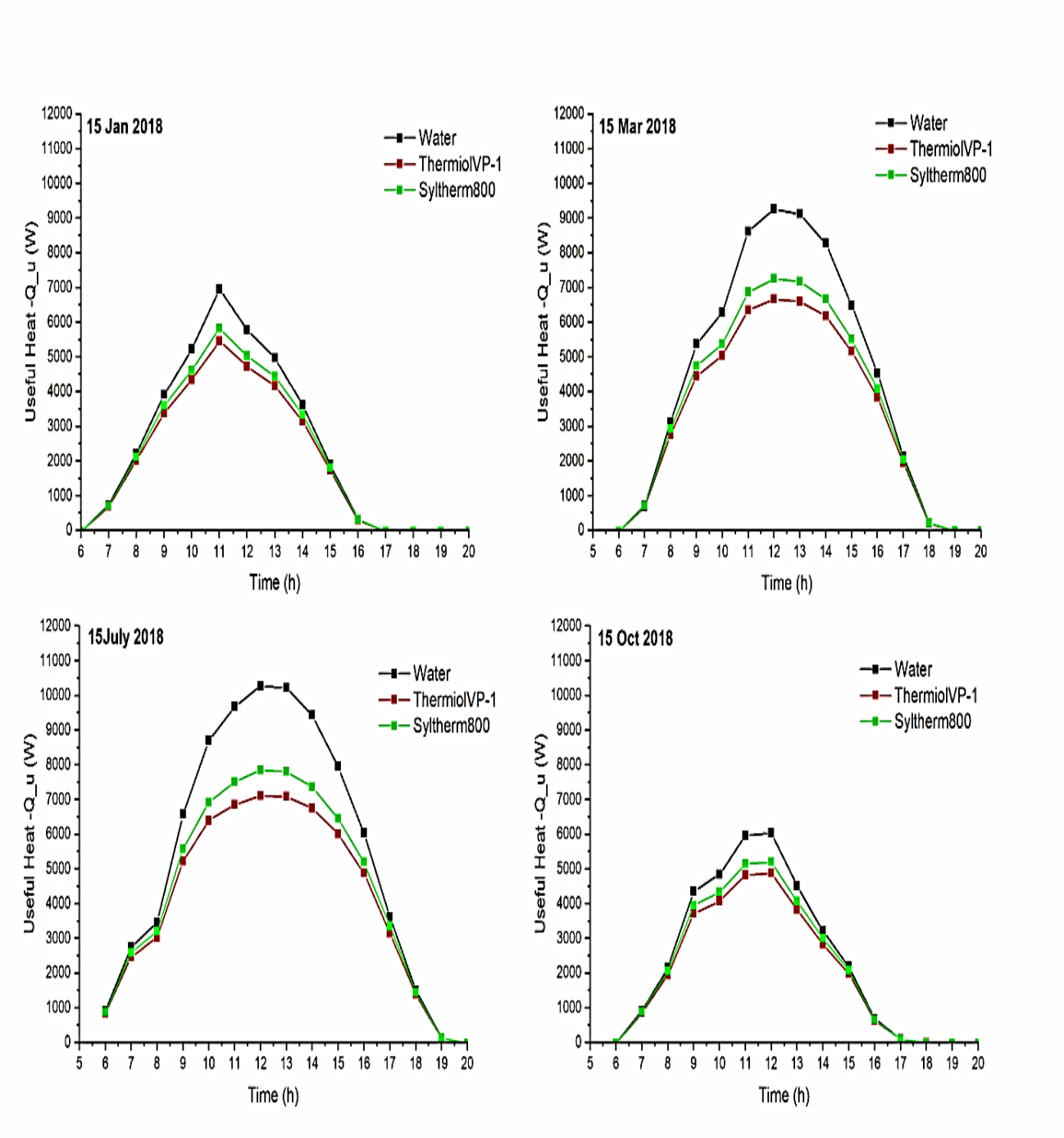

Fig.5.69.Variation of useful heat of Three Working Fluid with Time at Four Days in Year at Constant Mass Flow Rate ($\dot{m} = 0 \cdot 009267\ kg/s$)and Constant Inlet Temperature ($T_{in} = 323 \cdot 15K$).

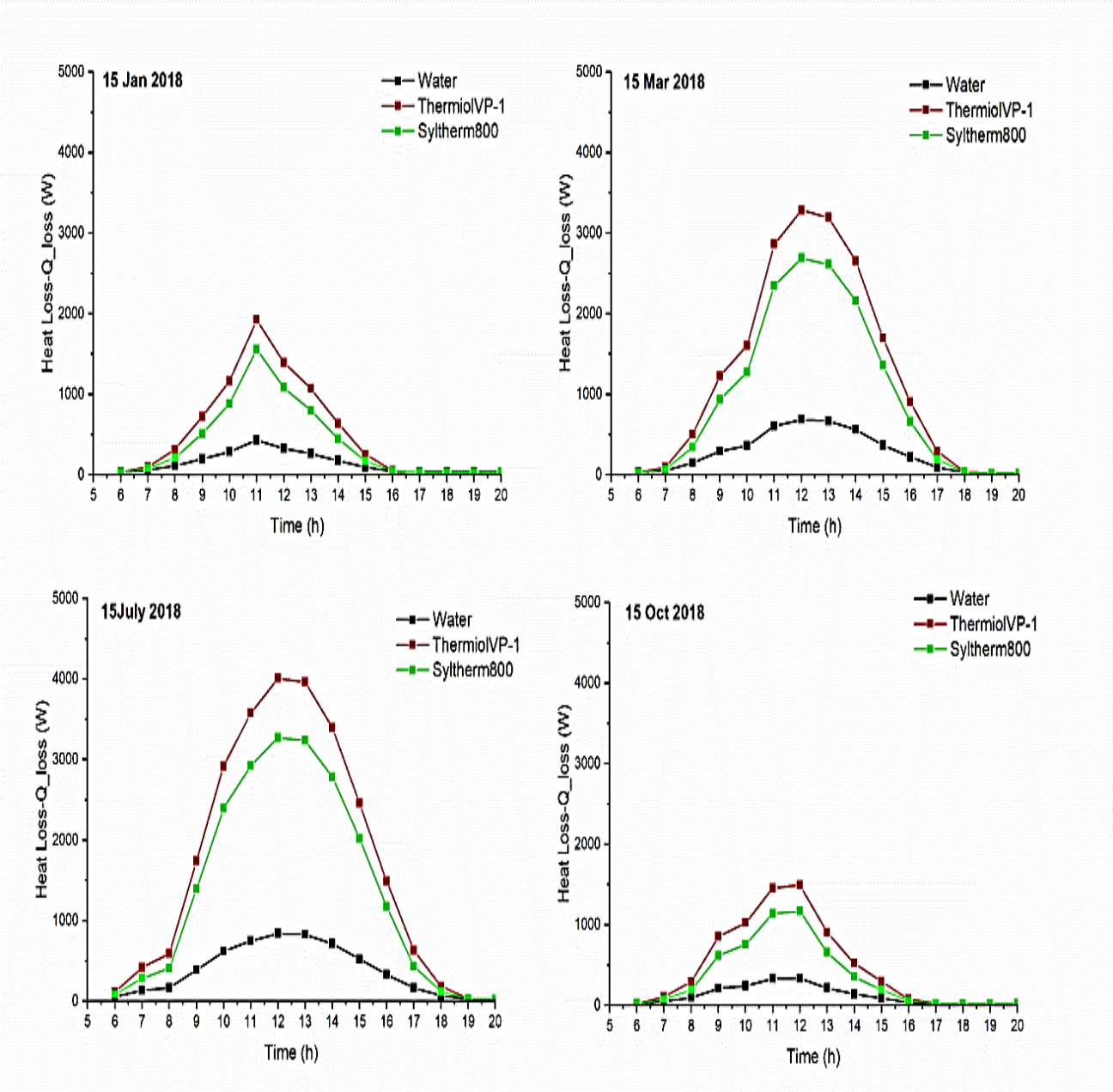

Fig.5.70.Variation of Heat Loss of Three Working Fluid with Time at Four Days in Year at Constant Mass Flow Rate ($\dot{m} = 0 \cdot 009267\ kg/s$)and Constant Inlet Temperature ($T_{in} = 323 \cdot 15K$).

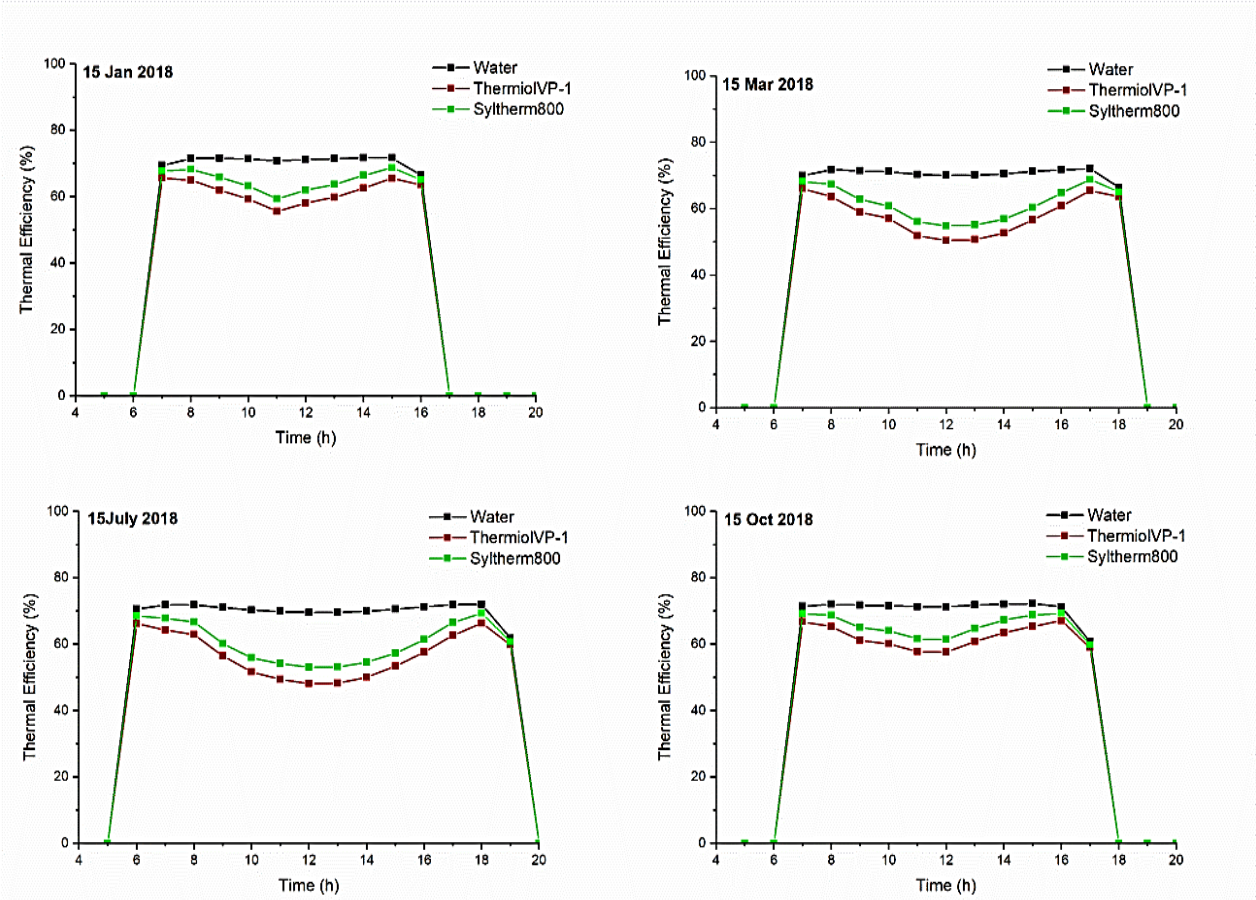

Fig.5.71. Variation of Thermal Efficiency of Three Working Fluid with Time at Four Days in Year at Constant Mass Flow rate ($\dot{m} = 0 \cdot 009267\ kg/s$)and Constant Inlet Temperature ($T_{in} = 323 \cdot 15K$).

5.3.7. The Effect of Mass Flow Rate on Performance of PTC

There are great effect of the mass flow rate on thermal performance of parabolic trough collector (PTC) .The results including the effect of the different of mass flow rate of working fluid, the mass flow rate of water inside absorber tube studied with four ranges (0.009267 Kg/s, 0.0139 Kg/s, 0.0278 Kg/s, 0.0556 Kg/s) with input temperature (323.15K). At constant weather conditions of 15 Jan 2018.

Figure 5.72 show the outlet temperature for PTC variation with time, with different mass flow rate (0.009267, 0.0139, 0.0278, 0.0556) Kg/s. The numerical simulation result shows in general that, with increasing the mass flow rate the outlet temperature for all working fluid is decrease, but note the working fluids Syltherm800 and TherminolVP-1 have higher outlet temperature than water. This is due to the thermal properties of these fluids. The maximum average outlet temperature of water, TherminolVP-1, and Syltherm800, are 411.6 K, 471.8K, and 472.3 K respectively, at mass flow rate 0.009267 Kg/s. The minimum average outlet temperature of water, TherminolVP-1, and Syltherm800, are 339.7 K, 362.0K, and 362.5 K respectively, at mass flow rate 0.0556 Kg/s Kg/s.

Figure 5.73 explain the useful heat variation with time for PTC with different mass flow rate. The percent of increasing of useful heat when using water as working fluid, with variation of mass flow rate four ranges (0.009267 Kg/s, 0.0139 Kg/s, 0.0278 Kg/s, 0.0556 Kg/s) are 0%, 1.5% , 2.9% , and 3.9% respectively. While for TherminolVP-1, with variation of mass flow rate four ranges (0.009267 Kg/s, 0.0139 Kg/s, 0.0278 Kg/s, 0.0556 Kg/s) are 0%, 6.5%, 13.2%, and 186.8% respectively, and for Syltherm800, with variation of mass flow rate four ranges (0.009267 Kg/s, 0.0139 Kg/s, 0.0278 Kg/s, 0.0556 Kg/s) are 0%, 6.8%, 14.5%, and 18.94% respectively. From these results deduce the mass flow very effect on the performance of PTC especially when using Syltherm800 and TherminolVP-1. This is due to the thermal properties of these oils.

Figure 5.74 show the heat loss variation with time from PTC, with difference working fluid. The results show the heat loss decreasing with increasing the mass flow rate, but the average heat loss for water with

variation of mass flow rate four ranges (0.009267 Kg/s, 0.0139 Kg/s, 0.0278 Kg/s, 0.0556 Kg/s) are 199.2 W, 143.5 W , 93.76 W , and 70 W respectively. While the average heat loss for TherminolVP-1 with variation of mass flow rate four ranges (0.009267 Kg/s, 0.0139 Kg/s, 0.0278 Kg/s, 0.0556 Kg/s) are 768.9 W, 560.2 W, 327.5 W, and 211.3 W respectively. And for Syltherm800, the average heat loss for TherminolVP-1 with variation of mass flow rate four ranges (0.009267 Kg/s, 0.0139 Kg/s, 0.0278 Kg/s, 0.0556 Kg/s) are 579.3 W, 373.7 W, 157.9 W, and 67.9 W respectively. Where the percent of decreasing in the average heat loss of PTC, by using TherminolVP-1, with variation of mass flow rate four ranges (0.009267 Kg/s, 0.0139 Kg/s, 0.0278 Kg/s, 0.0556 Kg/s) are 0% , 26.16%, 57.1%, and 72.3% respectively. And the Syltherm800, with variation of mass flow rate four ranges (0.009267 Kg/s, 0.0139 Kg/s, 0.0278 Kg/s, 0.0556 Kg/s) are 0%, 35.5%, 72.7.1%, and 88.3% respectively. While the water, with variation of mass flow rate four ranges (0.009267 Kg/s, 0.0139 Kg/s, 0.0278 Kg/s, 0.0556 Kg/s) are 0%, 28%, 52%, and 64% respectively.

Figure 5.75 explain the thermal efficiency variation with time for PTC, with difference working fluid, and different mass flow rate. The results that were reached in the numerical simulation, showed the highest average of thermal efficiency using water, TherminolVP-1, and Syltherm800 are 72.9%, 70.5%, and 73% respectively, at mass flow rate 0.0556 kg/s. While the lowest average thermal efficiency using water, TherminolVP-1, and Syltherm800 are 70.7%, 61.7%, and 65% respectively. at mass flow rate 0.009267 kg/s.

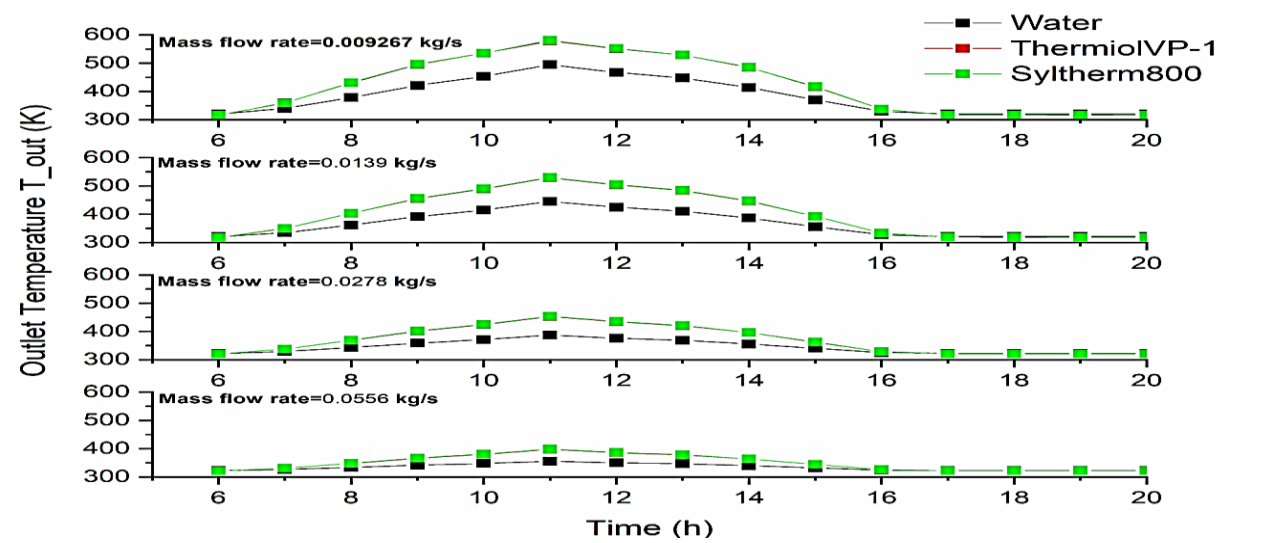

Fig.5.72 .Variation of Outlet Temperature of Three Working Fluid with Time at 15 Jan 2018 at Constant Inlet Temperature ($T_{in} = 323 \cdot 15K$) with Different Mass Flow Rate.

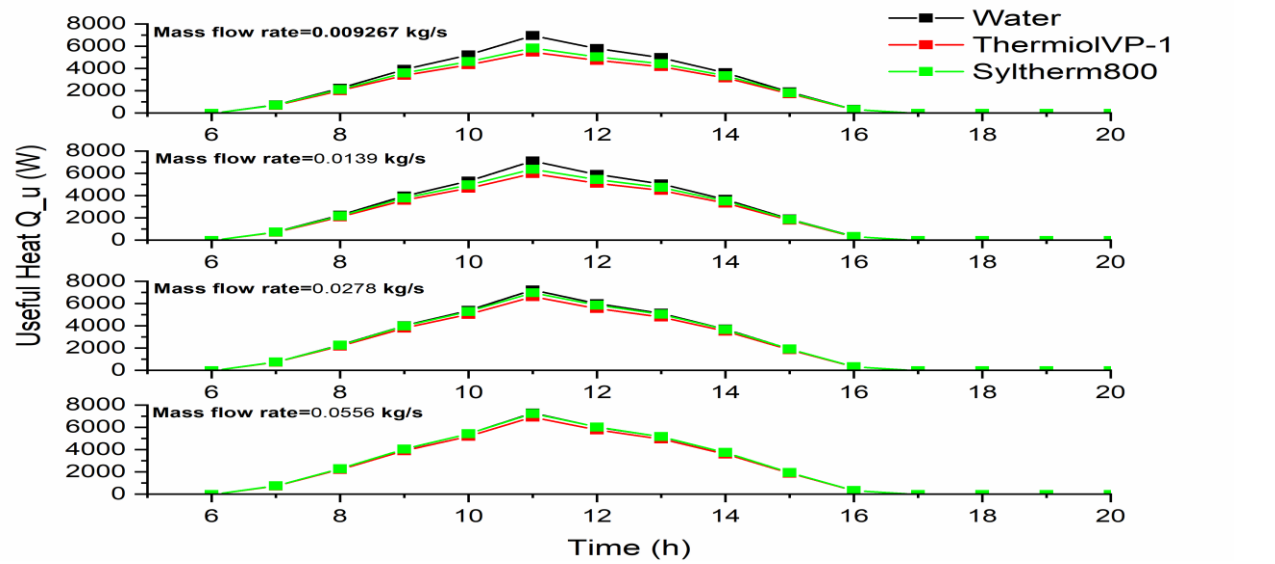

Fig.5.73. Variation of Useful Heat of Three Working Fluid with Time at 15 Jan 2018 at Constant Inlet Temperature ($T_{in} = 323 \cdot 15K$) with Different Mass Flow Rate

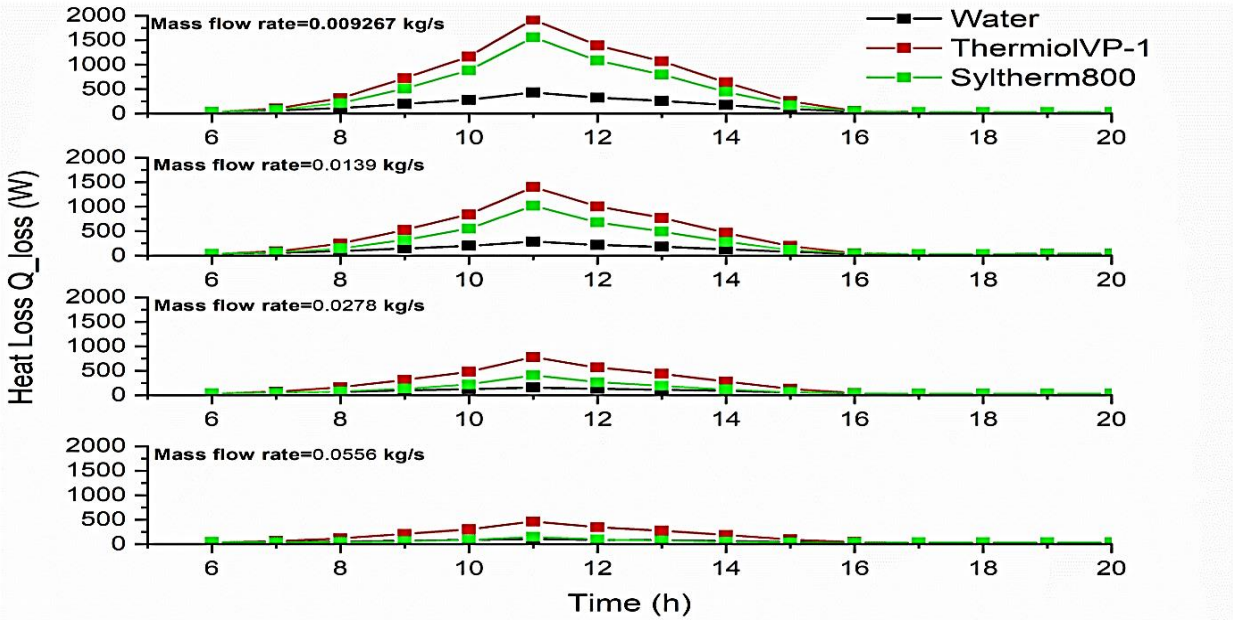

Fig.5.74. Variation of Heat Loss of Three Working Fluid with Time at 15 Jan 2018 at Constant Inlet Temperature ($T_{in} = 323 \cdot 15K$) with Different Mass Flow Rate

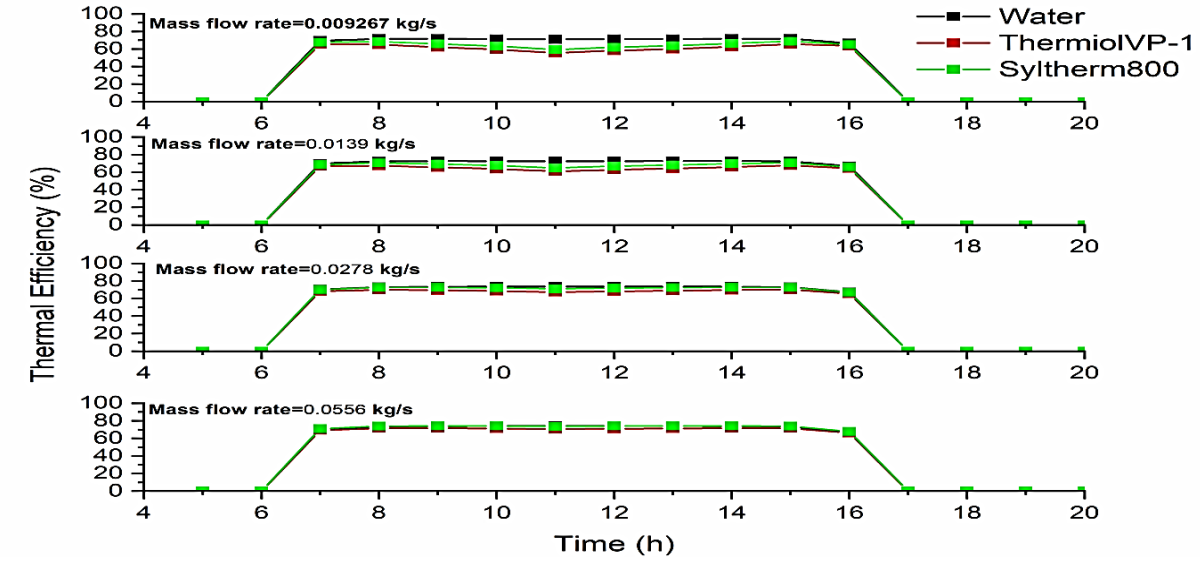

Fig.5.75 Variation of Thermal Efficiency of Three Working Fluid with Time at 15 Jan 2018 at Constant Inlet Temperature ($T_{in} = 323 \cdot 15K$) with Different Mass Flow Rate

5.3.8. The Effect of Inlet Temperature on Performance of PTC

The effect of the inlet temperature different on the thermal performance of Parabolic Trough Collector studied in this section, the input temperature of water ranges (323.15 K, 373.15 K, and 423.15 K), with mass flow rate (0.009267 Kg/s). The results obtained with increasing the inlet temperature the outlet temperature from PTC is increase as shown in figure 5.76, for all working fluid. But the useful heat small decreases with increase the inlet temperature as shown in figure 5.77. While the heat loss increasing for all working fluid as shown in figure 5.78. Also the thermal efficiency decreasing with increasing the inlet temperature as shown in figure 5.79. Overall PTC little drops in thermal performance, because the effect the inlet temperature on thermal properties of all working fluid used. Where in these numerical simulation obtained variable properties, it mean change with temperature.

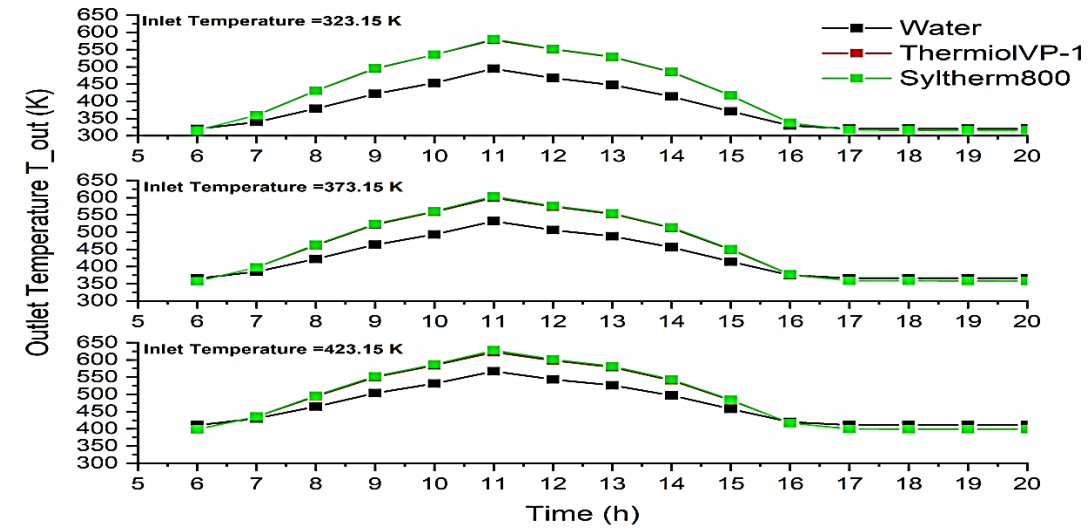

Fig.5.76 . Variation of Outlet Temperature of Three Working Fluid with Time at 15 Jan 2018 at Constant Mass Flow Rate ($\dot{m} = 0 \cdot 009267\ kg/s$) with Different Inlet Temperature.

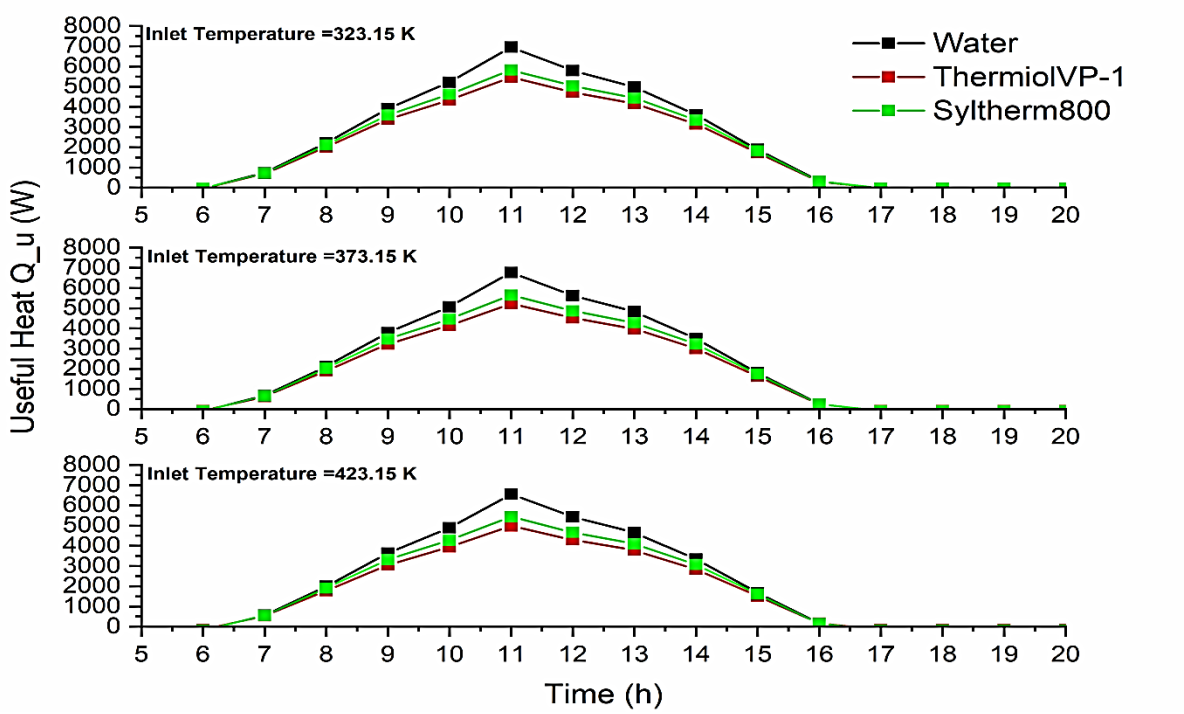

Fig.5.77. Variation of Useful Heat of Three Working Fluid with Time at 15 Jan 2018 at Constant Mass Flow Rate ($\dot{m} = 0 \cdot 009267\ kg/s$) with Different Inlet Temperature.

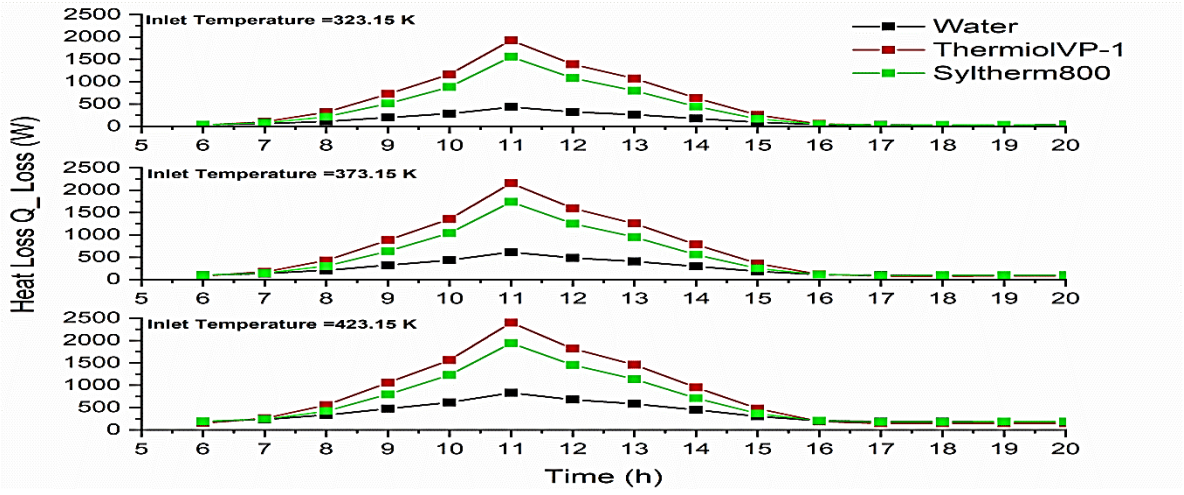

Fig.5.78. Variation of Heat Loss of Three Working Fluid with Time at 15 Jan 2018 at Constant Mass Flow Rate ($\dot{m} = 0 \cdot 009267\ kg/s$) with Different Inlet Temperature.

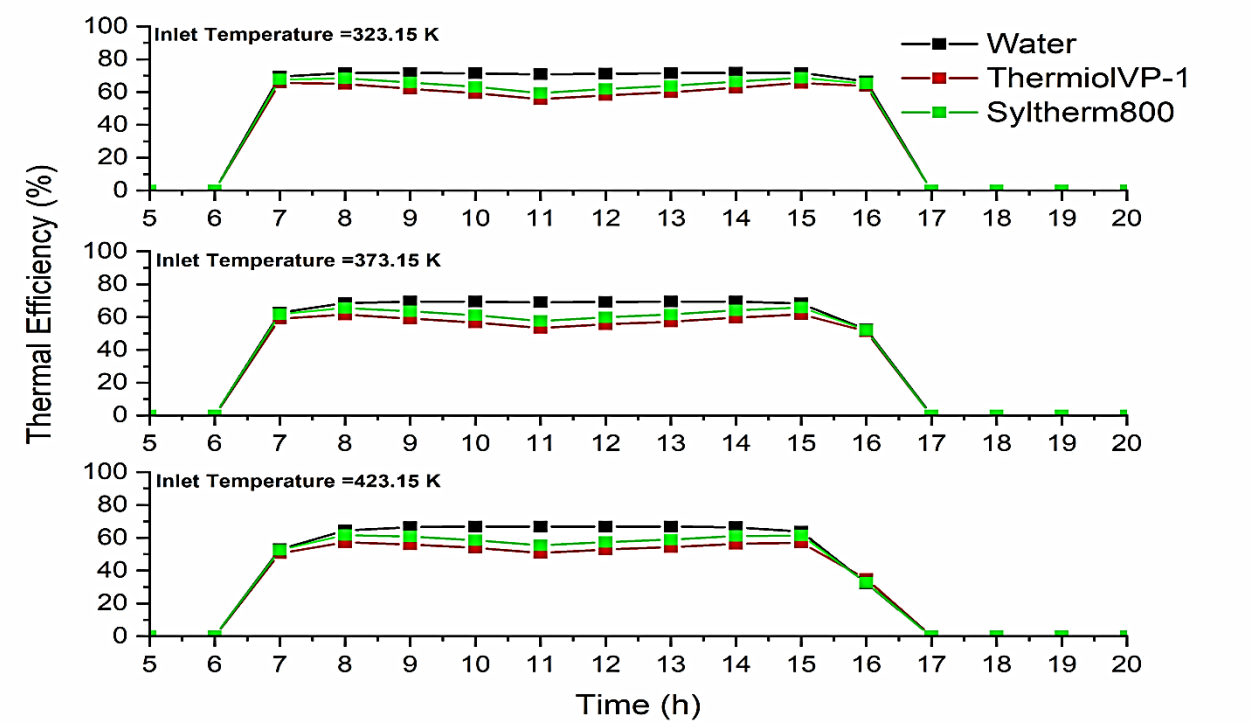

Fig.5.79. Variation of Thermal Efficiency of Three Working Fluid with Time at 15 Jan 2018 at Constant Mass Flow Rate ($\dot{m} = 0 \cdot 009267\ kg/s$) with Different Inlet Temperature.

Chapter Six

Conclusions and Recommendations

Chapter Six

Conclusions and Recommendations

6.1. Conclusions

In this study, experimental, and numerical conclusion present, the experimental and numerical conclusion investigation thermal performance of parabolic trough collector with different working fluids with many parameters that affect on the thermal performance, including absorber tube, working fluid flow rate inside the absorber tube, direction of the parabolic trough collector, absorptivity of absorber tube, reflectivity of reflective surface, and the nature of the working fluid. The working fluid has the greatest effect on the thermal performance of parabolic trough collector due to the physical properties of the working fluid, which indicates the ability of the working fluid to heat transfer process. In the east – west line direction with days of November 2^{nd},6^{th} ,7^{th} , and 10^{th} with water volume flow rate (4, 1. 2, and 3) L/min respectively, and in the south – north line direction with days of November 13^{th},14^{th}, 20^{th}, and 21^{st} with water volume flow rate (1,2,3, and4) L/min respectively. the following conclusions were drawn :

1- There are great effect of flow rate of working fluid on thermal performance of parabolic trough collector.

2- To increase thermal performance of PTC use working fluid with high value of thermal conductivity, and low value of specific heat.

3- The average error percentage of validation for output temperature , thermal efficiency, useful heat, and total heat losses were (0.337 % , 5.34 % , 5.02 % , 5.2%) respectively.

4- Low flow rate of working fluid have high temperature difference between inlet and outlet of working fluid.

5- High range of reflectivity of reflector surface give high thermal performance of PTC.

6- High range of absorptivity of absorber tube give high thermal performance of PTC.

7- Weather conditions have great effect of thermal performance of PTC.

8- High value of inlet temperature give high thermal performance of PTC.

9- To increase thermal performance increase reflectivity of reflective surface and increase absorptivity of absorber tube.

10- Best working fluid that may be utilized in a parabolic trough collector when compared to other working fluids. Syltherm800 provides high exit temperatures relative to water while maintaining water efficiency at large mass flow rates. The Syltherm800 is therefore

a suitable working fluid for PTC with a high inlet temperature and mass flow rate.

6.2. Recommendations

Based on the previous conclusions, we suggest the following recommendations.

1- Study the performance of parabolic trough collector using absorber tube with vacuum glass cover.
2- Study the performance of parabolic trough collector with using Nano working fluid.
3- Study the performance of parabolic trough collector with coating absorber tube by thermal black color.
4- Study the performance of parabolic trough collector with electrical tracking system.
5- With high level of output temperature use thermal oil as working fluid and prefer on water.
6- Study the performance of parabolic trough collector with heat exchanger and heat storge tank.

References :

[1] O. Ellabban, H. Abu-Rub, and F. Blaabjerg, "Renewable energy resources: Current status, future prospects and their enabling technology," *Renew. Sustain. Energy Rev.*, vol. 39, pp. 748–764, 2014, doi: 10.1016/j.rser.2014.07.113.

[2] J. O. Petinrin and M. Shaaban, "Renewable energy for continuous energy sustainability in Malaysia," *Renew. Sustain. Energy Rev.*, vol. 50, pp. 967–981, 2015, doi: 10.1016/j.rser.2015.04.146.

[3] S. Ahmed *et al.*, "renewables 2010 global status report renewable energy policy network for the 21st century REN21 convenes international multi-stakeholder leadership to enable a rapid global transition to renewable energy . It pro- motes appropriate policies that increase," *Nucl. Saf.*, no. September, p. 80, 2010, [Online]. Available: http://www.ren21.net.

[4] S. A. Kalogirou, "Solar thermal collectors and applications," *Prog. energy Combust. Sci.*, vol. 30, no. 3, pp. 231–295, 2004.

[5] R. Free, S. Energy, and P. O. Thermal, "Collection And Storage 3e Solar Energy Principles Of Thermal Collection And Storage 3e Read Free Solar Energy," pp. 1–31.

[6] G. Energy, "CO2 status Report," *IEA (International Energy Agency) Paris, Fr.*, 2019.

[7] "Renewable Energy Market Update," *Renew. Energy Mark. Updat.*, 2020, doi: 10.1787/afbc8c1d-en.

[8] S. Warambhe, "Carbon Tracker Initiative," in *World Scientific Encyclopedia of Climate Change: Case Studies of Climate Risk, Action, and Opportunity Volume 1*, World Scientific, 2021, pp. 63–69.

[9] S. Warambhe, "Solar Power–A Renewable Energy and Alternate Energy Sources," *Int. J. Renew. Energy its Commer.*, vol. 3, no. 2, pp. 8–14, 2017.

[10] N. M. Aljamali and M. N. A. Maged, “Review on Energy Stored in Solar Cells and Converted to Operate Laboratory Apparatus,” *J. Power Electron. Devices*, vol. 7, no. 2, pp. 1–9, 2021.

[11] Y. Tian and C. Y. Zhao, “A review of solar collectors and thermal energy storage in solar thermal applications,” *Appl. Energy*, vol. 104, pp. 538–553, 2013, doi: 10.1016/j.apenergy.2012.11.051.

[12] D. G. Nocera and M. P. Nash, “For the ‘“In This Issue”’ summary,” vol. 104, no. 42, 2007.

[13] G. A. Labrador, “Heat energy recapture and recycle and its new applications,” doi: 10.1126/science.aad1920.22.

[14] A. Alshahrani, S. Omer, Y. Su, E. Mohamed, and S. Alotaibi, “The technical challenges facing the integration of small-scale and large-scale PV systems into the grid: A critical review,” *Electron.*, vol. 8, no. 12, 2019, doi: 10.3390/electronics8121443.

[15] B. Norton, *Harnessing solar heat*, vol. 18. Springer, 2013.

[16] A. Rabl, *Active solar collectors and their applications*. Oxford University Press on Demand, 1985.

[17] L. M. Ayompe and A. Duffy, “Analysis of the thermal performance of a solar water heating system with flat plate collectors in a temperate climate,” *Appl. Therm. Eng.*, vol. 58, no. 1–2, pp. 447–454, 2013.

[18] A. Shriem, “Sustainable Seawater Desalination–Evaluation & Analysis of Solar Power & Energy Storage Technologies in Combination with Seawater Desalination & Brine …,” 2021, [Online]. Available: https://repositum.tuwien.at/handle/20.500.12708/17405.

[19] A. A. Hachicha, I. Rodríguez, R. Capdevila, and A. Oliva, “Heat transfer analysis and numerical simulation of a parabolic trough solar collector,” *Appl. Energy*, vol. 111, pp. 581–592, 2013, doi: 10.1016/j.apenergy.2013.04.067.

[20] S. Khanna, S. B. Kedare, and S. Singh, “Deflection and stresses in absorber tube of solar parabolic trough due to circumferential and axial flux variations on absorber tube supported at multiple points,” *Sol. Energy*, vol. 99, pp. 134–151, 2014, doi: 10.1016/j.solener.2013.11.005.

[21] Abengoa Solar, “A New Generation of Parabolic Trough Technology,” *SunShot CSP Progr. Rev. 2013*, no. April, 2013, [Online]. Available: http://energy.gov/sites/prod/files/2014/01/f7/csp_review_meeting_042513_price.pdf.

[22] S. E. Ghasemi and A. A. Ranjbar, “Thermal performance analysis of solar parabolic trough collector using nanofluid as working fluid: A CFD modelling study,” *J. Mol. Liq.*, vol. 222, pp. 159–166, 2016, doi: 10.1016/j.molliq.2016.06.091.

[23] G. J. Kolb and R. B. Diver, “conceptual design of an advanced trough utilizing a molten salt working fluid.,” Sandia National Lab.(SNL-NM), Albuquerque, NM (United States), 2008.

[24] J. D. McTigue *et al.*, “Hybridizing a geothermal power plant with concentrating solar power and thermal storage to increase power generation and dispatchability,” *Appl. Energy*, vol. 228, no. June, pp. 1837–1852, 2018, doi: 10.1016/j.apenergy.2018.07.064.

[25] J. I. Ortega, J. I. Burgaleta, and F. M. Tellez, “Central receiver system solar power plant using molten salt as heat transfer fluid,” *J. Sol. Energy Eng. Trans. ASME*, vol. 130, no. 2, pp. 0245011–0245016, 2008, doi: 10.1115/1.2807210.

[26] D. Kearney *et al.*, “Assessment of a molten salt heat transfer fluid in a parabolic trough solar field,” *J. Sol. Energy Eng. Trans. ASME*, vol. 125, no. 2, pp. 170–176, 2003, doi: 10.1115/1.1565087.

[27] S. Flueckiger, Z. Yang, and S. V. Garimella, “An integrated thermal and mechanical investigation of molten-salt thermocline energy storage,” *Appl. Energy*, vol. 88, no. 6, pp. 2098–2105, 2011, doi: 10.1016/j.apenergy.2010.12.031.

[28] H. L. Zhang, J. Baeyens, J. Degrève, and G. Cacères, “Concentrated solar power plants: Review and design methodology,” *Renew. Sustain. Energy Rev.*, vol. 22, pp. 466–481, 2013, doi: 10.1016/j.rser.2013.01.032.

[29] https://solarpaces.nrel.gov/by-technology, “No Title.” .

[30] I. Purohit, P. Purohit, and S. Shekhar, “Evaluating the potential of concentrating solar power generation in Northwestern India,” *Energy Policy*, vol. 62, pp. 157–175, 2013, doi: 10.1016/j.enpol.2013.06.069.

[31] R. Pitz-Paal, “Concentrating solar power,” *Futur. Energy Improv. Sustain. Clean Options Our Planet*, pp. 413–430, 2020, doi: 10.1016/B978-0-08-102886-5.00019-0.

[32] Https://lh3.googleusercontent.com/-, “No Title.” .

[33] C. Sharma, A. K. Sharma, S. C. Mullick, and T. C. Kandpal, “A study of the effect of design parameters on the performance of linear solar concentrator based thermal power plants in India,” *Renew. Energy*, vol. 87, pp. 666–675, 2016, doi: 10.1016/j.renene.2015.11.007.

[34] M. Chaanaoui, S. Vaudreuil, and T. Bounahmidi, “Benchmark of Concentrating Solar Power Plants: Historical, Current and Future Technical and Economic Development,” *Procedia Comput. Sci.*, vol. 83, no. May, pp. 782–789, 2016, doi: 10.1016/j.procs.2016.04.167.

[35] https://www.google.com/search?q=1.6+solar+concentr, “No Title.”

[36] N. Abed and I. Afgan, “An extensive review of various technologies for enhancing the thermal and optical performances of parabolic trough collectors,” *Int. J. Energy Res.*, vol. 44, no. 7, pp. 5117–5164, 2020, doi: 10.1002/er.5271.

[37] A. K. Hussein, M. Ghodbane, Z. Said, and R. S. Ward, “The effect of the baffle length on the natural convection in an enclosure filled with different nanofluids,” *J. Therm. Anal. Calorim.*, vol. 147, no. 1, pp. 791–813, 2022, doi: 10.1007/s10973-020-10300-1.

[38] T. A. Yassen, “Experimental and Theoretical Study of a Parabolic

Trough Solar Collector."

[39] M. Ouagued, A. Khellaf, and L. Loukarfi, "Estimation of the temperature, heat gain and heat loss by solar parabolic trough collector under Algerian climate using different thermal oils," *Energy Convers. Manag.*, vol. 75, pp. 191–201, 2013, doi: 10.1016/j.enconman.2013.06.011.

[40] J. Muñoz-Anton, M. Biencinto, E. Zarza, and L. E. Díez, "Theoretical basis and experimental facility for parabolic trough collectors at high temperature using gas as heat transfer fluid," *Appl. Energy*, vol. 135, pp. 373–381, 2014, doi: 10.1016/j.apenergy.2014.08.099.

[41] Y. T. Wu, S. W. Liu, Y. X. Xiong, C. F. Ma, and Y. L. Ding, "Experimental study on the heat transfer characteristics of a low melting point salt in a parabolic trough solar collector system," *Appl. Therm. Eng.*, vol. 89, pp. 748–754, Jul. 2015, doi: 10.1016/j.applthermaleng.2015.06.054.

[42] N. Singh Rajput, D. Dilipbhai Shukla, D. Rajput, and S. Kumar Sharm, "Performance Analysis of Flat Plate Solar Collector using Al 2 O 3 /Distilled Water Nanofluid: An Experimental Investigation," *Mater. Today Proc.*, vol. 10, pp. 52–59, 2019, doi: 10.1016/j.matpr.2019.02.188.

[43] M. Chafie, M. F. Ben Aissa, and A. Guizani, "Energetic end exergetic performance of a parabolic trough collector receiver: An experimental study," *J. Clean. Prod.*, vol. 171, pp. 285–296, 2018, doi: 10.1016/j.jclepro.2017.10.012.

[44] S. H and M. RS, "Experimental Analysis of Parabolic Trough Concentrating Collector Using Ethylene Glycol Based Mixture," *Innov. Energy Res.*, vol. 06, no. 01, pp. 1–7, 2017, doi: 10.4172/2576-1463.1000157.

[45] M. M. Tafarroj, R. Daneshazarian, and A. Kasaeian, *CFD modeling and predicting the performance of direct absorption of nanofluids in trough collector*, vol. 148. Elsevier Ltd, 2019.

[46] S. T. Hamidi, F. A. K. Fattah, and M. S. Ghanam, “Performance Improvement of the Parabolic Trough Solar Collector Using Different Types of Fluids with Numerical Simulation,” *J. Univ. Babylon Eng. Sci.*, vol. 26, no. 6, pp. 332–347, 2018, doi: 10.29196/jubes.v26i6.1437.

[47] “Heat transfer modeling of a parabolic trough solar collector with working fluid of Fe3O4 and CuO/Therminol 66 nanofluids under magnetic field,” *Appl. Therm. Eng.*, vol. 163, Dec. 2019, doi: 10.1016/j.applthermaleng.2019.114435.

[48] R. Malviya, A. Agrawal, and P. V. Baredar, “A comprehensive review of different heat transfer working fluids for solar thermal parabolic trough concentrator,” *Mater. Today Proc.*, vol. 46, no. xxxx, pp. 5490–5500, 2020, doi: 10.1016/j.matpr.2020.09.240.

[49] H. Olia, M. Torabi, M. Bahiraei, M. H. Ahmadi, M. Goodarzi, and M. R. Safaei, “Application of nanofluids in thermal performance enhancement of parabolic trough solar collector: State-of-the-art,” *Appl. Sci.*, vol. 9, no. 3, 2019, doi: 10.3390/app9030463.

[50] N. Boerema, G. Morrison, R. Taylor, and G. Rosengarten, “Liquid sodium versus Hitec as a heat transfer fluid in solar thermal central receiver systems,” *Sol. Energy*, vol. 86, no. 9, pp. 2293–2305, 2012, doi: 10.1016/j.solener.2012.05.001.

[51] M. Biencinto, L. González, E. Zarza, L. E. Díez, and J. Muñoz-Antón, “Performance model and annual yield comparison of parabolic-trough solar thermal power plants with either nitrogen or synthetic oil as heat transfer fluid,” *Energy Convers. Manag.*, vol. 87, pp. 238–249, 2014, doi: 10.1016/j.enconman.2014.07.017.

[52] O. Behar, A. Khellaf, and K. Mohammedi, “A novel parabolic trough solar collector model - Validation with experimental data and comparison to Engineering Equation Solver (EES),” *Energy Convers. Manag.*, vol. 106, pp. 268–281, 2015, doi: 10.1016/j.enconman.2015.09.045.

[53] E. Kaloudis, E. Papanicolaou, and V. Belessiotis, “Numerical

simulations of a parabolic trough solar collector with nanofluid using a two-phase model," *Renew. Energy*, vol. 97, pp. 218–229, Nov. 2016, doi: 10.1016/j.renene.2016.05.046.

[54] E. Bellos, C. Tzivanidis, K. A. Antonopoulos, and I. Daniil, "The use of gas working fluids in parabolic trough collectors – An energetic and exergetic analysis," *Appl. Therm. Eng.*, vol. 109, pp. 1–14, 2016, doi: 10.1016/j.applthermaleng.2016.08.043.

[55] E. Bellos, D. Korres, C. Tzivanidis, and K. A. Antonopoulos, "Design, simulation and optimization of a compound parabolic collector," *Sustain. Energy Technol. Assessments*, vol. 16, no. December 2017, pp. 53–63, 2016, doi: 10.1016/j.seta.2016.04.005.

[56] Y. Qiu, M. J. Li, Y. L. He, and W. Q. Tao, "Thermal performance analysis of a parabolic trough solar collector using supercritical CO2 as heat transfer fluid under non-uniform solar flux," *Appl. Therm. Eng.*, vol. 115, pp. 1255–1265, 2017, doi: 10.1016/j.applthermaleng.2016.09.044.

[57] E. Bellos and C. Tzivanidis, "A detailed exergetic analysis of parabolic trough collectors," *Energy Convers. Manag.*, vol. 149, pp. 275–292, 2017, doi: 10.1016/j.enconman.2017.07.035.

[58] E. Bellos, C. Tzivanidis, and K. A. Antonopoulos, "A detailed working fluid investigation for solar parabolic trough collectors," *Appl. Therm. Eng.*, vol. 114, pp. 374–386, 2017, doi: 10.1016/j.applthermaleng.2016.11.201.

[59] E. Bellos and C. Tzivanidis, "Parametric investigation of nanofluids utilization in parabolic trough collectors," *Therm. Sci. Eng. Prog.*, vol. 2, no. May, pp. 71–79, 2017, doi: 10.1016/j.tsep.2017.05.001.

[60] E. Bellos, C. Tzivanidis, I. Daniil, and K. A. Antonopoulos, "The impact of internal longitudinal fins in parabolic trough collectors operating with gases," *Energy Convers. Manag.*, vol. 135, no. March, pp. 35–54, 2017, doi: 10.1016/j.enconman.2016.12.057.

[61] P. D. Tagle-Salazar, K. D. P. Nigam, and C. I. Rivera-Solorio, "Heat

transfer model for thermal performance analysis of parabolic trough solar collectors using nanofluids," *Renew. Energy*, vol. 125, pp. 334–343, 2018, doi: 10.1016/j.renene.2018.02.069.

[62] E. Bellos and C. Tzivanidis, "Thermal analysis of parabolic trough collector operating with mono and hybrid nanofluids," *Sustain. Energy Technol. Assessments*, vol. 26, no. November, pp. 105–115, 2018, doi: 10.1016/j.seta.2017.10.005.

[63] B. Lamrani, A. Khouya, B. Zeghmati, and A. Draoui, "Mathematical modeling and numerical simulation of a parabolic trough collector: A case study in thermal engineering," *Therm. Sci. Eng. Prog.*, vol. 8, pp. 47–54, 2018, doi: 10.1016/j.tsep.2018.07.015.

[64] A. A. Hachicha, I. Rodríguez, R. Capdevila, and A. Oliva, "Numerical Analysis of Heat Transfer Enhancement in a Parabolic Trough Collector Based on Geometry Modifications and Working Fluid Usage."

[65] D. Korres, E. Bellos, and C. Tzivanidis, "Investigation of a nanofluid-based compound parabolic trough solar collector under laminar flow conditions," *Appl. Therm. Eng.*, vol. 149, no. January 2019, pp. 366–376, 2019, doi: 10.1016/j.applthermaleng.2018.12.077.

[66] E. Bellos and C. Tzivanidis, "Analytical expression of parabolic trough solar collector performance," *Designs*, vol. 2, no. 1, pp. 1–17, 2018, doi: 10.3390/designs2010009.

[67] E. C. Okonkwo, E. A. Essien, E. Akhayere, M. Abid, D. Kavaz, and T. A. H. Ratlamwala, "Thermal performance analysis of a parabolic trough collector using water-based green-synthesized nanofluids," *Sol. Energy*, vol. 170, no. February, pp. 658–670, 2018, doi: 10.1016/j.solener.2018.06.012.

[68] J. Liu, Y. He, and X. Lei, "Heat-transfer characteristics of liquid sodium in a solar receiver tube with a nonuniform heat flux," *Energies*, vol. 12, no. 8, 2019, doi: 10.3390/en12081432.

[69] M. A. Ehyaei, A. Ahmadi, M. E. H. Assad, A. A. Hachicha, and Z.

Said, “Energy, exergy and economic analyses for the selection of working fluid and metal oxide nanofluids in a parabolic trough collector,” *Sol. Energy*, vol. 187, no. March, pp. 175–184, 2019, doi: 10.1016/j.solener.2019.05.046.

[70] K. A. Ahmed and E. Natarajan, “Numerical investigation on the effect of toroidal rings in a parabolic trough receiver with the operation of gases: An energy and exergy analysis,” *Energy*, vol. 203, p. 117880, 2020, doi: 10.1016/j.energy.2020.117880.

[71] A. Mwesigye and İ. H. Yılmaz, “Thermal and thermodynamic benchmarking of liquid heat transfer fluids in a high concentration ratio parabolic trough solar collector system,” *J. Mol. Liq.*, vol. 319, 2020, doi: 10.1016/j.molliq.2020.114151.

[72] N. Abed, I. Afgan, A. Cioncolini, H. Iacovides, and A. Nasser, “Assessment and Evaluation of the Thermal Performance of VariousWorking Fluids in Parabolic Trough Collectors of Solar Thermal Power Plants under Non-Uniform Heat Flux Distribution Conditions,” *Energies*, vol. 13, no. 15, pp. 1–27, 2020, doi: 10.3390/en13153776.

[73] Y. M. Abdullatif, E. C. Okonkwo, and T. Al-Ansari, “Thermal Performance Optimization of a Parabolic Trough Collector Operating with Various Working Fluids Using Copper Nanoparticles,” *J. Therm. Sci. Eng. Appl.*, vol. 13, no. 5, 2021, doi: 10.1115/1.4049872.

[74] C. Tzivanidis, E. Bellos, D. Korres, K. A. Antonopoulos, and G. Mitsopoulos, “Thermal and optical efficiency investigation of a parabolic trough collector,” *Case Stud. Therm. Eng.*, vol. 6, pp. 226–237, 2015.

[75] E. Bellos, D. Korres, C. Tzivanidis, and K. A. Antonopoulos, “Design, simulation and optimization of a compound parabolic collector,” *Sustain. Energy Technol. Assessments*, vol. 16, pp. 53–63, 2016.

[76] J. H. Lienhard, “A Heat Transfer,” vol. 1.31, p. 698, 2008, [Online]. Available: http://www.ncbi.nlm.nih.gov/pubmed/21128847.

[77] N. Lorenzin and A. Abánades, “A review on the application of liquid metals as heat transfer fluid in Concentrated Solar Power technologies,” *Int. J. Hydrogen Energy*, vol. 41, no. 17, pp. 6990–6995, 2016, doi: 10.1016/j.ijhydene.2016.01.030.

[78] E. Bellos, C. Tzivanidis, K. A. Antonopoulos, and I. Daniil, “The use of gas working fluids in parabolic trough collectors – An energetic and exergetic analysis,” *Appl. Therm. Eng.*, vol. 109, pp. 1–14, Oct. 2016, doi: 10.1016/j.applthermaleng.2016.08.043.

[79] K. Bhagat and S. K. Saha, “Numerical analysis of latent heat thermal energy storage using encapsulated phase change material for solar thermal power plant,” *Renew. Energy*, vol. 95, pp. 323–336, 2016, doi: 10.1016/j.renene.2016.04.018.

[80] B. Lamrani, A. Khouya, B. Zeghmati, and A. Draoui, “Mathematical modeling and numerical simulation of a parabolic trough collector: A case study in thermal engineering,” *Therm. Sci. Eng. Prog.*, vol. 8, pp. 47–54, Dec. 2018, doi: 10.1016/j.tsep.2018.07.015.

[81] Dow Oil and Gas, “SYLTHERM 800 Heat Transfer Fluid,” pp. 1–28, 1997.

[82] T. Vp- and T. Vp-, “THERMINOL VP-1.”

[83] S. Mathew and G. Visavale, “CFD Analysis of a Heat Collector Element in a Solar Parabolic Trough Collector,” no. November, pp. 1–21, 2010, doi: 10.13140/2.1.3247.4241.

Appendices:

Appendix –A

Thermocouple Calibration

One of the temperature sensing equipment used in many engineering experiments is thermocouples. In the experimental work, 12 K-type thermocouples were used and calibrated using a data logger and a thermometer (mercury thermometer). Where all thermocouples are connected to the data logger and the other end of the temperature sensor is placed in a basin of pure water, the temperature of which is gradually raised from zero to 100 ºC with a step of 20 degrees. As shown in Figure and Table A.1 .

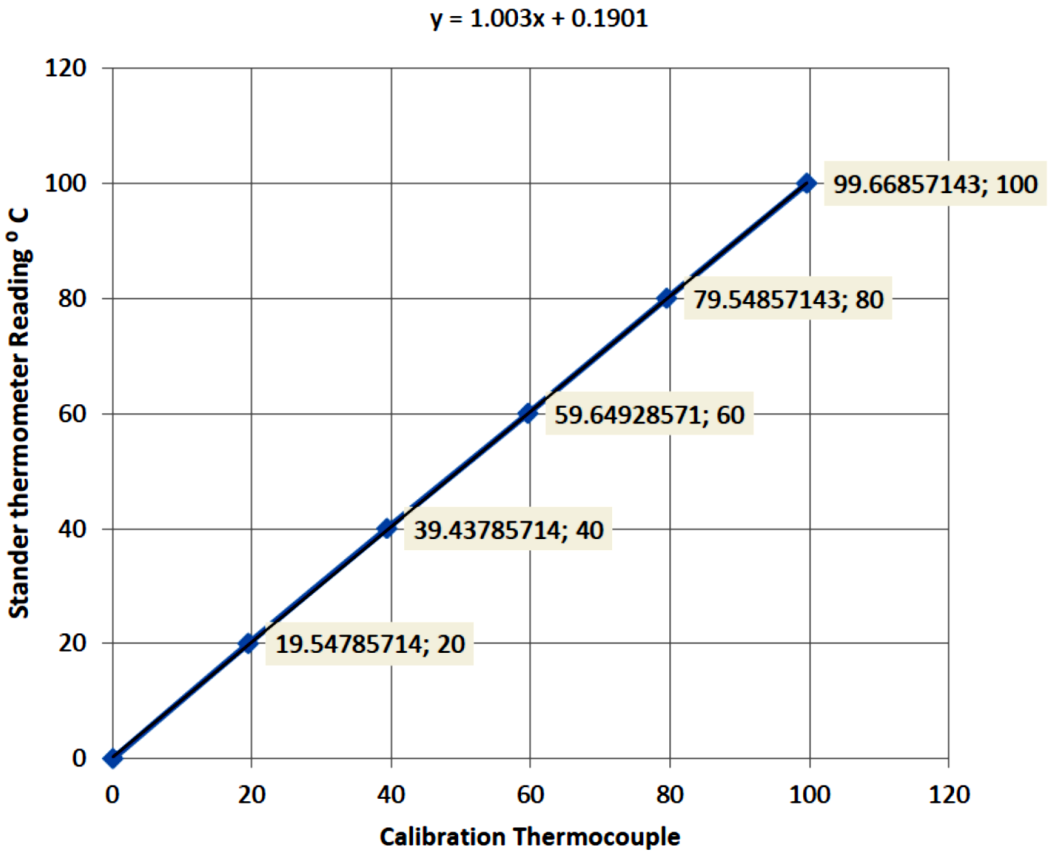

Figure A.1 . Calibration of thermocouples.

APPENDIX - B

WIND SPEED CALIBRATION

In this study, an AM-4206M anemometer was used to measure wind speed. It was calibrated with the Davis standard weather station installed above the ground in the Technical College of Engineering in Najaf / Iraq. Figure B-1 shows the results of the calibration.

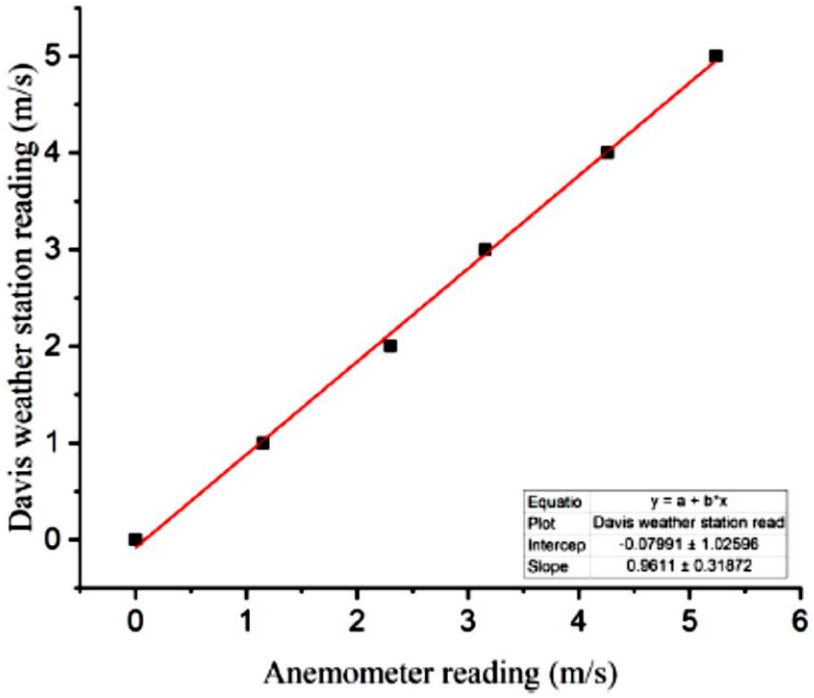

Figure .B1. Anemometer Calibration .

Appendix-C. Solar Meter Calibration:

Figure and table C.1. Represent the calibration process for the solar meter (Pyranometer) device which was used in this work**.**

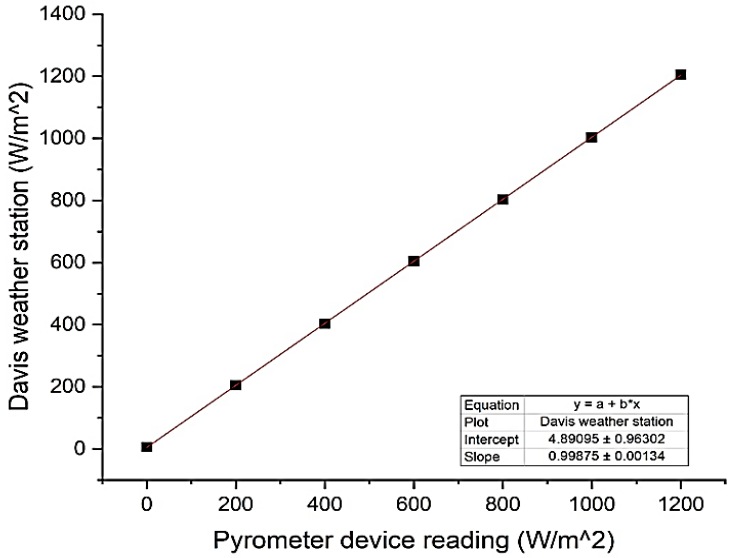

Figure C.1 solar meter calibration(Pyranometer)

Table C.1 solar meter characteristics (Pyranometer).

Property	**Value**
Model	SM206 - SOLAR
Temperature error	±0.38℃
Accuracy	±10W/m^2
Sample time	0.25 second
Operating under temperature effect	0ºC - 50ºC
Humidity	<80% RH
Dimension L/W/H	22 cm, 15cm, and 4.5cm
Battery	1 pcs 9V

Appendix. D - List of Publications.

1- Hussein Ali Jabbar , Dhafer Manea Hachim, Kareem J. Alwan'' Heat Transfer Fluids (HTFs) in Parabolic Trough Collector (PTC) : Review Study'' 1st International Conference on Achieving the Sustainable Development Goals (Istanbul-Turkey 2022).

2- Hussein Ali Jabbar , Kareem J. Alwan , Dhafer Manea Hachim'' Numerical Study on the effect of working conditions on the Performance of Parabolic Trough Collector at Al-Najaf city in Iraq'' 6th International Conference on Engineering Sciences (Ankara-Turkey 2023).

Heat Transfer Fluids in Parabolic Trough Collector (PTC) : A Review Study

Hussein Ali Jabbar [1, a)] , Dhafer Manea Hachim [1, b)] ,and Kareem J. Alwan [2, c)]

[1] *Engineering Technical College / Najaf, Al-Furat Al-Awsat Technical University ,31001, Najaf, Iraq.*
[2]*Najaf Technical Institute / Al-Furat Al-Awsat Technical University ,31001, Najaf, Iraq.*

[a)] Corresponding author: hussein.jabar.etcn@student.atu.edu.iq
[b)] coj.dfr@atu.edu.iq
[c)] karimjaefar@atu.edu.iq

Abstract. A solar thermal collector is a heat collector that absorbs heat via sunlight. It is a device that turns the thermal energy in sunshine or solar radiation into a useful and storable form. This energy is conveyed via electromagnetic radiation with wavelengths ranging from infrared (long) to ultraviolet (short). Solar energy is one of the cleanest and most versatile renewable energy sources when compared to other renewable energy sources. Solar trough collectors (PTC), Compound Parabolic Collectors (CPC), Linear Fresnel Collectors (LFC), Solar Towers, and Solar Dish Collectors are all types of solar concentrator systems. One of the most common types of solar concentrators is the parabolic trough collector (PTC). Working fluids, also known as heat transfer fluids (HTFs), are a crucial component of (PTC) that will be investigated. Water, thermal oil, molten salts, and gases are just a few of the working fluids used in the parabolic trough collector, all of which types operate in a temperature range. This research evaluates thermal performance of a parabolic trough collector by employing different heat transfer fluids (HTFs) at a temperature range up to 823 K under various operating conditions. The fundamental physical parameters, such as specific heat, density, viscosity, and thermal conductivity of working fluids (HTFs) and their output temperatures, thermal efficiency, advantages, disadvantages, and cost of the working fluids are also presented. After comparing the various working fluids which are used in parabolic trough collectors (PTC), it is found that Liquid Sodium is the most reliable heat transfer fluid (HTF) based on number of factors, including useful energy, thermal efficiency, low cost, high temperature operation range, and physical qualities in operation. Liquid sodium provides good thermal performance factors, including useful energy, thermal efficiency, low cost, and a high temperature operation range.

Keywords. Heat transfer fluids (HTFs), working fluids in Parabolic Trough Collector (PTC), Renewable energy (solar energy) .

INTRODUCTION

Renewable energy is natural energy that has no finite supply and may be used repeatedly without depletion. Energy is essential to our well-being because it helps us to be comfortable, productive, and live our lives as we like. Since the beginning of time, wood, water, and fossil fuels have been used to heat and power equipment. For nearly all types of tasks, we rely on one or more forms of energy [1]. A civilization's energy consumption is a barometer of its economic progress and growth [2]. Almost everything we see in our surroundings necessitates the use of energy in the manufacturing or transformation of a natural resource into a completed product. The clothing we wear, the food we eat, and the housing we live in are all examples of this [3]. Increasing global energy consumption because of the consequences [4], like rising carbon dioxide emissions and fossil resource depletion, are serious issue that the society must solve [5]. The cost rising of energy and changing lifestyle patterns [6], both are associated with high energy consumption, necessitating the usage of renewable also alternative energy sources. Solar energy, as well as , low-cost thermal and electrical energy, is a viable solution for all environmental concerns [7]. Solar collectors are devices that gather solar energy and convert it, at least in part, t thermal output. At the present, the most often usable

1st International Conference on Achieving the Sustainable Development Goals
AIP Conf. Proc. 2776, 050011-1–050011-12; https://doi.org/10.1063/5.0135997
Published by AIP Publishing. 978-0-7354-4441-6/$30.00

ACCEPTING LETTER

Dear authors:

Hussein Ali Jabbar

Kareem J. Alwan

Dhafer Manea Hachim

Thanks for submitting your paper to ICES2023.

Based on our reviewers comments your paper has been accepted for this conference

(Numerical Study on the effect of working conditions on the Performance of Parabolic Trough Collector at Al-Najaf city in Iraq) (code: ices-15)

Conference coordinator

Dr.Khawola F. Mahmoud

Numerical Study on the effect of working conditions on the Performance of Parabolic Trough Collector at Al-Najaf city in Iraq

Hussein Ali Jabbar [1)], Kareem J. Alwan [2)], Dhafer Manea Hachim [3)]

[1,3] Engineering Technical College / Najaf, Al-Furat Al-Awsat Technical University ,31001, Najaf, Iraq
[2] Najaf Technical Institute / Al-Furat Al-Awsat Technical University ,31001, Najaf, Iraq

Corresponding author: enghussein166@gmail.com

Abstract: Solar energy is one of the renewable energy types. A solar collector is a device that converts solar energy into thermal energy for use in the production of electricity. The most common form of solar collector used in solar power plants is a parabolic trough collector (PTC). The study aims to use a numerical CFD model using COMSOL Multiphysics 5.5 software to investigate the effect of different working conditions on the thermal performance of a solar Parabolic Trough Collector at Al-Najaf city in Iraq. Three different working fluids, such as Water, THERMINOL VP -1, and SYLTHERM800, were used. The influence of input temperature was considered at a range of temperatures between (323.15 – 423.15)K. In addition, various magnitudes of mass flowrate were selected between (0.00926 - 0.0556) kg/s. The developed numerical model was validated based on the literature's experimental results. The final results showed that water has a high maximum (average output temperature = 411.6 K, average thermal efficiency = 70.7%, average useful heat = 3560.1 W, and average heat loss = 199.2 W), while SYLTHERM800 has a maximum (average output temperature = 472.3K, average thermal efficiency = 65.0%, average useful heat = 3180 W, and average heat loss = 579.3 W) at mass flow rate 0.00926 kg/s, for 15 July 2018, Also obtained the flowing results for high mass flow rate (0.0556 kg/s), water has a high maximum (average output temperature = 339.75 K, average thermal efficiency = 72.9%, average useful heat = 3689.3 W, and average heat loss = 70.0 W), while SYLTHERM800 has a maximum (average output temperature = 362.5K, average thermal efficiency = 73.0%, average useful heat = 3691.4 W, and average heat loss = 67.9 W). The percentage error of validation results with literature article research for output temperature, thermal efficiency, useful heat, and total heat losses were (0.337%, 5.34%, 5.02%, 5.2%) respectively.

Keywords: Thermal performance of Parabolic Trough Collector , Working fluid , heat transfer fluid , Numerical study.

الخلاصة

واحد من تقنيات المركزات الشمسية هو المجمع الحوض المكافئ, مجمع الحوض المكافئ يجمع الاشعاع الشمسي الساقط على السطح العاكس و يعكسه على الانبوب الماص الذي يسخن سائل العمل المتدفق من خلاله الى المبادل الحراري ليكون بخار الانتاج الطاقة الكهربائية. خطوات عملية و عددية تم تقديمها في هذه الدراسة لفحص الاداء الحراري لمجمع الحوض المكافئ باستخدام سوائل عمل مختلفة , حيث تم في الخطوات العملية بعد تصميم و تصنيع جهاز مجمع الحوض المكافئ دراسة تأثير معدل التدفق الحجمي لماء على الاداء الحراري لمجمع الحوض المكافئ , و كذلك دراسة تأثير اتجاه مجمع الحوض المكافئ على اداءه الحراري. في التجارب العملية تم مقارنة بين اتجاه خط (شرق – غرب) و اتجاه خط (جنوب – شمال), حيث كانت الايام الخاصة باتجاه خط (شرق – غرب) هي (١٠,٧,٦,٢) تشرين الثاني و بمعدل تدفق حجمي (٣,٢,١,٤) لتر/الدقيقة بالتسلسل. و الايام الخاصة باتجاه خط (جنوب – شمال) هي (٢١,٢٠,١٤,١٣) تشرين الثاني و بمعدل تدفق حجمي (٤,٣,٢,١) لتر/الدقيقة بالتسلسل. النتائج وجدت ان اعظم درجة حرارة خروج للماء في اتجاه خط (شرق – غرب) بلغت (٣٣٦,٦٥ كلفن) في يوم (٦) تشرين الثاني ذو معدل تدفق حجمي للماء (١) لتر/الدقيقة , و هي اكثر من باقي ايام اتجاه خط (شرق – غرب) و هي (١٠,٧,٢) تشرين الثاني بنسبة (٥,٦ %, ٤%, ٦,٨ %) بالتسلسل. أعلى قيمة لدرجة حرارة خروج الماء في اتجاه خط (جنوب – شمال) بلغت (٣٢٨,٣٥ كلفن) في يوم (١٣) تشرين الثاني بمعدل تدفق حجمي للماء (١) لتر/الدقيقة و هي اعلى من بقية ايام اتجاه خط (جنوب – شمال) الباقية و هي (٢١,٢٠,١٤) تشرين الثاني و بنسبة (٣% , ٤% , ٥%) بالتسلسل. اعلى قيمة للكفاءة الحرارية لمجمع الحوض المكافئ في أتجاه خط (شرق – غرب) بلغت (٦٨,٧ %) في يوم (٦) تشرين الثاني و هي اعلى من باقي أيام (شرق – غرب) هي (١٠,٧,٢) تشرين الثاني بنسبة (٦٤% , ٢٤% , ٣٣%) بالتسلسل. أعلى كفاءة حرارية لمجمع الحوض المكافئ لأتجاه خط (جنوب – شمال) في يوم (١٤) تشرين الثاني حيث بلغت (٤٩,٥%) و هي اكثر باقي الايام اتجاه خط (جنوب – شمال) و هي (٢١,٢٠,١٣) تشرين الثاني بنسبة (١١% , ٨% , ٤%) بالترتيب. النتائج العملية النهائية وجدت ان بالمقارنة بين اتجاه خط (شرق – غرب) و اتجاه خط (جنوب – شمال) لافضل اداء حراري لمجمع الحوض المكافئ هو اتجاه خط (شرق – غرب).الدراسة العددية استندت

على المحاكاه بواسطة برنامج (COMSOL Multiphysic 6.0) لتحقق من الاداء الحراري لمجمع الحوض المكافئ باستخدام سؤائل عمل مختلفة منها (الماء , TherminolVP-1, Sytherm800). الدراسة العددية درست تأثير التدفق الحجمي لسوائل العمل المختلفة , و تأثير الانعكاسية بمعدلات (٠,٢٢٥ , ٠,٥ , ٠,٩٥) , و دراسة تأثير الامتصاصية بمعدلات مختلفة (٠,٥ , ٠,٧ , ٠,٩) و دراسة تأثير طقس مناخ مدينة النجف الاشرف و دراسة تأثير التدفق الكتلي لسوائل العمل و دراسة ثاتير اختلاف معدلات درجة حرارة الدخول على الاداء الحراري لمجمع الحوض المكافئ. النتائج وجدت ان ارتفاع درجة حرارة دخول السائل تتناسب طرديا مع درجة حرارة خروج السائل. الخصائص الفيزيائية لسوائل العمل مثل الكثافة و معامل التوصيل الحراري و اللزوجة ذو علاقة عكسية مع معدل درجة حرارة سائل العمل حيث ان بارتفاع درجة حرارة السائل تقل قيمة الخواص الفيزيائية لسائل العمل , ماعدا خاصية الحرارة النوعية تتناسب طرديا مع درجة حرارة سائل العمل حيث ان بزيادة درجة حرارة السائل تزداد الحرارة النوعية للسائل. في دراسة تأثير درجة حرارة دخول السائل حيث ان اقل معدل من درجة حرارة الدخول التي تبلغ (٣٢٣,١٥ كلفن) اعطت اعلى معدل من الكفاءة الحرارية بلغت (٧١,٢٥%) و اعلى معدل من الطاقة الحراري ة المكتسبة بلغت (٣٥٦٠ واط) و اقل معدل من الخسائر الحرارية بلغت (١٩٩,٢ واط). نستنتج ان سائل العمل(Sytherm800) هوسائل عمل الانسب يمكن ان يستخدم في مجمع الحوض المكافئ عند المقارنة بين السوائل العمل البقية (الماء , TherminolVP-1). سائل العمل (Sytherm800) من مميزاته هي نطاق درجة حرارة الخروج عالية مقارنة بالماء مع الحفاظ على كفاءة الماء عند معدلات التدفق الكتلي الكبيرة. لذلك فأن سائل العمل (Sytherm800) هو السائل العمل الانسب لمجمع الحوض المكافئ مع نطاق درجات الحرارة الدخول العالية و تدفق الكتلي العالي.

جمهورية العراق
وزارة التعليم العالي
جامعة الفرات الاوسط التقنية
الكلية التقنية الهندسية / النجف الاشرف

دراسة تحليلية للاداء الحراري لمجمع شمسي حوضي مكافئ

رسالة مقدمة الى

قسم هندسة تقنيات ميكانيك القوى في الكلية التقنية الهندسية – النجف – جامعة الفرات الاوسط التقنية كجزء من متطلبات نيل شهادة الماجستير في هندسة تقنيات ميكانيك الحراريات

تقدم بها

حسين علي جبار حمود

اشراف

الأستاذ الدكتور
ظافر مانع حاجم

الاستاذ المساعد
كريم جعفر علوان

2023

جمهورية العراق

وزارة التعليم العالي والبحث العلمي

جامعة الفرات الاوسط التقنية

الكلية التقنية الهندسية /النجف

دراسة تحليلية للاداء الحراري لمجمع شمسي حوضي مكافئ

حسين علي جبار حمود

ماجستير في هندسة تقنيات ميكانيك القوى / الحراريات

2023